Journal of Research of the National Bureau of Standards Vol. 46, No. 3, March 1951 Research Paper 2188

Refractive Indices of Maltose Solutions

Emma J. McDonald

The refractive indices of maltose hydrate solutions have been determined at 20° and at 25° C. Equations relating the refractive index to the percentage concentration of sugar have been prepared from the observed data by the method of averages. A table, giving the refractive indices of maltose solutions at 1-percent intervals over a range of 1 to 65 percent of maltose hydrate at both 20° and 25° C, is included.

I. Introduction

The disaccharide, maltose, has found extensive use in the food industry. Starch is converted into "soluble starch" by mild acid treatment, and this in turn is hydrolized to a mixture of maltose and dextrins by the enzymes of barley flour. Much of the maltose is not further purified but is used as a constituent of this mixture. Upon hydrolysis, maltose yields two glucose units, which are joined in the maltose molecule to form a 4-D-glucose D-glucoside. In the present investigation refractive index measurements have been made of aqueous maltose solutions at 20° and at 25° C. It is believed that these values will be of use in estimating the quantity of maltose present in solutions of the pure sugar, as well as in those containing maltose along with other sugars.

II. Purification of Maltose Hydrate

Maltose crystallizes from aqueous solution and from aqueous alcohol solution as maltose-H_2O. Considerable care is required to remove the last traces of dextrins. The preparation of the pure sugar by crystallization from alcohol, from acetic acid [1] and by deacetylation of the acetate [2] have been discussed in the literature.

The sugar used in this investigation was prepared by three recrystallizations of maltose from aqueous solution at approximately 5° C. The starting product was the chemically pure maltose of Pfanstiehl and of Eastman Kodak Co. The sugar was dissolved in water and the solution filtered through carbon, evaporated under reduced pressure, and crystallized in an ice bath with constant stirring. After the first crystallizations the carbon was omitted. The crystals were dried at room temperature, and finally at 50° C. They gave a very clear solution, were ash free, and had a specific rotation of +130.5 (water, C=4.73). This crystallization from water solution gives lower yields than when alcohol is used but has the advantage that small amounts of dextrose or dextrins remain in solution.

[1] T. S. Harding, Sugar **25,** 350 (1923).

[2] G. Zemplén, Ber. deut. chem. **59,** 1258 (1926); Ber. Ges. **60,** 2 1555 (1927); G. Zemplén and E. Pacsu, Ber. deut. chem. **62,** 1613 (1929); W. A. Mitchell, J. Am. Chem. Soc. **63,** 3534 (1941).

The maltose used for the refractive index determinations was found to contain 0.14 percent of moisture in excess of the theoretical 5.00 percent for maltose hydrate. This moisture content was determined by a procedure used previously in this laboratory by R. F. Jackson, who found that carefully prepared maltose hydrate dried at room temperature and finally at 50° C contained 5.13 percent of moisture rather than the theoretical 5.00 percent. He dried maltose to constant weight in a vacuum over P_2O_5. The initial drying temperature of 64° C was slowly increased to 105° C. In order to be assured that the loss of weight, in excess of 5.0 percent, was not due to decomposition, a sample of the sugar hydrate was allowed to come to equilibrium in an atmosphere whose vapor pressure was that of pure maltose hydrate. This vapor pressure was maintained by means of a mixture containing equal amounts of maltose hydrate and partially dehydrated maltose hydrate. A relatively small sample of the sugar hydrate after standing 255 hours at 56° C in this environment reached a constant weight and had lost 0.13 percent of its weight.

Tables 1 and 2 record data obtained by R. F. Jackson.

TABLE 1. *Drying of maltose hydrate in vacuum over* P_2O_5

Sample 1: 1.16355 g, moisture 5.14%				Sample 2: 1.1093 g, moisture 5.12%			
Temperature	Time	Loss	Total loss	Temperature	Time	Loss	Total loss
° C	*hr*	*mg*	*mg*	*° C*	*hr*	*mg*	*mg*
76	26	42.1	42.1	76	26	44.1	44.1
76	19	2.3	44.4	76	19	2.1	46.1
100	3	2.0	46.4	100	3	1.6	47.8
100	7	1.8	48.2	100	7	1.4	49.2
100	3	0.3	48.5	100	3	0.5	49.7
100	3.5	.6	49.1	100	3.5	.6	50.3
105	4	2.2	51.1	110	3	3.8	54.1
105	8	2.5	53.6	110	2.2	1.9	56.0
105	8.2	1.7	55.3	110	2	0.4	56.4
105	6.4	1.3	56.6	110	2	.3	56.7
105	10.3	1.8	58.4	110	4	0	56.8
105	6.8	0.4	58.8				
105	7.2	.5	59.3	Total	74.7		
105	6	.25	59.5				
105	4	.15	59.7				
105	4.5	.1	59.8				
105	4	0	59.8				
Total....	130.9						

UNIVERSITY OF MICHIGAN LIBRARIES

TABLE 2. *Maltose hydrate sample in atmosphere having vapor pressure of maltose.H_2O*

Temperature	Time	Loss	Total loss
°C	hr	mg	mg
36	40	0.65	0.65
56	40	.3	.95
56	40	.1	1.05
56	45	.2	1.25
54	45	−.1	1.15
55	45	0	1.15
Total	255	9.13%	

III. Measurements and Discussion of Results

The refractive index measurements were made on solutions whose concentrations varied from approximately 1 to 65 percent of maltose hydrate. All measurements were made under carefully controlled temperature conditions. Observations over the entire range of concentration were made on a Bausch & Lomb precision refractometer, and at the lower concentrations, a Zeiss dipping refractometer was used. These instruments were calibrated at this Bureau. A measurement of the refractive index of water [3] was made before and after that of each maltose solution, and proper corrections were applied. The value used was the average of four or five readings on a given solution. The maximum difference on a given solution never exceeded 0.00002 in refractive index. Each solution stood at least 4 hours to allow the maltose to reach equilibrium.[4]

Sixteen observations were made at 20°C and eight observations at 25°C. Equations relating the refractive index to the percentage concentration of sugar hydrate (p) were calculated by the method of averages from the observed data. Equations 1 and 2 express this relationship.

$$n_D^{20} = 1.33299 + 1.38914\times10^{-3}p + 4.7602\times10^{-6}p^2 + 2.0933\times10^{-8}p^3 - 6.124\times10^{-11}p^4 \quad (1)$$

$$n_D^{25} = 1.33250 + 1.38275\times10^{-3}p + 3.9303\times10^{-6}p^2 + 5.2527\times10^{-8}p^3 - 3.4994\times10^{-10}p^4 \quad (2)$$

Tables 3 and 4 contain the observed data, along with the calculated values. At 20°C the average deviation of the calculated values from those observed amounts to ±0.000024, whereas at 25°C the corresponding average deviation is ±0.000049. At both temperatures the deviations at the higher concentrations are greater than in the lower range. This may be attributed to the increased difficulty in the preparation and the handling of the solutions of higher concentration. The refractive indices in table 5 were calculated by means of eq 1 and 2. The temperature coefficient of maltose solutions appears to be very similar to that of sucrose solutions in this temperature range. The apparent decrease in temperature effect above 44-percent concentration is small and may be a result of experimental error. It is of the same order of magnitude as the deviation of the observed values from the calculated values. At 21°C a saturated maltose solution contains 46.4 percent of sugar; thus the solutions with concentration above 46.4 percent are supersaturated and are more subject to error due to shifting of the equilibrium products. It appears that a temperature coefficient of 0.00016 would be within the experimental error of the data for the concentration range above 23 percent.

TABLE 3. *Refractive indices of maltose solutions at 20° C*

Percentage of maltose hydrate	n_D^{20} (observed)	n_D^{20} (calculated) [a]	Observed−calculated
1.563	1.33518	1.33517	+0.00001
5.015	1.34008	1.34008	.00000
7.003	1.34294	1.34296	−.00002
12.929	1.35180	1.35179	+.00001
14.410	1.35404	1.35406	−.00002
20.512	1.36362	1.36366	−.00004
25.586	1.37200	1.37197	+.00003
25.197	1.37135	1.37132	+.00003
31.034	1.38126	1.38125	+.00001
36.666	1.39128	1.39124	+.00004
40.995	1.39918	1.39921	−.00003
44.801	1.40640	1.40641	−.00001
50.713	1.41807	1.41800	+.00007
55.537	1.42781	1.42782	−.00001
59.798	1.43674	1.43677	−.00003
65.529	1.44920	1.44922	−.00002
Average deviation ±0.000024			

[a] Equation 1 was used in obtaining calculated values.

TABLE 4. *Refractive indices of maltose solutions at 25° C*

Percentage of maltose hydrate	n_D^{25} (observed)	n_D^{25} (calculated) [a]	Observed−calculated
3.312	1.33709	1.33712	−0.00003
10.180	1.34707	1.34703	+.00004
12.530	1.35051	1.35054	−.00003
25.530	1.37026	1.37023	+.00003
39.837	1.39633	1.39626	+.00007
40.405	1.39725	1.39732	−.00007
50.992	1.41777	1.41783	+.00006
65.551	1.44842	1.44836	−.00006
Average deviation ±0.000049			

[a] Equation 2 was used in obtaining calculated values.

TABLE 5. *Refractive indices of maltose hydrate solutions at 20° and 25° C*

Percent	n_D^{20}	n_D^{25}	Δn	$\Delta n/\Delta t$
1	1.33428	1.33389	0.00049	0.00010
2	1.33579	1.33528	.00051	.00010
3	1.33720	1.33668	.00052	.00010
4	1.33862	1.33810	.00052	.00010
5	1.34006	1.33952	.00054	.00011
6	1.34150	1.34095	.00055	.00011
7	1.34295	1.34239	.00056	.00011
8	1.34442	1.34384	.00058	.00012
9	1.34589	1.34530	.00059	.00012
10	1.34738	1.34677	.00061	.00012
11	1.34887	1.34825	.00062	.00012
12	1.35039	1.34974	.00065	.00013
13	1.35190	1.35124	.00066	.00013
14	1.35343	1.35276	.00067	.00013
15	1.35497	1.35428	.00069	.00014

[3] L. W. Tilton and J. K. Taylor, J. Research NBS **20,** 419 (1938).
[4] H. S. Isbell and W. W. Pigman, J. Research NBS **18,** 183 (1937) RP969.

TABLE 5. *Refractive indices of maltose hydrate solutions at 20° and 25° C*—Continued

Percent	n_D^{20}	n_D^{25}	Δn	$\Delta n/\Delta t$
16	1.35652	1.35582	0.00070	0.00014
17	1.35808	1.35737	.00071	.00014
18	1.35965	1.35893	.00072	.00014
19	1.36124	1.36051	.00073	.00015
20	1.36283	1.36209	.00074	.00015
21	1.36444	1.36369	.00075	.00015
22	1.36606	1.36530	.00076	.00015
23	1.36770	1.36692	.00078	.00016
24	1.36934	1.36856	.00078	.00016
25	1.37100	1.37021	.00079	.00016
26	1.37267	1.37187	.00080	.00016
27	1.37435	1.37355	.00080	.00016
28	1.37604	1.37524	.00080	.00016
29	1.37775	1.37694	.00081	.00016
30	1.37946	1.37865	.00081	.00016
31	1.38120	1.38038	.00082	.00016
32	1.38294	1.38213	.00082	.00016
33	1.38470	1.38388	.00082	.00016
34	1.38647	1.38565	.00081	.00016
35	1.38825	1.38744	.00081	.00016
36	1.39004	1.38924	.00080	.00016
37	1.39185	1.39105	.00080	.00016
38	1.39367	1.39287	.00080	.00016
39	1.39551	1.39471	.00080	.00016
40	1.39735	1.39656	.00079	.00016
41	1.39922	1.39843	.00079	.00016
42	1.40109	1.40031	.00078	.00016
43	1.40298	1.40221	.00077	.00016
44	1.40488	1.40411	.00077	.00015
45	1.40680	1.40603	.00077	.00015
46	1.40873	1.40797	.00076	.00015
47	1.41067	1.40992	.00075	.00015
48	1.41263	1.41188	.00075	.00015
49	1.41460	1.41385	.00075	.00015
50	1.41658	1.41584	.00074	.00015
51	1.41858	1.41784	.00074	.00015
52	1.42059	1.41986	.00073	.00015
53	1.42262	1.42189	.00073	.00015
54	1.42466	1.42392	.00074	.00015
55	1.42672	1.42598	.00074	.00015
56	1.42878	1.42804	.00074	.00015
57	1.43087	1.43012	.00075	.00015
58	1.43296	1.43221	.00075	.00015
59	1.43508	1.43431	.00077	.00015
60	1.43720	1.43643	.00077	.00015
61	1.43934	1.43855	.00079	.00016
62	1.44150	1.44069	.00081	.00016
63	1.44367	1.44283	.00084	.00017
64	1.44585	1.44499	.00086	.00017
65	1.44805	1.44716	.00089	.00018

Results of work by F. W. Zerban and J. Martin, now in press (J. Assoc. Off. Agr. Chem.) on the refractive indices of maltose solutions at 20°C is in good agreement with the results obtained in this investigation. Previous work may be summarized as follows. Tolman and Smith [5] reported the refractive indices of maltose solutions of relatively low concentrations. In their discussion they state that the sugars were dried at 70°C under a diminished pressure of about 27 in.; no other comment is made as to the preparation of the sugar. The following refractive indices are those reported by these authors along with values obtained from table 5 of this investigation.

Percentage of maltose	n_D^{20} (T and S)	n_D^{20} (McD)
1.00	1.3343	1.3344
2.07	1.3357	1.3359
5.07	1.3402	1.3402
10.07	1.3477	1.3475
15.12	1.3555	1.3552
20.17	1.3637	1.3631

Pulvermacher [6] determined the refractive indices of maltose solutions whose concentrations varied from 1.16 to 19.40 percent of anhydrous sugar at 25°C. His results are reported to the fourth place, and the values are all higher by one in the third place than the results here presented. As the results reported in the same article by Pulvermacher are higher for glucose than the accepted values, it appears that perhaps some discrepancy persisted throughout his measurements.

WASHINGTON, October 23, 1950.

[5] L. M. Tolman and W. B. Smith, J. Am. Chem. Soc. **28**, 1476 (1906).
[6] G. Pulvermacher, Z. anorg. chem. **113**, 141 (1920).

UNIVERSITY OF MICHIGAN LIBRARIES

Journal of Research of the National Bureau of Standards Vol. 46, No. 3, March 1951 Research Paper 2189

Electrode Function (pH Response), Hygroscopicity, and Chemical Durability of Soda-Potash-Silica Glasses

Donald Hubbard, Mason H. Black, Sylvanus F. Holley, and Gerald F. Rynders

The pH response, hygroscopicity, and chemical durability of a series of Na_2O-K_2O-SiO_2 glasses have been investigated. The pH responses of electrodes prepared from these glasses are in accord with similar data previously reported for two other series of glasses, namely, Na_2O-CaO-SiO_2 and Na_2O-PbO-SiO_2, which showed that (1) glasses of low hygroscopicity produce electrodes whose pH response fall below the theoretical 59 millivolts per pH at 25° C predicted by the Nernst equation, and (2) electrodes prepared from glasses of poor chemical durability also fail to develop the full theoretical voltage.

Chemical durability determinations by an interferometer procedure indicate swelling of the glasses upon exposure to acid buffers and pronounced attack in alkaline solutions. During the investigation some limitations of the interferometer procedure for determining chemical durability of glass became evident. Glasses that had exhibited direct solution in the acid pH range were found to show swelling in the early stages of the exposure. This swollen layer then sloughed off giving the appearance of attack as previously interpreted.

Above 70 percent of SiO_2, glasses containing mixtures of Na_2O and K_2O have lower hygroscopicities than those having but a single one of these oxides.

The pH response-hygroscopicity curves appeared to reflect some of the critical compositions of the phase equilibrium diagram, with glasses in the composition range for alpha tridymite yielding electrodes with the optimum pH response characteristics.

I. Introduction

Previous studies of the chemical durability and hygroscopicity of optical glasses as a rapid test of their serviceability have demonstrated that these two properties are pertinent indicators of the suitability of glasses for measuring the hydrogen ion activity of aqueous solutions [1 to 5].[1] In every case studied, electrodes prepared from glasses of poor chemical durability failed to develop the theoretical voltage response indicated by the Nernst equation; $\Delta E = 0.000198\ T\Delta pH$ [1, 6, 7]. Equally obvious was the fact that glasses of very low hygroscopicity also failed to produce electrodes having satisfactory pH response [1, 6, 7]. In order to gain further information as to the universal validity of these findings, the hygroscopicity, chemical durability and pH response were studied for a series of Na_2O-K_2O-SiO_2 glasses.

II. Experimental Procedure

The pH responses of the experimental glasses were determined on electrodes of the Haber type [3] prepared by blowing thin walled bulbs on the end of tubing drawn from the molten glass. The resulting bulbs were filled with mercury for the inner electrical connection [8]. These metal filled electrodes were preferred to the conventional inner-solution filled types of glass electrodes [1], not only because of the simplicity of preparation, but also because a mercury filled electrode broken in service will not contaminate or alter the pH of the buffer solution involved. The voltage and pH measurements were made at room temperature with a Beckman pH meter, laboratory model G, using a well-conditioned glass electrode as the reference electrode.

The pH response values (mv per pH) were calculated from the electromotive force readings at pH 4.1 and 8.2. The voltage reading at pH 2 for the cell consisting of the experimental electrode and the reference electrode was taken as zero departure in every case. The values presented for the voltage departures represent in general the best performance obtained on any electrode from each glass. However, the life of electrodes varied from a few minutes to many weeks, depending upon the chemical durability of the glasses.

The procedure employed for obtaining the hygroscopicity data consisted in exposing approximately 1.5 g of powdered glass that passed a 150 mesh Tyler standard sieve, to the high humidity maintained by a saturated solution of $CaSO_4.2H_2O$ at 25° C [5, 6, 7]. All glasses were exposed for 1- and 2-hour periods and the results reported as milligrams of water sorbed per cubic centimeter of sample, that is, water sorbed times the density of the glass divided by the weight of the sample. To hasten equilibrium and uniformity throughout the humidity chamber, the walls were lined with a blotter wick and the atmosphere of the system circulated continously.

The chemical durability measurements of a semi-quantitative nature were obtained by an interferometer procedure [4, 9]. Specimens of the experimental glasses, after having been polished sufficiently flat to show interference bands when placed under a quartz optical flat, were partially immersed in Britton-Robinson universal buffer solutions at 80° C, covering the range from pH 2 to 11.8 [10]. The displacement of the bands due to surface alteration from the exposure was subsequently observed with a Pulfrich viewing apparatus. All results were reported for a 6-hour period, although some of the glasses were exposed for shorter periods of time in order to keep within the range limitations of the interferometer. In some extreme cases, the exposure time was reduced to 10 seconds and the value extra-

[1] Figures in brackets indicate the literature references at the end of this paper.

polated to 6 hours to keep the data consistent. Swelling is plotted as negative attack in the figures.

The compositions of the glasses were calculated from batch compositions and are identified in the illustrations as weight percent in the order Na_2O: K_2O:SiO_2.

III. Results and Discussion

Typical data for hygroscopicity, chemical durability, voltage departure, and pH response for the Na_2O-K_2O-SiO_2 glasses are given in table 1. For convenience of presentation and observation, the glasses are listed as five distinct series, namely, Na_2O-SiO_2, K_2O-SiO_2, Na_2O-K_2O-SiO_2 having 10 percent of K_2O, another having 10 percent of Na_2O, and a fifth set consisting of an incomplete short series of increasing percentages of SiO_2, in which the contents of Na_2O and K_2O are maintained equal on a weight percent basis. It is interesting to observe that each of these families of glasses passed through a composition range of optimum pH response (figs. 3 to 7), with a falling off on both sides of the optimum. Such a reversal does not appear for either the hygroscopicity or chemical durability values for the same families (figs. 4, 6, 7).

TABLE 1. *Hygroscopicity (water sorbed), pH response, and chemical durability of* Na_2O-K_2O-SiO_2 *glasses*

Glasses			Water sorbed		Voltage departure at pH—						pH response, 4.1 to 8.2	Chemical durability (attack) at pH—					
Na_2O	K_2O	SiO_2	1 hr	2 hr	2.0	4.1	6.0	8.2	10.2	11.8		2.0	4.1	6.0	8.2	10.2	11.8
%	%	%	mg/cm²	mg/cm²	mv	mv	mv	mv	mv	mv	mv/pH	Fringes	Fringes	Fringes	Fringes	Fringes	Fringes
40	0	60	320	----	0	95	183	285	375	466	12	[a]	[a]	[a]	[a]	[a](	[a]
35	0	65	210	----	0	90	182	274	370	451	13	[a]	[a]	[a]	[a]	[a]	[a]
32	0	68	176	445	0	70	157	252	330	..	14	180 swell	180 swell	180 swell	180 swell	108 swell	----------
30	0	70	159	379	0	68	148	229	307	397	19	72 swell	72 swell	72 swell	72 swell	18 swell	252
28	0	72	151	346	0	17	39	68	95	138	46	36 swell	36 swell	36 swell	36 swell	1/16 swell	120
26	0	74	130	309	0	21	34	51	62	88	51	18 swell	18 swell	18 swell	18 swell	[e]D	36
24	0	76	127	270	0	9	24	32	49	60	53	12 swell	12 swell	12 swell	8 swell	2½ swell	20
22	0	78	112	265	0	10	18	23	39	49	55	2½ swell	6−swell	6 swell	6−swell	?	6
20	0	80	108	256	0	10	17	25	37	49	55	2 swell	2 swell	2+swell	2 swell	1 swell	3
18	0	82	96	220	0	10	18	18	26	34	57	¾ swell	¾ swell	¾ swell	½+swell	?	3+
16	0	84	83	178	0	3	7	7	9	11	58	¼+swell	¼+swell	¼+swell	1/16 swell	?	2½
14	0	86	61	124	0	2	4	6	8	10	58	1/16 swell	1/16 swell	1/16 swell	--------	D	2−
12	0	88	52	104	0	10	18	32	45	54	55	D swell	D swell	D swell	--------	?	2
?	0	>88	37	----	0	31	55	78	107	.	47	[b]	[b]	[b]	[b]	[b]	[b]
?	0	>88	30	----	0	36	85	133	185	.	35	[b]	[b]	[b]	[b]	[b]	[b]
?	0	>88	24	----	0	74	167	252	341	.	15	[b]	[b]	[b]	[b]	[b]	[b]
0	0	100	11	----	[c]	[c]	[c]	[c]	[c]	[c]	0	[d]ND swell	ND	ND	ND	ND	1/2
0	36	64	446	1,146	0	96	208	304	407	503	7	[a]	[a]	[a]	[a]	[a]	[a]
0	34	66	384	956	0	89	209	310	418	500	7	[a]	[a]	[a]	[a]	[a]	[a]
0	32	68	344	835	0	85	167	257	359	431	16	[a]	[a]	[a]	[a]	[a]	[a]
0	30	60	259	636	0	77	145	220	292	370	23	270 swell	270 swell	270 swell	? swell	18 swell	Etched
0	28	72	202	406	0	43	100	170	259	332	28	126 swell	126 swell	126 swell	126 swell	Etched	1/4 swell, 2 min, 1 attack, 5 min.
0	26	74	157	352	0	17	68	125	181	239	32	72 swell	72 swell	72 swell	70 swell	36 swell	90
0	24	76	122	237	0	20	48	80	142	195	44	40 swell	40 swell	40 swell	40 swell	36 swell	Etched
0	22	78	97	184	0	22	42	64	93	149	49	18 swell	20 swell	20 swell	16 swell	18 swell	24
0	20	80	80	161	0	10	21	32	54	91	54	8 swell	8 swell	8 swell	6 swell	6 swell	14
0	18	82	67	136	0	12	16	18	40	68	57.5	3½ swell	3½ swell	3 swell	3 swell	2+ swell	2½
0	16	84	57	122	0	11	13	17	21	26	57.5	½ swell	½ swell	½ swell	½ swell	½ swell	2−
0	14	86	46	100	0	4	8	12	20	31	57	1/16 swell	1/16 swell	2/16 swell	2/16 swell	1/16 swell	2−
0	12	88	37	80	0	31	93	174	220	264	23	ND	ND	ND	D	D	2+
0	10	90	29	50	[e]	[e]	[e]	[e]	[e]	[e]	0	ND	ND	ND	ND	ND	1½+
0	8	92	23	29	[e]	[e]	[e]	[e]	[e]	[e]	0	ND	ND	ND	ND	ND	1+
0	6	94	19	20	[e]	[e]	[e]	[e]	[e]	[e]	0	ND	ND	ND	ND	ND	¾
30	10	60	325	750	0	110	215	332	477	575	5	[a]	[a]	[a]	[a]	[a]	[a]
27.5	10	62.5	262	635	0	92	187	307	407	490	8	540 swell	540 swell	540 swell	540 swell	D swell	Etched
25	10	65	225	530	0	90	180	290	392	470	11	360 swell	360 swell	360 swell	Pitted	Pitted	Do.
20	10	70	159	370	0	40	85	150	207	267	32	72 swell	72 swell	72 swell	72 swell	do	315
17.5	10	72.5	130	275	0	17	47	86	127	185	43	27 swell	27 swell	20 swell	20 swell	20 swell	162
15	10	75	110	210	0	22	31	42	57	87	54	15 swell	15 swell	15 swell	15 swell	6 attack	120
12.5	10	77.5	85	160	0	6	11	19	32	43	56	3 swell	3 swell	3− swell	3− swell	?	15
10	10	80	60	118	0	5	14	16	22	33	57−	1¼ swell	1¼ swell	1¼ swell	1¼ swell	½+ swell	1
5	10	85	41	81	[f]	[f]	[f]	[f]	[f]	[f]	?	D swell	D swell	D swell	D swell	D	1½
0	10	90	29	50	[e]	[e]	[e]	[e]	[e]	[e]	0	ND	ND	ND	ND	ND	1½+
10	30	60	400	899	0	99	190	305	405	----	8	1080 swell	1080 swell	1080 swell	1080 swell	500	Etched
10	25	65	262	600	0	92	182	272	365	455	14	360 swell	360 swell	360 swell	Pitted	Pitted	Do.
10	22.5	67.5	212	490	0	77	160	242	328	420	19	144 swell	144 swell	144 swell	do	do	Do.
10	20	70	172	389	0	62	137	187	255	320	28	72 swell	72 swell	72 swell	do	do	200
10	17.5	72.5	145	290	0	37	75	127	170	234	38	27 swell	27 swell	20 swell	20 swell	----------	90
10	15	75	117	220	0	10	29	43	63	89	51	12 swell	12 swell	12 swell	12 swell	6 swell	72
10	12.5	77.5	89	160	0	16	29	24	47	63	55	3 swell	3 swell	3 swell	2 swell	D	15
10	10	80	60	118	0	5	14	16	22	33	57−	1¼ swell	1¼ swell	1¼ swell	1¼ swell	½+ swell	1
10	5	85	45	92	0	15	30	50	67	80	50	D swell	D swell	D swell	D swell	Surface cut	¾
?	0	>88	24	-------	0	74	167	252	341	----	15	[b]	[b]	[b]	[b]	[b]	[b]
20	20	60	345	833	0	81	172	260	425	550	9	1080 swell	1080 swell	Pitted	720 swell	270 swell	Etched
17.5	17.5	65	235	570	0	112	209	304	415	510	12	360 swell	Pitted	360 swell	----------	----------	----------
15	15	70	165	375	0	60	128	192	280	375	27	72 swell	72 swell	72 swell	72 swell	60 swell	315
12.5	12.5	75	110	213	0	12	21	40	78	106	52	12 swell	12 swell	12 swell	12 swell	6 attack	60
10	10	80	60	118	0	5	14	16	22	33	57−	1¼ swell	1¼ swell	1¼ swell	1¼ swell	½+ swell	1
27.5	7.5	65	210	532	0	106	212	292	420	522	14	360 swell	360 swell	Pitted	Pitted	Pitted	Etched
12.5	22.5	65	250	580	0	126	233	314	450	550	12	300 swell	Pitted	do	----------	----------	----------
Corning 015			59	138	0	0	0	0	0	3	59	2/16− swell	2/16− swell	2/16 − swell	Surface cut	1/4 − attack	2

[a] Failed to maintain polish.
[b] No specimens available.
[c] No definite pH response.
[d] Not detectable.
[e] Detectable.
[f] Devitrification.

UNIVERSITY OF MICHIGAN LIBRARIES

1. Na_2O-SiO_2 Glasses

(a) Voltage Departure and Chemical Durability

The voltage departures and the accompanying durability characteristics of the Na_2O-SiO_2 family of glasses over the range from pH 2 to 11.8 are shown in figure 1 and figure 2, respectively. From figure 1 it is evident that beginning with electrodes from glass 40:60 the voltage departures (errors) decrease with increasing SiO_2 content to glass 14:86. Above this composition the electrodes for glasses containing larger percentages of SiO_2 become progressively worse.[2]

Figure 2 illustrates the occurrence of swelling in the acid range and attack at the higher alkalinities. These features are characteristic of many silicate glasses [4, 6, 7, 9]. The conflict of results in figure 2 and in earlier published work [12] indicating both positive and negative attack for similar glasses exposed to equivalent solutions draws attention to an interesting feature of glass behavior and to a limitation of the interferometer procedure for determining the chemical durability of glasses. In some of the recent work it has become increasingly evident that the interferometer procedure can give this type of confusing result depending on the time of exposure to the attacking solution. For example, the glass 28 percent of K_2O; 72 percent of SiO_2, upon exposure to the buffer solution pH 11.8 at 80° C,

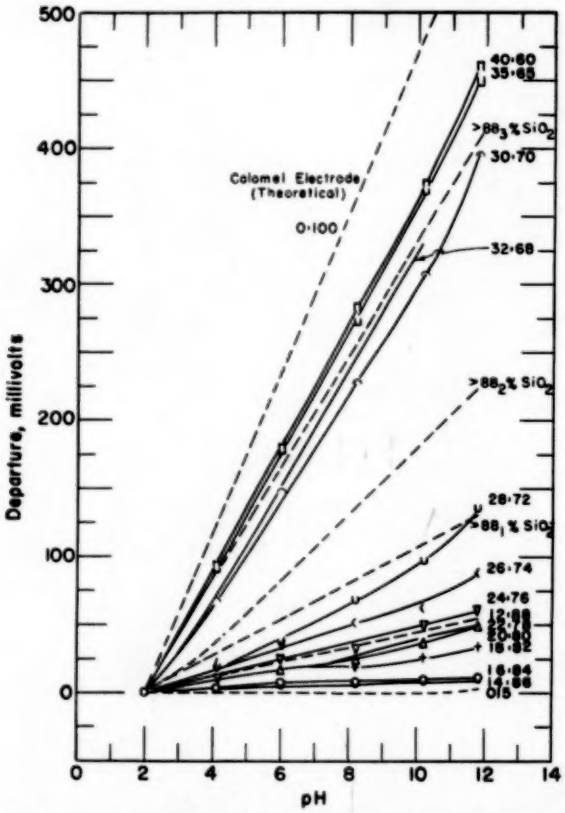

FIGURE 1. pH-*voltage departure curves for electrodes prepared from a series of* Na_2O-SiO_2 *glasses.*

Corning 015 is included for comparison.

[2] The pH response data for glasses labeled >88% SiO_2 were obtained from electrodes prepared from the glass of 88% of SiO_2 by leaching at 80° C for 1-, 2-, and 6-hour periods in 0.1 *N* HCl to remove Na_2O from the surface, followed by heating above the critical temperature. The accompanying hygroscopicity data were obtained on powdered samples similarly treated.

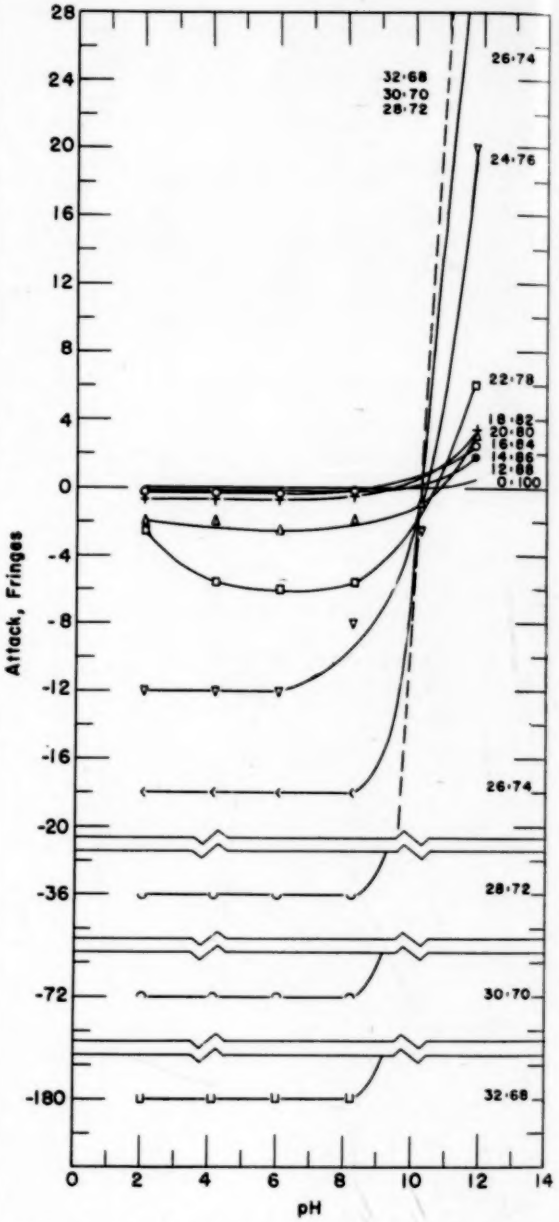

FIGURE 2. pH-*chemical durability curves for a series of* Na_2O-SiO_2 *glasses.*

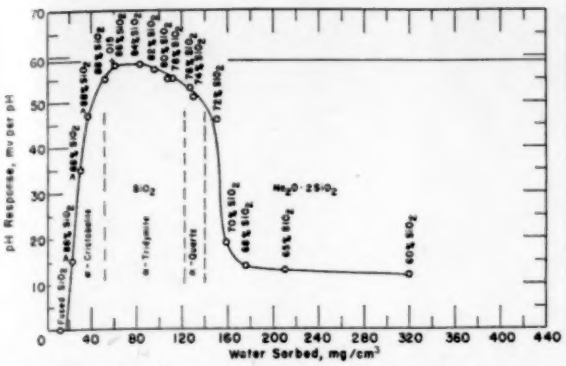

FIGURE 3. *Variation in* pH *response with increasing hygroscopicity for a series of* Na_2O-SiO_2 *glasses.*

Corning 015 electrode glass included for comparison. The approximate position at which the primary phase of the equilibrium diagram changes from SiO_2 to $Na_2O.2SiO_2$ is indicated by the broken lines.

exhibited a uniform swelling of one-fourth band after 2 minutes, but at the end of 5 minutes exposure a ragged attack of over one fringe was observed (table 1). This limitation of the interferometer method for measuring surface alteration was early suspected [6, 11, p. 155] but had not been observed. Any user of the interferometer procedure should be on the alert, especially when investigating glasses of very poor chemical durability. For such glasses, only by reducing the time of exposure to a minimum can it be demonstrated that the early stages of exposure produce swelling. Furthermore, if the surface alteration is greater than two or three fringes, it becomes increasingly difficult to ascertain if the alteration of the surface is one of swelling or solution.

(b) Hygroscopicity and pH Response

Figure 3 illustrates the variation in pH response with increasing hygroscopicity for the series of Na_2O-SiO_2 glasses listed in table 1. As was found for the Na_2O-CaO-SiO_2 and the Na_2O-PbO-SiO_2 glasses [6, 7] having a long hygroscopicity range, these glasses also exhibited a region of optimum pH response. Electrodes from glasses of low hygroscopicity failed to develop the full theoretical voltage of 59 mv/pH at 25° C, while those to the right of the optimum also failed to attain the full pH response. A glance at table 1 and figure 2 shows that these latter glasses have progressively poorer chemical durabilities with increasing hygroscopicity. In figure 3 the approximate position at which the primary phase, as shown by the equilibrium diagram, changes from SiO_2 to $Na_2O.2SiO_2$ is indicated by vertical broken lines [13].

(c) Hygroscopicity, Chemical Durability and pH Response Versus Composition

A better over-all picture of the interrelation between pH response, hygroscopicity, chemical durability, and composition for the Na_2O-SiO_2 glasses can be obtained from figure 4. The chemical durability curves presented are for the extremes of pH studied, namely pH 2 and 11.8. The divergence of these durability curves serves to emphasize the fact that swelling, plotted as negative attack, predominates in the acid range, while solution appears at high alkalinities, besides indicating the compositions at which marked durability departures appear. Further, a study of the pH response curve reveals that the hydrogen electrode function starts declining at approximately the same composition at which the chemical durability curves show a marked change [2, 4]. The approximate compositions at which a break has been reported in the specific volume curve for these glasses [14] and at which the primary phase of the equilibrium diagram changes from $Na_2O.2SiO_2$ to SiO_2 [13] are represented by

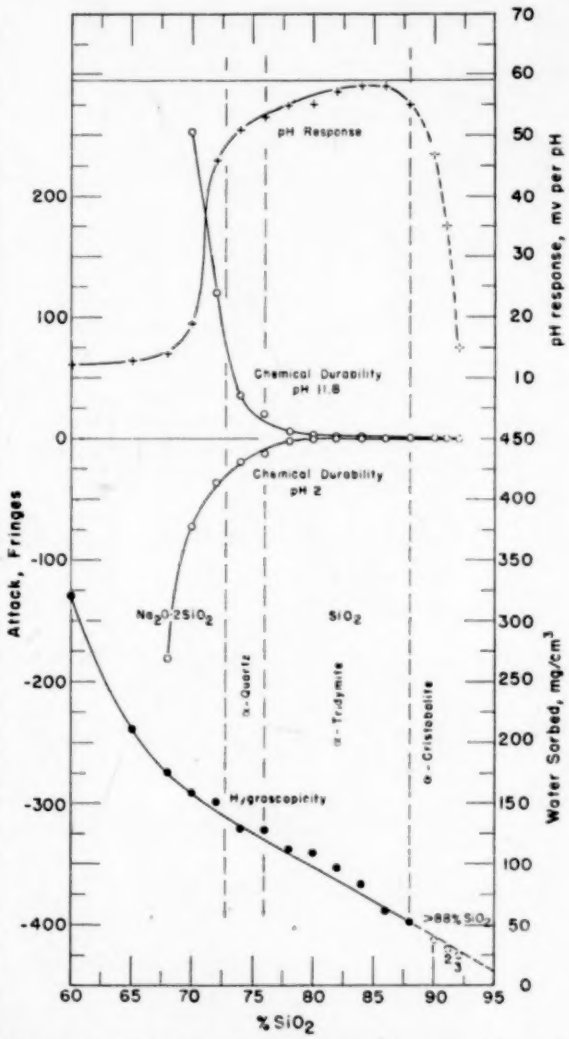

FIGURE 4. *Values for the* pH *response, hygroscopicity, and chemical durability at* pH *2 and 11.8 plotted against the percentage of* SiO_2 *for a series of* Na_2O-SiO_2 *glasses.*

broken lines. In earlier work on this system [12], a pronounced change in the slopes of the respective curves for voltage departure versus percentage of SiO_2, and apparent response to sodium ions versus percentage of SiO_2 also appeared near this same composition. The failure of electrodes from glasses of low hygroscopicity to develop the full theoretical voltage is also indicated in figure 4. Figures 3 and 4 show the optimum pH response for the Na_2O-SiO_2 glasses to lie within the composition range in which α-tridymite is the primary phase.

2. K_2O-SiO_2 Glasses

(a) Voltage Departure and Chemical Durability

Table 1 shows the voltage departure over the range pH 2 to 11.8 of electrodes prepared from the K_2O-SiO_2 glasses; and gives the accompanying durability characteristics for most of these glasses over the same pH range. As was the case with the Na_2O-SiO_2 glasses, the voltage departures (errors) decrease with increasing SiO_2 content to near 86 percent of SiO_2. Near this composition the improvement ceases, and it is followed by a reversal for higher percentage of SiO_2. No definite pH response was obtained for electrodes prepared from glasses having a SiO_2 content greater than 90 percent. These glasses also follow the two general rules: (1) electrodes prepared from glasses of very poor chemical durability fail to develop the full theoretical pH reponse, and (2) glasses of low hygroscopicity likewise fall short of the 59 mv/pH at 25°C indicated by the Nernst equation.

The chemical durability data of table 1 show the familiar swelling in the acid buffers and pronounced solution at the higher alkalinities. The same limitations of the interferometer procedure pointed out for the Na_2O-SiO_2 glasses are evident for the K_2O-SiO_2 glasses, and the same precautions are necessary in order to ascertain if the attack is positive or negative, that is, solution or swelling.

(b) Hygroscopicity and pH Response

The variation in pH response with increasing hygroscopicity for the K_2O-SiO_2 glasses (table 1) is qualitatively similar to that of the Na_2O-SiO_2 glasses. Electrodes prepared from the glasses of low hygroscopicity fell below the theoretical, and the glasses of high hygroscopicity characterized by very poor chemical durability also failed to give the full 59 mv/pH at 25°C. If the position at which changes in the primary phases of the equilibrium diagram appear [15] are superimposed on this data, the indicated reduction in pH response near the change from $K_2O.2SiO_2$ to $K_2O.4SiO_2$ is possibly transient as the pH response of all the glasses of very poor chemical durability continued to decrease until the electrodes failed. Electrodes from glasses of 76 percent and 78 percent of SiO_2 survived for 24 hours, whereas electrodes from the other glasses having smaller percentages of SiO_2 failed after much shorter service.

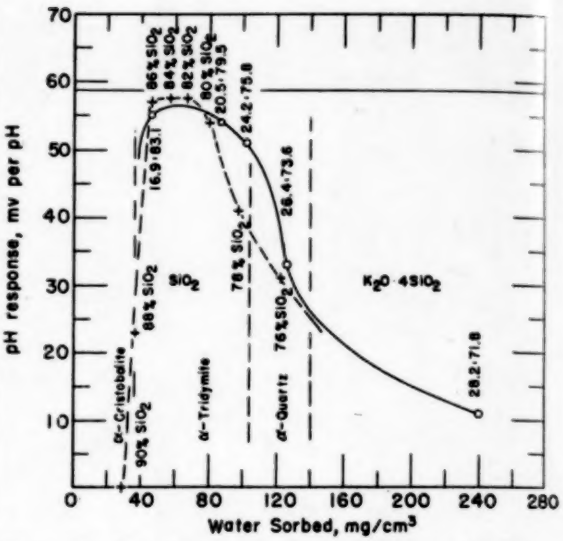

FIGURE 5. *Variation of* pH *response with increasing hygroscopicity for a limited series of* K_2O-SiO_2 *glasses previously reported.*

——, Compared with the present series; — — —, electrodes seasoned 24 hr.

In light of the present results, it seems desirable to reinterpret the pH response data previously presented for a limited series of K_2O-SiO_2 glasses [16]. Upon calculating the pH response for these "old" glasses between pH 4.1 and 8.2 (table 2), and plotting the values obtained against the hygroscopicity, the resulting curve is qualitatively similar to the curve for the present data, (fig. 5). The results as presented in the earlier publication had been calculated from the uncertain electromotive force data taken in the pH region of supposed maximum durability, giving values for pH response that appeared in contradiction to the upper voltage limits dictated by the Nerst equation. The present representation of these old data renders it in a more acceptable form. The approximate positions at which changes in the primary phase of the equilibrium diagram appear for this set of glasses [15] are inserted in this figure for the reader's inspection. Again it is apparent that the compositions of optimum pH response fall within the α-tridymite range.

TABLE 2. *Hygroscopicity and* pH *response of* K_2O-SiO_2 *glasses previously reported [16]*

Glasses		Water sorbed, 1 hr	pH response, 4.1 to 8.2
K_2O	SiO_2		
%	%	mg/cm.²	mv/pH
28.17	71.83	240	11
26.37	73.63	126	33
24.24	75.76	102	51
20.50	79.50	87	54
16.93	83.07	46	55

The differences in the performance of electrodes from the old and the new glasses may be attributed to either or both of the following factors. The old glasses were a part of a series of carefully analyzed glasses used for density determinations [14], whereas the compositions of the new series were calculated from batch composition. Electrodes of the old series were blown from tubes prepared by reworking pieces of the original glasses, while electrodes from the new glasses were prepared from tubes drawn from the melts at the time of pouring.

(c) Hygroscopicity, Chemical Durability, and pH Response Versus Composition

An over-all summary of the relationship between pH response, hygroscopicity, chemical durability, and composition for the K_2O-SiO_2 glasses can be plotted from table 1. As was the case with the Na_2O-SiO_2 glasses (fig. 4), glasses of low hygroscopicity and poor chemical durability failed to produce electrodes that developed the theoretical 59 mv/pH at 25°C. If the approximate compositions at which changes in the primary phase of the phase equilibrium diagram have been reported [15, 17] are superimposed on the K_2O-SiO_2 data of table 1, the compositions of optimum pH response fall in the range for which α-tridymite is the primary phase.

3. Na_2O-K_2O-SiO_2 Glasses

(a) Voltage departure and chemical durability

Three series of glasses, representing three cross sections of the Na_2O-K_2O-SiO_2 ternary diagram, were investigated for voltage and chemical durability characteristics. The voltage departures over the pH range 2 to 11.8 for these three series, are grouped in table 1. There is nothing unusual indicated by any of these voltage departures. The trends are qualitatively similar to the results shown by the Na_2O-SiO_2 and K_2O-SiO_2 series. The chemical durability characterized by swelling in the acid pH range and liberal solution of the glasses in the stronger alkaline buffers, improved with increased SiO_2 content.

(b) Hygroscopicity and pH Response

If the values for pH response and hygroscopicity for the Na_2O-K_2O-SiO_2 glasses containing 10 percent of K_2O and 10 percent of Na_2O are plotted, as was done for the Na_2O-SiO_2 glasses, curves are obtained which are similar to figure 3. Electrodes prepared from these glasses fit into the general pattern of performance, with those from glasses of low hygroscopicity failing to develop the full theoretical voltage, and those from glasses of poor chemical durability also falling well below the proper pH response. For these mixed alkali oxide glasses, those falling in the α-tridymite composition range indicated by the phase equilibrium diagram gave optimum performance [17].

(c) Hygroscopicity, Chemical Durability, and pH Response Versus Composition

The values for pH response, hygroscopicity, and chemical durability and their relation to the percentage SiO_2 are plotted in figures 6 and 7 for the two series of glasses containing 10 percent of K_2O and 10 percent of Na_2O. The approximate positions of the primary phases reported for the phase equilibrium diagram are included for inspection, and again they show that the region for α-tridymite produced electrodes which gave the optimum pH response [17].

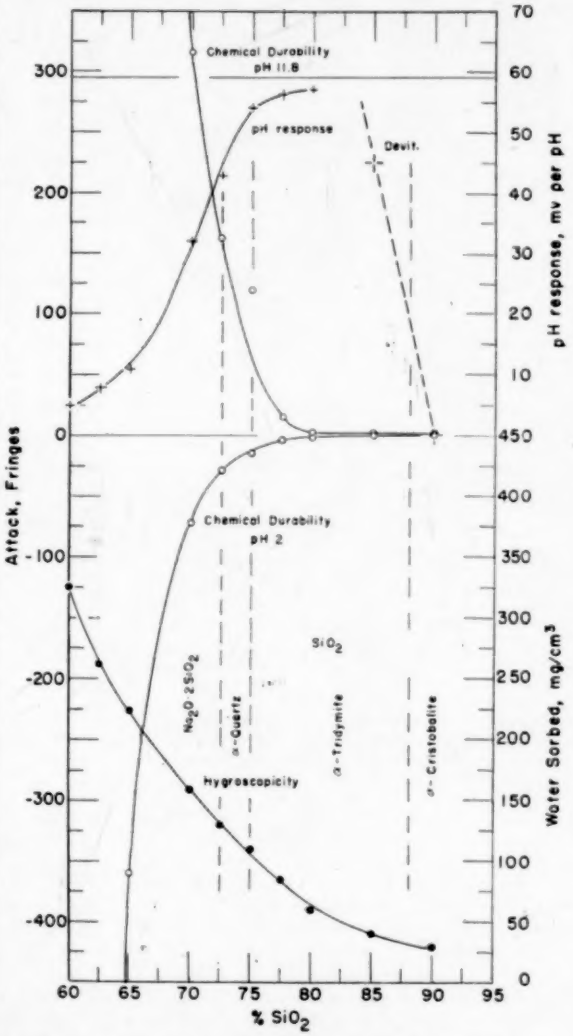

FIGURE 6. *Values for* pH *response, hygroscopicity, and chemical durability at* pH *2 and 11.8 plotted against the percentage of* SiO_2, *for a series of* Na_2O-K_2O-SiO_2 *glasses at 10 percent* K_2O *content.*

UNIVERSITY OF MICHIGAN LIBRARIES

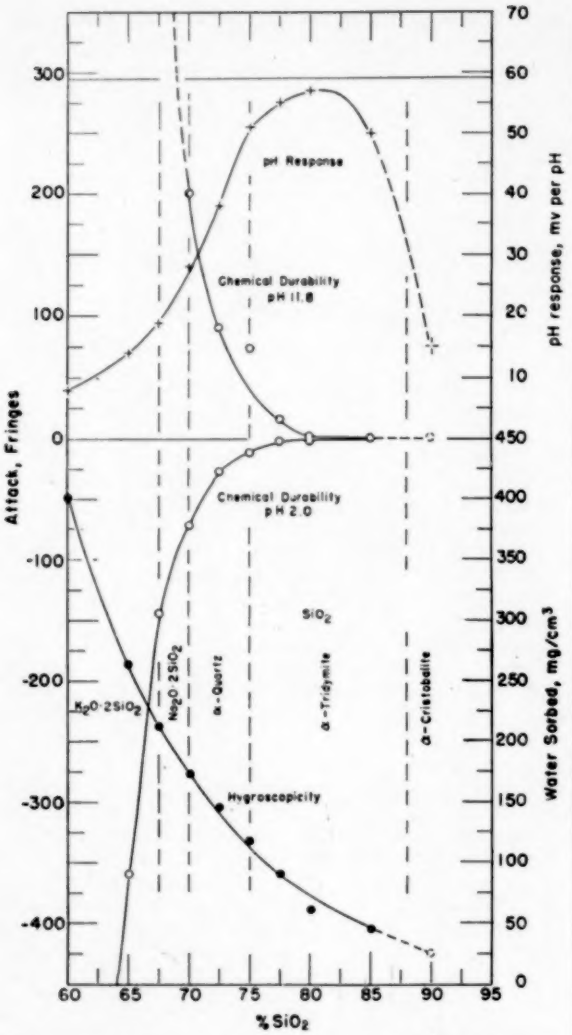

FIGURE 7. *Values for the* pH *response, hygroscopicity, and chemical durability at* pH_2 *and 11.8 plotted against the percentage of* SiO_2 *for a series of* Na_2O-K_2O-SiO_2 *glasses of 10-percent* Na_2O *content.*

4. Summary

An over-all picture of the relation between the hygroscopicity and composition for the Na_2O-K_2O-SiO_2 glasses is presented in the ternary diagram, figure 8. The iso-sorbs indicate the glass compositions of equal hygroscopicity based on the water "sorbed" by powdered specimens after 1-hour exposure to approximately 98 percent relative humidity at 25° C. The glass compositions that produced electrodes having a pH response as high as 56 mv/pH are included in the shaded portion of figure 8. A glance at the chemical durability data for the glasses included in this area show that most of these glasses have durabilities considerably inferior to Corning 015, indicating that the composition range for satisfactory electrodes is considerably more limited than the figure implies. Nevertheless, the same three groups are indicated for the Na_2O-K_2O-SiO_2 glasses that were found for the Na_2O-CaO-SiO_2 and Na_2O-PbO-SiO_2 glasses [6, 7] namely, group A, glasses that are too "dry" for successful electrodes; group B, glasses that produce electrodes that approach the theoretical pH response, and group C, glasses characterized by poor durability, which are too "wet."

The results obtained for the pH response, hygroscopicity, and chemical durability of the Na_2O-K_2O-SiO_2 glasses studied in this investigation add further evidence confirming the validity of the following generalizations: 1. Glasses of very low hygroscopicity yield electrodes whose pH responses fall appreciably below the theoretical 59 mv/pH at 25° C. 2. Electrodes prepared from glasses of poor chemical durability also fail to develop the full theoretical voltage.

The data for chemical durability gave further evidence that swelling of silicate glasses in acid buffers is more universal than generally realized. The Na_2O-SiO_2 and K_2O-SiO_2 glasses of very poor chemical durability were found to exhibit vigorous swelling in the early stages of exposure in the acid buffers. This brought out certain limitations of the interferometer procedure in differentiating between swelling and solution.

Electrodes prepared from those glasses that most nearly approximated the durability and hygroscopicity characteristics of Corning 015 approximated most nearly the theoretical pH response.

The pH response-hygroscopicity curves and the pH response-composition curves appear to reflect some

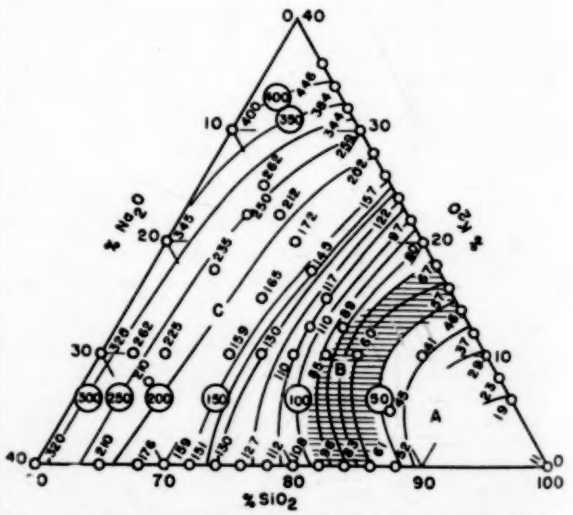

FIGURE 8. *Hygroscopicity of* Na_2O-K_2O-SiO_2 *glasses for 1-hr exposure, showing lines of equal hygroscopicity (iso-sorbs) and the shaded area over which electrodes prepared from these glasses developed as high as 56 mv per* pH.

of the critical compositions of the Na_2O-K_2O-SiO_2 phase equilibrium diagram. Perhaps the most interesting observation of the entire investigation is that the optimum pH response is shown by electrodes prepared from glasses that fall within the composition range in which α-tridymite is reported as the primary phase.

IV. References

[1] M. Dole, Glass electrode (John Wiley & Sons, Inc., New York, N. Y., 1941).

[2] W. S. Hughes, The potential difference between glass and electrolytes in contact with glass, J. Am. Chem. Soc. **44,** 2860 (1922).

[3] F. Haber and Z. Klemensiewicz, On electrical interfacial potentials, Z. physik. Chem. **67,** 385 (1909).

[4] Donald Hubbard, Edgar H. Hamilton, and A. N. Finn, Effect of the solubility of glass on the behavior of the glass electrode, J. Research NBS **22,** 339 (1939) RP1187.

[5] Donald Hubbard, Hygroscopicity of optical glasses as an indicator of serviceability, J. Research NBS **36,** 365 (1946) RP1706.

[6] Donald Hubbard, Given W. Cleek, and Gerald F. Rynders, Electrode function (pH response), hygroscopicity, and chemical durability of Na_2O-CaO-SiO_2 glasses, J. Research NBS **44,** 247 (1950) RP2076.

[7] Donald Hubbard, Mason H. Black, and Gerald F. Rynders, Electrode function (pH response), hygroscopicity, and chemical durability of soda-lead oxide-silica glasses, J. Research NBS **45,** 430 (1950) RP2154.

[8] M. R. Thompson, A metal-connected glass electrode, BS J. Research **9,** 833 (1932) RP 511.

[9] E. Berger, Grundsatzliches uber die chemische angreifbarkeit von glasen I, Glastech, Ber. dent. chem. Ges. **14,** 351 (1936).

[10] H. T. S. Britton, Hydrogen ions I, 3d. ed., 88c, p. 313 (D. Van Nostrand Co., Inc., New York, N. Y., 1943).

[11] Donald Hubbard and Edgar H. Hamilton, Studies of the chemical durability of glass by an interferometer method, J. Research NBS **27,** 143 (1941) RP1409.

[12] Gerald F. Rynders, Oscar H. Grauer, and Donald Hubbard, Electrode function (pH response) of the soda-silica glasses, J. Research NBS **41,** 273 (1948) RP1923.

[13] F. C. Kracek, The system Na_2O-SiO_2, J. Phys. Chem. **34,** 1583 (1930); J. Am. Ceram. Soc. **16,** 491 (1933).

[14] John C. Young, Francis W. Glaze, Conrad A. Faick, and Alfred N. Finn, Density of some soda-potash-silica glasses as a function of the composition, J. Research NBS **22,** 453 (1939) RP1187.

[15] F. C. Kracek, N. L. Bowen, and G. W. Morey, The binary system K_2SiO_3-SiO_2, J. Phys. Chem. **33,** 1857 (1929).

[16] Donald Hubbard, Electrode function (pH response) of potash-silica glasses, J. Research NBS **37,** 223 (1946) RP1743.

[17] F. C. Kracek, The system K_2SiO_3-$Na_2SiO_2SiO_2$, J. Phys. Chem. **36,** 2529 (1932).

WASHINGTON, August 8, 1950.

Journal of Research of the National Bureau of Standards Vol. 46, No. 3, March 1951 Research Paper 2190

Viscosity and Density of Molten Optical Glasses

Leo Shartsis and Sam Spinner

The viscosities and densities of 22 optical glasses, representing all types produced at the National Bureau of Standards, were measured by a counterbalanced-sphere method. The densities agreed with those obtained by a volumeter method, and the viscosities showed good agreement with those obtained with a small rotation viscometer.

Expansivities calulated from density results in the temperature range 1,000° to 1,200° C showed that flints are low, 15 to 22, barium crowns are intermediate, 22 to 37, and borosilicate crowns are high, 34 to 40 (microns/meter)/°C. The expansivities showed a positive correlation with the slope of the viscosity temperature curve.

The superiority of the theoretically derived Faxen correction of Stokes law over that of the empirical Francis formula was established by means of a freely falling sphere apparatus.

I. Introduction

The importance of the viscosity of glass in all phases of its manufacture is widely recognized. Certain useful empirical points such as the annealing temperature, softening temperature, strain point, etc., have been shown to be related to definite viscosities. In producing optical glass at this Bureau it has been found that the temperatures at which the stirring of the different kinds of optical glass is stopped and the pots removed from the furnace correspond to the same viscosity for all glasses. In addition to the practical reasons for studying viscosity, there is also the expectation that viscosity data will help to elucidate the structure of glasses.

The density of molten glasses as a function of temperature has not been investigated to any great extent. Expansivity is of interest to workers in glass and may be calculated from the change of density with temperature. As in the case of other fundamental properties, it may be expected that density studies will aid in determining the structure of glasses. In addition to its intrinsic interest, density data are necessary in the calculation of certain other properties, such as kinematic viscosity, some methods of measuring surface tension, etc.

II. Glasses Tested

The optical glasses tested were those regularly produced by the Bureau glass plant. Table 1 gives the compositions as computed from the proportions of the raw materials in the batch. The first column identifies the glass according to itts optical type, refractive index, and Abbe[1] value. Thus, *F* 5795/410 means a flint glass with a refractive index N_D= 1.5795, and Abbe value ν=41.0.

Although these compositions are considered fairly reliable because each pot holds from 900 to 1,500 lb. of glass, the computations neglect small amounts of material that are dissolved from the pot. Pot attack introduces chiefly silica and alumina into the glass, the amounts varying with the corrosiveness of the glass. The practice of adding cullet (broken glass from previous melts of the same composition) also introduces variations in composition. An all-cullet melt usually has a measurably higher viscosity along with lower density and refractive index than an all-batch melt because the former has dissolved more of the pot materials.

[1] The Abbe value $\nu=(N_D-1)/(N_F-N_C)$, where N_D is the refractive index for the sodium *D* line, and N_F and N_C are refractive indices for the hydrogen *F* and *C* lines, respectively.

III. Measurement of Viscosity

1. Sphere Method

(a) Apparatus

Figure 1 shows a diagrammatic view of the apparatus. A platinum sphere 1.5 cm in diameter is suspended by a thin platinum wire fastened by a thin chain to the center of the left-hand pan of an analyt-

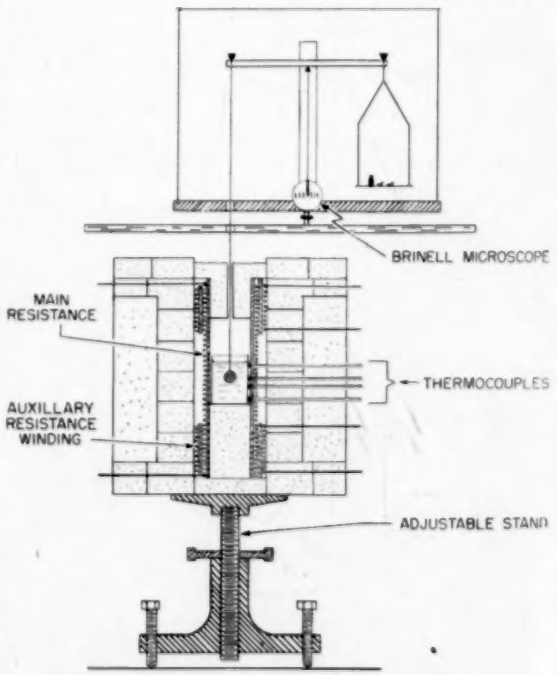

FIGURE 1. *Restrained sphere apparatus.*

TABLE 1. *Compositions of optical glasses, computed from batch*

Glass [a]	Melt number	Component oxides (weight percent)									Other oxides	Cullet
		SiO_2	PbO	BaO	B_2O_3	Na_2O	K_2O	ZnO	As_2O_3	Sb_2O_3		
												lb
F 5795/410	5613	53.1	35.5	0.7	.....	0.4	9.5	.....	0.2	0.6	.....	300
	7133	53.1	35.5	0.6	.....	.4	9.6	.....	.3	.5	.....	300
F 617/366	5618	45.6	43.1	.....	.....	5.0	5.8	.....	.5	.....	.....	300
	7045	45.6	43.1	.....	.....	4.7	6.1	.....	.5	.....	.....	775
F 620/362	5573	45.6	45.2	.....	.....	3.5	5.2	.....	.5	.....	.....	300
	5747											300
	8197	45.6	45.2	.....	.....	3.0	5.7	.....	.5	.....	.....	300
	4438	41.2	51.2	.....	.....	0.7	6.4	.....	.5	.....	.....	300
F 649/338	5943	41.2	51.1	.....	.....	0.7	6.5	.....	.5	.....	.....	300
	8187											300
	8189											300
F 666/324	7686	39.3	54.4	.....	.....	.....	6.0	.....	.3	.....	.....	300
F 689/309	7382	37.0	58.1	.....	.....	.....	4.6	.....	.3	.....	.....	None
F 720/293	7728	34.1	62.4	.....	.....	.....	3.2	.....	.3	.....	.....	All
F 754/277	8001	31.2	66.2	.....	.....	.....	2.3	.....	.3	.....	.....	300
F 923/209	8162	20.3	79.0	.....	.....	.....	0.4	.....	.3	.....	.....	None
CF 529/516	8217	65.4	10.0	0.2	.....	13.2	5.6	3.6	.2	1.8	.....	165
BaC 541/509	8072	58.8	.....	19.9	3.8	2.8	10.3	4.1	.3	.....	.....	300
BaC 5725/574	3247	49.7	.....	31.3	3.6	0.4	7.2	7.2	.2	0.4	.....	None
	3722	49.7	.....	30.8	3.6	.4	7.7	7.2	.2	.4	.....	300
	4581	45.2	.....	28.1	6.2	1.4	7.6	7.5	.3	.7	Al_2O_3 3.0	100
BaC 574/577	8171	47.4	.....	30.0	4.9	0.9	7.0	7.5	.3	.5	Al_2O_3 1.5	300
BaC 611/588	5666	38.3	0.2	42.8	10.7	.....	.....	.....	.4	.2	Al_2O_3 2.4, CaO 5.0	None
	7922	38.3	.2	42.8	10.7	.....	.....	.....	.4	.2	Al_2O_3 2.9, CaO 4.5	475
BaC 6109/572	8250	38.2	.2	42.8	6.7	.....	.....	4.2	.4	.2	Al_2O_3 4.9, CaO 2.3	None
BaC 617/550	5815	37.3	1.4	44.8	4.4	.2	0.4	5.6	.3	.7	Al_2O_3 4.9	300
	6903											
BaC 620/600	8085	37.8	.....	44.2	11.4	.....	.....	.....	.3	.2	CaO 3.6, BeO 2.3, ZrO_2 0.2	400
BaF 584/460	7631	49.8	18.8	13.4	.....	1.6	8.2	7.8	.5	.....	.....	200
BaF 588/534	3800	45.8	5.6	28.0	4.4	2.3	6.0	7.5	.4	.....	.....	200
BaF 604/435	3354	45.7	23.3	14.3	.....	.....	8.2	8.1	.4	.....	.....	None
	3849											200
BaF 605/435	7660	45.7	24.3	13.6	.....	.....	7.9	8.1	.4	.....	.....	200
LC 512/605	6980	71.9	.....	.....	5.0	14.7	5.0	.....	.....	1.2	CaO 2.2	100
LC 523/586	5718	70.2	.....	.....	1.5	14.0	2.5	.....	.....	1.2	CaO 9.4, Cl 0.7, SO_3 0.5	100
	6988											100
BSC 511/635	5407	68.8	.....	.....	8.5	7.8	14.7	.....	.2	.....	.....	100
	7656											100
BSC 517/645	8097	66.3	.....	.....	12.5	7.5	12.0	1.2	.5	.....	.....	300
	8223											550
	3703	66.4	.....	.....	12.4	8.4	11.8	0.5	.5	.....	.....	150
	5371	66.6	.....	.....	12.2	8.4	11.8	.5	.5	.....	.....	550
BSC 540/645	8244	69.0	.....	3.0	11.0	9.2	7.1	.....	.5	.....	Al_2O_3 0.2	300
	6471	63.4	.....	.....	13.0	.....	6.2	.....	.4	.....	BeO 2.0, SrO 10.0, Li_2O 5.0	None

[a] F = flint, BaC = barium crown, LC = light crown, BaF = barium flint, BSC = borosilicate crown, CF = crown flint.

ical balance. Upward or downward motion of the ball in the liquid is produced by changing the weights on the right-hand pan of the balance. The velocity of the ball is indicated by the motion of the balance pointer, which is observed through a Brinell microscope. The sample of glass is in the cylindrical platinum viscosity crucible (2 in. in diameter and 3 in. high).

The furnace (fig. 1) is supported on an adjustable stand by means of which it can be moved vertically. Over the ends of the main platinum alloy resistance winding there are two smaller separately controlled auxiliary windings to control vertical thermal gradients. Temperatures are measured by means of three thermocouples (Pt vs Pt-10 percent Rh), which can be pushed into contact with the crucible, which contains the molten glass. Another thermocouple placed near the center of the crucible is connected to a potentiometer-type controller, by means of which the temperature is held constant during a determination. The power to the furnace is supplied through a 3 KVA constant voltage transformer. A water-cooled copper shield protects the ba ance from the heat of the furnace.

The apparatus was calibrated with a liquid of known viscosity.

(b) Measurement of Viscosity of Calibrating Liquid

Preliminary studies of the method and calibrations of the apparatus were made with NBS Standard Oil P used for calibrating viscometers. As the viscosity values available did not cover so large a range as was desired, additional viscosity values at other temperatures were obtained with a freely falling sphere apparatus.

Figure 2 is a diagrammatic sketch of this apparatus. It consists of two concentric glass tubes, each about 24 in. long with liquid from a thermostatically controlled bath circulated through the annular space between them. A thermometer inserted through a hole in the upper rubber spacer measures the temperature of the thermostatically controlled liquid. The central tube is a 100-ml burette with the stopcock portion removed and is closed at both ends by rubber stoppers. A short piece of 6-mm glass tubing with a piece of rubber tubing over the lower end projects through a hole in the upper stopper. This piece of rubber tubing is of small bore and sufficiently flexible to hold different sizes of ball bearings above the test liquids until they are released by pushing down on a glass rod inside the glass tubing.

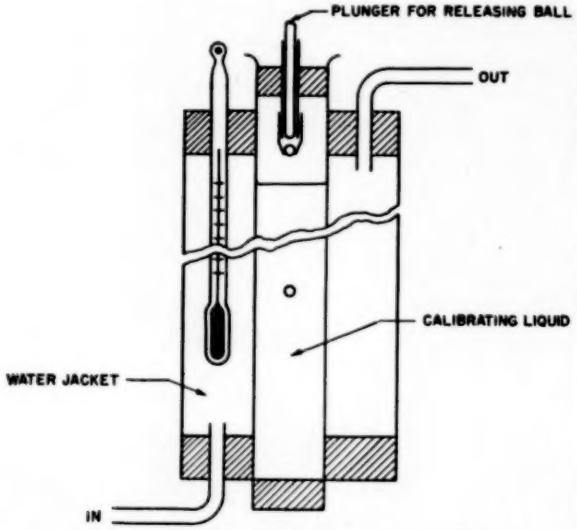

FIGURE 2. *Freely falling sphere apparatus.*

The inside diameter of the burette was measured at several places by means of a cathetometer microscope while the burette was immersed in a liquid of index 1.51 contained in a glass vessel with plane parallel walls. The average of nine such measurements was 1.489 cm with a standard deviation of 0.3 percent. The distance between even numbered milliliter marks on the burette was likewise measured at many different places. The average obtained for 21 measurements was 0.5831 cm/ml with a standard deviation of 0.3 percent.

The spheres used were ball bearings, some of steel and some of brass. Each one was measured with a micrometer to approximately 0.0001 in. and weighed to 0.1 mg on an analytical balance. Most of the balls were $\frac{1}{8}$, $\frac{3}{16}$, and $\frac{1}{4}$ in. in diameter. A few measurements were made with $\frac{5}{16}$- and $\frac{3}{8}$-in. balls.

Each ball was held in the holder above the liquid for a length of time considered sufficient to allow it to reach the temperature of the test liquid. Velocities were measured after the ball had traveled a considerable distance through the liquid, usually 6 cm or more.

For the calculation of viscosity the usual form of Stokes law was modified as follows:

$$F=(W-\tfrac{1}{6}\pi d^3\rho)g, \tag{1}$$

where

F=driving force
W=weight of the sphere in grams
d=diameter of sphere in centimeters
ρ=density of the test liquid in grams per cubic centimeter
g=gravitational constant, 980 dynes/cm.

When constant velocity is reached, the resisting force, according to Stokes, is

$$R=3\pi\eta_s dv, \tag{2}$$

where

R=resisting force
η_s=viscosity in poises, according to Stokes
v=velocity in centimeters per second.

At equilibrium, $F=R$ from which it can be shown that

$$\eta_s=\frac{(w-1/6\pi d^3\rho)g}{3\pi dv}=\frac{(W-1/6\pi d^3\rho)gt}{3\pi d(0.5831N)}, \tag{3}$$

where

t=time in seconds
N=number of milliliter divisions traversed in time, t.

As Stokes law is accurate only for a sphere in a medium of infinitely large extent, a correction for the boundary conditions is necessary. Several such correction formulas have been proposed and used. In this study it was considered desirable to compare the Faxen [1] [2] correction with the one proposed by Francis [2]. The Faxen correction is

$$F_a=1-2.104d/D+2.09\left(\frac{d}{D}\right)^3-0.95\left(\frac{d}{D}\right)^5, \tag{4}$$

where

d=diameter of sphere
D=diameter of test vessel.

The Francis correction F_r is given by the equation

$$F_r=\left(1-\frac{d}{D}\right)^{2.25}.$$

After each correction was calculated it was multiplied by the value obtained from Stokes law. Thus

$$\eta_{F_a}=\eta_s F_a,$$

$$\eta_{F_r}=\eta_s F_r.$$

Table 2 gives the results obtained. To compare the two corrections, the data have been classified into groups of approximately equal temperature, although there was some temperature drift during a set of determinations. The densities of the test liquid were measured by the Engine and Lubrication Section of this Bureau with a picnometer method.

[2] Figures in brackets indicate the literature references at the end of this paper.

TABLE 2. *Comparison of viscosity correction formulas*

Temperature	Ball diameter, d	Weight	Number of divisions	Time	Viscosity by—		
					Stokes, η_s	Faxen, η_{Fa}	Francis, η_{Fr}
°C	cm	g		sec	Poises	Poises	Poises
33.40	0.3183	0.1323	70	613.8	576	328	335
33.40	.4755	.4394	70	402.8	840	330	354
33.36	.6345	1.0430	70	354.8	1,316	331	377
33.34	.4755	.4389	70	399.8	833	327	351
33.31	.3190	.1330	70	616.4	580	330	337
Avg. 33.36	---	---	---	-----	----	329	351
Standard deviations	---	---	---	-----	----	1.5	15.1
Capillary flow	---	---	---	-----	----	328	-----
29.63	.6345	1.0430	52	370.8	1,719	433	493
29.60	.6345	1.0430	52	367.8	1,705	429	489
29.60	.4755	.4394	70	546.6	1,140	448	480
29.55	.3170	.1305	72	865.7	782	447	456
29.50	.6365	1.1873	70	422.9	1,806	452	515
29.45	.6345	1.0430	70	490.4	1,819	458	522
29.42	.4755	.4395	72	570.6	1,157	455	487
29.38	.3185	.1326	72	880.3	804	458	468
29.40	.4750	.4900	70	489.7	1,158	456	488
Avg. 29.50	---	---	---	-----	----	448	489
Standard deviations	---	---	---	-----	----	10.1	19.4
Capillary flow	---	---	---	-----	----	442	-----
26.61	0.3167	0.1305	72	1,114.8	1,009	577	589
26.58	.3162	.1302	72	1,112.8	1,007	577	588
26.71	.3162	.1303	66	1041.8	1,029	589	601
26.83	.4752	.4386	76	764.2	1,466	577	617
26.90	.6345	1.0430	70	629.0	2,333	587	669
27.18	.3162	.1298	70	1,049.0	973	557	569
27.27	.3180	.1319	70	1,035.0	969	553	564
27.35	.4752	.4388	70	678.5	1,414	556	596
27.40	6345	1.0430	70	582.4	2.160	544	619
Avg. 26.98	---	---	---	-----	----	569	601
Standard deviations	---	---	---	-----	----	15	30
Capillary flow	---	---	---	-----	----	570	-----
11.95	0.3167	0.1300	67	4,356.2	4,214	2,411	2,460
11.95	.4755	.4390	68	2,831.4	6,073	2,387	2,556
11.99	.6345	1.0430	80	2,807.4	9,110	2,294	2,612
11.95	.4742	.4925	78	2,867.0	6,119	2,413	2,582
12.00	.7916	2.0196	70	2,727.2	15,695	2,436	2,849
12.06	9515	3.4812	66	3,105.4	27,110	2,695	2,726
Avg. 11.98	---	---	---	-----	----	2,439	2,631
Standard deviations	---	---	---	-----	----	123	125
19.20	0.3175	0.1324	88	2,772.8	2,079	1,188	1,212
19.06	.4755	.4394	76	1,558.6	2,994	1,177	1,260
19.06	.6345	1.0430	76	1,338.8	4,573	1,151	1,311
19.06	.7915	2.0186	70	1,412.6	8,125	1,261	1,474
19.12	.3167	.1308	68	2,164.5	2,079	1,189	1,214
Avg. 19.10	---	---	---	-----	----	1,193	1,294
Standard deviations	---	---	---	-----	----	37	116
11.78	0.6345	1.0430	70	2,679.5	9,937	2,502	2,849
11.80	.7920	2.0188	72	3,069.1	17,149	2,656	3,107
11.82	.6363	1.1834	70	2,274.6	9,681	2,425	2,762
11.82	.4755	.4394	70	2,996.3	6,248	2,456	2,630
11.82	.4755	.4940	74	2,790.4	6,276	2,467	2,642
11.82	.3177	.1493	70	4,044.1	4,355	2,486	2,538
Avg. 11.81	---	---	---	-----	----	2,499	2,755
Standard deviations	---	---	---	-----	----	74	176

Inspection of the data in table 2 shows that the viscosities calculated with the Faxen correction are on the average lower than those obtained, using the Francis correction. The reproducibility of the Faxen results is better, as judged by the size of the standard deviations. Viscosity data supplied by the Engine and Lubrication Section, using a capillary flow method, are in better agreement with the Faxen results than with the Francis values. The Francis values have a distinct tendency to become larger as the ball size increases. For these reasons, only the results obtained with the Faxen correction received any further consideration.

An equation was fitted by the method of least squares to the Faxen data shown in table 2, as well as to other data obtained with the freely falling sphere method at lower temperatures and with the capillary flow results at temperatures between 30° and 60°C. The equation took the following form [3]

$$L=218.98+1.3914\ (t-30)+0.00163\ (t-30)^2, \quad (6)$$

where

t = °C
L = 1301/log 2000 η.

(c) Calibration

In making calibrations, the furnace as replaced by a thermostatically controlled bath, and the cylindrical platinum viscosity crucible was placed in a liquid-tight brass container (fig. 3).

When the apparatus reached the desired temperatures, weights were placed on the right-hand pan of the balance, and the time required for the balance pointer to move a selected number of scale divisions was measured with a stop watch. At low viscosities where the velocity was high, a large test distance was selected in order to get as accurate a time measurement as possible. Furthermore, at low viscosities the balance pointer was brought a considerable distance away from the region where the velocity was to be measured, in order to allow the sphere to reach an equilibrium velocity before approaching the test distance. At high viscosities where the velocity of

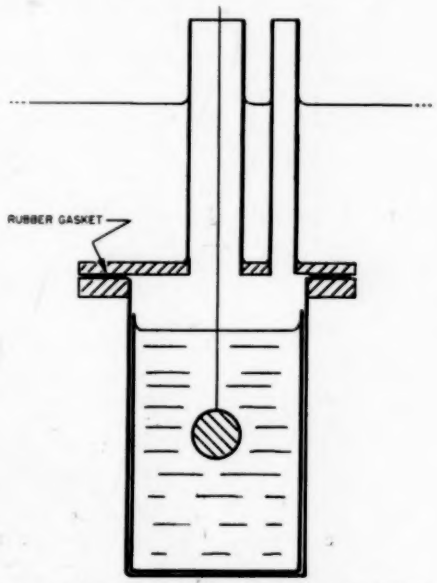

FIGURE 3. *Liquid-tight container for use in calibrations.*

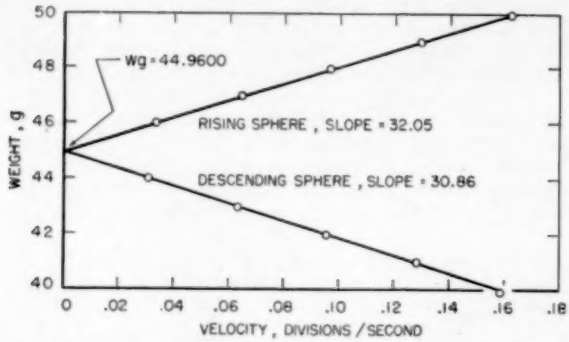

FIGURE 4. *Effect of weight on velocity of counterbalanced platinum sphere in calibrating liquid at −7.88° C.*

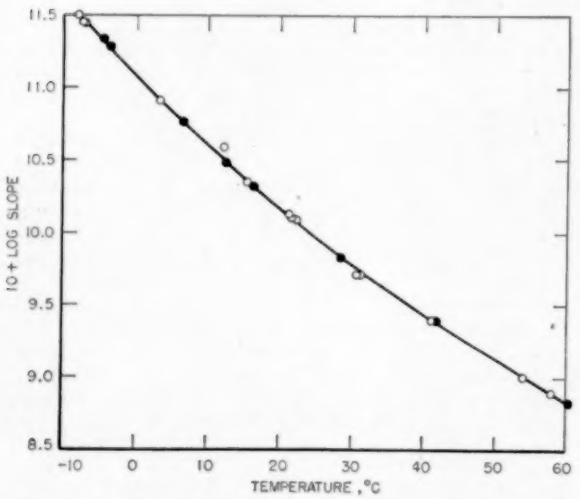

FIGURE 5. *Logarithm of the average slopes of the weight-versus-velocity curves of a series of calibrations plotted against the Centigrade temperature.*

Open circles represent old data, whereas filled circles represent the latest data.

the sphere was low the selected test distance was small, and the starting position of the pointer was closer to the measuring region in order to save time. In all cases, however, the zero of the balance scale divided the test distance into halves. The weights were selected to give a range of velocities in both directions.

Figure 4 shows in graphical form the effect of different weights of the sphere. At weights greater than the weight of the sphere in the test liquid the motion is upward, at lower weights the motion is downward. The load versus velocity curve is a straight line. The slope of the rising line is usually greater than that of the descending line. The difference in the slopes of the two curves is attributed to the influence of the liquid adhering to the wire. In practice the average slope was used in making calculations.

The effect of temperature on the slope of the load-velocity curves was determined over the temperature range −5 to +60° C. Figure 5 shows a plot of the results obtained. The filled circles represent the latest data, whereas the circles represent the data obtained in a similar series of experiments about a year before. The agreement indicates that the results were not significantly affected by the wear to which the crucible and sphere were subjected during the course of many measurements made during that year.

Previous experience had shown that a plot of log viscosity versus log slope could be represented by a straight line. Figure 6 shows a plot of data from a previous set of calibrations to illustrate this point. A straight line fitted by the method of least squares to the data obtained in the last set of calibrations gave the following equation

$$\text{Log } \eta = 1.0266\ (10 + \log S) - 7.4070, \qquad (7)$$

upon which all the viscosity results reported in this study are based. S is the slope of the load versus velocity curve.

If it is assumed that $\eta = KS$, where K is an instrumental constant and K is solved for, it will be noted that K is not constant but increases with viscosity. The probability is that the friction and inertia of the balance is at least partially responsible for the increase of K with viscosity. Part of the applied force is needed to move the balance; therefore, the sphere moves more slowly than if the whole force were acting on it. This effect results in a steeper slope than would otherwise be the case and K must be correspondingly smaller. As the retarding effect is a larger fraction of the total force at low viscosities, where low loads are used, the constant is smaller at low viscosities. The increase of calibration constant

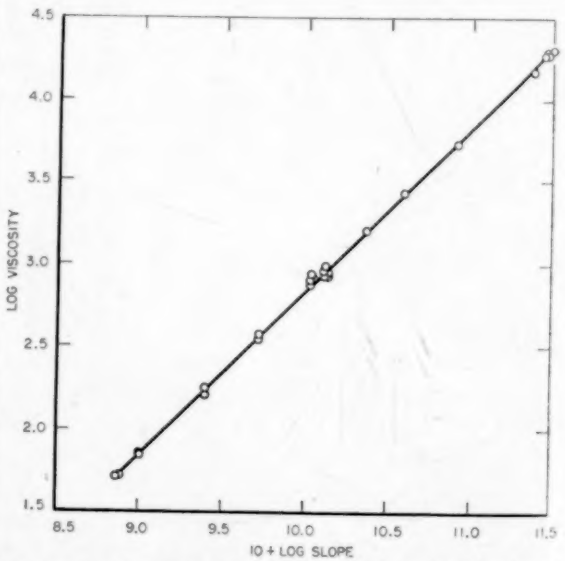

FIGURE 6. *Logarithm of the viscosity of the calibrating liquid plotted against the logarithm of the average slopes of the weight-versus-velocity curves of a series of calibrations.*

was noted by other workers using the restrained falling sphere method, one of whom [4] investigated the possibility that his glass was showing non-Newtonian behavior.

Additional evidence that friction and inertia are the causes of the change in K with increasing viscosity is to be found in the experience of investigators who worked with large balances [5]. These workers used balances with long beams in order to minimize side motion of the sphere. Their results show a larger change of K with viscosity than was found in the present study.

It is interesting to calculate the value of K by assuming Stokes law and the Faxen correction to apply. This calculation neglects the effect of the small platinum ring that is welded to the sphere, and to that part of the supporting wire that is immersed in the test liquid. As the neglected portions introduce a viscous traction that is not considered, the calculated K should be higher than the observed one.

Thus according to Faxen's modification of Stokes law

$$\eta = \eta_s F_a = \frac{(W - W_g) g F_a}{3\pi d V_c}, \tag{8}$$

where

W = weight of sphere in air
W_g = weight of sphere in test liquid
V_c = velocity in centimeters per second.

As $$S = \frac{W - W_g}{V_n}$$

where

V_n = velocity in balance divisions per sec, and $K = \eta/S$,

$$K = \frac{g F_a V_n}{3\pi d V_c}. \tag{9}$$

By measurement with a cathetometer microscope it was found that the movement of the balance pointer across six scale divisions was equal to a vertical travel of the ball of 2.3 mm. Thus $V_N = 26.09\ V_c$, and

$$K = \frac{26.09 g F_a}{3\pi d}. \tag{10}$$

The inside diameter of the viscosity crucible was 5.2 cm and the diameter of the sphere (d) 1.5 cm. Thus $d/D = 0.288$, $F_a = 0.4586$, and $g = 980$.

These values substituted in eq 10 yield a value of 825. The observed constant as computed from eq 7 varied from about 670 to about 800 over the range of viscosities measured during the calibrations.

(d) Procedure With Glasses

The test glasses were moulded into solid cylinders designed to fill the crucible with molten glass to a depth of 3 in. The moulded glass blank was placed in the platinum crucible and slowly heated to about 500° C in an electrically heated laboratory muffle furnace. Then it was quickly transferred to the viscosity furnace, which was previously heated to about 1,300° C. The ball was then lowered to a position above the molten glass. The furnace was raised slowly by means of the adjustable stand until the bottom of the sphere touched the molten glass. This position could be readily observed by first imparting to the ball a pendulum-like motion, which was quickly damped when the ball touched the surface of the viscous glass melt. The furnace was then raised 1.5 in. to allow sufficient immersion for the sphere.

Measurements of load versus velocity were made at 100-deg C intervals, decreasing the temperature until the glass was too viscous to allow the ball to move under reasonable loads and convenient times. Each time the temperature of the furnace was decreased 100 deg C, the furnace was raised 0.74 mm to compensate for the change in the relative position of the sphere caused by shrinkages of the furnace, the glass in the crucible, and the supporting platinum wire. The change in the level of the glass in the crucible was measured in a separate experiment by means of a platinum contact rod mounted on a scale outside the furnace.

2. Rotational Viscometer Method

Prior to work with the sphere method, some viscosity measurements were made with a small rotation viscometer that has already been described in the literature [6]. This apparatus was limited to measurements below 1,100° C.

IV. Measurement of Density

1. Sphere Method

By extrapolating the load-velocity lines (fig. 4) back to zero velocity, W_g, the weight of the sphere in the test liquid can be obtained. The average of the two values obtained was used. In general, after the load-velocity points were plotted straight lines were drawn by inspection. Two well-fitting points, covering as large an interval of load as the data permitted, were selected from each line. Calculations of S and W_g were made from the selected points as follows: Let W_1 and W_2 be the weights at the two selected points and V_1 and V_2 be the corresponding velocities.

Then

$$S = \frac{W_2 - W_g}{V_2} = \frac{W_1 - W_g}{V_1},$$

from which

$$W_g = \frac{W_1 V_2 - W_2 V_1}{V_2 - V_1}. \tag{11}$$

The density corrected for the effect of surface tension on the suspending wire was computed from the following equation

$$\rho = \frac{W - (W_g - 0.46\pi d\sigma/g)}{V_0 (1 + 3\alpha t)}, \tag{12}$$

where

ρ = density of the liquid in grams per cubic centimeter,

W = weight of platinum sphere plus that portion of the suspending wire immersed in the test liquid,

d = diameter of suspending wire in centimeters,

σ = surface tension of the test liquid (known from previous work [7]),

α = linear thermal expansion of platinum,

V_0 = volume of sphere at room temperature,

0.46 = Wilhelmy correction for the effect of surface tension on thin wires, [8] and

t = temperature in deg C.

The volume of the sphere plus that portion of the suspending wire immersed in the test liquid was determined by measuring the buoyant effect of distilled water,

$$V_0 = \frac{W - \left(W_s - \frac{0.46\pi d\sigma_0}{g}\right)}{\rho_0} \qquad (13)$$

where ρ_0 is the density of distilled water at the temperature at which V_0 was determined.

2. The Volumeter Method

(a) Principle of Method

Early in 1943 a project to measure the density of optical glasses at high temperatures with a volumeter method was initiated by B. Fonoroff. This method enables the calculation of the volume of a given weight of glass by determining the position of the surface of a melt in a calibrated crucible. The position of the surface is obtained by locating the top of the crucible with reference to a scale outside the furnace, finding the position of the glass surface on the same scale and taking the difference as a measure of the volume. This method avoids errors due to expansion of the furnace and the crucible supports. Thermal expansion of that part of the crucible above the glass level is compensated by making the measurements with a rod of the same material as the crucible and in thermal equilibrium with it.

(b) Apparatus

A diagram of the apparatus is shown in figure 7. The furnace was wound with three separate coils of platinum alloy resistance wire. A uniform temperature throughout a large portion of the furnace could be obtained by adjusting the current in each coil. Three noble-metal thermocouples (indicated by crosses in fig. 7) were used to measure the temperature.

The long-necked platinum crucible (shaped like a volumetric flask) has a flat horizontal lip at the mouth. The crucible could be raised while in the furnace by means of a sillimanite tube (not shown in fig. 7), which extended downward through a hole in the center of the furnace floor.

The depth gage consisted of an upright steel rod square in cross section and graduated in millimeters,

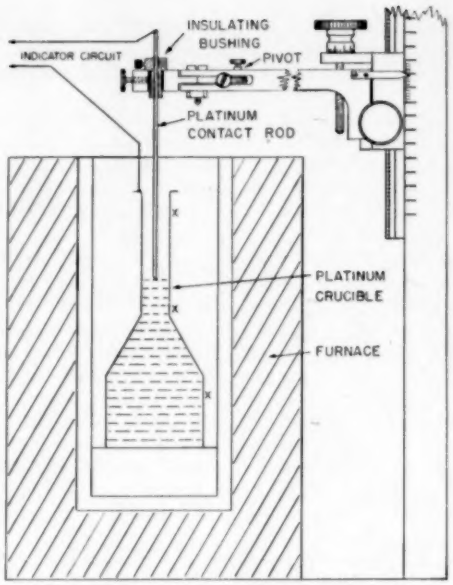

FIGURE 7. *Volumeter apparatus.*
Small crosses mark location of thermocouples.

and a movable arm that supported a rod of the same material as the volumeter. The contact could be turned through a small horizontal arc by means of a pivot located near the end of the movable arm. This enabled one to set the rod over the lip of the crucible or over its center without moving the crucible or the depth gage. The arm could be moved vertically by means of a rack and pinion arrangement. Fine adjustments of the position of the arm were made with a micrometer screw. The head of the screw was graduated into 50 divisions, and, as two revolutions of the screw corresponded to a vertical motion of 1 mm, the smallest measurable motion was 0.01 mm. The rod and crucible were connected in series with a neon glowlamp and a source of current, so that the appearance of a light indicated contact.

(c) Calibration

Before each determination of the expansion of a glass sample the volumeter was calibrated at room temperature. The crucible was filled to within 1 cm of the top with a dilute electrolyte solution of known density and then weighed. The position of the surface of the liquid was determined with the depth gage. The movable arm was then raised and contact made with the lip of the crucible. The distance between the liquid surface and the lip corresponded to a definite volume at room temperature. About 1 ml of solution was removed with a pipette, the position of the liquid surface with respect to the lip redetermined, and the volumeter reweighed. These operations were repeated until the level of the solution was at the base of the neck of the crucible. From the known density of the weights of the solution, the

volumes corresponding to the various depths of the liquid surface were calculated. As the neck of the crucible was found to be very uniform in diameter, a calibration chart was made that showed volume of the liquid corresponding to any depth in the crucible.

(d) Procedure

Samples of optically homogeneous glass were crushed to conveniently sized pieces in a steel mortar. A magnet was passed over the glass to remove magnetic particles and the sample was then washed and dried.

The crucible, filled with the crushed glass, was weighed and lowered into the furnace, which had previously been heated to 1,400° C. When the glass had melted the crucible was raised until the lip was just below the top of the furnace, and additional portions of glass were cautiously added from a weighing bottle by means of a platinum spatula. Several such additions were made until the glass level was a few centimeters from the top of the crucible. The melt was then stirred with a platinum wire to remove bubbles. The amount of glass removed by this process was determined by weighing the rod before and after stirring.

The temperature was lowered at a rate of 50° C/hour, depth readings being made at half-hour intervals. As the lip measurement changed relatively little with temperature, the measuring rod was kept just above it most of the time and frequent readings were taken. When the time approached for ascertaining the depth of the glass, the rod was swiveled into position over the center of the crucible and lowered to a position very close to the surface of the glass. Temperature readings were then made, contact made with the glass, and the temperature again measured. Then the rod was raised, swiveled over the lip, about 2 minutes allowed for temperature equilibrium, and the height of the lip ascertained again. The two lip readings were averaged, as were the temperature readings.

Measurements were made during continuous cooling until such low temperatures were reached (approximately 700° C) that consistent measurements were not obtained. The temperature was then raised in 25-deg steps, holding at each step until concordant depth readings were obtained.

The volume corresponding to a given depth was read from the calibration chart. This was the volume at the temperature of calibration and was adjusted to the temperature of test by the use of the following formula

$$V_t = V_0(1+\alpha t+\beta t^2),$$

where

V_t = volume at temperature t° C,

V_0 = volume at 0° C

$\alpha = 2.4\times10^{-5}$

$\beta = 6.0\times10^{-9}$.

[1] The constants α and β were calculated from linear expansion data obtained from the Thermal Expansion Section of this Bureau.

V. Viscosity Results

1. Sphere Viscometer Data

The viscosities obtained with the restrained sphere method are given in table 3. In the glass industry it is common practice to compare viscosities in terms of the temperature required to attain a given viscosity. Table 4 presents the experimental results in this form. Smooth curves were drawn through the points representing log viscosity versus temperature attained in each determination. The temperatures corresponding to the selected viscosities were then estimated from this curve. A comparison of reproducibility in terms of temperature at a given viscosity is thus made available in table 4. Beneath each average is the result obtained by estimation from a smooth curve drawn through all the data on that glass when more than one set of observations was available. The two sets of curves and the estimates derived from them were prepared by different investigators.

TABLE 3. *Viscosity of optical glasses—sphere method*

F = flint; BaC = barium crown; LC = light crown; BaF = barium flint; BSC = borosilicate crown; BF = crown flint

T	Log η	T	Log η	T	Log η
°C		°C		°C	
F5795/410	7133	F649/338	8187	F689/309	7382
1,298	2.526	1,310	1.812	985	3.153
1,200	2.927	1,200	2.300	883	3.742
1,100	3.388	1,100	2.699	802	4.556
999	4.000	1,000	3.247	760	5.060
897	4.755	897	3.869	1,305	1.783
805	5.720	796	4.827	1,150	2.361
1,293	2.528			922	3.530
1,202	2.940	F649/338	8189		
1,190	3.417			F720/293	7728
1,003	4.003	1,290	1.961		
907	4.707	1,200	2.306	1,311	1.429
804	5.698	1,099	2.736	1,204	1.900
1,288	2.570	999	3.241	1,104	2.277
1,198	2.967	900	3.902	1,000	2.785
1,095	3.437	801	4.771	895	3.461
991	4.052	711	5.833	800	4.278
895	4.764			698	5.600
		F666/324	7686	1,296	1.608
F617/366	7045			1,198	1.917
		1,308	1.828	1,099	2.287
1,332	1.851	1,210	2.228	1,000	2.765
1,214	2.234	1,103	2.670	905	3.366
1,099	2.535	999	3.215	804	4.235
1,000	3.062	897	3.927	704	5.506
898	3.665	803	4.806		
795	4.478	740	5.550	F754/277	8001
744	5.076	1,307	1.885		
1,297	1.904	1,199	2.250	1,305	1.249
1,203	2.171	1,099	2.692	1,198	1.600
1,100	2.574	999	3.177	1,103	1.985
998	3.048	907	3.786	1,000	2.436
900	3.638	801	4.786	900	3.056
802	4.407	750	5.399	800	3.845
751	4.950			697	5.132
		F689/309	7382	1,298	1.280
F620/362	8197			1,199	1.610
		1,305	1.716	1,100	1.985
1,300	2.019	1,204	2.148	1,000	2.432
1,200	2.320	1,103	2.533	900	3.012
1,101	2.779	1,000	3.000	800	3.828
1,000	3.294	900	3.713	690	5.178
900	3.939	798	4.583		
803	4.734	734	5.444	F923/209	8162
750	5.278	1,288	1.816		
1,296	1.990	1,190	2.166	800	1.750
1,203	2.347	1,088	2.612	702	2.654
1,103	2.770				
999	3.285				
902	3.900				
804	4.750				

TABLE 3.—*Viscosity of optical glasses—sphere method*—Con.

T	Log η
°C	
CF529/516	8217
1,306	2.275
1,200	2.636
1,099	3.102
1,000	3.621
900	4.260
802	5.120
1,303	2.239
1,208	2.627
1,103	3.090
995	3.651
905	4.221
801	5.125
BaC541/599	8072
1,298	2.320
1,202	2.707
1,100	3.270
991	3.989
897	4.947
850	5.568
1,304	2.326
1,203	2.728
1,100	3.260
998	4.013
898	4.939
844	5.595
BaC574/577	8171
1,296	1.956
1,198	2.483
1,100	3.087
990	3.926
892	5.034
1,300	1.995
1,200	2.480
1,101	3.082
996	3.854
886	5.100
843	5.803
BaC5725/574	4581
1,326	1.838
1,250	2.177
1,200	2.396
1,097	2.967
996	3.724
895	4.772
BaC611/588	7922
1,300	1.976
1,203	2.487
1,101	3.055
998	3.856
897	4.980
818	6.148
1,306	1.993
1,202	2.457
1,100	3.037
1,099	3.815
998	4.798
800	6.376
BaC6109/572	8250
1,297	1.751
1,196	2.207
1,099	2.816
1,002	3.680
902	5.009
1,297	1.714
1,198	2.209
1,100	2.830
1,000	3.739
900	5.094
829	6.278

T	Log η
°C	
BaC617/550	6003
1,304	1.877
1,198	2.324
1,096	2.992
1,005	3.719
1,003	3.748
895	5.112
BaC620/600	8085
1,305	1.520
1,204	1.603
1,103	2.229
1,005	3.116
897	4.670
1,304	1.130
1,200	1.626
1,101	2.239
1,002	3.147
899	4.614
847	5.703
BaF584/460	7631
1,302	2.370
1,207	2.738
1,096	3.303
1,000	3.992
900	4.823
809	5.950
1,305	2.378
1,200	2.730
1,099	3.313
996	4.013
895	4.951
BaF604/435	3849
1,318	2.182
1,209	2.616
1,103	3.175
996	3.994
905	4.812
1,300	2.244
1,202	2.637
1,103	3.197
1,003	3.918
888	5.014
1,296	2.272
1,192	2.628
1,097	3.205
996	3.958
897	4.958
797	6.262
1,310	2.126
1,203	2.597
1,103	3.156
998	3.922
896	4.980
BaF605/435	7660
1,282	2.285
1,195	2.673
1,097	3.200
998	3.951
914	4.757
LC512/605	6980
1,301	2.131
1,197	2.544
1,095	3.055
1,004	3.574
906	4.334
1,301	2.137
1,201	2.507
1,000	2.998
1,005	3.552
894	4.449
801	5.494

T	Log η
°C	
LC523/586	6988
1,307	2.314
1,195	2.689
1,095	3.221
995	3.807
894	4.674
844	5.246
1,300	2.297
1,203	2.621
1,100	3.149
1,000	3.768
900	4.619
BSC511/635	7656
1,312	1.960
1,202	2.433
1,101	3.005
1,000	3.574
898	4.512
808	5.674
1,300	2.075
1,203	2.422
1,100	2.982
1,000	3.607
901	4.402
803	5.748
BSC517/645	8244
1,318	1.979
1,202	2.497
1,104	2.990
999	3.701
892	4.815
796	6.045
1,310	2.074
1,202	2.533
1,100	3.056
996	3.739
899	4.691
803	6.020
BSC517/645	8097
1,206	2.392
1,105	2.894
1,005	3.567
897	4.550
1,282	2.062
1,205	2.365
1,108	2.872
1,000	3.597
897	4.547
805	5.832
BSC517/645	8223
1,290	2.025
1,202	2.419
988	3.650
884	4.887
788	6.246
1,302	2.030
1,198	2.416
1,100	2.949
1,006	3.611
908	4.532
BSC540/645	6471
1,310	1.677
1,219	1.915
1,108	2.326
995	3.016
898	3.690
805	4.744
1,297	1.640
1,183	2.124
1,097	2.369
998	2.913
901	3.584

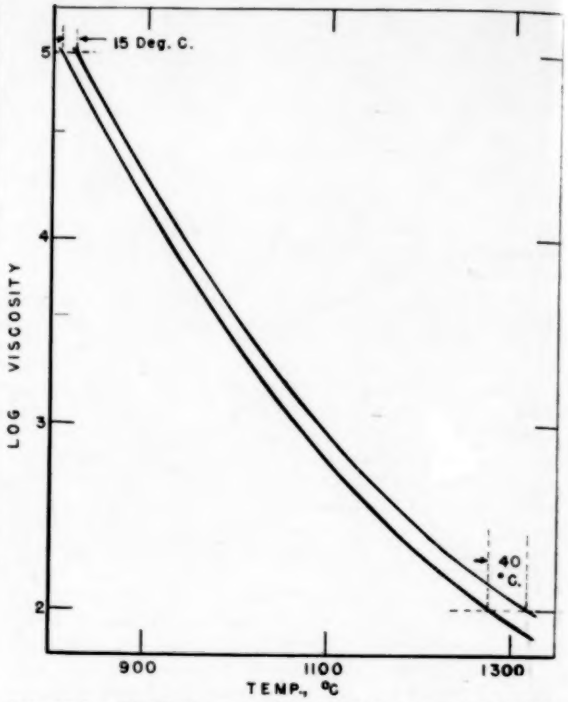

FIGURE 8. *Idealized curves of log viscosity versus temperature.*
The vertical distance between the two curves is the same throughout.

There are certain implications in the method of presenting viscosity data in the manner commonly done in the glass industry that are often overlooked. Statements frequently occur in the literature to the effect that the reproducibility is better in the low temperature range than in the high one. It is important to note that this assertion is a necessary consequence of the nature of the viscosity versus temperature curve. Figure 8 shows two hypothetical log viscosity versus temperature curves that are meant to represent two determinations on the same glass. The separation between the curves has been deliberately exaggerated, and the assumption has been made that the percentage difference in viscosity between the two sets of determinations at any given temperature is constant. This procedure is equivalent to finding that the difference in log viscosity of the two curves is the same at any temperature.

In spite of the fact that the vertical differences between the two curves are always the same, the curves appear to come closer together as the viscosity rises. The eye judges the distance between the two curves by their separation along a perpendicular to the curves themselves rather than either the vertical or horizontal distance. As the curves become steeper their perpendiculars become more nearly horizontal, and the eye sees the separation more and more along the horizontal, that is, the temperature difference. The vertical separation can increase and yet, depending upon the slope of the viscosity-temperature curve,

TABLE 4. *Viscosities of optical glasses by sphere method*

F=Flint; BaC=barium crown; LC=light crown; BaF=barium flint; BSC=borosilicate crown; CF=crown flint. Values in brackets are extrapolated

Glass type	Melt	Temperature, ° C, at which log η is—									
		1.5	2.0	2.5	3.0	3.5	4.0	4.5	5.0	5.5	6.0
F 5795/410	7133	.....	.....	1,305 1,289 [1,304]	1,184 1,189 1,192	1,080 1,085 1,083	999 1,003 999	930 934 929	872 874 [871]	826 823	.....
	Average	.....	.....	1,302	1,188	1,083	1,000	931	873	824	.....
	From average curve	.....	.....	1,304	1,185	1,083	1,000	930	875	828	.....
F 617/366	7045	.....	1,255 1,258	1,113 1,117	1,010 1,007	922 921	851 852	793 793	751 746	.....	.....
	Average	.....	1,256	1,115	1,008	922	852	793	748	.....	.....
	From average curve	.....	.....	1,117	1,008	922	850	794	748	.....	.....
F 620/362	8197	.....	1,307 1,293	1,157 1,168	1,054 1,056	967 962	892 890	830 831	776	.....	.....
	Average	.....	1,300	1,162	1,055	964	891	830	.....	.....	.....
	From average curve	.....	1,292	1,163	1,055	964	889	830	775	.....	.....
F 649/338	8187	.....	1,267	1,149	1,044	956	877	828	.....	.....	.....
	8189	.....	1,279	1,152	1,044	958	888	828	780	738	.....
	Average	.....	1,273	1,150	1,044	957	882	828	.....	.....	.....
	From average curve	.....	1,274	1,147	1,033	958	885	827	780	.....	.....
F 666/324	7086	.....	1,265 1,270	1,143 1,137	1,034 1,029	954 947	889 881	833 828	786 782	744 741	.....
	Average	.....	1,268	1,140	1,032	950	885	830	784	742	.....
	From average curve	.....	1,267	1,141	1,030	948	883	829	782	743	.....
F 689/309	7982	.....	1,240 1,233	1,111 1,111	1,012 1,012	931 931	859 859	806 808	763 764	730	.....
	Average	.....	1,236	1,111	1,012	931	859	807	764	.....	.....
	From average curve	.....	1,233	1,111	1,010	926	856	806	764	.....	.....
F 720/293	7728	1,293	1,178 1,174	1,056 1,051	965 958	890 884	828 828	779 781	739 741	704 704	.....
	Average	.....	1,176	1,054	962	887	828	780	740	704	.....
	From average curve	.....	1,174	1,054	964	890	827	780	739	704	.....
F 754/277	8001	1,223 1,241	1,101 1,096	990 986	908 902	838 838	784 780	740 740	704 702	.....	.....
	Average	1,227	1,098	988	905	838	782	740	703	.....	.....
	From average curve	1,230	1,098	986	903	834	782	738	702	.....	.....
CF 529/516	8217	.....	.....	1,235 1,238	1,121 1,122	1,023 1,022	938 938	869 870	813 814	.....	.....
	Average	.....	.....	1,236	1,122	1,022	938	870	814	.....	.....
	From average curve	.....	.....	1,237	1,122	1,020	937	872	814	.....	.....
BaC 541/599	8072	.....	.....	1,250 1,259	1,147 1,146	1,063 1,066	991 1,000	937 942	892 892	855 851	.....
	Average	.....	.....	1,254	1,146	1,064	996	940	892	853	.....
	From average curve	.....	.....	1,252	1,147	1,064	995	938	893	853	.....
BaC 5725/574	4581	.....	1,289	1,181	1,091	1,020	969	924	886	.....	.....
BaC 574/577	8171	.....	1,286 1,299	1,195 1,197	1,113 1,113	1,039 1,041	982 981	935 934	895 893	860	.....
	Average	.....	1,292	1,196	1,113	1,040	982	934	894	.....	.....
	From average curve	.....	1,292	1,196	1,114	1,040	980	932	894	860	.....
BaC 6109/572	8250	.....	1,237 1,236	1,146 1,148	1,076 1,079	1,019 1,023	974 978	936 939	903 906	874	844
	Average	.....	1,236	1,147	1,078	1,021	976	938	904	.....	.....
	From average curve	.....	1,236	1,148	1,076	1,021	974	937	904	875	844
BaC 611/588	7922	.....	1,296 1,304	1,200 1,194	1,111 1,105	1,038 1,036	983 980	935 932	895 892	859 856	826 822
	Average	.....	1,300	1,198	1,108	1,037	982	934	894	858	824
	From average curve	.....	1,300	1,196	1,109	1,036	981	934	894	859	826
BaC 617/550	6903	.....	1,271	1,162	1,086	1,028	981	940	903	.....	.....
BaC 620/600	8085	1,221 1,222	1,136 1,136	1,066 1,069	1,010 1,015	969 972	935 937	906 905	878	856	.....
	Average	1,222	1,136	1,068	1,012	970	936	906	.....	.....	.....
	From average curve	1,226	1,134	1,068	1,015	972	937	906	879	856	.....
BaF 584/460	7631	.....	.....	1,265 1,258	1,153 1,152	1,061 1,069	987 998	932 940	885 [889]	843	.....
	Average	.....	.....	1,262	1,152	1,065	992	936	887	.....	.....
	From average curve	.....	.....	1,265	1,152	1,069	1,000	940	887	843	[806]
BaF 604/435	3849	.....	.....	1,236 1,232 1,220 1,223	1,135 1,135 1,128 1,129	1,058 1,058 1,054 1,051	995 993 992 989	939 939 939 939	886 890 893 [894]	851	817
	Average	.....	.....	1,228	1,132	1,055	992	939	891	.....	.....
	From average curve	.....	.....	1,235	1,135	1,054	991	937	892	.....	.....

TABLE 4. *Viscosities of optical glasses by sphere method*—Continued

F=Flint; BaC=barium crown; LC=light crown; BaF=barium flint; BSC=borosilicate crown; CF=crown flint. Values in brackets are extrapolated

Glass type	Melt	Temperature, ° C, at which log η is—								
		1.5	2.0	2.5	3.0	3.5	4.0	4.5	5.0	5.5	6.0
BaF 605/435	7660	.....	.....	1,233	1,133	1,055	993	940	[892]	.....	.....
BSC 511/635	7656	.....	1,303	1,190	1,102	1,011	949	899	856	814	.....
		.....	1,190	1,096	1,014	950	898	856	813	.....	.....
	Average	.....	.....	1,190	1,099	1,012	950	898	856	814	.....
	From average curve	.....	1,302	1,189	1,097	1,014	949	898	857	820	.....
BSC 517/645	8097	.....	.....	1,183	1,087	1,013	954	902	.....	.....	.....
		.....	1,300	1,177	1,086	1,012	951	901	861	826	.....
	Average	.....	.....	1,180	1,086	1,012	952	902	.....	.....	.....
	From average curve	.....	1,299	1,180	1,087	1,012	954	901	859	825	.....
BSC 517/645	8244	.....	1,314	1,201	1,103	1,025	971	925	883	843	800
		.....	1,327	1,210	1,109	1,027	969	923	881	843	804
	Average	.....	1,320	1,206	1,106	1,026	970	924	882	843	802
	From average curve	.....	1,310	1,200	1,106	1,029	966	916	874	836	802
BSC 517/645	8223	.....	1,296	1,185	1,093	1,017	961	916	875	838	804
		.....	[1,310]	1,179	1,092	1,019	961	911	.....	.....	.....
	Average	.....	1,303	1,182	1,092	1,018	961	914	.....	.....	.....
	From average curve	.....	1,300	1,181	1,088	1,014	963	910	872	.....	.....
BSC 540/645	6471	.....	1,192	1,078	997	924	867	824	.....	.....	.....
		.....	1,197	1,070	983	914	.....	.....	.....	.....	.....
	Average	.....	1,194	1,074	990	919	.....	.....	.....	.....	.....
	From average curve	.....	1,194	1,076	989	920	867	823	.....	.....	.....
LC 512/603	6980	.....	.....	1,208	1,106	1,016	944	[880]	.....	.....	.....
		.....	.....	1,203	1,100	1,013	945	889	842	800	.....
	Average	.....	.....	1,206	1,103	1,014	944	.....	.....	.....	.....
	From average curve	.....	.....	1,205	1,100	1,013	945	888	840	800	.....
LC 523/586	6988	.....	.....	1,242	1,135	1,045	969	912	864	[823]	.....
		.....	.....	1,233	1,129	1,041	969	912	.....	.....	.....
	Average	.....	.....	1,238	1,132	1,043	969	912	.....	.....	.....
	From average curve	.....	.....	1,240	1,129	1,042	968	912	865	.....	.....

TABLE 5. *Viscosity of optical glasses by rotational viscometer*

F=flint; BaC=barium crown; LC=light crown; BSC=borosilicate crown

T	Log η	T	Log η	T	Log η
F 5795/410	5613	F 649/338	4438	BaC 617/550	5815
°C		°C		°C	
1,102	3.394	1,110	2.700	999	4.003
1,052	3.695	1,054	2.988	951	4.548
1,002	4.013	996	3.336	901	5.326
954	4.387	995	3.335		
902	4.813	949	3.635	LC 523/586	5718
853	5.231	948	3.631		
798	5.792	904	3.945	1,094	3.214
		852	4.411	1,053	3.458
F 617/366	5617	805	4.859	1,003	3.785
		756	5.502	954	4.172
1,096	2.649			901	4.648
1,050	2.876	BaC 5725/574	4581		
998	3.119			BSC 511/635	5407
951	3.403	1,101	2.942		
902	3.705	1,049	3.293	1,100	2.985
850	4.096	998	3.675	1,047	3.308
799	4.504	952	4.129	999	3.649
751	4.991	899	4.743	949	4.090
		851	5.409	902	4.554
F 620/362	5573	1,101	2.917	848	5.147
		1,048	3.292	799	5.806
1,098	2.740	1,002	3.649		
1,048	2.986	953	4.112	BSC 517/645	5371
1,000	3.222	902	4.688		
953	3.496	850	5.392	1,099	2.875
903	3.839			1,096	2.884
854	4.230	BaC 611/588	5666	1,051	3.153
802	4.708			1,000	3.532
755	5.164	1,101	2.248	953	3.931
		1,048	2.727	901	4.482
F 649/338	4438	1,006	3.138	850	5.140
		952	3.751	800	5.862
1,102	2.726	905	4.436	1,091	2.899
1,044	3.008	847	5.547	1,054	3.156
992	3.290			1,004	3.517
955	3.538	BaC 617/550	5815	951	3.967
896	3.957			904	4.459
854	4.315	1,098	3.100	850	5.120
799	4.882	1,052	3.485	814	5.662
754	5.389			800	5.969

the curves will appear to come closer together. Thus the reproducibility in the high viscosity range may actually become worse and yet appear better when expressed as a temperature difference at the same viscosity. In figure 8 the reproducibility is constant, yet one can readily see that whereas the temperature difference at log $\eta=2$ is 40 deg C, that at log $\eta=5$ is only 15 deg C.

2. Rotational Viscometer Data

Preliminary measurements were made with a small rotation viscometer, which has already been described in the literature [7]. This apparatus was limited to measurements below 1,100° C. Table 5 gives the results obtained, and table 6 shows these results in terms of temperature at certain selected viscosities as obtained by interpolation from smooth curves.

3. Comparison of Sphere and Rotational Viscometer Data

Table 7 gives a comparison between the results obtained with the rotation and sphere methods. Of the four glasses with nominally identical compositions, BaC 617 glass shows up as the worst; and all attempts to find the cause for the extreme deviation in this case proved fruitless. No additional sample of melt 5815 was available, so the possibility of an error could not be verified. The other three glasses where direct comparison is possible show fair agreement, the average difference between them being 5 deg.

TABLE 6. *Viscosity of optical glasses by rotational viscometer*

F=flint; BaC=barium crown; LC=light crown; BSC=borosilicate crown. Figures in brackets are extrapolated values

Glass	Melt	Temperature, ° C, at which log η is —							
		2.5	3.0	3.5	4.0	4.5	5.0	5.5	6.0
F 5795/410	5613	.....	.....	1,083	1,004	939	880	827	.....
F 617/366	5618	.....	1,025	935	862	802	749	.....	.....
F 620/362	5573	.....	1,045	953	882	822	771	.....	.....
F 649/338	4438	.....	1,046	960	890	835	787	[745]	.....
		.....	1,051	968	899	841	794	.....	.....
	Average	.....	1,048	964	894	838	790	.....	.....
BaC 5725/574	4581	.....	1,093	1,020	955	919	879	.....	.....
		.....	1,089	1,020	964	918	877	.....	.....
	Average	.....	1,091	1,020	964	918	878	.....	.....
BaC 611/588	5666	1,080	1,019	970	932	900	874	849	.....
BaC 617/550	5815	.....	[1,111]	1,051	999	955	920	892	[868]
LC 523/586	5718	.....	.....	1,047	974	916	.....	.....	.....
BSC 511/635	5407	.....	1,097	1,019	958	907	861	820	[785]
BSC 517/645	5371	.....	1,076	1,003	946	899	860	824	.....
		.....	1,076	1,007	948	900	858	822	.....
	Average	.....	1,076	1,004	947	900	859	823	.....

TABLE 7. *Viscosity of optical glasses*

F=flint; BaC=barium crown; LC=light crown; BSC=borosilicate crown. Figures in brackets are extrapolated values

Glass	Melt	Method of measurement	Temperature, °C, at which log η is—						
			2.5	3.0	3.5	4.0	4.5	5.0	5.5
F 5795/410	5613	Rotation	.....	.....	1,083	1,004	939	880	827
	7133	Sphere	.....	.....	1,080	999	930	872	826
F 617/366	5618	Rotation	.....	1,025	935	862	802	749	.....
	7045	Sphere	.....	1,008	922	852	793	748	.....
F 620/362	5573	Rotation	.....	1,045	953	882	822	.....	.....
	8197	Sphere	.....	1,055	964	891	830	.....	.....
F 649/338	4438	Rotation	.....	1,048	964	894	838	790	.....
	8189	Sphere	.....	1,044	958	888	828	780	.....
BaC 5725/574	4581	Rotation	.....	1,091	1,020	964	918	878	.....
	4581	Sphere	.....	1,091	1,020	969	924	886	.....
BaC 611/588	5666	Rotation	1,080	1,019	970	932	900	874	849
	7922	Sphere	1,198	1,108	1,037	982	934	894	858
BaC 617/550	*5815	Rotation	.....	[1111]	1,051	999	955	920	.....
	*6903	Sphere	.....	1,086	1,028	981	940	903	.....
BSC 511/635	*5407	Rotation	.....	1,097	1,019	958	907	861	820
	*7656	Sphere	.....	1,102	1,011	949	899	856	814
BSC 517/615	5371	Rotation	.....	1,076	1,004	947	900	.....	.....
	8097	Sphere	.....	1,086	1,012	952	902	.....	.....
	8223	.....do	.....	1,092	1,018	961	914	.....	.....
LC 523/586	*5718	Rotation	.....	.....	1,047	974	916	.....	.....
	*6988	Sphere	.....	.....	1,043	969	912	.....	.....

* Nominally identical compositions.

The effect of composition differences on the viscosity of glasses causes difficulty in comparing results of the two methods. However, in some cases the differences in composition are so small that a comparison seems valid. Thus, considering F 5795 the average differences between the two methods is about 5 deg because only small differences in composition are present (table 1). In the case of F 617 the only apparent difference is a substitution of 0.3 percent of Na_2O for K_2O but melt 5618 has 775 lb of cullet to only 300 lb for melt 7045. This means that 5618 probably has more alumina and may account for its higher viscosity at the higher temperatures. In the case of F 620 there has been a substitution of 0.5 percent of Na_2O for K_2O in melt 5573 as compared to 8197. The effect of such substitutions is hard to predict because it has been shown [9] that such substitutions may either raise or lower the viscosity, depending upon the composition of the base glass. In this case the substitution of Na_2O for K_2O lowered the viscosity. In the case of BaC 611 melt 7922 would be expected to be more viscous than melt 5666 because it has 0.5 percent more Al_2O_3 and 0.5 percent less CaO. However, the difference is very large in the high-temperature range and the fact that 475 lb of cullet was used in melt 7922, whereas the fact that none was used in 5666 helps to account for this. In the case of BSC 517 the compositions are considerably different, so that comparison between the two methods is not valid. Melts 8097 and 8223 have nominally identical compositions, but the latter melt had 250 lb more cullet than the former and therefore shows the higher viscosity.

VI. Density Results

1. Sphere Method

Figure 9 shows a plot of the density of the calibrating liquid versus temperature. The straight line represents densities obtained by a picnometer method. The circles represent the density data obtained with the restrained falling sphere apparatus. The average deviation of the circles from the straight line is about 5 in the fourth significant figure.

Table 8 gives interpolated values of density of optical glasses at 100-deg C intervals obtained with the restrained sphere method. Densities of glasses at room temperature were obtained by measuring the buoyant effect of distilled water. The average difference between nominally duplicate determinations at 1,300° and 1,200° C is about 3 in the fourth significant figure. This difference rises to about 5 at 1,100° and 1,000° C. At high viscosities (approximately 5,000 poises) the density results become unreliable.

The expansivities as computed from density changes in the range 1,000° to 1,200° C are given in the last column of table 8. The precision of these expansivities is rather low. On the whole, the flints, barium flints, and crown flints have low expansivities, whereas the borosilicate crowns have high ones. The expansivities of the barium crowns show a general tendency to increase with index of refraction and density.

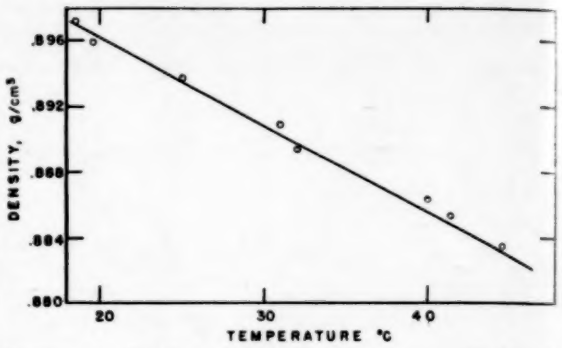

FIGURE 9. *Density of calibrating liquid versus Centigrade temperature.*

Circles represent restrained sphere data, straight line represents picnometer data.

TABLE 8. *Density and expansivity of molten optical glasses by sphere method*

F=flint; BaC=barium crown; LC=light crown; BaF=barium flint; BSC=borosilicate crown; CF=crown flint

Glass	Melt	Determination number	Density (g/cm³) at—								Expansivity (1,000° to 1,200° C)
			1,300° C	1,200° C	1,100° C	1,000° C	900° C	800° C	700° C	Room	
											(μ/m)/°C
F 5795/410	7133	1	3.035	3.046	3.051	3.076	.....	.....	.....	3.230	16
		2	3.040	3.048	3.058	3.073	.....	.....	.....	.....	.....
		3	3.025	3.037	3.052	.....	.....	.....	.....	.....	.....
		avg	3.033	3.044	3.054	3.074	.....	.....	.....	.....	.....
F 617/366	7045	1	3.271	3.289	3.307	3.330	3.347	3.362	.....	3.545	19
		2	3.276	3.296	3.315	3.332	3.350	.....	.....	.....	.....
		avg	3.274	3.292	3.311	3.331	3.348	.....	.....	.....	.....
F 620/362	8197	1	3.346	3.357	3.375	3.388	3.406	.....	.....	3.602	19
		2	3.350	3.363	3.382	3.404	3.417	.....	.....	.....	.....
		avg	3.348	3.360	3.378	3.396	3.412	.....	.....	.....	.....
F 649/338	8187	1	3.595	3.610	3.632	3.656	.....	.....	.....	3.871	20
	8189	1	3.598	3.611	3.630	3.650	3.670	.....	.....	.....	.....
		avg	3.596	3.610	3.631	3.653	.....	.....	.....	.....	.....
F 666/324	7686	1	3.728	3.743	3.762	3.786	3.806	.....	.....	4.016	20
		2	3.734	3.747	3.767	3.790	3.800	.....	.....	.....	.....
		avg	3.731	3.745	3.764	3.788	3.803	.....	.....	.....	.....
F 689/305	7382	1	3.928	3.950	3.969	3.988	4.014	.....	.....	4.219	18
		2	3.932	3.952	3.973	3.993	4.016	.....	.....	.....	.....
		avg	3.930	3.951	3.971	3.990	4.015	.....	.....	.....	.....
F 720/293	7728	1	4.172	4.194	4.218	4.243	4.274	.....	.....	4.491	20
		2	4.170	4.192	4.217	4.244	4.270	.....	.....	.....	.....
		avg	4.171	4.193	4.218	4.244	4.272	.....	.....	.....	.....
F 754/277	8001	1	4.414	4.440	4.466	4.496	4.522	4.566	4.591	4.776	22
		2	4.414	4.440	4.468	4.499	4.529	4.557	.....	.....	.....
		avg	4.414	4.440	4.467	4.498	4.526	4.562	.....	.....	.....
F 923/209	8162	1	.....	.....	.....	.....	.....	5.737	5.772	5.977	.....
CF 529/516	8217	1	2.492	2.504	2.509	2.522	2.536	.....	.....	2.708	16
		2	2.482	2.504	2.515	2.528	2.542	.....	.....	.....	.....
		avg	2.486	2.504	2.512	2.525	2.539	.....	.....	.....	.....

TABLE 8. *Density and expansivity of molten optical glasses by sphere method*—Continued

F = flint; BaC = barium crown; LC = light crown; BaF = barium flint; BSC = borosilicate crown; CF = crown flint

Glass	Melt	Determination number	Density (g/cm³) at—								Expansivity (1,000° to 1,200° C)
			1,300° C	1,200° C	1,100° C	1,000° C	900° C	800° C	700° C	Room	(μ/m)/°C 25
BaC 541/509	8072	1	2.580	2.607	2.620	.....	.....	.....	.....	2.854	.....
		2	2.580	2.602	2.617	.....	.....	.....	.....	.....	.....
		avg	2.580	2.604	2.618	.....	.....	.....	.....	.....	.....
BaC 5725/374	4581	1	2.831	2.858	2.882	2.895	.....	.....	.....	.....	28
BaC 574/577	8171	1	2.904	2.914	2.934	2.951	.....	.....	.....	3.180	21
		2	2.898	2.913	2.922	2.947	.....	.....	.....	.....	.....
		avg	2.901	2.914	2.928	2.949	.....	.....	.....	.....	.....
BaC 6109/572	8250	1	3.207	3.222	3.249	3.278	.....	.....	.....	3.518	30
		2	3.207	3.222	3.251	3.278	.....	.....	.....	.....	.....
		avg	3.207	3.222	3.250	3.278	.....	.....	.....	.....	.....
BaC 611/588	7922	1	2.883	2.900	2.924	.....	.....	.....	.....	3.177	27
		2	2.884	2.902	2.924	2.945	.....	.....	.....	.....	.....
		avg	2.884	2.901	2.924	.....	.....	.....	.....	.....	.....
BaC 617/550	6903	1	3.363	3.368	3.390	3.413	.....	.....	.....	3.652	23
BaC 620/600	8085	1	3.089	3.120	3.154	3.196	3.224	.....	.....	3.490	37
		2	3.081	3.109	3.147	3.190	.....	.....	.....	.....	.....
		avg	3.085	3.114	3.150	3.193	.....	.....	.....	.....	.....
BaF 584/460	7631	1	3.067	3.084	3.087	3.109	.....	.....	.....	3.286	15
		2	3.069	3.088	3.102	3.122	.....	.....	.....	.....	.....
		avg	3.068	3.086	3.094	3.116	.....	.....	.....	.....	.....
BaF 604/435	3949	1	3.265	3.281	3.286	.....	.....	.....	.....	3.488	16
		2	3.262	3.276	3.296	3.321	.....	.....	.....	.....	.....
		3	3.221	3.236	3.253	3.263	.....	.....	.....	.....	.....
		4	3.247	3.263	3.280	3.301	.....	.....	.....	.....	.....
		avg	3.249	3.264	3.281	3.295	.....	.....	.....	.....	.....
BaF 605/435	7660	1	3.267	3.271	3.296	3.301	.....	.....	.....	3.487	.....
LC 512/605	6980	1	2.223	2.236	2.252	2.276	.....	.....	.....	2.481	26
		2	2.223	2.241	2.257	2.272	.....	.....	.....	.....	.....
		avg	2.223	2.238	2.254	2.274	.....	.....	.....	.....	.....
LC 523/586	6988	1	2.301	2.309	2.320	2.325	.....	.....	.....	2.512	16
		2	2.302	2.313	2.323	2.334	.....	.....	.....	.....	.....
		avg	2.302	2.311	2.322	2.330	.....	.....	.....	.....	.....
BSC 511/635	7656	1	2.180	2.201	2.222	2.254	.....	.....	.....	2.468	34
		2	2.177	2.203	2.221	2.247	.....	.....	.....	.....	.....
		avg	2.178	2.202	2.222	2.250	.....	.....	.....	.....	.....
BSC 517/645	8244	1	2.221	2.236	2.259	2.278	.....	.....	.....	2.506	35
		2	2.219	2.238	2.259	2.287	.....	.....	.....	.....	.....
		avg	2.220	2.237	2.259	2.282	.....	.....	.....	.....	.....
BSC 517/645	8097	1	2.215	2.235	2.259	.....	.....	.....	.....	2.497	38
		2	2.211	2.228	2.252	2.277	2.307	.....	.....	.....	.....
		avg	2.213	2.232	2.256	.....	.....	.....	.....	.....	.....
BSC 517/645	8223	1	2.199	2.215	2.236	2.267	.....	.....	.....	.....	40
		2	2.185	2.215	2.231	2.263	.....	.....	.....	.....	.....
		avg	2.192	2.215	2.234	2.265	.....	.....	.....	.....	.....
BSC 540/645	6471	1	2.269	2.272	2.292	2.316	2.341	.....	.....	2.561	37

2. Volumeter Method

Figure 10 shows a plot of the data obtained with the volumeter on BaF 604. In this instance the data obtained in both the cooling and heating schedules showed good agreement. In other cases where the agreement between the two schedules was not good, the difference was traced to devitrification. An estimate of the liquidus temperature of the glass could be made from study of the density data. The sharp drop in density occurring at about 1,350° C was probably due to the formation of bubbles in the glass. It was noted that the surface of the melt was covered with fairly large bubbles and could not be freed from them by stirring as long as the temperature was above 1,350° C. Below this temperature the bubbles were observed to disappear gradually, first receding to the periphery of the crucible, leaving a clear area in the middle, and then disappearing for the most part. The increase in slope of the density-temperature curve below about 950° C is suspected to be caused by nonuni-

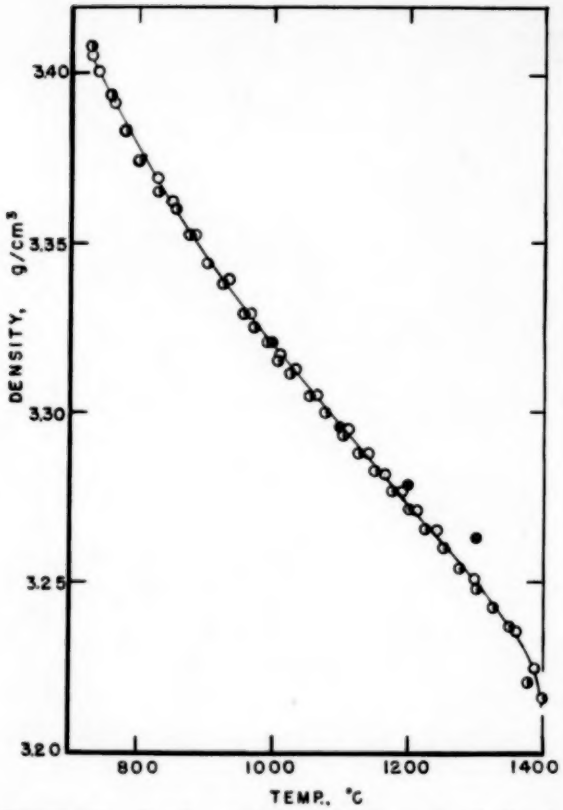

FIGURE 10. *Density of* BaF *604/435 versus Centigrade temperature.*

Half-filled circles show volumeter data obtained on 50° C/hour cooling schedule, open circles show volumeter data on reheating in 25-deg C steps, both on Melt 3354. Filled circles represent sphere data on Melt 3849, which is of the same nominal composition (see table 1).

form drainage of the highly viscous glass in this temperature range. For these reasons only the density data in the region between 950° and 1,200° C are considered reliable.[4]

The points enclosed by filled circles (fig. 10) represent the density data obtained by the counterbalanced sphere method on the same kind of glass from a different pot. However the nominal compositions are identical, and thus a comparison between the two methods is possible. Between 1,000° and 1,200° C the agreement is excellent. At 1,300° C the ball method yielded high values. At this temperature there are probably a few small seeds (bubbles) in the melt, but their presence should not cause much error in the volumeter method; the error should be in the direction of too large a volume and hence too low a density. In the case of the ball method, a bubble that attaches itself to the ball will make the ball appear to be lighter; hence the buoyant effect will appear too large, and too great a density will be calculated. Figure 11 shows another comparison between the ball and volumeter methods on two glasses of nominally identical compositions. Here, also, the value at 1,300° is too high. Other glasses measured by both methods are not comparable because of differences in composition.

Table 9 gives the data that were obtained by the volumeter method over the range where such data were considered reliable. The agreement between nominally duplicate measurements is satisfactory. It is probable that the temperature coefficient of density over the range where such data are valid is more reliable than similar data obtained with the ball method because the volumeter method is intrinsically a differential method.

As expansivity data for some glasses were available in both the low (25° to 600° C) and high (900° to 1,300° C) temperature ranges, the total expansion curve in the range from 25° to 1,300° C could be constructed (fig. 12). The lower part of figure 12 shows a plot of the expansivity of BSC 517/64.5. The data from room temperature to the softening point were obtained on a sample from Melt 3246 by J. B. Saunders [10] with an interferometer method. The data on a sample from Melt 3703 from 900° C and above were obtained with the volumeter. The two filled circles represent the mean expansivity over a 200-deg C interval plotted at the midpoint. The broken line indicates the interpolation that was adopted. The continuation of the open circles below *P* indicates the observed slumping of the specimen. The curve in the upper part of figure 12 was obtained by integration of the expansivity curve. The open and half-filled circles represent two different determinations with the volumeter. At the lower temperatures where the data are unreliable because of poor drainage the half-filled circles show the direction of the error from this cause.

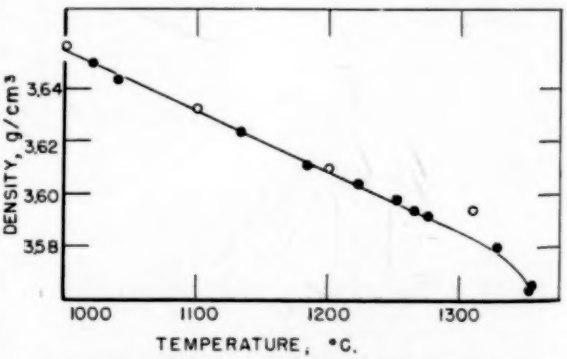

FIGURE 11. *Density of F 649/33.8 versus temperature.*

Curve represents volumeter data on Melt 5943 (filled circles), and open circles represent sphere data on Melt 8187. These melts have nominally identical composition (table 1).

[4] For those who may wish to use this or a similar method for obtaining accurate densities, it is suggested that the glass be covered with a layer of a molten salt. The volume-temperature relationships of such a salt have to be known or determined, and of course one should be picked that will not severely attack the glass. The high fluidity of most molten salts is such that they will readily drain off the walls of the crucible and thus allow density measurements to extend to lower temperatures than are possible without their use. High accuracy in the knowledge of the volume-temperature relationship of the salt is not necessary, as only a relatively small amount need be used.

TABLE 9. *Density and expansivity of optical glasses by volumeter method*

F = flint; BaC = barium crown; BaF = barium flint; BSC = borosilicate crown

Glass	Melt	Density (g/cm³) at							Expansivity
		1300 °C	1200° C	1100° C	1000° C	900° C	800° C	Room	
									(μ/m)/°C
F. 620/362	5747	3.360	3.380	3.402	3.423	3.446	3.470	.....	21
F 640/338	5943	3.387	3.609	3.631	3.654	3.678	.....	.....	21
BaF 588/534	3800	2.996	3.024	3.052	3.082	3.118	.....	3.317	34
		3.000	3.027	3.055	3.087	3.120	.....	.....	.....
		2.999	3.025	3.053	3.085	3.119	.....	.....	.....
	avg	2.998	3.025	3.053	3.085	3.119	.....	.....	.....
BaF 604/435	3354	3.259	3.273	3.296	3.319	3.346	3.376	3.483	23
		3.249	3.272	3.294	3.317	3.342	3.366	.....	.....
	avg	3.254	3.272	3.295	3.318	3.344	3.371	.....	.....
BaC 5725/574	3247	2.936	2.959	2.979	3.008	3.039	.....	3.201	26
		2.933	2.958	2.984	3.016	.....	.....	.....	.....
	avg	2.934	2.958	2.982	3.012	.....	.....	.....	.....
BaC 5725/574	3722	2.915	2.938	2.968	2.994	3.028	.....	.....	31
BSC 517/645	3703	2.199	2.226	2.261	2.294	.....	.....	2.505	47
		2.196	2.228	2.257	2.293	.....	.....	.....	.....
	avg	2.198	2.227	2.259	2.294	.....	.....	.....	.....

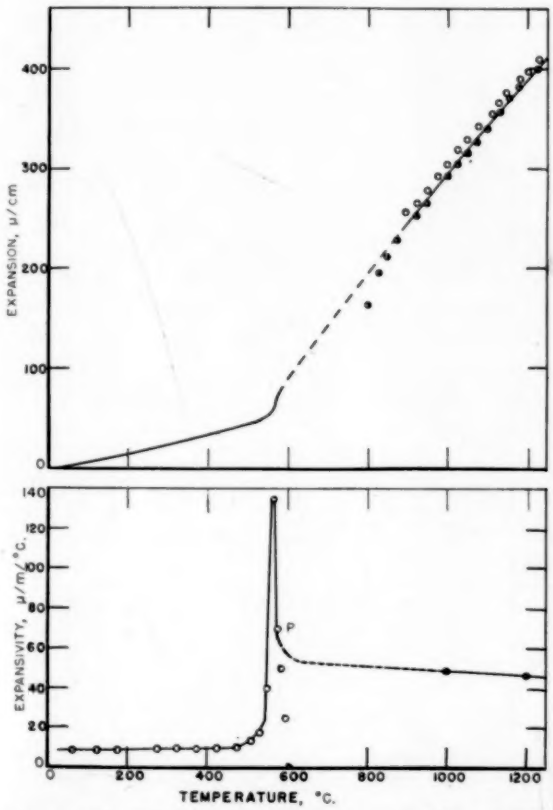

FIGURE 12. *Thermal expansion and expansivity of BSC 517/64.5 as a function of temperature.*

Data from room to approximately 600° C on Melt 3246 by interferometer method. Data above 800° C on Melt 3703 by volumeter method. Each of the two filled circles represents the mean expansivity over a 200-deg C interval plotted at the midpoint.

Two features of interest may be noted concerning the expansivity curve. One is that although the expansivity in the low temperature range increases with temperature, the reverse relationship seems to hold in the liquid range. The second point of interest is that the expansivity shows a decrease before the interferometer softening point is reached that is not due to slumping of the specimen.

Saunders was able to demonstrate this point in an ingenious experiment. He used a plane parallel polished specimen plate with a hole in the center. This plate was placed between two fused silica flats in such manner that interference fringes could be observed through the air space in the hole, as well as between the polished faces of the specimen itself. The conditions were such that the pressure of the upper silica flat was negligible. Figure 13 shows a plot of the results obtained. In the temperature region 650° to 690° C there occurs a slowing down of the precipitous drop of the expansion coefficient. In this temperature range the specimen did not slump as judged by the appearance of the interference fringes between the polished faces of the specimen. The dashed line indicates the probable further course of the expansion coefficient if the specimens had not slumped from this region onward. The sharp drop in expansion coefficient actually observed beyond the 650° to 690° C region was due to slumping of the specimen plate as evidenced by the curving of the interference fringes between the faces of the specimen.

VII. Discussion

Data on viscosity and density of glass melts are of value in explaining molding properties of glasses, behavior to stirring and fining during the melting cycle, performance of the glass as it is cooled, etc. The data also indicate class difference in expansivity among the major types of optical glasses. Because

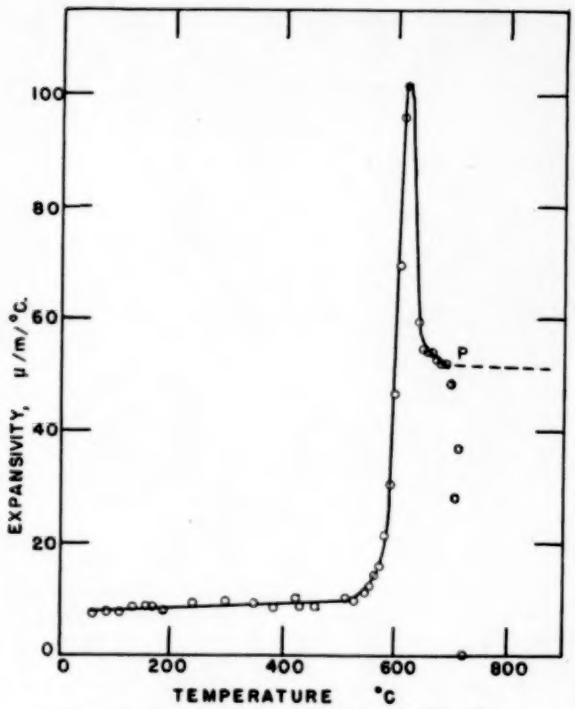

FIGURE 13. *Thermal expansivity of BSC 517/64.5.*

of the lack of systematic variation in composition of the glasses studied, it is not possible, however, to establish close correlation of viscometric and density data with composition. Further, as viscosity curves may cross, a statement regarding one temperature region may be invalid in another region. Figure 14 illustrates this point. Here BaC 620 is less viscous at 1,300° C and more viscous at 850° C than any of the other glasses represented. In general, when comparing the viscosity of glasses it is necessary to compare viscosity versus temperature relationships.

1. Temperature Coefficient of Viscosity and Molding of Glass

The slope of the viscosity-temperature curve is a property in which the glass technologist is very much interested. In general, the optical flints as a group show relatively small slopes; that is, the viscosity does not change rapidly with temperature, whereas barium crowns as a group show relatively large slopes. This is related to the ease with which these glasses may be formed or pressed, as will be shown.

The practical glassworker calls a glass that he can form or shape with ease a "sweet," or "long," glass. If, while he works with the glass, it stiffens so that he has to reheat frequently, he calls it a "sour," or "short," glass. Sweetness and sourness of glass depend upon the rate of cooling, which is a complicated function of the temperature, the size of the piece, the color, etc. Thus, if two glasses at the same initial temperature were cooled at the same rate, sweetness would be inversely related to the slope of the viscosity-temperature curve. The glass with a viscosity that changed slowly with fall in temperature would be in the proper viscosity range for easy working for a longer time than the sour glass with a rapid change of viscosity with temperature.

The slope of the viscosity-temperature curve is, however, not the only factor in practical rating of sweetness and sourness. Glass is taken from the furnace at the top of its working range. Other things being equal, the glass with working range in a higher temperature region will cool faster and therefore be more sour.

An attempt was made to evaluate the molding qualities of the glasses by taking into account the temperature difference between two selected viscosities and dividing that by the square of the higher temperature. The two viscosities selected were log $\eta = 2.5$ and 3.5. These viscosities are in the range for lamp working and were selected because such data were available on a great many optical glasses. As cooling of the glass takes place by radiation as well as conduction, the square of the temperature was selected on a trial basis. Table 10 shows the data obtained. The sweetness index $(T_1 - T_2)/(T_1^2)$ is seen to be high for the optical flints, low for the barium crowns, and intermediate for the others. In order to test the validity of this concept of sweetness index with practical observation, a questionnaire was submitted to five molding crew supervisors who were asked to place 22 glass types in order of increasing difficulty in pressing optical lens blanks. A rank correlation of +0.93 was found between the average order as estimated by the supervisors and that calculated from the sweetness index.

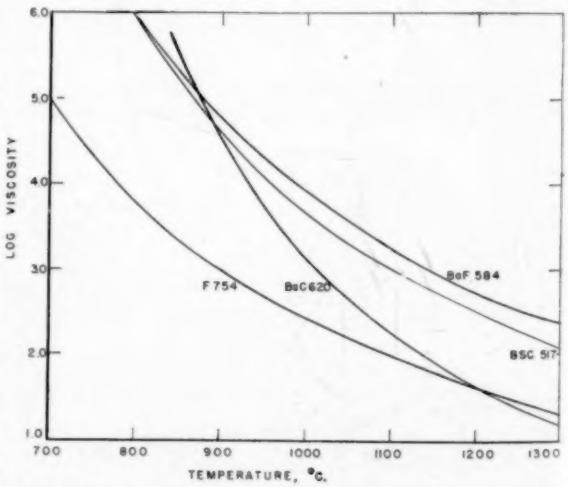

FIGURE 14. *Curves of log viscosity versus temperature of some typical optical glasses.*

TABLE 10. *Some properties of optical glasses*

Glass	Melt	T_1 at log η =2.5	T_2 at log η =3.5	T_1-T_2	Sweetness index, $\frac{T_1-T_2}{T_1^2}$	Expansivity (1,000° to 1,200° C),	Slope of log η vs. temperature, $\frac{1}{T_1-T_2}$
		°C	°C	°C		$(\mu/m)/°C$	
F 5795/410	7133	1,302	1,083	219	129×10^{-6}	16	456×10^{-6}
F 617/366	7045	1,115	922	193	155	19	518
F 620/362	8197	1,162	964	198	146	19	505
F 649/338	8187 & 9	1,150	957	193	146	20	518
F 666/324	7686	1,140	950	190	146	20	526
F 689/309	7382	1,111	931	180	146	18	556
F 720/293	7728	1,054	887	167	150	20	599
F 754/277	8001	988	838	150	157	22	667
CF 529/516	8217	1,236	1,022	214	140	16	467
BaC 541/599	8072	1,254	1,064	190	121	25	526
BaC 5725/574	4581	1,181	1,020	161	115	28	621
BaC 574/577	8171	1,196	1,040	156	116	21	641
BaC 6109/572	8250	1,147	1,021	126	96	30	794
BaC 611/588	7922	1,198	1,037	161	112	27	621
BaC 617/550	6903	1,162	1,028	134	99	23	746
BaC 620/600	8085	1,068	970	98	86	37	1020
BaF 584/460	7631	1,262	1,065	197	124	15	507
BaF 604/435	3849	1,228	1,055	173	115	16	578
BSC 511/635	7656	1,190	1,012	178	125	34	561
BSC 517/645	8097	1,180	1,012	168	120	38	595
BSC 517/645	8244	1,206	1,026	180	124	35	556
BSC 517/645	8223	1,181	1,014	168	120	40	595
BSC 540/645	6471	1,074	919	155	134	37	645
LC 512/605	6980	1,206	1,014	192	132	26	521
LC 523/586	6988	1,238	1,043	195	127	16	513

2. Expansivity and Temperature Coefficient of Viscosity

The last two columns of table 10 give the expansivity (col. 7) in the liquid range (approximately 1,000° to 1,200° C) as calculated from density data, as well as the slope (col. 8) of the curve of log η versus temperature in the region between log η=2.5 and 3.5. Figure 15 shows a plot of these data. There is a general correlation indicating a common factor in these two properties. This common factor may be the change in attractive force between molecules or molecular groupings with change in temperature. As we are dealing with many kinds of groupings, the correlation cannot be expected to be high. The flints are found in the lower left hand part of figure 15, and within the group there is a general tendency for the slope to increase with the expansivity. Similarly, the barium crowns as a group are found in the central part of the diagram and also show a tendency for the slope to increase with increasing expansivity. The borosilicate crowns as a group show the highest expansivities accompanied by only moderate slopes, and within the group there is some trend for the slope to increase with expansivity.

3. Expansivity and "Breaks"

In the transfer process of making optical glass, [11] the proper cooling of the pot of glass after removal from the melting furnace is of the utmost importance in order for the glass to break into large usable pieces. In the case of flints, cooling at 18 deg C/hr through the critical temperature region (where the rapid expansion region begins, fig. 12) results in satisfactory breaks, whereas the same procedure causes unsatisfactory results (vacuum bubbles, shattering, onions [11]) when applied to borosilicate crowns [12]. For satisfactory breaks with borosilicates the cooling rate has to be lowered to at least 16 deg C/hr. It seems probable that this difference in behavior is partially accounted for by the lower expansivity of the flints in the liquid range as compared to that of the borosilicates. As the pot is cooled, the surface of the glass reaches a temperature at which it becomes rigid while the glass in the hotter interior is still fairly liquid. With further cooling the glass in the center of the pot tries to contract much more than the rigid surface glass (because it has a higher expansion, fig. 12) thus producing some of the stresses that break the glass. As the ratio of the expansivities in the liquid region to that in the solid region is much less for flints than for borosilicates, the flints can endure a greater cooling rate than the borosilicates and still produce satisfactory breaks.

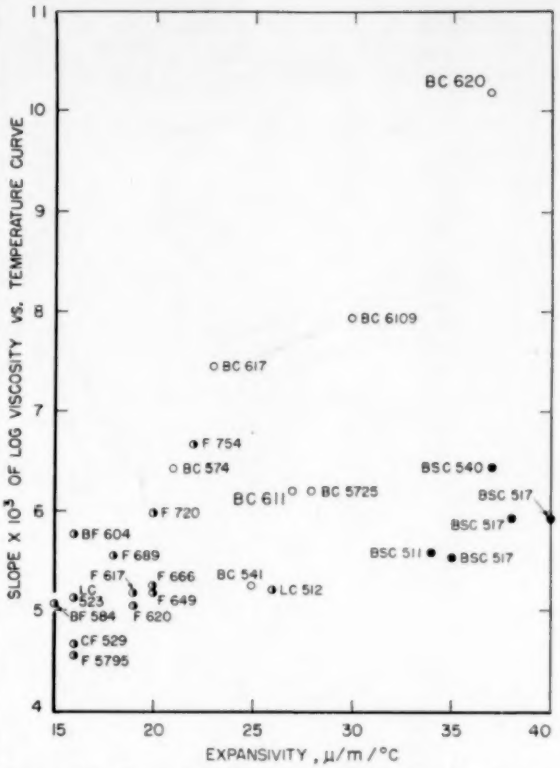

FIGURE 15. *Expansivity versus the slope of the viscosity-temperature curve.*

VIII. Summary and Conclusion

1. Viscosities and densities of molten optical glasses were measured with a counterbalanced-sphere method. The sphere apparatus is simple, rugged, and has stood up well with continued use.

2. The densities obtained with the sphere method agree well in the temperature range 1,000° to 1,200° C with those obtained by measuring the volume of a given weight of glass contained in a platinum volumetric flask.

3. Comparison of viscosity results obtained with the sphere method and a rotation viscometer has shown good agreement.

4. Expansivities calculated from density results obtained with the sphere method in the temperature range 1,000° to 1,200° C indicate that the expansivity in this range is from 2 to 3.5 times that in the solid range (100° to 400° C). The flints and barium flints as a group have the lowest expansivity, the barium crowns are intermediate, and the borosilicate crowns have the highest expansivities. A correlation was found between expansivity in the liquid range and the slope of the viscosity-temperature curve.

5. A numerical value for the ease of making optical glass pressing was calculated from viscosity data. This index was found to correlate well with estimates made by molding supervisors.

6. The Faxen correction of Stokes law was found to be superior to the Francis formula.

IX. References

[1] L. R. Bacon, J. Frank Inst. **221,** 251 (1936).
[2] A. W. Francis, Physics **4,** 403 (1933).
[3] C. S. Cragoe, World Petroleum Congress **2,** 529 (1933).
[4] V. H. Stott, E. Irvine, and D. Turner, Proc. Roy. Soc. (London) [A], **108,** 154 (1925).
[5] G. Heidtkamp and K. Endell, Glastech. Ber. **14,** 89 (1936).
[6] William N. Harrison, Robert E. Stephens, and Stephen M. Shelton, J. Research NBS **20,** 39 (1938) RP1063.
[7] Leo Shartsis and Alden W. Smock, J. Research NBS **38,** 341 (1947) RP1771.
[8] L. Wilhelmy, Pogg. Ann. **119,** 177 (1863).
[9] James P. Poole and Maxwell Gensamer, J. Am. Ceram. Soc. **32,** 220 (1949).
[10] J. B. Saunders, Private communication.
[11] Manufacture of Optical Glass and of Optical Glass Systems, Ordnance Dept. Document No. 2037 (1921).
[12] D. Hubbard, Private communication.

WASHINGTON, October 5, 1950.

Journal of Research of the National Bureau of Standards Vol. 46, No. 3, March 1951 Research Paper 2191

Calorimetric Properties of Diphenyl Ether From 0° to 570°K

George T. Furukawa, Defoe C. Ginnings, Robert E. McCoskey, and Raymond A. Nelson

The heat capacity, enthalpy, and entropy of diphenyl ether from 0° to 570° K are calculated from experimental heat capacities obtained by using an adiabatic vacuum calorimeter and a Bunsen ice calorimeter. The heat of fusion and the triple-point temperature are given as 17,216 ±17 absolute joules mole^{-1} and 300.03 ±0.01° K, respectively. Heat of combustion experiments in a bomb calorimeter gave the value −6,135.64 ±0.88 absolute kilojoules mole^{-1} for the standard heat of combustion of the liquid at 30° C. The standard heats of combustion and formation are computed for both liquid and solid at 25° C. The standard entropy and Gibbs free energy of formation for the solid at 25° C are given as −590.1 ±0.5 absolute joules deg^{-1} mole^{-1} and 143.8 ±0.9 absolute kilojoules mole^{-1}, respectively.

I. Introduction

Frequently in calorimetry it is desirable to have access to standard substances whose thermal properties are accurately known to calibrate and test calorimeters under conditions of actual use. Water has been used quite extensively as a standard substance in heat capacity and latent heat of vaporization calorimeters, but it has a relatively limited temperature range of application due to its rather rapid vapor pressure increase above 100° C and its large change in volume on freezing. Often the choice of a standard is dictated by the calorimeter design, consequently there should be a number of standards from which to select the most suited. In heat-capacity calorimetry, as well as in other types of calorimetry, the basic requirements for any standard substance are high chemical stability; high purity, which can be attained and retained easily; reproducibility of physical state; and easy manipulation in the calorimetric apparatus. It is advisable to test heat capacity calorimeters under conditions such that the heat capacity of the calorimetric system is closely the same whether it contains the standard material or the test material. If a standard of high heat capacity per unit volume is available, this condition can be met easily by adjusting its quantity in the calorimeter.

Diphenyl ether has been known to be relatively stable and to be obtainable in a high state of purity by fractional distillation followed by crystallization. As this material melts close to room temperature, it is being developed at this Bureau for use in triple-point cells, as a thermostatic medium at its melting point and in a modified Bunsen calorimeter. The accurate measurement of the thermal properties of diphenyl ether is desirable for these applications as well as for improvement in design of high-temperature heat-transfer equipment in which diphenyl ether is being used in the form of diphenyl-diphenyl ether eutectic mixture.

The heat capacity of diphenyl ether was measured between 18° and 573° K, using two calorimeters widely different in design. An adiabatic vacuum calorimeter was used from 18° to 360° K, and a "drop" method was used from 273° to 573° K with an accurately thermostated furnace and an improved Bunsen ice calorimeter. The two methods overlap in the temperature range between 273° to 360° K, where they serve to check each other. The triple point and heat of fusion were measured in the adiabatic vacuum calorimeter. An isothermal jacket water calorimeter was used for the determination of heat of combustion.

II. Low-Temperature Calorimetry

1. Apparatus

The melting-point studies and heat-capacity measurements from 18° to 360° K were made with an adiabatic vacuum-type calorimeter essentially the same as that described in the paper on 1,3-butadiene by Scott, et al [1].[1] Briefly, the apparatus and procedure were as follows. The diphenyl ether, freed of air and water, was sealed in a copper container, which in turn was suspended inside an evacuated adiabatic shield system. The copper sample container had a volume of about 60 ml and was provided with a central well for a thermometer and heater. For rapid dissipation of heat to the sample, copper vanes radiated out from this well. No part of the sample was more than 2 mm from the copper vanes. A thin coating of pure tin was applied to the inner surfaces of the container to provide an inert surface to the sample and to solder the vanes in place. The outer surface of the container, as well as the adjacent surface of the adiabatic shield, were polished to cut down the effect of heat transfer by radiation. The heat transfer by convection was made negligible by pumping the vacuum space to 10^{-5} mm Hg or better. During an experiment the shield temperature was kept, at all times, equal to that of the sample container surface by controlling the shield heaters, using constantan-chromel *P* thermels to integrate surface temperatures. One set of three-junction thermels and another of two-junction thermels were used. In the melting-point studies and heat-capacity experiments, the electrical energy introduced into the sample and container was determined by means of a precision potentiometer in conjunction with a volt box and a

[1] Figures in brackets indicate the literature references at the end of this paper.

standard resistor. The time was measured by using a precision interval timer operated on standard 60 cycles furnished by the Radio Section of this Bureau. This timer was compared periodically with time signals from the Time Section and found not to vary by more than 0.02 sec for any heating period, which was never less than 2 min. The initial and final temperatures of a heating interval were measured by means of a platinum resistance thermometer and a G–2 Mueller bridge. The platinum resistance thermometer was calibrated at this Bureau above 90° K on the International Temperature Scale [2] and between 10° to 90° K on a provisional scale [3], which consists of a set of platinum resistance thermometers calibrated against a gas thermometer. The resistance of the thermometer was frequently checked at the ice point, and the small fluctuations observed were too insignificant to affect the results of the measurements. The volt box, standard resistor, potentiometer, and bridge were calibrated recently at this Bureau.

2. Purity and Triple-Point Temperature

The diphenyl ether used in this investigation was purified by F. L. Howard of this Bureau by means of a fractional distillation followed by 25 fractional crystallizations. A portion of this diphenyl ether was treated by the following procedure in order to remove the dissolved air and water. The material was slowly frozen in a glass bulb during evacuation; then after melting, this process was repeated. After distilling the sample completely into a second bulb, the process of slow freezing while evacuating was repeated again. A portion (36.7724 g in vacuum) of this sample was transferred to the copper container by gravity, and the container was sealed with solder.

The purity of this air-free diphenyl ether was determined calorimetrically from the melting-point studies. In this method the equilibrium temperatures are measured at various increasing liquid-solid ratios as determined from the electric energy input, heat of fusion, and heat capacity of the system. The experimental data are treated on the assumption that Raoult's law is obeyed and no solid solution is formed in the concentration range under investigation. The simplified equation, $N_2 = A\Delta T$, is used to represent the relation between mole fraction impurity, N_2, and the depression, ΔT, of the triple point. The cryoscopic constant, A, is calculated from $A = L_f/RT_t^2$, where L_f is the heat of fusion, R the gas constant and T_t the triple-point temperature. The observed equilibrium temperatures are plotted against $1/F$, the reciprocal of the fraction of material in the liquid state. This curve is extrapolated to $1/F = 0$ to obtain the triple point of the pure substance, and the slope of this curve is multiplied by the cryoscopic constant to obtain mole fraction impurity.

The purity of diphenyl ether was determined before and after the heat-capacity measurements to ascertain whether any chemical change had taken place under the conditions inside the calorimeter

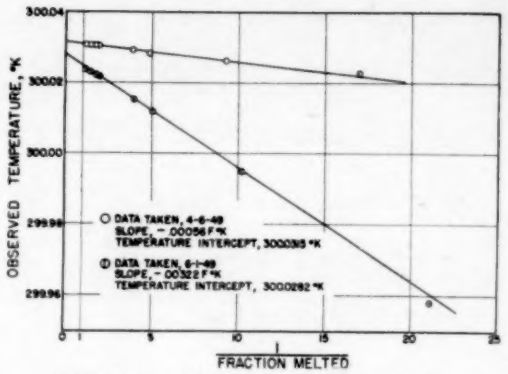

FIGURE 1. *Melting curves of diphenyl ether.*

sample container. Table 1 and figure 1 show the results of these measurements. Although the inside of the container is completely covered with pure tin, which is considered to be inert, the results show that the liquid soluble-solid insoluble impurity has increased from 0.000013 to 0.000074 mole fraction. This is rather surprising compared to only 0.00002 mole fraction increase indicated in the high-temperature measurements mentioned in a later section. Perhaps the inner surface of the sample container used with the adiabatic calorimeter has a catalytic effect on the decomposition of diphenyl ether even as low as 360° K. As the absolute purity is still high, the impurities would have only a negligible influence on the heat capacities.

TABLE 1. *Melting points of diphenyl ether*

$N_2 = 0.0230\,\Delta T$

Before the heat-capacity measurements		
$1/F$	$T_{obs.}$	$T_{calc.}$
17.01	300.0231	300.0219
9.33	300.0264	300.0262
4.90	300.0285	300.0287
3.93	300.0292	300.0293
2.01	300.0308	300.0304
1.79	300.0306	300.0305
1.50	300.0306	300.0307
1.26	300.0308	300.0308
1.00	.....	300.0309
Temperature intercept, 300.0315° K. Impurity, 0.000013 mole fraction.		
After the heat-capacity measurements		
$1/F$	$T_{obs.}$	$T_{calc.}$
21.11	299.9581	299.9603
10.25	299.9651	299.9652
5.05	300.0122	300.0118
4.02	300.0154	300.0153
2.00	300.0219	300.0217
1.79	300.0223	300.0220
1.50	300.0231	300.0234
1.27	300.0240	300.0241
1.00	.....	300.0250
Temperature intercept, 300.0282° K. Impurity, 0.000074 mole fraction.		

The difference in the two temperature intercepts, 300.0315° and 300.0282° K,[2] amounting to 3.3 mdeg is believed to have been caused by small changes in the resistance thermometer and bridge between periods of the measurements. This change, however, does not affect the slope of the melting curve, as it only causes a parallel displacement in temperature. For a given set of measurements the temperatures agreed to within a few tenths of a millidegree. Considering the calibration uncertainties in the bridge and platinum resistance thermometer and uncertainty in the absolute temperature scale, the triple point of diphenyl ether is taken to be 300.03±0.01° K.

The third column of table 1 gives temperatures obtained from the equation $T_t - T_{calc} = N_2/AF$. Here N_2 is the mole fraction impurity calculated from the experimental data. The relation between the results in the second and third columns shows that Raoult's law was followed quite closely. The value of the cryoscopic constant A used in all the calculations is 0.0230 deg^{-1}.

3. Heat of Fusion

The latent heat of fusion of diphenyl ether was determined by adding electric energy continuously from a temperature a few degrees below the triple point to a temperature above the triple point. The quantity of energy was corrected for the heat capacity of the material plus the container on both sides of the triple point and for a small amount of premelting caused by the presence of impurities. The heat of fusion was determined soon after the first purity measurements, thus the premelting corrections have been calculated on the basis of 0.000013 mole fraction impurity. The results and corrections are tabulated in table 2. $\int C dT$ is the sum of the heat capacity corrections above and below the triple point. The mean value obtained for three determinations is 17,216 abs j mole^{-1}, and the mean deviation is ±2 abs j mole^{-1}. Considering the arbitrariness involved in the heat-capacity correction a probable error[3] of ±0.1 percent is assigned. The value for the heat of fusion is taken as 17,216 ±17 abs j mole^{-1}.

TABLE 2. *Heat of fusion of diphenyl ether*

Mole weight, 170.20 g; mass of sample, 36.7724 g

Defined calorie = 4.1840 abs j.

Temperature interval	Total energy	$\int C dT$	Premelting correction	L_f
°K	*abs j*	*abs j*	*abs j*	*abs j*
298.4668 to 305.2408	4357.49	639.47	1.34	3719.36
296.1288 to 303.6634	4404.12	685.48	0.54	3719.18
295.5214 to 303.0956	4401.96	682.00	.30	3720.26
Mean				3719.60
Mean deviation				±0.44
Heat of fusion { 101.152±0.012[a] abs j g^{-1} / 17,216 ±2[a] abs j mole^{-1}				

[a] These values are mean deviations.

4. Heat Capacity

The heat capacity of the diphenyl ether sample (36.7724 g mass) plus the container was measured from 18° to 360° K in the adiabatic vacuum calorimeter. Between 18° and 80° K solid and liquid hydrogen were used to cool the material and above 80° K liquid air, solid carbon dioxide, and ice were used. During heat-capacity experiments in the temperature range 18° to 30° K, where the heat-capacity curve changes rapidly in slope, the temperature change per heating interval was about 2 deg. The interval was increased to 4 or 5 deg up to 100° K, and above this temperature intervals of 6 to 10 degrees were used.

Nine series of experiments were made on the full container in the solid range, and the temperature ranges covered were 20° to 98° K, 15° to 29° K, 13° to 100° K, 88° to 234° K, 215° to 295° K, 125° to 295° K, 105° to 216° K, 90° to 105° K, and 101° to 205° K. Five series of experiments in the liquid range consisted of the following temperature ranges: 302° to 367° K, 304° to 370° K, 305° to 367° K, 303° to 320° K, and 321° to 348° K. Six series of experiments were made on the empty container, and the temperature ranges were 13° to 35° K, 15° to 31° K, 28° to 60° K, 90° to 370° K, 50° to 119° K, and 279° to 342° K. Curvature corrections were applied to these measurements wherever significant, using the relation given by Osborne, et al. [4]:

$$Z_{T_m} = Q/\Delta T - \left(\frac{\partial^2 Z}{\partial T^2}\right)_{T_m} \frac{\Delta T^2}{24} \cdots \qquad (1)$$

Z_{T_m} is the corrected heat capacity at the mean temperature, T_m, of the interval ΔT; Q is the electrical energy added; and $(\partial^2 Z/\partial T^2)_{T_m}$ is the second derivative of the heat capacity with respect to temperature at T_m. The observed results (corrected for curvature) were plotted on a large scale as deviations from an approximate empirical equation and a smooth curve was drawn through the deviation points. The smooth deviation curve and the empirical equation were then used to obtain smoothed heat capacities at equally spaced integral temperatures. Similar heat-capacity experiments were made with the empty container, and the results were treated in the same manner. The weight of the container was different for the experiments with and without the sample. This arose from small differences in the weights of the copper filling tube and solder for the two experiments. Corrections for these differences in weights were applied to the smoothed heat capacities for the empty container from known heat capacities of copper and solder. The deviations of experimental

[1] All temperatures expressed in degrees Kelvin were obtained from the relation °K = °C + 273.1600.

[3] For these experiments a true probable error cannot be statistically computed. The values given are estimates arrived at by examining contributions to the inaccuracy from all known sources, and they are to be considered (unless stated otherwise) as the authors' best estimate of the error, which is just as likely to be exceeded as not.

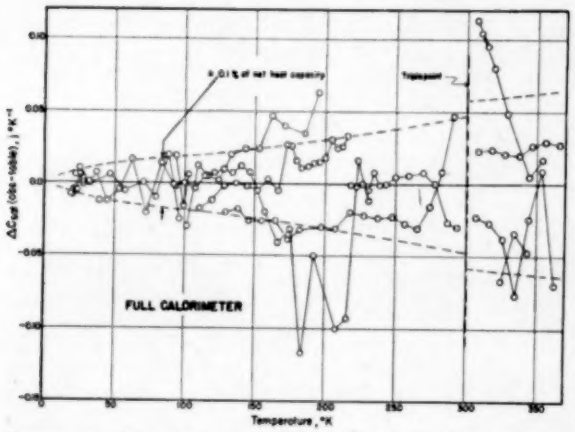

FIGURE 2. *Deviations of experimental heat capacities (corrected for curvature) from smoothed values for the container plus diphenyl ether.*

The experiments in a single series of measurements are connected by lines.

heat capacities from the smoothed values for the full and empty container are shown in figures 2 and 3. Most of the points lie within 0.1 percent of the net heat capacity. The net heat capacities were calculated, using the equation given by Hoge [5],

$$C_{\text{sat.}} = \frac{Z_2 - Z_1 - T\frac{d}{dT}\left[\frac{dp}{dT}(V - m v_c)\right]}{m/M}, \tag{2}$$

where Z_2 and Z_1 are the tabulated heat capacities for the full and empty container, respectively, at the same temperature T; p is the vapor pressure; m is the mass of sample; M is the molecular weight of diphenyl ether; V is the volume of the container; and v_c is the specific volume of the condensed phase. The term involving the vapor correction was not actually used, for it does not contribute significantly to the results obtained with the low-temperature adiabatic calorimeter. At 360° K this vapor correction amounts to only 0.002 percent. The values of heat capacity listed in table 4 from 18° to 300° K are those obtained from these calculations. The heat-capacity values below 18° K in this table were obtained by extrapolation, using the Debye equation,

$$C_{\text{sat.}} = 59.91 D\left(\frac{112}{T}\right), \tag{3}$$

fitted to the heat capacity at 18°, 20°, and 22° K. The values tabulated between 300° and 360° K were obtained by adjusting the slight differences between the results with the low-temperature adiabatic calorimeter and the ice calorimeter. The method of adjustment is discussed in a later section.

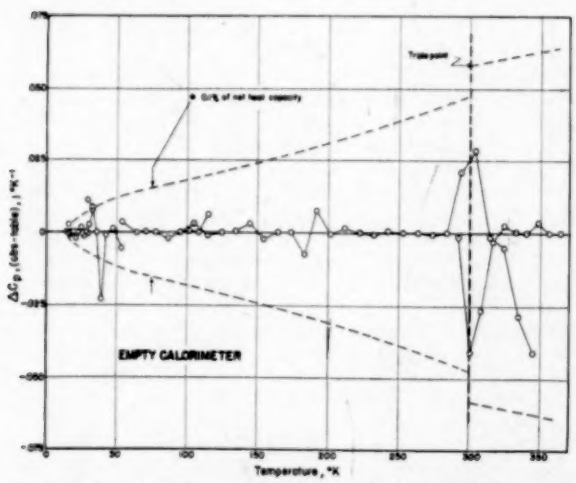

FIGURE 3. *Deviations of experimental heat capacities (corrected for curvature) from smoothed values for the empty container.*

The experiments in a single series of measurements are connected by lines.

5. Reliability of Heat-Capacity Results Obtained With the Low-Temperature Adiabatic Calorimeter

The precision of the heat-capacity experiments is shown in figures 2 and 3 of the previous section, in which the results (corrected for curvature) of the individual measurements are plotted as deviations from smoothed heat-capacity values for sample plus container and for container alone. As the experiments were made over a wide temperature range instead of a series of experiments over the same temperature interval, it is believed that a statement of average deviation is misleading in this situation. The conditions, particularly the heating rate, in the calorimeter were made as close as possible in the two series of experiments, so that certain systematic additive errors would cancel out. As a further check, the heat-capacity experiments were made at heating rates of 0.9 and 1.5 deg/min. Under these conditions large heat leaks dependent upon heating rate should be detectable, but the results obtained with the two heating rates showed no obvious differences on the large-scale deviation plot. In the two sets of measurements, although precaution was taken to install the sample container in the same position within the adiabatic shield system, it is possible that there were some differences in the positioning of the thermels and leads. Any error from this source is indeterminate, but it is believed that the probable error is not greater than ± 0.05 percent.

The effect of impurities on the heat-capacity results is considered to be negligible.

Upon consideration of the above uncertainties the probable error of ± 0.2 percent is assigned to the heat-capacity values above 50° K in table 4. Below 50° K the accuracy is less, increasing to about 1 percent at 18° K.

III. High-Temperature Calorimetry

1. Method and Apparatus

The enthalpy measurements at higher temperatures, which supplement the heat-capacity measurements made from 18° to 360° K, covered the range 273° to 573° K (0° to 300° C). These were carried out by essentially the same method and apparatus as used previously in measurements on sodium up to 900° C [6]. In brief, the method is as follows. The sample, sealed in its container, is suspended in a furnace until it comes to the chosen constant temperature, as measured by a platinum resistance thermometer. It is then dropped into a Bunsen ice calorimeter, which measures the heat evolved by the sample plus container in cooling to 0° C. A similar experiment is made with the empty container at the same temperature. The change in enthalpy of the sample between 0° C and the temperature in the furnace is computed from the difference in the two values of heat. The heat capacity can be derived from enthalpy values of the sample so determined for a series of temperatures.

The sample was taken from the same supply as that used in the low-temperature measurements. A sample of about 8 g of the solid was melted and transferred to a monel container (volume, about 11 ml), which was similar to the container used in earlier measurements on *p*-xylene [7]. In order to remove most of the air and water in the sample, the container was heated to about 100° C while evacuating the space above the sample. The method of sealing the container while still evacuating is shown in figure 4. One end of the container is made with a threaded projection, which can be temporarily sealed to a connecting fitting by means of a tin gasket, *C*. The container can be evacuated and filled through the filling tube, *B*. The actual sealing of the container is at the gold gasket, *D*, which is attached to the bottom end of the monel screw insert. Rotation of the screw insert for sealing is accomplished by the screw driver, *A*, which is sealed from the atmosphere by a packing not shown. In this way, it is possible to retain all the advantages of a valve with a packing, but reduce the mass and thereby the heat capacity, of the sealed container to a minimum. Also, the mass of the metal container is definite and not dependent on a soldered seal, as in the low temperature adiabatic calorimeter.

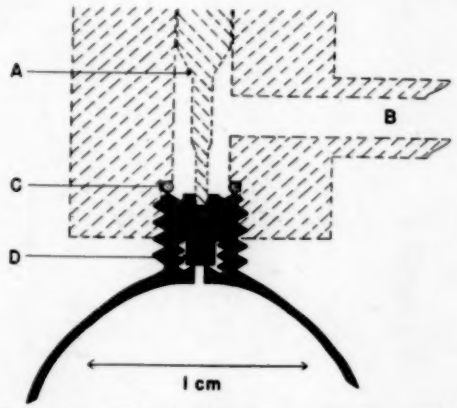

FIGURE 4. *Filling device and the seal for the capsule.*
A, Screw driver; B, filling tube; C, tin gasket; D, gold gasket.

2. Results

The results of the individual experiments are given in columns 2 and 3 of table 3. The measured heats listed are obtained from the mass of mercury drawn into the ice calorimeter, using the calorimeter calibration factor [6] of 270.46 abs j/g of mercury.

About 100 measurements were made, of which 56 were made with 7.8152 g (in vacuum) of sample in the container and the remainder with the empty container. The diphenyl ether was found to be solidified at 0° C in all experiments. Hence, every enthalpy calculated from a drop experiment starting with the liquid includes the heat of fusion. The sample was initially in the liquid state in all experiments except a few at furnace temperatures of 25.00° and 26.60° C (just below the triple point). In these experiments, the sample was solidified by dropping into the ice calorimeter prior to holding the solid sample in the furnace. By also making experiments with the supercooled liquid at the same temperatures as with the solid, there was obtained by differences the heats of fusion of 17,059 and 17,071 abs j mole^{-1} at 25.00° and 26.60° C, respectively. Upon extrapolation to the triple point, 26.87° C, using the heat capacities of solid and liquid found with the low-temperature adiabatic vacuum calorimeter, these values yield respectively 17,154 and 17,085 for the heat of fusion at the triple point. These values are lower by 0.3 and 0.7 percent, respectively, than the corresponding value of 17,216 abs j mole^{-1} found with the adiabatic calorimeter, and are considered much less reliable than the latter value. This is partly because of the small absolute uncertainty inherent in all measurements of heat by the ice calorimeter and partly because the sample used in the ice-calorimeter measurements was much smaller, so that a trace of impurity soluble in the diphenyl ether may have caused enough premelting at these temperatures to explain part of the discrepancy.

The difference between the measured heats for the empty container and the container with sample (columns 2 and 3 in table 3) gives essentially the enthalpy change in the sample between 0° C and the temperature involved. Actually, to get the true enthalpy change, this difference was corrected by an equation given by Osborne [8],

$$[Q]_1^2=[q-pV+mH+(V-m\,v)L/(v'-v)]_1^2, \qquad (4)$$

where $[Q]_1^2$ is the heat evolved in cooling a closed container in which there is a liquid in equilibrium with its vapor from temperature 2 to temperature 1;

TABLE 3. *Experimental results with the furnace and ice calorimeter*

Furnace temperature	Measured heat		[a] Enthalpy change of the $(C_6H_5)_2O$		
	Empty container	With $(C_6H_5)_2O$	Observed	Calculated from equation 5	Observed minus calculated
°C	*abs j*	*abs j*	*abs j mole*$^{-1}$	*abs j mole*$^{-1}$	*abs j mole*$^{-1}$
		[b] 366.8			
		[b] 367.4			
		[b] 367.9			
		370.1			
		368.0			
		368.4	5,146		
		366.7			
		368.3			
	132.8	368.1			
	132.5	368.2			
	131.8	368.2			
	131.9	368.6			
[c] 25.00 (solid)	131.6	1150.3			
	129.9	1151.0			
	132.1	1148.2			
	132.0	1150.1			
		1154.4			
		1150.0	22,206	22,209	−3
		1152.7			
		1149.9			
		1151.8			
[c] 25.00 (liquid)		1153.2			
		1153.5			
		1152.0			
		395.9			
		394.5			
[c] 26.60 (solid)		394.9			
		[d] 397.1			
		[d] 397.7			
		[d] 397.7			
[c] 26.60 (liquid)		[d] 397.2			
		1181.1			
		1179.4			
	[e](258.2)				
	262.3				
	264.2	1600.4			
	263.8	1597.5			
50.00	264.1	1598.9	29,078	29,042	+36
	263.5	1598.5			
	264.2				
	262.6				
	263.4				
	264.6				
	400.5				
	397.5				
75.00	398.1				
	[e](410.4)				
	399.2				
	535.2				
	535.0	2531.2			
	534.9	2531.0			
100.00	534.0	2536.0	43,484	43,548	−64
	536.8	2528.6			
	534.2				
	534.6				
	809.1	3528.7			
	809.1	3528.2			
150.00	810.1	3527.0	59,203	59,176	+27
	809.1	[e](3521.0)			
	1089.8	4578.6			
	1084.9	4574.5			
200.00	1092.3	4575.6	75,922	75,927	−5
	1089.2	4574.6			
	1089.7				
	1372.1	5687.6			
	1374.0	5685.5			
250.00	1373.4	5681.2	93,856	93,799	+57
		5679.8			
	1660.4	6837.4			
300.00	1660.3	6837.2	112,754	112,794	−40
	1658.9	6837.8			

[a] The contribution from vaporization has been eliminated.
[b] Not included in the mean because for these experiments the diphenyl ether was frozen rapidly, using dry ice.
[c] State of the sample at the furnace temperature.
[d] Experiment made after the higher-temperature experiments. The preceding three experiments of this set were made before the diphenyl ether had been heated above 150° C.
[e] Rejected by Chauvenet's criterion.

q is the contribution to Q made by the empty container, shields, and suspension wire: p is the vapor pressure of the liquid; V is the volume of the container; m is the total mass of liquid and vapor; H is the enthalpy per unit mass of the "saturated" liquid (i. e., at pressure p); v' and v are the specific volumes of saturated vapor and liquid, respectively; and L is the enthalpy of vaporization per unit mass. The maximum value of each of the two correction terms that convert measured heats $([Q-q]_1^2)$ to get true enthalpy $[H]_1^2$ amounted to only 0.05 percent at the highest temperature, 300° C. The mean values of enthalpy listed in column 4 of table 3 have been corrected in this way and converted to molal basis.

The mean values of enthalpy of the liquid diphenyl ether at each temperature (26.87° to 300° C) were fitted by an equation whose constants were determined by least squares:

$$H_t(\text{liquid})-H_0(\text{solid})=15657.2+256.4649t+0.224409t^2, \quad (5)$$

where $H_t(\text{liquid})-H_0(\text{solid})$ is the enthalpy difference in abs j mole^{-1} (mole wt=170.20) between the liquid at $t°$ and the solid at 0° C. In evaluating the constants, equal weight was given to values of enthalpy, and at each temperature a weighting factor was used to correspond to the number of determinations made at that temperature.[4] The values calculated from eq 5 are given in column 5 of table 3.

Values of $C_{\text{sat.}}$ the heat capacity of the "saturated" liquid (in equilibrium with its vapor), were calculated from the thermodynamic relation

$$C_{\text{sat.}}=\left(\frac{\partial H}{\partial T}\right)_{\text{sat.}}-V_{\text{sat.}}\left(\frac{dp}{dT}\right)_{\text{sat.}}, \quad (6)$$

where $V_{\text{sat.}}$ is the molal volume of the liquid and p the vapor pressure. The values of $(\partial H/\partial T)_{\text{sat.}}$ were determined by differentiating eq 5. The maximum contribution of the last term in the temperature range studied is at 300° C, and amounts to 0.15 percent of the heat capacity. The values of heat capacity so calculated may be represented by the equation

$$C_{\text{sat.}}=0.448818(T-273.16)+256.4649-V_{\text{sat.}}\left(\frac{dp}{dT}\right)_{\text{sat.}}. \quad (7)$$

The values of heat capacity listed in table 4 at temperatures of 370° K and above are those calculated from this equation.

[4] Actually, the weighting factor used was $(1/a+1/b)^{-1}$, where a and b are the number of runs on the empty and the filled container, respectively, as it is the difference between the enthalpies of these two, which determines the net enthalpy of the sample.

TABLE 4. *Heat capacity, enthalpy, and entropy of solid and liquid diphenyl ether at saturation pressures*

T	$C_{sat.}$	$(H_{sat.}-H^{\circ}_0)$	$(S_{sat.}-S_0)$
	SOLID		
° K	*abs j deg⁻¹ mole⁻¹*	*abs j mole⁻¹*	*abs j deg⁻¹ mole⁻¹*
2	0.027	0.014	0.009
4	.213	.213	.068
6	.718	1.077	.240
8	1.699	3.401	.567
10	3.283	8.272	1.105
12	5.497	16.952	1.889
14	8.272	30.670	2.941
16	11.52	50.413	4.255
18	14.91	76.845	5.807
20	18.06	109.83	7.542
22	21.17	149.08	9.409
24	24.29	194.54	11.386
26	27.33	246.11	13.451
28	30.30	303.81	15.585
30	33.16	367.29	17.769
32	35.88	436.39	19.998
34	38.48	510.77	22.262
36	40.95	590.25	24.526
38	43.28	674.50	26.806
40	45.44	763.18	29.087
42	47.45	856.11	31.351
44	49.34	952.95	33.597
46	51.13	1053.4	35.827
48	52.85	1157.4	38.040
50	54.53	1264.8	40.235
55	58.41	1547.3	45.614
60	61.92	1848.2	50.856
65	65.14	2166.0	55.928
70	68.11	2499.2	60.881
75	70.97	2846.9	65.693
80	73.77	3208.8	70.344
85	76.52	3584.6	74.888
90	79.19	3973.8	79.347
95	81.80	4376.4	83.704
100	84.35	4791.8	87.959
105	86.90	5219.9	92.129
110	89.49	5661.0	96.231
115	92.15	6115.0	100.28
120	94.82	6582.5	104.25
125	97.53	7063.3	108.18
130	100.26	7557.7	112.06
135	103.04	8066.0	115.89
140	105.88	8588.3	119.68
145	108.77	9124.9	123.46
150	111.72	9676.2	127.19
155	114.68	10243	130.90
160	117.64	10823	134.59
165	120.64	11419	138.25
170	123.70	12030	141.91
175	126.80	12656	145.54
180	129.98	13298	149.15
185	133.20	13956	152.75
190	136.45	14632	156.35
195	139.75	15321	159.94
200	143.09	16028	163.53
205	146.47	16751	167.10
210	149.88	17493	170.68
215	153.35	18251	174.23
220	156.86	19027	177.81
225	160.41	19820	181.37
230	164.00	20630	184.94
235	167.65	21459	188.50
240	171.32	22306	192.07
245	175.05	23173	195.65
250	178.83	24058	199.22
255	182.64	24962	202.79
260	186.49	25884	206.37
265	190.37	26825	209.96
270	194.25	27787	213.55
275	198.15	28769	217.16
280	202.04	29770	220.77
285	205.98	30789	224.38
290	209.94	31829	227.98
295	213.98	32888	231.61
298.16	216.56	33569	233.91
300	218.06	33969	235.25
300.032	218.25	33975	235.27

TABLE 4. *Heat capacity, enthalpy, and entropy of solid and liquid diphenyl ether at saturation pressures*—Continued

T	$C_{sat.}$	$(H_{sat.}-H^{\circ}_0)$	$(S_{sat.}-S_0)$
	LIQUID		
° K	*abs j deg⁻¹ mole⁻¹*	*abs j mole⁻¹*	*abs j deg⁻¹ mole⁻¹*
300.032	268.42	51188	292.61
310	272.71	53884	301.45
320	277.17	56634	310.18
330	281.71	59428	318.78
340	286.25	62268	327.25
350	290.79	65153	335.62
360	295.35	68084	343.87
370	299.90	71060	352.03
380	304.39	74082	360.08
390	308.86	77148	368.05
400	313.33	80259	375.93
410	317.89	83415	383.72
420	322.36	86617	391.43
430	326.84	89863	399.07
440	331.30	93155	406.64
450	335.77	96491	414.13
460	340.32	99872	421.56
470	344.71	103298	428.93
480	349.16	106769	436.23
490	353.60	110284	443.48
500	358.04	113845	450.66
510	362.48	117450	457.80
520	366.92	121100	464.88
530	371.35	124794	471.91
540	375.78	128534	478.89
550	380.19	132318	485.83
560	384.63	136148	492.72
570	389.05	140022	499.57

3. Reliability of Results With Ice Calorimeter

In order to check the over-all accuracy of operation of the apparatus, heat-capacity experiments were made at temperatures of 25° and 250° C with water sealed in the container. In these tests, it was convenient for comparison of the results to make two series of measurements similar to those described in the measurements with water [9]. One series was made with the container mostly full of water, while the other series was made with a small amount of water. The results of the experiments compare very favorably with the results of the earlier work [9] with an adiabatic calorimeter. The average heat capacity from 0° to 250° C, as measured with the present apparatus, is about 0.02 percent lower than that measured with the earlier apparatus, with a reproducibility of about ±0.02 percent. This is well within the accuracy of the earlier work. At 25° C the reproducibility of the present apparatus was relatively poor, giving a value of about ±0.14 percent for the average deviation of the mean. In spite of this, the measured average heat capacity from 0° to 25° C was only about 0.05 percent lower than the accepted accurate value [9].

The reliability of the results may be considered in two ways. First, there is the reproducibility or precision of the experiments. The average deviation of a single experiment from the mean at a given temperature was ±0.19 percent in the case of the empty containers and ±0.09 percent in the case of the containers with the sample. As the enthalpy of the sample was about two to three times as great

as that of the empty container, the larger deviations with the empty container are not so important. At a given temperature the calculated probable error of the mean of the net enthalpy of liquid diphenyl ether, referred to that of the solid at 0° C, is about 0.04 percent. This error is about the same at all furnace temperatures.

In addition to the reproducibility of the results, there must be considered the sources of systematic errors. Many such errors have already been considered in other measurements with this apparatus [10] and will not be reviewed here. The ice-point reading of the platinum resistance thermometer was frequently redetermined during the measurements. On the basis of the small changes thereby noted, small corrections were applied to the heat measurements for deviations from the nominal temperatures. As these corrections were always less than 0.01 percent of the heat measured, it is believed that errors in the temperature scale did not appreciably affect the values of heat capacity.

Another source of systematic error is the effect of impurity in the sample. The measurements with the low-temperature adiabatic calorimeter indicated that the impurities in the sample amounted to only about 0.000013 mole fraction. However, in these measurements, considerable effort was made to remove both air and water. In the measurements with the ice calorimeter, some solid sample was melted and quickly transferred to the sample container, which was heated while pumping before sealing the capsule. Under these conditions, it seems improbable that the impurities amounted to more than 0.00005 mole fraction, a value that may be neglected insofar as effect on the heat-capacity values reported. However, small impurities affect greatly the measurements on the heat of fusion where the enthalpy of the solid is measured at temperatures close to the triple point. For example, in the measurements at 26.60° C (triple point=26.87° C), the measurements with the ice calorimeter gave a value of the enthalpy of the solid that corresponded to a heat of fusion value about 0.7 percent lower than that obtained with the adiabatic calorimeter. This difference could be explained by an impurity of about 0.00005 mole fraction in the sample. It is believed that the heat of fusion value obtained with the adiabatic calorimeter is the more accurate value.

Another factor affecting the reliability of the results is the question of the chemical stability of the diphenyl ether at the higher temperatures. The rate of spontaneous decomposition of diphenyl ether at 300° C does not seem to have been estimated previously. As this is the highest temperature to which the sample was subjected, a number of enthalpy determinations were made on the solid at 26.60° C (0.27 deg below the triple point) before and after several hours of heating to the higher temperatures.

Considering only the mean results of these two sets, it appears that the apparent relative enthalpy was greater in the second set of experiments by 47 abs j $mole^{-1}$. This corresponds to 0.3 percent more of the sample melted. It can readily be shown that this would be caused by an increase in impurity of only 0.00002 mole fraction. Here again, this impurity would not affect the reliability of the heat-capacity results, although it would have some significance in the heat of fusion value calculated from the measurements on the solid at 26.60° C.

Another source of systematic error lies in the uncertainty in the mass of the sample. The mass of the empty container was 0.0033 g less during the experiments with the empty container than it was before introducing the sample. The mass of the sample was taken to be the difference in weight of the full container and the container after removing the sample. It is possible that some material other than the sample was removed in this process, in which case, an uncertainty of as large as 0.04 percent might exist in the mass of the sample. The other sources of error, such as temperature measurement, calorimeter calibration factor, variation in heat loss on dropping the sample from the furnace, and possible slightly inaccurate correction for condensation of vapor inside the container, are estimated each to contribute an uncertainty to the enthalpy and heat capacity of from 0.01 to 0.02 percent.

Considering these various sources of error, it is believed that the values of relative enthalpy represented by eq 5 have the probable error of ± 0.15 percent, except below 100° C, where the probable error must be considered greater. Similarly, it was estimated that the values of heat capacity of the liquid as determined by the ice calorimeter (eq 7) have the probable error of ± 0.25 percent, except near 25° and 300° C, where the course of the enthalpy curve is more uncertain.

IV. Tabulated Heat Capacities

In the temperature range 300° to 360° K, values of heat capacity are obtained with both the low-temperature adiabatic calorimeter and the ice calorimeter. The values, except between 300° and 320° K, are displaced almost parallel from each other, the displacement being about 0.45 abs j deg^{-1} $mole^{-1}$. This difference between the two sets of values, however, is smaller than the estimates of absolute error claimed with the two methods. The results with the two methods were adjusted so that continuity exists in the heat capacity curve between the overlap range and the range above 360° K. The problem of continuity at 300° K does not arise because the heat-capacity curve is discontinuous at the triple-point temperature (300.03° K). The results from the two methods were adjusted with the following considerations. The enthalpy experiments with the ice-calorimeter method decrease in sensitivity with approach to the ice point; furthermore, derivatives of the enthalpy equation become less accurate toward the end of the experimental temperature range. The shield control in the adiabatic vacuum calorimeter becomes a little unwieldy at higher temperatures, and at the same time heat transfer by radiation can be significant if any unknown thermal gradients exist in the calorimeter.

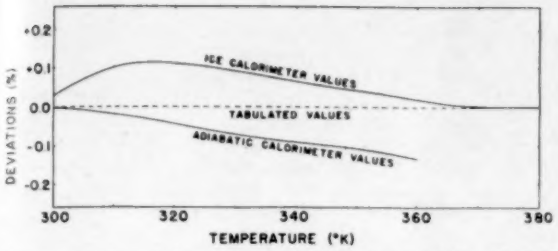

FIGURE 5. *Comparison of smoothed heat capacities obtained by the two experimental methods with the final values in table 4.*

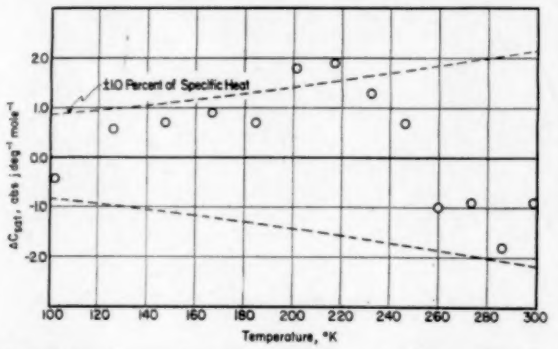

FIGURE 6. *Comparison of the values of heat capacity given in table 4 with the results of Smith and Andrews.*

The base line represents the values from the table.

The results from the ice calorimeter were given progressively greater weight toward 360° K and the results from the adiabatic vacuum calorimeter greater weight toward 300° K. A comparison of the results from these two calorimeters with the adjusted tabulated values from table 4 is given in figure 5, which shows that the maximum difference is about 0.13 percent.

The survey of literature revealed only one publication on the heat capacity of diphenyl ether. Smith and Andrews [11] measured the heat capacity from 100° to 300° K, using a heat conduction calorimeter. In figure 6 these results are compared with the tabulated values of table 4. In general, the values given by these authors are higher below 246° K and lower above this temperature. The over-all discrepancy amounts to about ±1 percent; the maximum discrepancy amounts to 1.2 percent. These authors claimed an accuracy of 1 percent for their apparatus.

V. Combustion Calorimetry

1. Apparatus and Procedure

The apparatus and procedure used in measuring the heat of combustion, with the exception of the Wheatstone bridge used in measurement of temperature, have been described in several previous publications [12, 13, 14]. The bridge used is a special Mueller type instrument with gold-chromium alloy resistance coils, which have negligible temperature coefficient of resistance so that the bridge does not need to be thermostated. The energy equivalent of the calorimetric system was determined by six experiments with NBS Standard Sample 39f, benzoic acid, using the value 26,433.8 abs j/g mass (weight in vacuum), previously obtained in this laboratory [15, 16, 17], for the heat of combustion of this substance under the standard conditions of the bomb process. The mean value obtained for the energy equivalent is 13,976.42 abs j deg^{-1}, and the standard deviation of the mean is ±0.64 abs j deg^{-1}. (See footnote a, table 5 for the definition of standard deviation.)

The observed heat of combustion in each experiment was corrected for the heat of stirring and the heat transfer between the jacket and calorimeter, for the energy used in firing the charge and for the energy of formation of nitric acid in the bomb. The observed values of the heat of combustion of diphenyl ether were reduced to $-\Delta U_c^\circ$ [18], the decrease in intrinsic energy accompanying the combustion reaction

$$C_{12}H_{10}O_{(l)}+14O_{2(g)}=12CO_{2(g)}+5H_2O_{(l)}$$

with the components in their thermodynamic standard states at 30° C. In the above reaction the standard state for diphenyl ether was taken as that of the liquid at 1-atm pressure.

Three combustion experiments were made with the samples of diphenyl ether in an open platinum crucible, and three with the samples enclosed in thin-walled glass bulbs [19, 20] flattened on opposite sides. The method for filling the bulbs is described in the references given. The weight of the glass in each bulb was about 0.05 g. There was no significant difference in the results obtained by the two methods.

The carbon dioxide formed in the combustion was absorbed in Ascarite and weighed, following the procedure described by Prosen and Rossini [21]. The absorption train, however, did not contain any provision to oxidize and absorb products of incomplete combustion. When the escaping bomb gases in each experiment were tested for carbon monoxide, using a NBS colorimeter method [22], only negligible traces of carbon monoxide were found.

2. Results

Table 5 gives the results of the heat of combustion measurements, where $-\Delta U_B$ is the observed heat of combustion under the conditions specified by the volume of the bomb (381 ml), the mass of water (1 g) placed in the bomb and the data given in columns 1 and 3; and $-\Delta U_c^\circ$ represents the decrease in intrinsic energy accompanying the combustion reaction when the components of the reaction are in their appropriate thermodynamic standard states at 30° C.

Except for the first experiment, in which the weight of the sample was apparently in error, the values obtained for the masses of carbon dioxide formed in the combustion are lower than the corresponding values calculated stoichiometrically from

TABLE 5. *Heat of combustion of diphenyl ether*

Defined calorie = 4.1840 abs j

Mass of sample	Initial O_2 pressure at 30° C	Mass of CO_2	Heat of combustion at 30° C	
			$-\Delta U_B^\circ$	$-\Delta U_C^\circ$
Burned in platinum crucible				
g	*atm*	*g*	*abs j/g* CO_2	*abs j/g* CO_2
1.13500	31.1	3.52667	11613.33	11606.00
1.08319	30.4	3.35893	11616.98	11609.84
1.09104	30.4	3.38367	11620.74	11613.59
Burned in glass bulb				
1.12596	31.4	3.49271	11613.26	11605.87
1.10658	30.3	3.43144	11616.85	11609.68
0.99321	29.2	3.08082	11612.05	11605.06
Mean				11608.06
Standard deviation of the mean [a]				±1.34

	kj/mole	*kcal/mole*
$-\Delta U_C^\circ$ (*l*, 30° C)	[b] 6130.60 ±0.88	[b] 1465.25 ±0.21
$-\Delta H_C^\circ$ (*l*, 30° C)	[b] 6135.64 ±0.88	[b] 1466.45 ±0.21
$-\Delta H_C^\circ$ (*l*, 25° C)	[b] 6136.36 ±0.88	[b] 1466.63 ±0.21
$-\Delta H_C^\circ$ (*c*, 25° C)	[b] 6119.24 ±0.88	[b] 1462.53 ±0.21

[a] Standard deviation of the mean as used above is defined as $[\Sigma d^2/n\,(n-1)]^{\frac{1}{2}}$; where d is the difference between a single observation and the mean, and n is the number of observations.

[b] The value following the ± sign is a measure of the precision of the result, which is defined as follows [23]:

$$s = Q\sqrt{(s_E/E)^2+(s_Q/Q)^2+(s_R/R)^2+(s_H/H)^2},$$

In this expression, s_E is the standard deviation of the mean of the results of the series of experiments with benzoic acid to determine E, the energy equivalent of the calorimetric system; s_Q is the standard deviation of the mean of the results of the series of experiments to determine the heat of combustion, Q, of the diphenyl ether; s_R/R is an allowance of 5×10^{-4} for the standard deviation of the value used for the heat of combustion of benzoic acid; s_H/R is an allowance of 5×10^{-4} for the standard deviation associated with the determination of the amount of the combustion reaction from the mass of carbon dioxide formed.

the masses of the sample burned. Excluding the first experiment, the average difference between the observed and calculated masses of carbon dioxide is 0.05 percent. The masses of carbon dioxide formed in the combustion of NBS Standard Sample 39f, benzoic acid, before and after the work with diphenyl ether agreed with the calculated values on the average within 0.010 percent. The low experimental value for the carbon dioxide formed in the combustion of diphenyl ether is probably due to air and water absorbed by the sample before the combustion experiment was made. These impurities have practically no effect on the value obtained for the heat of combustion per gram of carbon dioxide formed.

In table 5 are listed the values obtained for the heat of combustion per mole of liquid diphenyl ether at 30° C and of both liquid and solid at 25° C. The calculations were based on the mass of carbon dioxide formed in the combustion reaction, using the mean $-\Delta U_C^\circ$ per gram of carbon dioxide given in the same table and the value 44.010 g for the molecular weight of carbon dioxide. The results at 25° C were obtained, using the values of heat capacity and heat of fusion of diphenyl ether obtained in this work, together with the values of the heat capacity of gaseous carbon dioxide and oxygen and liquid water given in references [9, 24].

VI. Derived Thermal Properties

1. Enthalpy and Entropy

In table 4, columns 3 and 4, the values of enthalpy and entropy, respectively, are tabulated at integral temperatures for intervals of 2 deg from 0° to 50° K, 5 deg from 50° to 300° K, and 10 deg from 300° to 570° K. For most purposes any intermediate values can be obtained by linear interpolation or more accurately by quadratic interpolation. These properties were obtained by evaluating the thermodynamic relations

$$H_{\text{sat.}}-E_0^\circ=\int_0^T C_{\text{sat.}}\,dT+L_f+\int_0^T V_{\text{sat.}}\left(\frac{dp}{dT}\right)_{\text{sat.}}dT, \quad (8)$$

$$S_{\text{sat.}}-S_0=\int_0^T \frac{C_{\text{sat.}}\,dT}{T}+\frac{L_f}{T_t}, \quad (9)$$

where E_0° is the internal energy of the solid diphenyl ether at absolute zero to which the enthalpy values are referred. S_0 is the entropy of the solid at absolute zero, which is considered to be zero for diphenyl ether. The other symbols have the same significance as previously indicated. The term $\int_0^T V_{\text{sat.}}(dp/dT)_{\text{sat.}}dT$ in the enthalpy equation was not applied up to 360° K; even at 570° K, the contribution from this term is only 0.03 percent. The term L_f (heat of fusion) in both expressions obviously is not applicable below the triple point. Below 18° K eq 8 and 9 were evaluated analytically, using the Debye heat capacity function given in eq 3. Between 18° and 570°K these equations were evaluated by tabular integration, using Lagrangian four-point integration coefficients. When the enthalpy values from tabular integration were checked in the interval from 370° to 570° K by evaluating the enthalpy eq 5, the discrepancy was found to be only 3 abs j mole^{-1}. No attempt was made to fit the tabulated values of heat capacity, enthalpy, or entropy between 18° and 370° K to an equation. The internal consistency of tabular integration in this lower temperature range, however, was checked by evaluating the thermodynamic identity:

$$\int_0^T (S_{\text{sat.}}-S_0)dT=T(S_{\text{sat.}}-S_0)-\int_0^T C_{\text{sat.}}\,dT-L_f. \quad (10)$$

Considering the accuracy claimed for the heat-capacity values and the uncertainty involved in the Debye extrapolation, a probable error of ±0.2 percent is assigned to the tabulated values of enthalpy above 50° K and a probable error of ±0.4 abs j deg^{-1} mole^{-1} to entropy in the whole temperature range.

2. Standard Heat of Formation

The standard heat of formation for both liquid and solid diphenyl ether at 298.16° K was calculated from the values of standard heat of combustion for this

material listed in table 5 and from the accepted standard heat of formation for liquid water ($-285{,}840\pm42$ abs j mole^{-1}) and carbon dioxide ($-393{,}513\pm45$ abs j mole^{-1}) [24] by evaluating the relation:

$$\Delta H_f^\circ = \Sigma\Delta H_f^\circ \text{ (products)} - \Delta H_\omega^\circ, \qquad (11)$$

where ΔH_f° is the standard heat of formation; and $\Sigma\Delta H_f^\circ$ (products) is the sum of the standard heats of formation for the products of the combustion reaction. The results so obtained are given by

$$\text{Solid, } \Delta H_{f_{298.16^\circ K}}^\circ = -32.11\pm0.93 \text{ abs kj mole}^{-1}\ ^{5}$$

$$\text{Liquid, } \Delta H_{f_{298.16^\circ K}}^\circ = -14.99\pm0.93 \text{ abs kj mole}^{-1}\ ^{5}$$

3. Standard Entropy of Formation

The standard entropy of formation for solid diphenyl ether at 298.16°K was computed from the standard entropies of diphenyl ether (table 4), graphite (5.720 ± 0.050 abs j deg^{-1} mole^{-1}), gaseous hydrogen (130.574 ± 0.010 abs j deg^{-1} mole^{-1}), gaseous oxygen (205.073 abs j deg^{-1} mole^{-1}) [25] by evaluating the expression:

$$\Delta S_f^\circ = S_C^\circ - \Sigma S_E^\circ. \qquad (12)$$

in which ΔS_f° is the standard entropy of formation; and the subscripts C and E indicate the compound and the element, respectively. The standard entropy of formation for diphenyl ether so obtained is

$$\Delta S_{f_{298.16^\circ K}}^\circ = -590.1\pm0.5 \text{ abs j deg}^{-1} \text{ mole}^{-1}.$$

The assigned probable error was estimated from the probable errors in the standard entropy for diphenyl ether and the elements.

Actually, in carrying out the above calculation the tabulated entropy (table 4) was used directly without correcting to standard state. The amount of this correction can be obtained using the following thermodynamic expression:

$$\left(\frac{\partial S}{\partial P}\right)_T = -\left(\frac{\partial V}{\partial T}\right)_P. \qquad (13)$$

There are no data for the temperature coefficient of expansion for solid diphenyl ether around 298° K, consequently the densities of solid diphenyl ether at 20° C and the liquid at 30° C [26] were used to calculate the maximum possible correction. This correction amounts to 0.02 abs j deg^{-1} mole^{-1}, which does not significantly affect the value of standard entropy of formation.

[5] The precision was determined by evaluating the expression:

$$s = \sqrt{(12s_1)^2+(5s_2)^2+(s_3)^2}$$

where s_1 and s_2 are the standard deviations of the mean of the heat of combustion values for carbon dioxide and water, respectively. s_3 is the precision s given in footnote b, table 5.

4. Standard Gibbs Free Energy of Formation

The standard Gibbs free energy of formation for solid diphenyl ether at 298.16° K was obtained from the values of standard heat and entropy of formation given in previous sections by evaluating the relation:

$$\Delta F_f^\circ = \Delta H_f^\circ - T\Delta S_f^\circ. \qquad (14)$$

The value so obtained is

$$\Delta F_{f_{298.16^\circ K}}^\circ = 143.8\pm0.9 \text{ abs kj mole}^{-1}.$$

The probable error of ±0.9 abs kj mole^{-1} was obtained from statistical combination of the probable errors assigned to the various data used in the calculation.

VII. Discussion

The results of the purity determination indicate that diphenyl ether can be prepared in a state of extremely high purity. This material can be purified quite easily by slow fractional crystallization at room temperature. There is the question of chemical stability with the adiabatic vacuum calorimeter, but the heat of fusion results with the ice calorimeter indicate that even after several hours at 570° K in contact with monel the impurity increased by only 0.00002 mole fraction. No conclusion can be drawn without additional data in regard to the chemical reactivity of diphenyl ether with different metals.

There is implied in one set of enthalpy experiments (table 3) with the ice calorimeter that perhaps conditioning of the diphenyl ether crystal might affect the results of the experiments. The results indicate that the enthalpy is slightly lower for the material when cooled in dry ice. This difference is, however, so small that it is difficult to ascertain whether the effect is real or not. The experiments in the solid range with the adiabatic vacuum calorimeter do not indicate any unusual discrepancy in the results, although the material was subjected to extreme treatments such as freezing rapidly with liquid air and freezing slowly across a vacuum with ice. In the melting-point studies the diphenyl ether required relatively long periods for temperature equilibrium. This, however, is not uncommon with compounds of high molecular weight.

The results of the heat capacity experiments indicate that diphenyl ether is a suitable standard to be used in heat capacity calorimeters below 600° K. It might be possible to use this material above this temperature, but the increase in vapor correction would be undesirable. The material should be provided freed of air and water in ampoules of suitable volume.

As indicated by the 0.05-percent discrepancies in the weighed carbon dioxide from the stoichiometric value, the solubility of air and water in diphenyl ether is relatively high, for there is incomplete

combustion. Considering the difficulties involved in preventing the test material from being exposed to the atmosphere in combusiton calorimetry, diphenyl ether is undesirable as a combustion standard.

The authors express their indebtedness to several members of the Bureau—to F. L. Howard for purifying the diphenyl ether, to R. B. Scott for many helpful suggestions in the use of the adiabatic vacuum calorimeter, to T. B. Douglas and Anne F. Ball for help in taking the measurements and calculating the results with the ice calorimeter, and to R. S. Jessup for many suggestions and help with the combustion bomb calorimeter.

VIII. References

[1] R. B. Scott, C. H. Meyers, R. D. Rands, Jr., F. G. Brickwedde, and N. Bekkedahl, J. Research NBS **35,** 39 (1945) RP1661.
[2] H. F. Stimson, J. Research NBS **42,** 209 (1949) RP1962.
[3] H. J. Hoge and F. G. Brickwedde, J. Research NBS **22,** 351 (1939) RP1188.
[4] N. S. Osborne, H. F. Stimson, T. S. Sligh, and C. S. Cragoe, BS Sci. Pap. **20,** 65 (1925) S501.
[5] H. J. Hoge, J. Research NBS **36,** 111 (1946) RP1693.
[6] D. C. Ginnings, T. B. Douglas, and Anne F. Ball, J. Research NBS **45,** 23 (1950) RP2110.
[7] R. J. Corruccini and D. C. Ginnings, J. Am. Chem. Soc. **69,** 2291 (1947).
[8] N. S. Osborne, BS J. Research **4,** 609 (1930) RP168.
[9] N. S. Osborne, H. F. Stimson, and D. C. Ginnings, J. Research NBS **23,** 197 (1939) RP1228.
[10] D. C. Ginnings and R. J. Corruccini, J. Research NBS **38,** 593 (1947) RP1797.
[11] R. H. Smith and D. H. Andrews, J. Am. Chem. Soc. **53,** 3661 (1931).
[12] H. C. Dickinson, Bul. BS **11,** 189 (1914) S230.
[13] R. S. Jessup and C. B. Green, J. Research NBS **13,** 469 (1934) RP721.
[14] D. E. Roberts, W. W. Walton, and R. S. Jessup, J. Research NBS **38,** 627 (1947) RP1801.
[15] R. S. Jessup, J. Research NBS **29,** 247 (1942) RP1499.
[16] R. S. Jessup, J. Research NBS **36,** 421 (1946) RP1711.
[17] NBS Circular 475, p. 22 (1949).
[18] E. W. Washburn, BS J. Research **10,** 525 (1933) RP546.
[19] T. W. Richards and F. Barry, J. Am. Chem. Soc. **37,** 993 (1915).
[20] R. S. Jessup, J. Research NBS **18,** 115 (1937) RP966.
[21] E. J. R. Prosen and F. D. Rossini, J. Research NBS **27,** 289 (1941) RP1420.
[22] M. Shepherd, Anal. Chem. **19,** 77 (1947).
[23] F. D. Rossini and W. E. Deming, J. Wash. Acad. Sci. **29,** 416 (1939).
[24] Selected values of chemical thermodynamic properties NBS Circular 500 (Dec. 31, 1947).
[25] F. G. Brickwedde, M. Moskow, and J. G. Aston, J. Research NBS **37,** 263 (1946) RP1747; H. W. Woolley, R. B. Scott, and F. G. Brickwedde, J. Research NBS **41,** 379 (1948) RP1932; H. W. Woolley, J. Research NBS **40,** 163 (1948) RP1864; The NBS–NACA Tables of thermal properties of gases, Tables 7.10 and 9.10.
[26] D. I. Zhuravlev, J. Phys. Chem. (USSR) **9,** 876 (1937).

Washington, September 6, 1950.

Journal of Research of the National Bureau of Standards Vol. 46, No. 3, March 1951 Research Paper 2192

Compressibility of Natural and Synthetic High Polymers at High Pressures

Charles E. Weir

Compression data ($-\Delta V/V_0$) are reported between 1,000 and 10,000 atmospheres for the following materials: dry cellulose, polyvinylidene chloride (Saran), polyethylene, polymonochlorotrifluoroethylene (Kel-F), polytetrafluoroethylene (Teflon), a polyester (Selectron 5003), and raw rubbers, Hycar OR25, Hycar OR15, Neoprene, and Thiokol ST. All compression curves are smooth except that for polytetrafluoroethylene, which shows a transition at 5,500 atmospheres, resulting in a change in volume ($\Delta V/V_0$) of approximately 2 percent. Coefficients of the cubic equations, $-\Delta V/V_0 = a(P-2000) + b\ (P-2000)^2 + c\ (P-2000)^3$ fitted to the data are as follows: Cellulose: $a=9.26\times10^{-6}$, $b=-3.25\times10^{-10}$, $c=2.93\times10^{-15}$; polyvinylidene chloride (Saran): $a=2.17\times10^{-5}$, $b=-1.90\times10^{-9}$, $c=8.73\times10^{-14}$; polyethylene: $a=1.89\times10^{-5}$, $b=-1.45\times10^{-9}$, $c=6.10\times10^{-14}$; polymonochlorotrifluoroethylene (Kel-F): $a=9.89\times10^{-6}$, $b=-4.74\times10^{-10}$, $c=8.29\times10^{-15}$; polyester (Selectron 5003): $a=1.76\times10^{-5}$, $b=-1.23\times10^{-9}$, $c=4.82\times10^{-14}$; Hycar OR25: $a=2.26\times10^{-5}$, $b=-2.03\times10^{-9}$, $c=9.09\times10^{-14}$; Hycar OR15: $a=2.17\times10^{-5}$, $b=-2.03\times10^{-9}$, $c=9.42\times10^{-14}$; Neoprene: $a=2.04\times10^{-5}$, $b=-1.75\times10^{-9}$, $c=7.66\times10^{-14}$; Thiokol ST: $a=1.92\times10^{-5}$, $b=-1.41\times10^{-9}$, $c=6.07\times10^{-14}$. Compressibilities calculated from these equations show fictitious minima circa 10,000 atmospheres, although the equations represent the data satisfactorily to 10,000 atmospheres. The data given compare favorably with those obtained on similar materials by previous workers.

I. Introduction

In a previous paper [1] [1] the design, construction, and use of apparatus for measurement of volume change of solids (or liquids) at high pressure was described. The apparatus was applied to a determination of the compression of leather and collagen in the forementioned report. This equipment has been applied subsequently for measurement at room temperature of compression of a number of other materials that fall into the two general categories of high polymeric substances and minerals. The data on compression of minerals is primarily of geological interest and will be reported elsewhere. The results of experiments on high polymers are of particular interest here and constitute the subject of this report.

II. Experimental Method and Treatment of Data

The apparatus and experimental procedure have been described in detail previously [1, 2], and will not be discussed fully here. Briefly, an experiment consists of forcing a leakproof piston into the bore of a heavy-walled cylinder, which contains the specimen immersed in a suitable pressure-transmitting liquid (Varsol, a mixture of naphthenes boiling between 150° and 200° C). Combination of the measurements of depth of penetration of the piston and the internal hydrostatic pressure—made at each 1,000 atm—with measurements obtained from a similar experiment in which the specimen is replaced by a steel bar of comparable volume, permits a calculation of the compression of the specimen. Suitable equations for the calculation, as well as values of the constants of the vessel and the Varsol required, have been given previously [2, 1].

[1] Figures in brackets indicate the literature references at the end of this paper.

Measurements were made in the pressure range 1,000 to 10,000 atm. The upper limit of 10,000 atm was self-imposed as a result of a crack existing in the ram, while the lower limit of 1,000 atm is imposed in this type of experiment by frictional forces between packing washers and the bore of the vessel.

The notation used here conforms to that followed for many years by workers at the Geophysical Laboratory of the Carnegie Institute of Washington. The compression $-\Delta V/V_0$ is defined as $-(V_p - V')/V_0$, where V_p is the volume at pressure P; V' is the volume at the experimental reference pressure of 2,000 atm; and V_0 is the initial volume at atmospheric pressure. The subscript zero may be taken to refer to zero atmospheres, since in these and most other high-pressure measurements, the volume change occurring between 0 and 1 atm is insignificant. The compression occurring between 1 and 2,000 atm is designated by $-\Delta V'/V_0$ and is equal to $-(V'-V_0)/V_0$. This compression which is not measured in these experiments is referred to as the initial compression.

Estimation of the initial compression that occurs between 1 and 2,000 atm was made by successive extrapolations of tentative calculations of compression to 1 atm rather than by the least squares method previously described [1]. While this extrapolation is not to be construed as more than moderately accurate, it is believed sufficiently accurate for the following reason: The required initial compression enters the calculation in a correction term that is usually small. Errors in assessment of the initial compression of as much as a few tenths of a percent result in negligible variation in the measured values between 1,000 and 10,000 atm. However, if the compression is reckoned from 1 atm, the initial compression ($-\Delta V'/V_0$, 1 to 2,000 atm) must be added to the measured values, and the final results will be subject to at least as much uncertainty as is involved in the initial compression. To eliminate this uncer-

tainty, all data and calculations are based on the experimental reference pressure of 2,000 atm, at which $-\Delta V/V_0$ is taken to be zero. Values at 1,000 atm therefore appear as negative compressions, which as a result of the previously mentioned frictional forces, are less reliable than data at higher pressures.

In the present experiments no serious attempt was made to establish the presence of slow plastic flow under hydrostatic pressure. Most observations made during measurements, however, indicate that if such a process occurs a much longer time than was used here must be employed for its detection. Pressure equilibrium in these measurements appeared to be obtained in 15 to 20 minutes following each pressure change, a period of time ordinarily required for establishment of thermal equilibrium [1]. Observations made during measurements were indicative of an instantaneous response to pressure changes in all specimens except Thiokol rubber. The agreement of data obtained in duplicate measurements made on some specimens also tends to indicate negligible permanent set.

During the course of these experiments the dial gage, which was used to measure the depth of penetration of the piston, was remounted directly on the ram itself. Measurements with all rubber samples were made with this arrangement. All other data were obtained with the dial gage mounted on the top platen of the press.

III. Materials Studied

There is a scarcity of data on behavior of all polymeric materials in this pressure range, but the choice of materials to be studied was dictated by the Varsol used as the confining liquid. Only those available materials expected to be resistant to swelling by Varsol were studied. The following materials were investigated:

Cellulose.—A sample of purified cotton was compressed into cylindrical form for test and was dried at 100° C in vacuum (<2 mm Hg) for 48 hours. This specimen is referred to as dry cellulose, and had a density of 1.521 g/cm³ at 20° C, as measured by hydrostatic weighing in Varsol [1].

Polytetrafluoroethylene (*Teflon*).—One sample of Teflon, denoted sample A, was an opaque, grey rod having a density of 2.236 g/cm³ at 20° C. The previous history of this sample is unknown. Sample B was obtained from the E. I. Dupont de Nemours & Co., and was a rod of mottled greyish color having a density of 2.219 g/cm³ at 20° C. The mottled appearance was caused by dispersed dark material in the greyish bulk of the rod.

Polymonochlorotrifluoroethylene (*Kel-F*).*—A sheet of this material was available for test. The material was transparent with a slight opalescence and had a density of 3.168 g/cm³ at 20° C. A bundle of strips of suitable width, cut from the sheet, comprised the test specimen.

Polyethylene.—A molded rod, which served as test specimen, had a density of 0.917 g/cm³ at 20° C.

*This material is of uncertain origin and history.

Polyvinylidenechloride (*Saran*).—A sheet of this substance was available for study.

The material was very dark in color, and had a density of 1.099 g/cm³ at 20° C. A bundle of strips cut from the sheet formed the test specimen.

Polyester.—A molded rod of this material was made of Selectron 5003, and was a brittle rigid product having a slightly yellowish cast. The density was found to be 1.190 g/cm³ at 20° C.

All rubbers studied were raw stock containing no fillers or added vulcanizing agents, as follows:

Hycar OR25.—A molded cyclinder of density 0.972 g/cm³ at 20° C.

Hycar OR15.—A molded cylinder of density 0.964 g/cm³ at 20° C.

Neoprene.—A rough cylinder cut manually from an irregularly shaped piece of raw stock. This sample was probably partially crystalline, and had a density of 1.134 g/cm³ at 20° C.

Thiokol ST.—A test specimen formed by stacking disks of rubber cut from an irregularly shaped piece of raw material. The density of the specimen was 1.298 g/cm³ at 20° C.

IV. Results and Discussion

1. Synthetic Plastics and Cellulose

The results of measurements made on cellulose, polyethylene, polymonochlorotrifluorethylene, polyvinylidene chloride, and a polyester are given in table 1.

The initial volume (at 1 atm), V_0; the volume at the reference pressure (2,000 atm), V'; the compression assumed between 1 and 2,000 atm, $-\Delta V'/V_0$; and the density, ρ, are given at the head of the appropriate sections of the table. In some instances duplicate measurements were made on the same specimens to ascertain the reproducibility. Such duplicates are referred to as run 1 and run 2, and the average of the values obtained appears as a separate column in these instances. The last column of each section contains calculated values of compression obtained by solving the equation: $-\Delta V/V_0 = a(P-2000)+b(P-2000)^2+c(P-2000)^3$, which was fitted to the data by the method of least squares. The appropriate values of the constants of the equation are compiled in tabular form in table 4.

The large compressions experienced by the synthetic materials are to be noted. The decrease in volume of these materials appears to be approximately inversely related to the density, a relationship that has been pointed out frequently by Bridgman [3]. The synthetic polymers are generally more compressible than the natural polymers cellulose and leather reported previously [1]. The dense Kel-F, however, is less compressible than leather and nearly equally compressible as cellulose.

The synthetic materials were weighed in air before and after test to ascertain the amount of absorption of Varsol. The increase in weight noted for all synthetics of table 1, except for polyvinylidene chloride, amounted to no more than 5 mg. Poly-

TABLE 1. *Compression of natural and synthetic polymers*

Pressure	Dry cellulose (purified cotton)		Polyvinylidene chloride (Saran)				Polyester (Selectron 5003)	
	V_0=10.527 ml V'=10.290 ml $-\Delta V'/V_0$=0.0225 $\rho_{20°}$=1.521		V_0=11.377 ml V'=10.694 ml $-\Delta V'/V_0$=0.060 $\rho_{20°}$=1.699				V_0=16.031 ml V'=15.390 ml $-\Delta V'/V_0$=0.040 $\rho_{20°}$=1.190	
	Measured, $-\Delta V/V_0$	Calculated, $-\Delta V/V_0$	Measured			Calculated, $-\Delta V/V_0$	Measured, $-\Delta V/V_0$	Calculated, $-\Delta V/V_0$
			Run 1 $-\Delta V/V_0$	Run 2 $-\Delta V/V_0$	Average, $-\Delta V/V_0$			
atm								
10,000	0.0534	0.0548	0.0959	0.0962	0.0960	0.0963	0.0867	0.0864
9,000	.0497	.0499	.0889	.0888	.0888	.0884	.0716	.0795
8,000	.0441	.0434	.0808	.0807	.0808	.0804	.0717	.0718
7,000	.0380	.0386	.0717	.0714	.0716	.0717	.0634	.0633
6,000	.0304	.0320	.0612	.0616	.0614	.0618	.0538	.0538
5,000	.0245	.0248	.0501	.0495	.0498	.0502	.0431	.0431
4,000	.0178	.0172	.0368	.0364	.0366	.0364	.0306	.0307
3,000	.0090	.0080	.0210	.0204	.0207	.0199	.0163	.0164
2,000	.0000	.0000	.0000	.0000	.0000	.0000	.0000	.0000
1,000	*−.0104	−.0096	*−.0259	*−.0260	*−.0260	−.0237	----------	−.0189

Pressure	Polyethylene V_0=14.742 ml V'=14.004 ml $-\Delta V'/V_0$=0.050 $\rho_{20°}$=0.917				Polymonochlorotrifluoroethylene (Kel-F) V_0=8.036 ml V'=7.835 ml $-\Delta V'/V_0$=0.025 $\rho_{20°}$=3.168			
	Measured			Calculated, $-\Delta V/V_0$	Measured			Calculated, $-\Delta V/V_0$
	Run 1 $-\Delta V/V_0$	Run 2 $-\Delta V/V_0$	Average, $-\Delta V/V_0$		Run 1 $-\Delta V/V_0$	Run 2 $-\Delta V/V_0$	Average, $-\Delta V/V_0$	
10,000	0.0895	0.0892	0.0894	0.0897	0.0523	0.0537	0.0530	0.0529
9,000	.0826	.0823	.0824	.0822	.0490	.0481	.0485	.0488
8,000	.0745	.0743	.0744	.0744	.0439	.0439	.0439	.0440
7,000	.0660	.0658	.0659	.0659	.0387	.0383	.0385	.0386
6,000	.0562	.0558	.0560	.0563	.0329	.0321	.0325	.0326
5,000	.0450	.0447	.0448	.0453	.0255	.0256	.0256	.0256
4,000	.0327	.0327	.0327	.0325	.0185	.0180	.0182	.0180
3,000	.0178	.0180	.0179	.0175	.0101	.0094	.0097	.0095
2,000	.0309	.0309	.0309	.0309	.0000	.0000	.0000	.0000
1,000	----------	*−.0205	*−.0205	−.0204	*−.0089	*−.0104	*−.0096	−.0105

* Values not used in least squares determinations of constants of empirical equations.

vinylidene chloride, however, was observed to be covered with minute blisters after test. This specimen absorbed 0.4 g of Varsol, corresponding to 3.2-percent increase in weight during test. While the effect of absorbed Varsol on compressibility is not known, it is probably small, and the data given for polyvinylidene chloride are most probable essentially correct. This absorption of Varsol does create some uncertainty in the present measurements.

The data of table 1 are shown graphically in figure 1, in which the compression, $-\Delta V/V_0$, is plotted against the pressure. The corresponding compressibilities, $(-1/V_0)\ (dV/dP)$, obtained by differentiation and solution of the appropriate equations, are plotted as functions of the pressure in figure 2.

It is noted in figure 2 that while the compressibilities of the synthetic polymers decrease to approximately one-third of their original values at the extreme pressure, the compressibility of cellulose has decreased much less. In particular, the polymonochlorotrifluoroethylene, which exhibits approximately the same compression as cellulose, differs markedly from cellulose in compressibility. It will be noted that a minimum compressibility is indicated in figure 2 at approximately 10,000 atm. This minimum is fictitious, being due to the cubic equation that was used to represent the data.

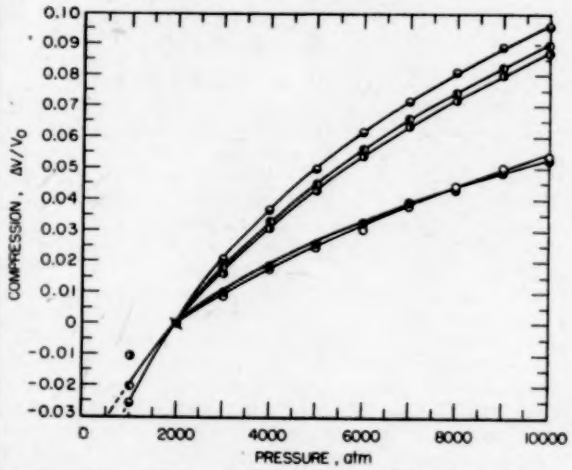

FIGURE 1. *Compression of synthetic plastics and cellulose.*

◒, Polyvinylidene chloride (Saran); ◑, polyester (Selectron 5003); ◐, polyethylene; ●, polymonochlorotrifluoroethylene (Kel-F); ○, cellulose.

Parks and Richards [4] and Bridgman [5] have reported compression data on polyethylene. Parks and Richards studies were confined to pressures below 2,000 atm. The data presented here are in sub-

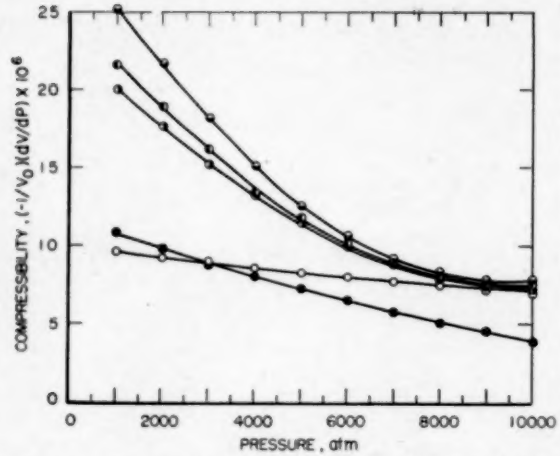

FIGURE 2. *Compressibilities of synthetic plastics and cellulose.*

◒, Polyvinylidene chloride (Saran); ◑, polyester (Selectron 5003); ◐, polyethylene; ●, polymonochlorotrifluoroethylene (Kel-F); ○, cellulose.

stantial agreement with their results at 1,000 and 2,000 atm, as far as can be ascertained, since their data are given graphically. However, the compressibility of 5.5×10^{-5}/atm at 1 atm reported by them is not obtained by extrapolation of the cubic equation fitted to these data. Bridgman [5] reported data on the compressibilities of three samples of polyethylene of differing molecular weights to a maximum pressure of 40,000 kg/cm². The present data are in fair agreement with his data at corresponding pressures but in general appear to show slightly higher compressions. The differences are of the general order of a few tenths of a percent in compression.

2. Polytetrafluoroethylene

Measurements made on polytetrafluoroethylene (Teflon) differed from all others in that a transition was observed at 5,500 atm. The transition was anticipated in view of previous studies at atmospheric pressure [6], and it was subsequently found that Bridgman [5] had reported this transition under pressure. As the present data differ somewhat from those of Bridgman, it is believed they may be of interest.

Original measurements were made in duplicate on a specimen of uncertain origin—sample A. Observations clearly showed a transition at 5,500 atm, but the volume of the specimen was too small to permit accurate evaluation of the volume change at the transition. The difference in volume between this specimen and the reference steel bar generally used was so large that the data were undesirably sensitive to small variations in the assumed initial compression. A larger specimen of material—sample B—was procured from the manufacturer and tested. Within experimental error of a few atmospheres, the transition was found at the same pressure in these two specimens. No effort was made to do more than locate the transition with sample A, all serious measurements at this point being conducted with

TABLE 2.—*Compression of polytetrafluoroethylene at 25.5° C (Teflon)*

Pressure	Sample A V_0=6.565 ml V'=6.368 ml $-\Delta V'/V_0$=0.030 $\rho_{25}°$=2.236			Sample B V_0=21.241 ml V'=20.604 ml $-\Delta V'/V_0$=0.030 $\rho_{25}°$=2.219	Transition region, sample B	
	Run 1 $-\Delta V/V_0$	Run 2 $-\Delta V/V_0$	Average, $-\Delta V/V_0$	$-\Delta V/V_0$	Pressure	$-\Delta V/V_0$
atm					atm	
10,000	0.0987	0.0987	0.0987	0.0908	5,753	0.0672
9,000	.0932	.0945	.0938	.0830	5,590	.0616
8,000	.0861	.0864	.0862	.0858	5,493	.0557
7,000	.0783	.0799	.0791	.0784	5,452	.0524
6,000	[a].0696	[a].0700	[a].0698	[a].0694	5,390	.0469
5,000	.0359	.0349	.0354	.0389	5,280	.0425
4,000	.0251	.0254	.0252	.0267	.....	.....
3,000	.0138	.0136	.0137	.0149	.....	.....
2,000	.0000	.0000	.0000	.0000	.....	.....
1,000	−.0166	−.0215	−.0190	−.0192	.....	.....

[a] $-\Delta V/V_0$ resulting from transition 0.0235.

sample B, which was of such volume that variations in assumed initial compression produced only small differences in compression. As the temperature was not controlled, all data refer to the average ambient temperature of 25.5° C. The results obtained on these measurements are shown in table 2.

The original volumes, measured densities, volumes assumed at 2,000 atm, and the initial compressions used are given at the head of each section of the table. Measurements made in the transition region are given at the right of the table. The data are shown graphically in figure 3.

The transition is observed as the large compression caused by a small pressure change in the range about 5,500 atm. The transition occurs over a definite pressure range, and is not, therefore, considered to take place at a fixed pressure. The change of volume at transition is estimated to be 2.35 percent of the original volume, a value in substantial agreement with the 2.26 percent reported by Bridgman [5]. The transition, however, is reported by Bridgman to occur at 6,500 kg/cm² (≈6,300 atm) as compared to the 5,500 atm observed here. Rela-

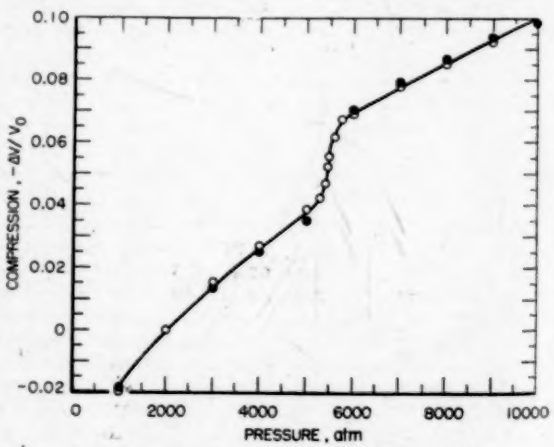

FIGURE 3. *Compression of polytetrafluoroethylene.*

● Sample A; ○ sample B.

tive volume changes at beginning and end of transition are also at variance with Bridgman's values, but this discrepancy is due almost entirely to the difference in the initial compression of 0.0300 used here as compared with the 0.0527 used by Bridgman. Substantially larger compressions reported here are not due to this factor, at least in sample B in which a change of 0.0200 of the initial compression changes the compression calculated at 10,000 atm by only 0.2 percent. The differences between these data and those of Bridgman [5] may arise from differences in samples or in temperature of measurement, but no other explanations can be offered.

Suitable equations to represent the compression of this material were not obtained, as too few points were obtained above or below the transition to permit accurate curve fitting. However, comparisons of curves and data permit the conclusion that this material is slightly less compressible than polyethylene above the transition, and considerably less compressible below the transition pressure. It is much more compressible than polymonochlorotrifluoroethylene however, over the whole range studied. The divergence of the behavior of these three materials is marked, particularly, as no analogous transition occurs for polyethylene or polymonochlorotrifluoroethylene in this pressure range or even up to 40,000 kg/cm² for polyethylene [5].

3. Raw Rubbers

Compression data on raw rubbers are given in table 3. The pertinent volume and density figures are given at the head of each section, while the corresponding constants of the cubic equations fitted to the data are compiled in table 4.

These results show that the compression of the rubbers is of the same general numerical order of magnitude as that of the synthetic polymers that are not elastomers (table 1). Despite the wide variety of chemical compositions involved in the samples, there is relatively little change in compression. It seems, therefore, that the compression of these types of materials is governed largely by the gross nature of the chainlike structure, and is influenced to a lesser degree by details of the molecular structure.

Weights of specimens taken before and after test showed the following pickup of Varsol: Thiokol ST, 0.31 percent; Hycar OR15, 0.11 percent; Hycar OR25, 0.09 percent; Neoprene, 4.8 percent. As a portion of the increase in weight at least is very probably due to Varsol held in void spaces, it is believed that, except for Neoprene, the compression data given are not subject to uncertainty arising from absorption of varsol. The Neoprene specimen, which was obviously porous, absorbed Varsol with visible surface swelling, and the effect of this absorption on the compression is not known.

A difference in behavior between Thiokol ST and the other rubbers was noted during the measurements. The Thiokol rubber appeared to react sluggishly to pressure changes in contrast to the instantaneous response exhibited by the other rubbers. No explanation can be given for this behavior.

TABLE 3. *Compression of raw rubbers*

Pressure	Hycar OR-25		Hycar OR-15	
	V_o=21.074 ml $-\Delta V'/V_o$=0.060	V'=19.810 ml $\rho_{25°}$=0.972	V_o=19.343 ml $-\Delta V'/V_o$=0.060	V'=18.182 ml $\rho_{25°}$=0.964
	Measured, $-\Delta V/V_o$	Calculated, $-\Delta V/V_o$	Measured, $-\Delta V/V_o$	Calculated, $-\Delta V/V_o$
atm				
10,000	0.0969	0.0969	0.0922	0.0925
9,000	.0898	.0895	.0858	.0853
8,000	.0818	.0818	.0781	.0779
7,000	.0732	.0734	.0696	.0698
6,000	.0632	.0636	.0602	.0606
5,000	.0516	.0518	.0495	.0495
4,000	.0375	.0377	.0363	.0361
3,000	.0203	.0206	.0203	.0198
2,000	.0000	.0000	.0000	.0000
1,000	[a]−.0265	−.0246	[a]−.0265	−.0237
	Neoprene		Thiokol ST	
	V_o=17.711 ml $-\Delta V'/V_0$=0.0525	V'=16.781 ml $\rho_{25°}$=1.134	V_o=19.786 ml $-\Delta V'/V_o$=0.050	V'=18.797 ml $\rho_{25°}$=1.298
	Measured, $-\Delta V/V_o$	Calculated, $-\Delta V/V_o$	Measured, $-\Delta V/V_o$	Calculated, $-\Delta V/V_o$
10,000	0.0908	0.0909	0.0940	0.0941
9,000	.0839	.0837	.0859	.0858
8,000	.0763	.0763	.0775	.0773
7,000	.0680	.0681	.0683	.0682
6,000	.0587	.0587	.0577	.0580
5,000	.0476	.0477	.0464	.0465
4,000	.0347	.0345	.0331	.0332
3,000	.0187	.0188	.0180	.0178
2,000	.0000	.0000	.0000	.0000
1,000	[a]−.0245	−.0221	[a]−.0227	−.0205

[a] Values not used in least squares determinations of constants of empirical equations.

The data of table 3 are shown graphically in figure 4, and the corresponding compressibilities calculated from the equations given in table 4 are shown in figure 5.

The compressibilities shown in figure 5 decrease rapidly with pressure, and appear to level off at about 10,000 atm. This apparent minimum is the

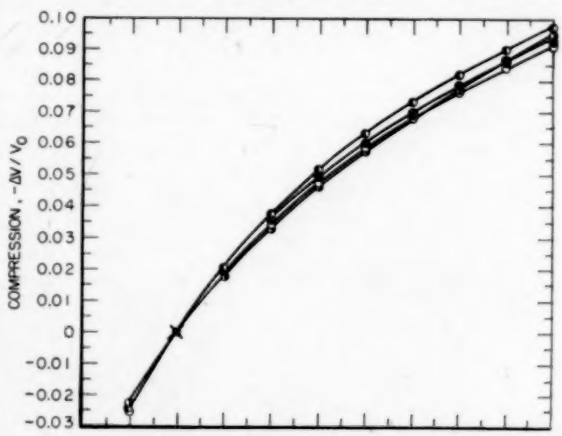

FIGURE 4. *Compression of raw rubbers.*

●, Hycar OR25; ◐, Hycar OR15; ○, Neoprene; ◑, Thiokol ST.

direct result of the equations used for calculation, all of which exhibit a minimum in the first derivative at about 10,000 atm. A pronounced similarity exists between the compressibility curves of figure 5 and most of those of figure 2.

Compressibility data on rubber have been reported by a few other workers, all of whom, as far as can be ascertained, studied rubbers that were vulcanized. Copeland [7] presented data that cannot be conveniently compared with the present results. The data of Scott [8], obtained on rubbers with varying sulfur contents, terminate at a maximum pressure of 800 bars. Extrapolation of his data at 25°C on rubber of 3-percent sulfur content yields a compressibility of approximately 26×10^{-6}/atm at 1,000 atm, which is numerically comparable with the values shown in figure 5. The present data, however, on extrapolation will not give the high compressibilities shown by Scott at pressures below 800 bars. Bridgman [3] reported the compressions of a number of vulcanized rubbers, some of which contained filler at a few pressures up to 25,000 kg/cm², but the present values are slightly higher at corresponding pressures. Bridgman also reported a discontinuity in the pressure-compression ($-\Delta V/V_0$) curves of some samples that most probably corresponds to the second-order transition [9]. This discontinuity is not shown by Adams and Gibson [10] who worked with similar rubbers, or by the present data on raw rubbers. The present data agree well at low pressures with the results obtained by Adams and Gibson on a rubber sample containing 4 percent of sulfur. At higher pressures the present values are slightly lower, a difference probably due to differences in rubbers studied. The cubic equations obtained by these authors are very similar to the present equations. Adams and Gibson noted the minimum compressibility at 10,000 atm previously mentioned as arising from the cubic equation used to represent the data.

The absence of the discontinuity reported by Bridgman [3] in this study, and that of Adams and Gibson [10] is puzzling, and no explanation can be offered. It is important to note, however, that the maximum decrease in volume on compression

TABLE 4. *Constants of empirical equation* [a]
$-\Delta V/V_0 = a(P-20000)+b(P-20000)^2+c(P-20000)^3$

Material	Constants [a]		
	$a\times10^5$	$-b\times10^9$	$c\times10^{14}$
Dry cellulose	0.926	0.325	0.283
Polyvinylidene chloride (Saran)	2.17	1.90	8.73
Polyester (Selectron 5003)	1.76	1.23	4.82
Polyethylene	1.89	1.45	6.10
Polymonochlorotrifluoroethylene (Kel-F)	0.989	0.474	0.829
Hycar OR-25	2.26	2.03	9.09
Hycar OR-15	2.17	2.03	9.42
Neoprene	2.04	1.75	7.66
Thiokol ST	1.92	1.41	6.07

[a] Constants given are applicable at room temperature (20°C to 25°C) over the pressure range 2,000 to 10,000 atm.

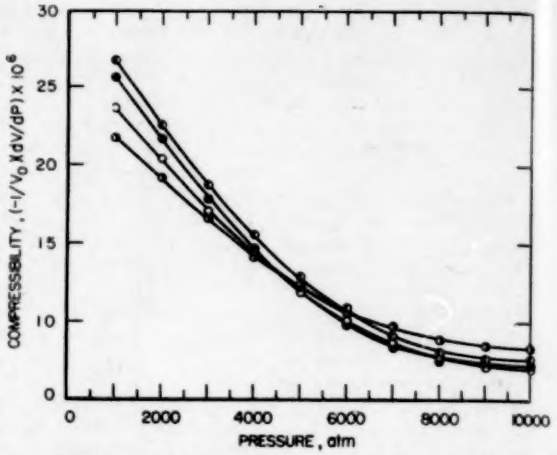

FIGURE 5. *Compressibilities of raw rubbers.*
●, Hycar OR25; ◐, Hycar OR15; ○, Neoprene; ◑, Thiokol ST.

of approximately 15 percent is far in excess of the decrease in volume of approximately 6 percent, which occurs between room temperature and −65°C —the second-order transition temperature of natural rubber—as a result of thermal contraction. As the transition temperatures of most of the rubbers subjected to pressure here are above −65° C [9, 11], the discrepancy is even greater and indicates that the second-order transition is not a result of change in volume alone.

The measurements reported here were made by the author in the laboratories of the Geophysical Laboratory of the Carnegie Institution of Washington. The author is indebted to workers of the Geophysical Laboratory for their suggestions and encouragement, as well as the use of their facilities, without which these measurements could not have been completed.

V. References

[1] C. E. Weir, J. Research NBS **45,** 465 (1950) RP2160.
[2] L. H. Adams, E. D. Williamson, and J. Johnston, J. Am. Chem. Soc. **411,** 12 (1919).
[3] P. W. Bridgman, Proc. Am. Acad. Arts Sci. **76,** 9 (1945).
[4] W. Parks and R. B. Richards, Trans. Faraday Soc. **45,** 203 (1949).
[5] P. W. Bridgman, Proc. Am. Acad. Arts Sci. **76,** 71 (1948).
[6] H. A. Rigby, C. Bunn, Nature **164,** 583 (1949); R. N. Work, National Bureau of Standards, unpublished.
[7] L. E. Copeland, J. Applied Phys. **19,** 434 (1948).
[8] A. H. Scott, J. Research NBS **14,** 99 (1935) RP760.
[9] R. F. Boyer and R. S. Spencer, Advances in colloid science II, chapter I, H. Mark and G. S. Whitby (Interscience Publishers Inc., New York, N.Y., 1946).
[10] L. H. Adams and R. E. Gibson, J. Wash. Acad. Sci. **20,** 213 (1930).
[11] R. N. Work, National Bureau of Standards, unpublished.

WASHINGTON, September 26, 1950.

Journal of Research of the National Bureau of Standards Vol. 46, No. 3, March 1951 Research Paper 2193

Formulas and Graphs for Representing the Interchangeability of Fuel Gases

Elmer R. Weaver

When gas-burning appliances have been adjusted to give satisfaction with a gas of one composition, and are then supplied with gas of a different composition, changes are usually noted in the characteristics of the flames produced. When no change can be seen or measured, the gases are said to be "exactly interchangeable." When undesirable changes do not occur to a greater extent than the person using the term thinks permissible, the gases are usually still called "interchangeable" with the omission of the adverb. No entirely satisfactory method has ever been found for predicting or representing the extent to which different gases depart from exact interchangeability. In this paper a set of six "indexes" is given for specifying and predicting from the composition of any two fuel gases the extent of the effects that occur when one is substituted for another. Four of these indexes are new. Their derivation is given, and their application is shown by comparison with the results of extensive experimentation of the American Gas Association. They are shown to represent the results of observation somewhat better than any method previously proposed.

I. Introduction

The problem of determining in advance the effect of changing the composition of the fuel gas supplied to a city on the operation of the many appliances in use is one of great practical importance. To this general problem have been devoted many extensive, expensive, and time-consuming studies based on experience, on theory, on laboratory observation, and on combinations of them. The various reports dealing with the problem would fill several volumes, yet no entirely satisfactory answer of general applicability has been obtained.

It will make the subject more tangible to cite some actual cases. About the year 1930 a supply of natural gas became available to the Washington Gas Light Co. At that time, the Company was delivering to the city a carburetted water-gas of 600 Btu/cu ft. Natural gas promised economies, but natural gas simply could not have been burned in existing appliances without a difficult period of readjustment and redrilling or replacement of burners and appliances. Accordingly, the Company set itself the problem of modifying the natural gas by mixing it with gases it could manufacture from coke, coal, and oil or from the natural gas itself to obtain a product that could be substituted for the carburetted water-gas without adversely affecting the use of a million or more burners of every conceivable design and purpose. To avoid complications in connection with the selling price of the gas, the Company chose the limitation that the new supply should have the same heating value as the old. With some guidance from the experience of others, but mainly by the empirical method of trying many mixtures made in numerous ways with appliances of many types, the Company succeeded admirably in its purpose. However the solution applied only to the set of conditions existing in Washington and not generally to the replacing or mixing of gases of other types. Had satisfactory formulas been available to represent "interchangeability," most of the time and cost of the experimental investigation could have been saved.

Recently, the Company that supplies Milwaukee with a mixture of coke-oven and carburetted water-gas found itself without plant capacity to meet winter peaks at a time when a transmission line to deliver natural gas from the Texas fields was nearing completion. It was not economical to build additional machinery to serve only as a supplementary source of supply during a few days, or at most a few months of a year or two while the natural gas line was being completed. Propane or butane were available, but the problem arose as to whether they could be safely introduced during peak loads, and in what quantity and with what other practicable modifications of the gas supply. Similar problems are faced by the gas companies in many localities.

The term interchangeability has come to represent the degree to which the operation of gas appliances is affected by substituting one gas for another. If no difference in the service rendered can be observed or measured, if flames on all burners are equally stable (that is, do not tend more or less to flash back or to "lift" from the burners), if there is no more tendency for carbon monoxide or soot to be liberated from one gas than from the other, the gases may be said to be exactly interchangeable. It is necessary to use the adverb if this ideal condition is to be indicated, for the term interchangeable is also applied to pairs of gases that do not give identical results but cause no more change of one kind or another than the user of the term thinks permissible.

Because service can be unsatisfactory in one or more of several ways, gases may be interchangeable in one respect but not in another. They are usually interchangeable, in the practical sense of causing no serious trouble, with some appliances but not with others; and they may be practically interchangeable in one direction but not in the reverse. For example, appliances that have been given ordinary adjustments while supplied with natural gas usually have a rather wide margin of safety from flash back (burning with primary air inside the burner) but a narrow margin of safety from "lifting" (blowing of the flames away from the burner ports). Hence,

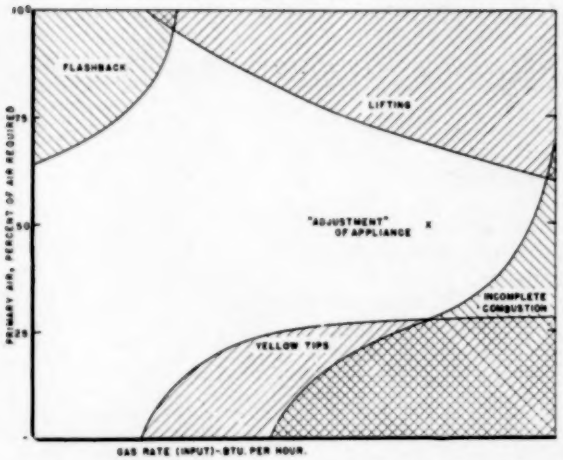

FIGURE 1. *Conventional diagram to show appliance "adjustment" in relation to limits of satisfactory operation.*

When the point representing adjustment is within the unshaded area, the operation of the appliance is considered "satisfactory".

appliances that have been using a slow-burning natural gas will usually give no trouble if a considerably more rapidly burning gas, such as a mixture of the natural gas with 25 percent of coke-oven gas, is substituted; but if appliances should be adjusted for the second gas and the first were then supplied, a great deal of trouble from lifting might be anticipated.

In the course of an investigation of domestic gas-burning appliances begun at this Bureau in 1915, the relations between the design of appliances, the composition of the gas supplied to them, and their performance in service were approximately determined. It was found that, in addition to the primary requirement that the burning gas produce as much heat as is wanted, there are four conditions, already mentioned and usually referred to as "limiting" conditions, that must always be met if service is to be satisfactory or even safe. They are: Flames must not (1) lift, (2) flash back, (3) liberate carbon as indicated by yellow tips, or (4) burn incompletely with the liberation of carbon monoxide. In order to describe the conditions under which failures occur in one or more of these respects, a diagram was devised that has since become conventional in the fuel gas industry. One such diagram is shown in figure 1.

In this figure the point X represents the rate at which heat is produced by combustion (commonly called the "input" of the burner to distinguish it from the "output" of heat in hot water or other material leaving the appliance) and the rate at which primary air enters the burner of an individual appliance under a particular set of conditions of gas supply and mechanical setting. These two rates are subject to easy mechanical adjustments of valves, orifices, and air shutters, and they are conveniently referred to collectively as "the adjustment" of the appliance. On the same diagram the four "limiting conditions" are represented by curves, the positions of which depend on the composition of the gas and on details of burner design not easily changed, such as the size and number of ports. For a given appliance the limiting curves are changed only by a change of composition of the gas, not by changes of orifice, air-shutter, or gas pressure; these affect the "adjustment" only. The position with respect to these limiting curves of a point representing the existing adjustment of an appliance shows whether the appliance is safe from each of the four hazards and by how wide a margin. A mechanical model of this diagram was constructed and exhibited by this Bureau at the 1925 convention of the American Gas Association. On this model a "point" (a small black disk) moved automatically to represent accurately the effects of any change in the proportions of the eleven most common constituents of fuel gases on the rate of liberation of heat and on the entrainment of primary air into the burner. The curves representing the limiting conditions also moved to show the effects of every change of composition of the gas supplied to a typical appliance, but the representation was only approximate. Because different appliances show very different limiting curves it was considered impracticable to represent all of them satisfactorily by a single diagram or a single mathematical formula without extensive additional research involving observations of many appliances with a large number of gas mixtures. Plans were made to conduct such a research at the Bureau and much of the necessary equipment had been purchased, but the project had to be abandoned for lack of funds.

In 1927 the American Gas Association (abbreviated AGA) began a 6-year study of interchangeability called the Mixed Gas Reserach, of which it was said in the final report, [1][1] that "detailed results * * * are contained in twenty-five progress reports of the Testing Laboratory comprising nearly 2,000 typewritten pages * * * Approximately 175,000 separate tests and examinations were conducted during this study, involving the preparation and examination of more than 250 different gas mixtures". The investigation resulted in the development of a general formula, called "C=the index of change in performance of appliances," which was first made public in 1936 during the Federal Trade Commission's investigation of public utilities. This index will be referred to in the present paper as "AGA Index C." Its derivation and significance will be discussed in the following section.

It is easily shown (1) that at a constant pressure the heat "input" into an appliance is determined by a characteristic of the appliance and by $H/\sqrt{D}$, where H is the heating value, and D is the density of the gas usually expressed as specific gravity, and (2) that the fraction of the air required for complete combustion,[2] which is introduced as primary air is

[1] Figures in brackets indicate the literature references at the end of the paper.

[2] By the "air required for complete combustion" is meant the number of cubic feet of air that contains just enough oxygen to combine chemically with the combustible constituents of 1 cu ft of the fuel gas to convert them to carbon dioxide and water. This number will be briefly called the "air requirement" of the gas and be represented by the symbol A.

proportional to $\sqrt{D}/A$. For most gases there is a nearly constant relation between air requirement and heating value (approximately 9 cu ft of air is required per 1,000 Btu). Heating values and specific gravities of gases are commonly reported, air requirements rarely. Hence it is often convenient to substitute H for A and to consider $H/\sqrt{D}$ (or its reciprocal) a measure of two of the most important properties which determine interchangeability. (Of course, the more accurate $A/\sqrt{D}$ should be substituted when primary air is considered, if the necessary data are available). In 1934 in Bureau Circular 405 [2], the significance of $H/\sqrt{D}$ as a partial measure of interchangeability was pointed out. In the same publication it was shown that at least one additional factor, the "ignition velocity" or "speed of flame propagation," which can be represented approximately by a number S[3] must be considered in any decision regarding interchangeability. However, no attempt was made to combine S and $H/\sqrt{D}$ into any general formula for interchangeability such as AGA Index C.

In 1938 an AGA committee made an investigation to select gases for appliance tests that would be representative of the gases in use throughout the United States. The results are described in Report 847 of the AGA Testing Laboratories [3]. Although the number of gases experimented with was small in comparison with the Mixed Gas Research or the investigations described hereafter, certain important data are given in more detail and will have use in this paper.

In 1941 Knoy [4], who was concerned primarily, with substitutions involving liquefied petroleum gases, published a formula for interchangeability that has received wide acceptance.

In 1946 the AGA Laboratories published, as Research Bulletin 36 [5], an account of an investigation of interchangeability, during which 18 appliances were adjusted successively with 3 natural gases of somewhat different characteristics, and after each adjustment were supplied with from 18 to 48 other gases of widely different compositions and properties. The results are reported in enough detail to make them much more valuable to a student of the subject than the available results of the Mixed Gas Research. By this time it was recognized that no one formula could represent accurately the interchangeability of gases with respect to all important properties, and three "interchangeability index" for "yellow tips," "lifting," and "flashback," designated I_Y, I_L, and I_F, respectively, were developed. Collectively these three indexes give an excellent representation of the effects observed. The very important question of whether an interchange of gases would result in "incomplete combustion", meaning the liberation of carbon monoxide, was answered by the observation that combustion was complete in all cases in which the gases were interchangeable with respect to each of the three properties represented by indexes. Hence, no formula for interchangeability with respect to completeness of combustion was considered necessary. For brevity this report will be referred to simply as Bulletin 36.

In the spring of 1948 a preliminary report of a somewhat similar investigation of the results of supplying a wide variety of gases to 28 burners was made [6] by J. F. Anthes, Chairman of the Committee in charge of the investigation. When the observed results were compared with the predictions of the previously evolved formulas, the agreements were not very satisfactory. In his presentation of the report Anthes called attention to this fact and expressed the hope that even more satisfactory formulas would be developed in the future. For brevity, reference [6] will be called the Anthes Report.

Accepting Anthes' statement as a broad invitation to anyone to try to develop more useful formulas, the writer undertook to repair the omission of a quantitative connection between the partial formulas $H/\sqrt{D}$ (or $A/\sqrt{D}$) and S of Circular 405 and to see whether they could be made to predict quantitatively the probable interchangeability with respect to flashback and lifting as judged by all data easily available. The first application of a new index to lifting among the gases described in the Anthes Report, was more successful than anticipated; and while less success was met in dealing with Bulletin 36, the writer was encouraged to develop formulas for all four limiting conditions of service, lifting, flashback, yellow-tips, and incomplete combustion. The resulting formulas appeared to represent all available observations a little better than do the three indexes of Bulletin 36, and are simpler to apply.

However, at the time of the Anthes Report, the experimental study of the subject was being greatly extended by the American Gas Association, and many of the important details even of the first investigation remained to be published. It could not be certain that further work would not show the new formulas to be of limited application or unsatisfactory accuracy, in which case their premature publication would have resulted only in further confusion of an already tangled subject. Subsequently, the observations made in the AGA investigation were published in four reports designated Research Reports 1106 A, B, C, and D [7 to 10]. Comparisons of the formulas based initially on approximately 40 gas mixtures of the preliminary report with several hundred mixtures described in Bulletin 36 and the complete reports of the later work have shown their general applicability to the problems of interchangeability with enough certainty to merit the publication of a thorough analysis of the subject. The derivation of the new formulas will be explained and their relation to earlier formulas shown with the object of making the whole subject more understandable.

II. Graphic Representation of the Performance of Appliances and General Formulas for Interchangeability

So many different symbols have been used for the same thing, and the same symbol has been used for

[3] The valuation of S will be described later.

so many different things in the numerous papers on interchangeability, that to use each in its original sense would be confusing unless accompanied by excessive explanation. An attempt has been made to simplify the use of symbols, as the result of which the discussion and even quotation of some work will not be in terms of the original symbols. For example, in the papers of the Bureau and in some of the AGA reports, heating value has been represented by (H); in others it has been represented by (h). In all AGA papers and in this paper also properties of the gas with which an appliance is adjusted are represented by the subscript (a); but in some AGA reports the properties of gases subsequently supplied to the appliance are represented by the subscript (t) for "test" gas, in others by (s) for "substitute" gas. In this paper the last two subscripts have simply been omitted.

The following symbols are used in this paper:

a=subscript used with another symbol to indicate a property of the gas with which an appliance was adjusted. The same symbol without subscript indicates the same property of a gas "substituted" for the adjustment gas.

A=cubic feet of air required for the complete combustion of 1 cu. ft. of gas.

A_P=cubic feet of air required for the complete combustion of the gas that enters the burner in 1 hour.

$b, c, \ldots$ =fractions of given chemical constituents of a gas mixture.

C=a general "index of interchangeability". Usually identified as AGA Index C or Knoy Index C.

C=a constant. Used several times to represent different numbers.

D=density of gas expressed as specific gravity referred to air as unity.

E, F=factors used in computing K, the "chemical composition factor" in "AGA Index C".

F=a factor used in computing flame speed S.

H=heating value of gas in Btu per cubic foot.

I="input", or rate at which heat is produced in an appliance, in Btu per hour.

k=a "constant" representing the "adjustment" of an appliance that determines the rate of flow of gas into the burner. k depends on the size and form of the "orifice."

k'=a second "constant" which represents the design and adjustment of the burner. Its value depends on the "air-shutter opening," the form of the "mixing-tube," the size and number of the burner "ports" and some other things.

K=a constant used in two of the AGA "indexes".

K=the "chemical composition factor" used in evaluating "AGA Index C".

L=the "lifting constant" used in the AGA indexes. It is designated F in Bulletin 36.

$M=H_aD_a/H_gA_gD$=AGA "index representing change in performance of appliance with variations in heating value and/or specific gravity with no appreciable change in combustion characteristics".

N=number of "readily liberated atoms" of carbon per hundred molecules of gas. All carbon atoms of unsaturated and cyclic hydrocarbons and all but one atom per molecule of saturated hydrocarbons are considered to be readily liberated. Hence, N represents the number of carbon atoms in hydrocarbons minus the number of molecules of saturated hydrocarbons.

p=gas pressure at the orifice.

P=primary air in a burner expressed as a percentage of the air required for complete combustion.

Q=percentage of oxygen in fuel gas. It is designated O_2 in Bulletin 36.

R=ratio of number of atoms of hydrogen in all forms of combination in the fuel gas to the number of carbon atoms in the hydrocarbons (carbon monoxide is excluded).

S=maximum flame speed in a mixture of the gas with air, expressed as a fraction of flame speed for hydrogen.

T=the "yellow tip constant" used in computing the AGA index of interchangeability with respect to yellow tips.

V=cubic feet of gas that enters the burner in 1 hour.

Z=percentage of inert constituents (nitrogen and carbon dioxide) in fuel gas. It is designated E in Bulletin 36.

I_F=AGA index for flashback. For gases that are exactly interchangeable with respect to flashback, $I_F=1$.

I_L=AGA index for lifting. For gases that are exactly interchangeable with respect to lifting, $I_L=1$.

I_Y=AGA index for yellow tips. For gases that are exactly interchangeable with respect to yellow tips, $I_Y=1$.

$J_A=\quad A\sqrt{D_a}/A_a\sqrt{D}$=index of interchangeability with respect to air supply. When $J_A=1$, the total quantity of air required to burn each gas is the same, the fraction of this introduced as primary air is the same, and, unless there are unusual convective effects, the excess oxygen in the flue products is the same, and there is the same hazard of liberation of large quantities of carbon monoxide through "smothering" of the flame.

$J_F=S/S_a-1.4\ J_A+0.4$=proposed index for flashback. For gases that are exactly

interchangeable with respect to flashback, $J_F=0$.

$J_H=H\sqrt{D_a}/H_a\sqrt{D}$=index of interchangeability with respect to rate at which heat is produced. For gases exactly interchangeable in this respect, $J_H=1$.

$J_I=J_A-0.366\ R/R_a-0.634$=proposed index for incomplete combustion. For gases exactly interchangeable in this respect, $J_I=0$.

$J_L=J_A\dfrac{S}{S_a}\dfrac{100-Q}{100-Q_a}$= proposed index of interchangeability with respect to lifting. For gases that are exactly interchangeable with respect to lifting, $J_L=1$.

$J_Y=J_A-1+(N-N_a)/110$=proposed index for interchangeability with respect to yellow tips. For gases that are exactly interchangeable in this respect, $J_Y=0$.

The purpose of using fuel gas is always to heat something, and the first measure of service is the rate at which heat is supplied. Nearly all gas-burning appliances are given by their manufacturers an input rating, expressed in Btu per hour, at which the most favorable results are to be expected. The rate in cubic feet per hour at which gas flows through an orifice is equal to $k\sqrt{p/D}$, where k is a constant for the orifice involving its form and area, D is the density of the gas, usually expressed as specific gravity referred to air, and p is the pressure at the orifice. The rate at which heat is supplied, in Btu per hour, commonly referred to as the "input", I, is the product of the rate of flow and the heating value of the gas, H, that is, $I=k\sqrt{p}\times H/\sqrt{D}$. The equation is written in this way to distinguish $H/\sqrt{D}$, which is a characteristic of the gas, from the pressure, p, and from k, which is a characteristic of the mechanical construction and adjustment of the appliance. If an appliance is adjusted to give the desired heating effect with a gas of heating value H_a and specific gravity D_a and, without changing anything else, is then supplied with another gas of heating value H and specific gravity D, then

$$\frac{I}{I_a}=\frac{H\sqrt{D_a}}{H_a\sqrt{D}} \qquad (1)$$

where I_a and I are the inputs or the rates at which heat is produced when burning the adjustment gas and the substitute gas, respectively. The quantity $H\sqrt{D_a}/H_a\sqrt{D}$ is thus a measure or, to use the term favored in the AGA reports, an index, of interchangeability of the two gases with respect to the rate at which heat is produced when the two gases are delivered to an appliance at the same pressure. If the gases are exactly interchangeable, the index is unity.[4]

The satisfactory application of the heat depends not only on its rate of supply but on what is loosely called the type of flame, which is often described qualitatively in the gas industry as "hard" or "soft". Perhaps the most tangible effects of practical importance connected with the type of flame are the space within which combustion is completed, and the relation of this space to efficiency and completeness of combustion. The amount of heat liberated in a given space is sometimes called the intensity of the flame and is important in many industrial and laboratory applications but not very significant in most domestic uses.

With most gases, when the flame is too soft, hydrocarbons are decomposed to produce solid carbon, which gives a yellow color to the flame. The solid particles of carbon are harder to oxidize completely than are gases and tend to escape from the flame as soot and discolor nearby objects. This is the reason for the desire to avoid yellow tips, the appearance of which is usually taken as one of the limits of satisfactory operation of appliances.

The principal factor in determining the degree of hardness of a flame is the fraction of the air required for complete combustion that is introduced as primary air. The higher this is the "harder" is the flame; in fact, this fraction is the usual quantitative measure of hardness used in the study and testing of appliances. An alternative measure sometimes used is the heating value of the primary mixture (gas and air within the burner). With the gases usually encountered in public supplies, from coke-oven gas to butane, there is little difference in the appearance or useful properties of flames produced with equal percentages of primary air (referred to total air required), provided the flames are stable and not very close to the yellow-tip limit.

The number of cubic feet of primary air injected into a burner by 1 cu ft of gas is directly proportional to the square root of the specific gravity of the gas. Hence, the ratio of primary air to total air required is $k'\sqrt{D}/A$, where A is the number of cubic feet of air required for the combustion of 1 cu ft of gas, and k' is a constant characteristic of the appliance. If an appliance is adjusted to have a desirable flame with one gas of specific gravity D_a and air requirement A_a, the flame of another gas of specific gravity D and air requirement A will have the same percentage of primary air and the same desirable qualities (to the extent that primary air determines them) if $A\sqrt{D_a}/A_a\sqrt{D}=1$. If this expression, which will be called an index of interchangeability with respect to the injection of primary air, is less than one, the substituted gas will produce a harder flame, if greater than one, a softer flame than the gas with which the adjustment was made. We will call the expression J_A.

In almost every case in which an interchange of gases is otherwise practicable, the air required per heat unit is nearly identical for the two gases. For example, AGA Report No. 487 lists 16 natural gases with heating values from 705 to 1,260 Btu/cu ft and 20 manufactured gases from 400 to 600 Btu/cu ft as representative of all the gases of the two types supplied to the public in 1938 ("mixed gases",

[4] In order to conform to the type of symbols to be used later for other "indexes" of performance $H\sqrt{D_a}/H_a\sqrt{D}$ will also be called J_H. J will be used, in general, to indicate indexes derived in this paper and to distinguish them from the indexes derived by the American Gas Association, which has similarly employed I.

usually mixtures of the two types were placed in another category). All the natural gases required from 9.3 to 9.5 cu ft of air per 1,000 Btu. The extreme variation among manufactured gases was between 8.3 and 9.0 cu ft/1,000 Btu with only 3 of the 20 gases outside the range of 8.5 to 8.8. As interchange without readjustment of appliances is far from feasible between gases as different as those in the two groups, a practical problem of interchangeability rarely arises in which the air required per 1,000 Btu of the gases involved differs by more than 2 or 3 percent. Hence, within this rather small margin we can consider air required as proportional to heating value and write

$$\frac{A_a\sqrt{D}}{A\sqrt{D_a}}=\frac{H_a\sqrt{D}}{H\sqrt{D_a}} \text{ (approx.)}$$

which makes the index of interchangeability with respect to the injection of primary air the same as the index of interchangeability with respect to the rate of heat supply.

There is not only some gain in convenience from reducing the two indexes to one; a more important consideration is that the approximate heating values and specific gravities of gases from various sources or distributed in different places are commonly reported, but air requirements are not. For example, an appliance manufacturer who supplies different orifices or other burner parts for such widely different gases as coal gas, natural gas, and propane, and who knows the range of good adjustment with each, should have no difficulty in learning the heating value and specific gravity of the gas in a certain city nor in determining from them with what combination of parts an appliance may be expected to give satisfactory service.

It was mentioned in the introduction that in the study and testing of appliances it has long been customary to represent diagrammatically the two major variables, primary air and "input," in the performance of appliances. It will be desirable to develop this idea more fully than was done in connection with figure 1. In figure 2 heat input (I), expressed in Btu per hour, is plotted with respect to primary air (P), expressed again as a percentage of total air required. Suppose an appliance is adjusted, with burner valve wide open, to produce the conditions indicated by the point marked X_a when burning gas (a). If the pressure at the orifice is gradually reduced, by closing the burner value or otherwise, the changing conditions can be represented by a series of points along the line N_a, which represents the "normal injection" of primary air by gas (a) at any rate of input. If we partially close the air-shutter, the change of conditions will be represented by moving vertically downward from point X_a. Other changes in the appliance itself that will affect gas flow or the entrainment of air are easily pictured. If we control the entry of both gas and air into the burner, it is possible to observe experimentally conditions under which flames lift from the ports or flash back, become yellow, or liberate carbon monoxide.

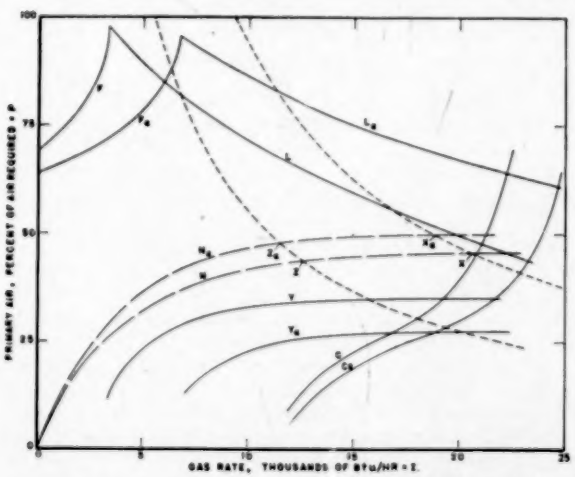

FIGURE 2. *Conventional diagram of appliance adjustment and performance showing changes in the diagram to represent the effects of a change in the composition of the gas supplied.*

The conditions under which these failures occur can be separated on the diagram from those under which they do not occur by curves such as L_a, F_a, Y_a, and C_a. Under all conditions above and to the right of the lifting curve L_a, flames may be expected to blow from the ports. Points above and to the left of F_a represent conditions under which flash back occurs. Those below Y_a represent conditions under which yellow tips appear, and those below and to the right of C_a represent conditions under which combustion is incomplete and carbon moxoxide appears.

If without changing the pressure or any of the mechanical adjustments of the appliances we substitute another gas for (a), the point on the diagram representing the input and type of flame is shifted from X_a to another position X, the coordinates of which are given by multiplying or dividing, those of X_a by the appropriate indexes.

$$I=I_a\frac{H\sqrt{D_a}}{H_a\sqrt{D}}=I_aJ_H.$$

$$P=P_a\frac{A_a\sqrt{D}}{A\sqrt{D_a}}=\frac{P_a}{J_a}.$$

As a step in preparing a general expression for interchangeability, the committee in charge of the Mixed Gas Research decided to make use of the quotient I/P. It was explained that: "Examination of this ratio shows that as its value is increased either by increasing I or reducing P the tendency will be toward incomplete combustion. As the value of I/P is lowered, the tendency will be toward faulty burner performance as evidenced by noisy operation, noisy flame extinction or flashback." It was not stated that increasing the value of I/P by increasing I and by decreasing P have opposite tendencies so

far as lifting is concerned, as can be seen readily from the diagram.

When comparing two gases,

$$\frac{I}{P}=\frac{I_a}{P_a}\cdot\frac{H\sqrt{D_a}}{H_a\sqrt{D}}\cdot\frac{A\sqrt{D_a}}{A_a\sqrt{D}}=\frac{I_a}{P_a}\frac{HAD_a}{H_aA_aD}$$

$M=HAD_a/H_aA_aD$ was called the "index representing change in performance of appliance with variations in heating value and/or specific gravity with no appreciable change in combustion characteristics." For the usual case, in which heating value is proportional to air requirement or nearly so, M is substantially equal to the square of $H\sqrt{D_a}/H_a\sqrt{D}$ and has the same significance as a means of judging the performance of appliances. If cases occurred in which the proportionality between heating value and air required did not hold and there were no complications, M should be a slightly better index of interchangeability with respect to lifting and incomplete combustion than $H\sqrt{D_a}/H_a\sqrt{D}$ but not as good as $A\sqrt{D_a}/A_a\sqrt{D}$. As an index for flashback the reverse should be true. Actually, however, other factors complicate the problem so much that the three indexes, without further modification, are equivalent for practical purposes. They show well enough the effect of the change of gas supply on the heat input and the primary air; on the diagram they locate the point X with respect to the coordinate axes. However, we are often more concerned in avoiding the dangerous or disagreeable results of lifting, flashback, and liberation of carbon monoxide and soot than with the rate and intensity of heating. The danger of encountering these difficulties is represented on the diagram by the relation of the point X to the several limiting curves, the positions of which shift with changes of the gas supply typically as representing by limiting curves L, F, Y, and C. The initial positions of the limiting curves and the shifts that occur when the gas is changed depend to some extent on the design of the appliances and make accurate generalization difficult; but, in any case, we are concerned with the sum of the shift of point X toward the limiting curve and of the curve toward X.

What has here been explained graphically was stated in algebraic form in the Mixed Gas Research Report as follows: " . . . The effect of variations in chemical composition and superimposed on changes in heating value and/or specific gravity could be accounted for by

$$\boldsymbol{C}=\boldsymbol{M}+(\boldsymbol{K}_a-\boldsymbol{K}),$$

where

$\boldsymbol{C}$=index indicating change in performance of appliances, and

$\boldsymbol{K}$=a factor depending on chemical composition."

In our diagram $(\boldsymbol{K}_a-\boldsymbol{K})$ should be represented by the displacement of the limiting curve. Actually the displacements of the several curves are of different magnitudes and, as will be shown later, appear to depend on different functions of composition. In the case of flashback and lifting they are even in opposite directions. The impossibility of representing these divergent effects by a single expression is the reason why $\boldsymbol{C}$, the general AGA "index in change of performance of appliances", has not been more successful.

In the attempt to find a suitable function of composition to represent the changes of limiting conditions "a large number of expressions were devised for $\boldsymbol{K}$ and subsequently discarded". The final selection, made by a combination of theory and observation, was

$$\boldsymbol{K}=HA/5000\ \boldsymbol{EF},$$

in which H and A have their previous significance, $\boldsymbol{E}$ is the heat capacity, between 60° and 1,600° F of the "theoretical products of combustion" of 1 cu ft of the gas, and $\boldsymbol{F}$ is the summation of the product of the fraction by volume of each chemical constituent and a constant characteristic of that constituent. This constant is proportional to the heat capacity of the products of combustion of the gas divided by the velocity of flame in a mixture of the gas with the amount of air required for complete combustion. For a pure gas $\boldsymbol{K}$ would simplify to the product of heating value, air required for combustion, flame velocity, and an arbitrary constant divided by the square of the heat capacity of the products of combustion. The heat capacity of the products of combustion is nearly proportional to the air required and to heating value; hence, these factors tend to cancel and to leave the "chemical composition factor" roughly proportional to flame velocity in a mixture of gas with the air required for complete combustion. The cancellation is not complete, however, and a plot of $\boldsymbol{K}$ with respect to flame speed only for various gases shows a nonlinear relation with considerable scattering.

In the Knoy formula interchangeability is judged from relative values of $(H-175)/\sqrt{D}$ instead of the expression $H/\sqrt{D}$ previously discussed. The expression was derived by considering the heating value of the primary mixture of gas and air in the burner, rather than the ratio of primary air to air required, to be the measure of good adjustment. It was further assumed that the primary mixture should normally have a heating value of 175 Btu/cu ft and that air required is proportional to heating value, an assumption previously discussed. For further details of the derivation, the original article should be consulted.

III. Data Available for the Study of Interchangeability

It was stated in the Report of the Mixed Gas Research that "while certain assumptions have been necessary the value of the final formula depends not so much on the correctness of these assumptions or hypotheses as the degree to which it satisfactorily serves to yield results that are in agreement with those actually obtained by careful experimentation".

With this statement the writer is in complete agreement; it applies equally to all formulas that have been or may be developed.

The only data at present available to the author that show the results of a sufficiently numerous and varied lot of interchanges in enough detail to make the empirical evaluation of the formulas satisfactorily are those in Bulletin 36 and Research Reports No. 1106A, B, C, and D, of the American Gas Assoc.

In the work reported in Bulletin 36, 18 appliance burners were adjusted to burn a "high Btu natural gas." Then 23 "supplemental" gases of varied types were supplied to the same burners at the same pressure and without readjustment of the appliances. Most of the supplemental gases were also mixed with the adjustment gas to give 25 additional "substitute" gases,[5] making 48 substitutions in all. With each of the substitute gases observations were made of lifting, flashback, and yellow tips, and the number of burners that failed in each respect was recorded.

Two similar series of observations were made with a "high methane natural gas" and a "high inert natural gas" as the adjustment gas. The second series involved eight supplemental gases and 10 additional mixtures with the adjustment gas. The third series included 14 original substitute gases and 8 additional mixtures. In all, there were 88 substitutions of another gas for an adjustment gas and, in effect, $88 \times 18 \times 3 = 5{,}742$ observations that an individual appliance did or did not fail with respect to one of three limiting conditions when one gas was substituted for another.

The tests recorded in Research Reports 1106-A, B, C, and D were similar but much more extensive. The number of appliance burners was increased to 28. There were six adjustment gases that were compared with 98, 65, 57, 72, 94, and 13 substitute gases, of which 29, 30, 23, 27, 33, and 13, respectively, were unmixed supplemental gases. Instead of giving each appliance a single adjustment, supplying all gases at a single pressure, and reporting only one degree of failure with respect to three limiting conditions, appliances were given three successive adjustments, and supplied with gas at three different pressures; and failures were recorded for four limiting conditions. Moreover, the degree of failure with respect to lifting and yellow tips was recorded in two categories.

[5] The term "supplemental" gas reflects the principal purpose of the AGA investigation, which was to determine to what extent gas from the regular source of supply (the adjustment gas) could be supplemented when necessary with gas of different characteristics from another source. The term will be retained to distinguish gas of the second type from its mixtures with the adjustment gas, made to determine how much of the supplemental gas could be used. Except when this distinction is to be made, both the supplemental gases and their mixtures will continue to be referred to as "substitute" gases, meaning, merely that they are the gases substituted for the adjustment gas after the appliances were adjusted. In Research Report 1106, the adjustment gases are given numbers less than 10. Supplemental gases are numbered from 11 upward. Their mixtures with the adjustment gases were indicated by the percentage of the supplemental gas in the mixture. No numbers were assigned to the gases in Bulletin 36, but it will be convenient in mentioning individual gases to use the same system, numbering the adjustment gases 1, 2, and 3, and the supplemental gases 11 to 37 in the order in which they appear in the tables showing the results of experiments. Combining the numbers with a letter, N (for natural gas) for those given in Bulletin 36, or A, B, C, or D for the various sections of Report 1106 permits unambiguous reference to any one of the large numbers of gases used or to any observation recorded during the study. Thus, N3–12–60 represents the comparison of the third adjustment gas referred to in Bulletin 36 with a mixture of 60 percent of supplemental gas 12 with 40 percent of adjustment gas 3. B2 represents the adjustment gas 2 used in the tests recorded in Section B of Research Report 1106, and A1–19–20 represents a mixture containing 20 percent of gas 19 and 80 percent of gas 1, as recorded in Research Report 1106–A.

In order to specify the kind of adjustment given appliances and the extent of the failures observed, flame characteristics were given the following designations:

−5 flames: Distinct yellow in outer mantles, or large volumes of luminous yellow tips on inner cones. Flames deposit soot on impingement.
−4 flames: Slight yellow streaming in the outer mantles, or yellow fringes on tops of inner cones. Flames deposit no soot on impingement.
−3 flames: Inner cones broken at top, lazy wavering flames.
−2 flames: Faint inner cone.
−1 flames: Inner cone visible, very soft tips.
0 flames: Inner cones rounded, soft tips.
+1 flames: Inner cones and tips distinct.
+2 flames: Inner cones distinct and pointed.
+3 flames: Short inner cones, flames may be noisy.
+4 flames: Flames tend to lift from ports, but become stable after short period of operation.
+5 flames: Flames lifting from ports, with no flame on 25 percent or more of the ports.
FB: Flames flash back through the ports.

Observations were made with appliances that had been adjusted to have flames of the types −2, 0, and +2. All of these are within the range of what we would normally consider good adjustment. Actually, in any large number of homes the range of appliance adjustment will be found to include many cases of −3 and +3 flames and some −4 and +4 flames. The pressures employed were 2.5, 5, and 7.5 in. of water column, a range that is to be encountered in most localities. These pressures are referred to, respectively, as 0.5 normal, normal, and 1.5 normal. With some appliances when testing for completeness of combustion, the maximum pressure employed was 6.25 in. of water column (1.25 normal).

It may be helpful to represent these conditions of adjustment on the conventional diagram. If we define our limit of operation with respect to lifting as that at which flames lift from 25 percent of the ports and our yellow tip limit as that at which flames pass from the −4 to the −5 classification and assume that equal ranges in the percentage of primary air are represented by each of the specied flame characteristics, the initial adjustments of the appliances would be as shown in figure 3. Each short, heavy line represents one set of conditions of pressure and adjustment with the adjustment gas.

It is the main purpose of this paper to show to what extent the proposed indexes of interchangeability will serve to predict what will happen when a gas supply is changed in a city with the usual range of pressures and existing appliance adjustments. As none of the initial conditions of pressure and adjustment employed in the AGA investigation are to be considered unusual, they will be treated alike in the statistical use of the information. Thus, if one burner flashed back under two conditions of adjustment and at each of two pressures, it will be recorded as four

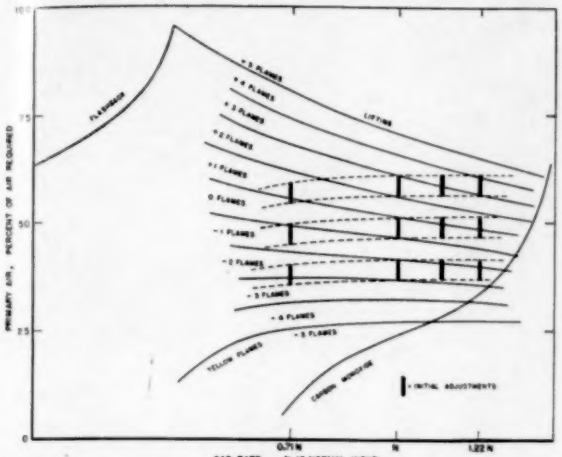

FIGURE 3. *Initial adjustments of appliances in experiments described in Report 1106, as they would appear on the conventional diagram for a typical appliance.*

failures just as though four burners had flashed back under one condition.

In the course of the experimental work it was found that certain appliances were much more prone to failures of certain types than other appliances. When several of these had been tested without failure it was considered unnecessary to test the others. The number of appliances tested, as well as the number of failures is scrupulously recorded; but for the purpose of this paper, no use can be made of the number of burners tested. Only the number of recorded failures will be used. In most cases this is probably the same number that would have been found had all the appliances been tested, but it is not necessarily so, and in some cases it is rather certainly not true. Had the purpose of the AGA investigation been to test existing or future formulas for interchangeability, it is probable that enough appliances would have been tested with each gas to make certain that no further failures would occur with the others; but the primary purpose seems to have been to establish the amount of "supplemental" gas that can be mixed with the base gas normally delivered without exceeding the limits of practical interchangeability. For this purpose, it was sufficient to know that so large a number of appliances had failed that the gas could not be considered even to approach interchangeability whatever the untested burners might have done. The result of this variation in the number of appliances tested will be discussed later in connection with the application of the data.

IV. Derivation of a New Index to Represent Lifting

As explained in the introduction, the present attempt to derive improved formulas for representing the effects of changing the gas supplied to an appliance began with a combination of the two quantities represented by (S) and $H/\sqrt{D}$, later changed to $A/\sqrt{D}$, to predict lifting and flash back.

The derivation of (S), a coefficient intended to represent the approximate maximum velocity with which flame will travel in any mixture of the gas with air, is not fully explained in Circular 405 and has been changed a little. There are many obstacles in the way of computing flame speed simply and accurately; to avoid this several assumptions have been made. As the result is to be judged by the success of its application, no attempt will be made to justify them in detail. The principal assumption is that the maximum flame velocity in mixtures of two fuel gases is a linear function of the volumes obtained by adding to each gas in the mixture the volume of air required for its complete combustion. The assumptions made lead to the method for the calculation of (S) which follows:

$$S=\frac{aF_a+bF_b+cF_c\cdots}{A+5Z-18.8Q+1},$$

in which a, b, c, . . . are the fractions by volume of various combustible constituents of the fuel gas, F_a, F_b, F_c, . . . are corresponding values of the coefficient F listed in table 1, A has its usual meaning, the volume of air required to burn one volume of gas, and Z and Q are, respectively, the fraction by volume of inert gases, chiefly carbon dioxide and nitrogen, and of oxygen in the fuel. To obtain the factor, F, the recorded maximum ignition velocity in mixtures of the combustible with air was expressed as a percentage of the maximum ignition velocity of hydrogen with air and multiplied by 1 plus the number of cubic feet of air required to burn 1 cu ft of the gas. The coefficient 5, by which the fraction of inert constituents in the gas mixture is multiplied, is larger than corresponds to the volume of inert as a fraction of ultimate products of combustion. The coefficient was obtained in trying to fit the formula to the results of appliance tests. It may be explained in part on the ground that usually we are

TABLE 1. *Properties of gases used in computing interchangeability by the methods proposed in this paper*

Gas	Chemical formula	Total heating value, H	Specific gravity, D	Air required to burn, A	Flame speed factor, F[a]
Carbon monoxide	CO	315.3	0.97	2.39	61
Hydrogen	H_2	318.5	.07	2.39	339
Methane	CH_4	994.1	.55	9.55	148
Ethane	C_2H_6	1757	1.04	16.71	301
Propane	C_3H_8	2535	1.56	23.87	398
Butane	C_4H_{10}	3330	2.09	31.03	513
Ethylene	C_2H_4	1572	0.97	14.32	454
Propylene	C_3H_6	2337	1.45	21.48	674
Acetylene	C_2H_2	1464	0.91	11.93	776
Benzene	C_6H_6	3700	2.70	35.79	920
Atmospheric nitrogen	N_2	-----	0.97	-----	----
Carbon dioxide	CO_2	-----	1.53	-----	----
Oxygen	O_2	-----	1.11	(−4.78)	----
Air	-----	-----	1.00	-----	----

[a] $F=(A+1)\ S$, where $A+1$ is the number of cubic feet occupied by a mixture of 1 cu ft of gas with enough air for its complete combustion, and S is the speed of flame in such a mixture in percentage of the speed in the corresponding mixture of hydrogen and air.

really concerned with primary mixtures in the burners containing much less air than is required for complete combustion, so that inert in the gas constitutes a larger fraction of the total in the primary mixture than in a mixture containing all the air required for combustion. Partly it may result from the fact that we are usually working on a steep portion of the curve representing the relation of flame velocity to primary air, where the effect of added diluent is excessive. The factor for oxygen simply cancels as much nitrogen as is contained in an equivalent volume of air.

The two limits of appliance operation under consideration, lifting and flash back, are more closely related to the chemical reactions involved in combustion with primary and secondary air than to the quantity of heat liberated, and it is therefore more direct and may be more accurate to consider $A/\sqrt{D}$ rather than $H/\sqrt{D}$ as the major variable. To be consistent, the abscissa of a diagram such as figure 1 should be changed to represent the total volume of air required to burn the volume of gas supplied to the appliance rather than the "heat input". When nothing but the supply of gas is changed, the point X, determined by the previous mechanical adjustment of the appliance, will then follow accurately a reciprocal curve (i. e., the product of ordinate and abscissa is constant) instead of following such a curve only approximately. The principal reason for using $H/\sqrt{D}$ originally, that the heating value of a prospective gas supply is often known when its composition is not, is no longer of importance since (S) cannot be computed unless the composition is known.

In order to find an experimental relation between S and $A/\sqrt{D}$, it was necessary to consider the results of determining the lifting curves of a single appliance with each of a large number of gases. For this purpose AGA Report 847 [3] supplied the necessary data. The curves in Report 847 that represent the conditions under which lifting occurs with a given test burner have been replotted in figure 4, with the volume of air required to burn all the gas supplied to the appliance as abscissa in place of heat input. Curves lettered A through P represent the lifting limits for gases identified by the same letters in Report 847. A reciprocal curve, Y, has been drawn to represent a fixed mechanical adjustment of an appliance, the condition assumed to exist in the definition of interchangeability. The fact that this adjustment remains unchanged gives us definite relations between gas and primary air, so that either can represent both when dealing with a third variable, such as flame speed (S). The intersection of Y with the lifting curve of one of the gases represents the flow of gas and primary air that would just produce incipient lifting if it occurred, not the flow that actually occurs. The difference between the two is the margin of safety against lifting. Hence, if we can determine a relation between (S) and one of the coordinates of the intersection of Y with the lifting curve, we will be in position to express the hazard of lifting quantitatively.

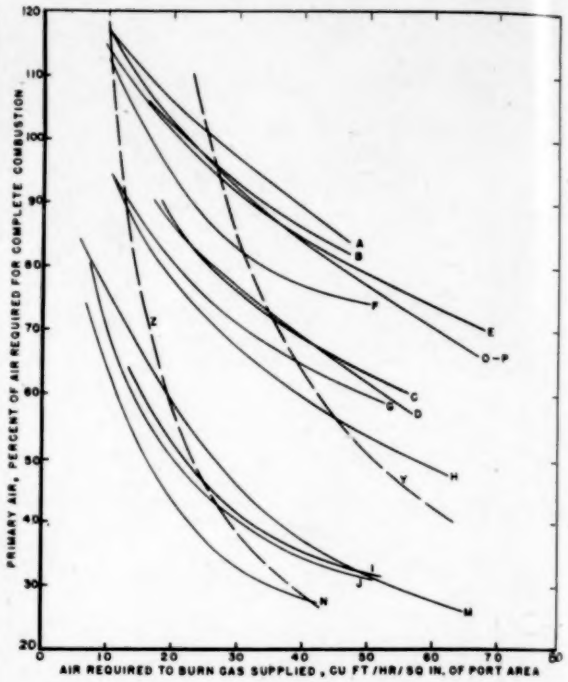

FIGURE 4. *Lifting curves of AGA Report 847 replotted with rate of flow of primary air as abscissa.*

Curves Y and Z represent constant mechanical adjustments.

The primary air at which lifting occurs with the adjustment represented by Y is plotted with respect to flame-speed (S) by the open circles of figure 5. A straight line through the origin (the origin is not on the figure) represents the results about as well as they can be represented by any simple relation. To show the effect of a different adjustment of the appliance and to include the natural gases, another reciprocal curve (Z) has been drawn in figure 4. Its construction and significance are the same as those of (Y), except that a very different mechanical adjustment of the appliance is represented. The intersections of curve Z with the various lifting curves are shown on figure 5 by solid dots, which scatter rather widely from the simple relation of direct proportionality between (S) and the percentage of primary air at which lifting occurs, represented by the broken line. Apparently they could be better represented by such a curve as the unbroken one.

It is our purpose, if possible, to choose a relationship through which interchangeability of various gases with respect to lifting can be represented by a single formula. If a different relation exists between the properties of the gases and the performance of a single appliance after a change of the size of orifice and perhaps of the primary air openings, we would wish to base our formula on the conditions most nearly representative of those existing in service. For the most numerous group of gases, this is undoubtedly the condition of adjustment represented

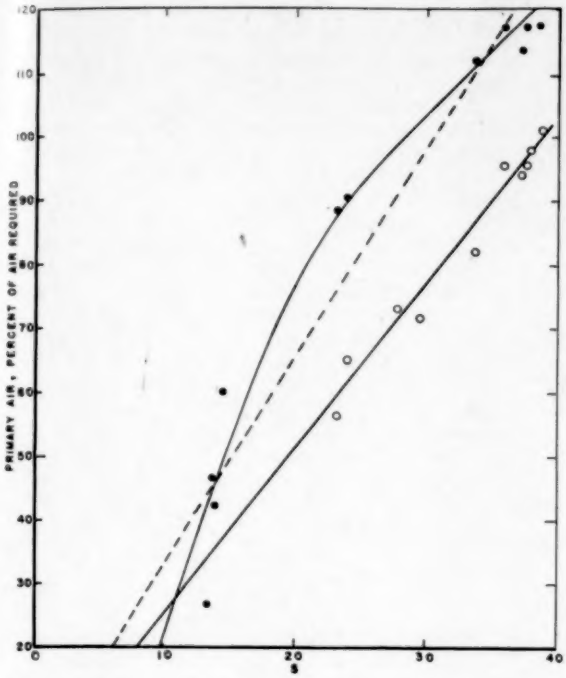

FIGURE 5. *Primary air that would cause lifting at relative rates corresponding to fixed mechanical adjustments of burners.*

Data from Figure 4.

by (*Y*) rather than by (*Z*). We do not often encounter in practice an appliance taking through the burner more than 100 percent of the air required for combustion, nor one with so low an input rating as 1,450 Btu per hour per square inch of port area, the greatest input with adjustment *Z* of any except the natural gases. It is not quite certain that the curvature of the solid curve is not the result of inaccuracies in either the values of (*S*) or of the positions of the lifting curves intersected by line (*Z*). The extreme ends of such curves are ordinarily of little interest and are determined only with considerable difficulty. The displacement to the right of the points at the upper end of the curve may also be explained by the fact that, as the percentage of primary air increases beyond that at which flame speed is a maximum, additional air slows down instead of accelerating the ignition velocity. A line drawn through the approximate average of points representing the more rapidly burning gases and the slow-burning natural gases passes close to the origin. Finally, the range of compositions covered by curve (*Z*) is much greater than the range of practical interchangeability, and our formulas need cover only ranges within which interchange can generally be made. For all these reasons, as well as for simplicity, it was decided to represent practical interchangeability by direct proportionality between (*S*) and the fraction of primary air at which lifting occurs.

An additional reason for this choice appears when we consider lifting, not among appliances supplied at constant pressure and without mechanical adjustment of any kind, but among those in which desired rates of heating are set at the time of use by means of the burner valve. They include top burners and broilers of cooking appliances and a majority of space heaters. With these appliances we have to consider whether lifting will occur at the maximum desired rate of heat input, which may be considered constant. To obtain an approximate answer to the problem, the lines representing a constant input of 4,000 Btu per hour per square inch of port area were drawn on the original figures of Report 847, and their intersections were plotted in figure 6. An approximation to proportionality between (*S*) and the fraction of the air that passes through the burner when lifting occurs is again apparent.

Expressing this proportional relation in terms of our symbols for gas properties,

$$S=k\sqrt{D}/A \text{ or } AS/\sqrt{D}=k,$$

in which k is a constant representing a characteristic of the appliance independent of the gas supplied to it. If we use letters with the subscript (a) to represent properties of the gas with which the appliance was adjusted and letters without subscript to represent any other gas, exact interchangeability would be indicated if

$$AS\sqrt{D_a}/A_aS_a\sqrt{D}=1,$$

and the degree of departure from exact interchangeability is indicated by the coefficient $AS\sqrt{D_a}/A_aS_a\sqrt{D}$

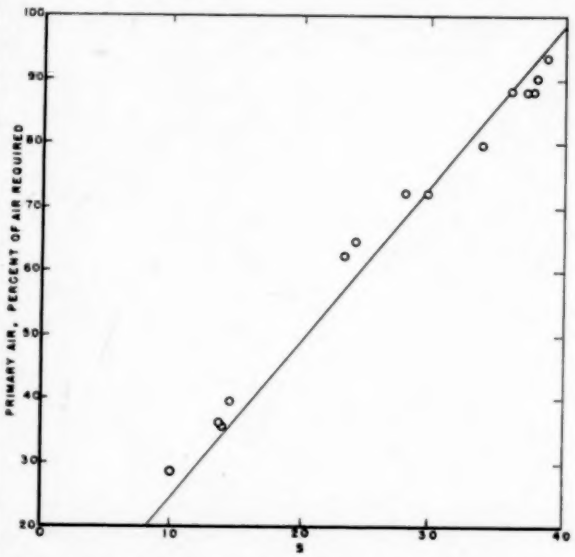

FIGURE 6. *Primary air that would cause lifting from appliances with an input of 4,000 Btu per hour per square inch of port area.*

Data from AGA Report 847.

which, in conformity with AGA phraseology, may be called an index of interchangeability with respect to lifting. It will be designated J_{L-1} to distinguish it from the corresponding AGA index I_L and from a modification to be designated J_L.

The merits of the new index were first tested by plotting S/S_a with respect to $A\sqrt{D_a}/A_a\sqrt{D}$ for the gases described in the Anthes Report. The result was figure 7.

The Anthes report was a preliminary condensation of Research Report 1106A and did not state the number or extent of failures (whether +4 or +5 flames) of appliances but only whether the unmixed supplementary gas was or was not considered by the investigators to be interchangeable with respect to each limiting condition, and, if not, what percentage of it could be mixed with the adjustment gas.

If the new index accurately indicates the behavior of all appliances, then in such a plot as figure 7, the points representing any number of gases that are identical ("exactly interchangeable" among themselves) in their tendency to lift should lie on a reciprocal curve representing a constant value of the index. Such a curve is, of course, determined by any one point. The points representing every gas more susceptible to lifting should lie on one side of the curve, and those representing gases less susceptible to lifting should lie on the other side. In figure 7, all supplemental gases that were reported as interchangeable with the adjustment gas with respect to lifting are represented by circles. All supplemental gases reported not interchangeable are represented by crosses. The adjustment gas itself is represented by two concentric circles. As it could be assumed that any mixture of a supplemental gas with the adjustment gas would be interchangeable with the latter if the supplemental gas was itself interchangeable, the "limiting mixtures", the determination of which involved only conditions other than lifting were also represented by circles. When lifting was mentioned as one of the conditions that made the substitute gas noninterchangeable, the properties of the mixture regarded as "limiting" are represented by L. Points representing limiting mixtures should fall near to but on the safe side of a curve separating the gases which gave trouble from those which did not. Since lifting was the only limiting condition with five of the original substitute gases and was only one of two or more limiting conditions with the others, it should not be surprising to find that some of the limits were determined primarily by other factors, and that they are well on the safe side with respect to lifting.

Had some of the appliances been adjusted initially to incipient lifting, the curve separating the interchangeable from the noninterchangeable gases should have passed through or very close to the concentric circles that represent the adjustment gas.

It can be seen at a glance that, so far as this set of data is concerned, the index is in almost exact agreement with the reported observations. When the observations reported in Bulletin 36 were plotted in the same manner, the agreement with the formula was much less satisfactory. In Bulletin 36 the number of appliances that showed lifting with each gas was given. Figures 8 to 10, representing the result of substitutions for each of the three adjustment gases, are like figure 7 except for a change of scale and the substitution of the number of appliances that failed for the crosses of the earlier figure. Had the index

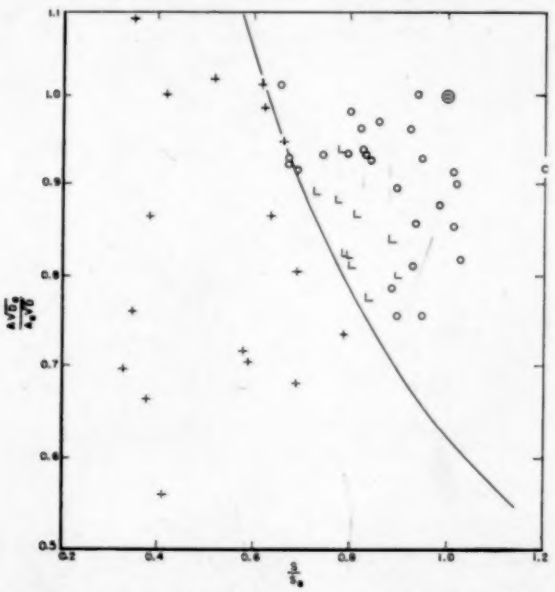

FIGURE 7. *Observations of lifting and committee's estimates of limiting mixtures as recorded in the Anthes Report.*

(+) represents gases considered not interchangeable because of lifting; (O) gases that were interchangeable, and (L) limiting mixtures.

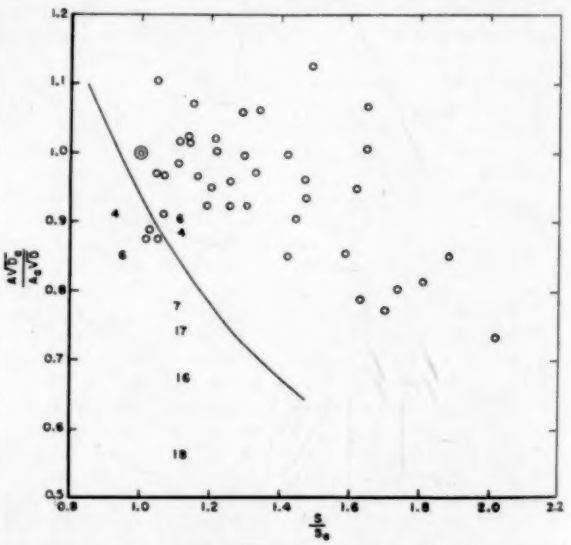

FIGURE 8. *Observed lifting after appliances were adjusted with "high-Btu" natural gas.*

From Bulletin 36, numbers represent number of recorded cases of lifting with substitute gas.

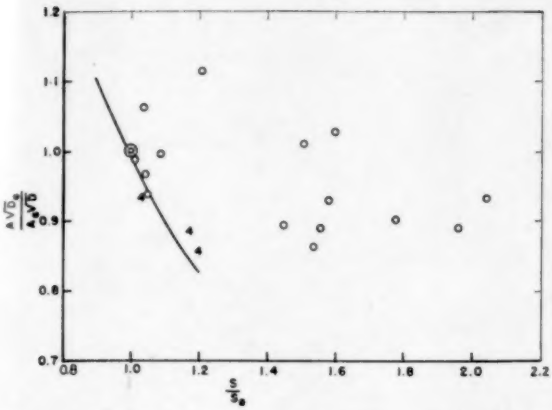

FIGURE 9. *Observed lifting after appliances were adjusted with "high-methane" natural gas.*

From Bulletin 36.

perfectly represented the observations in this case, not only should all zeros have fallen on one side of a single reciprocal curve and all other numbers on the other side, but of two numbers the greater should always have been farther from the curve.

Inspection showed that of the gases that produced lifting more readily than would have been predicted from their indexes, a large proportion contained butane and air. In cases in which air is present its amount is, of course, subtracted from the volume needed to burn the fuel portion when the "air required for complete combustion" is computed. With an appliance injecting just this amount of air the sum of the air injected and that already in the gas is the correct amount needed to meet the chemical requirements of combustion. However, few

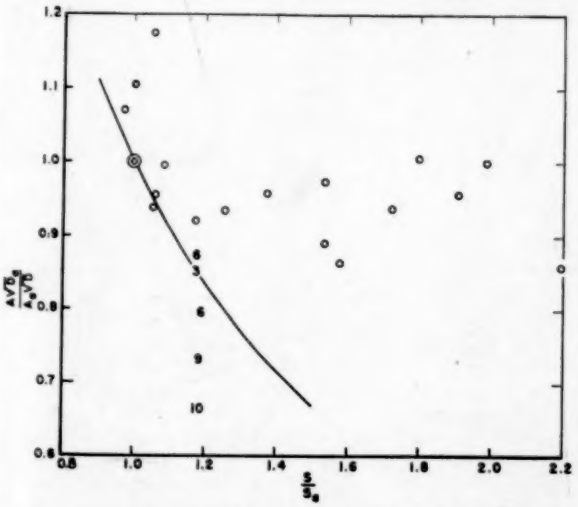

FIGURE 10. *Observed lifting after appliances were adjusted with "high inert" natural gas.*

From Bulletin 36.

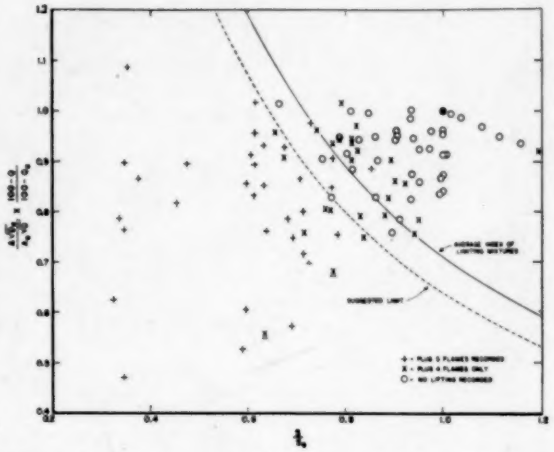

FIGURE 11. *Observations of lifting recorded in AGA Report 1106–A.*

Value of J_A modified to take account of oxygen in the gas.

appliances are used with 100 percent of primary air. With a slow-burning gas, such as natural gas or butane, it is not uncommon for lifting to begin at 25 to 30 percent of primary air and, as failure is judged by the appearance of lifting from any of the burners under observation, it is with the lowest limits of lifting that we are really concerned. At these low percentages of primary air, the primary mixture is not correctly accounted for by the formula. For example, if a butane-air mixture of 1,000 Btu/cu ft injects just 100 percent of the "air required", about 8 percent of the air in the primary mixture enters the burner with the gas, and only 92 percent is injected. If the burner is now adjusted to take "25 percent of the air required", the air injected is actually 25 percent of 92 percent, or 23 percent of that needed to burn the fuel, but 8 percent enters with the gas, making a total of 31 percent instead of the 25 percent indicated by formula. The error involved in ignoring the oxygen in the gas is great enough to make a big difference in the usable gas rate, as will be appreciated after a glance at the gently sloping lifting curves at the bottom of figure 4.

From this discussion it appears that a correction to the index for lifting may be needed when the gas contains much oxygen. An inspection of the data indicated that the trouble with the formula would be reduced if the value of $A/\sqrt{D}$ for each gas is multiplied by the fraction by volume of all constituents of the gas except oxygen. The index for lifting is then conveniently written

$$J_L = \frac{S A \sqrt{D_a}(100-Q)}{S_a A_a \sqrt{D}(100-Q_a)},$$

where Q is the percentage by volume of oxygen in the gas.

To test the application of J_L, values of $[A\sqrt{D_a}(100-Q)]/[A_a\sqrt{D}(100-Q_a)]$ have been plotted with

respect to S/S_a for the data reported in Research Report 1106–A in figure 11, and for the data of Bulletin 36 in figure 12. In figure 11, substitute gases that showed any $+5$ flames are marked $+$ and those that produced $+4$ flames only are marked X. This seemed more informative than entering the number of "failures" of either type. The solid reciprocal curve represents the average values of J_L for the mixtures considered "limiting" by the AGA committee in charge of the investigation. The broken line represents the present writer's judgment of a limiting value for the index in this case. Two points marked X are underscored. They will be referred to later in a discussion of the reliability of the data.

In figure 12 the three plots corresponding to figures 8 to 11 have been superimposed. Dots have been placed below numbers representing observations made with "high methane" natural gas and above numbers representing "high inert" gas. The numbers representing adjustments with "high Btu" gas are without dots. The horizontal scale is the same for the three sets of data; the vertical scale has been shifted to bring the curves drawn to represent the limits of interchangeability into coincidence at the abscissa $S/S_a=1$. One of the more interesting things about the figure is that it shows rather clearly the different margins between lifting and the adjustments with the three different adjustment gases.

It may be of interest to compare the form of the new index J_L with the AGA index for lifting I_L, which is defined in Bulletin 36 by the equation

$$I_L=\frac{K_a/f_a a_s}{f_s a_a(K_s-\log\,(f_a/f_s))},$$

in which subscripts a and s represent properties of "adjustment" gas and "substitute" gas, respectively, and

$$K_a=F_a/D_a \qquad K_s=F_s/D_s$$

$$f_a=1000\sqrt{D_a}/H_a \qquad f_s=1000\sqrt{D_s}/H_s$$

$$a_a=100A_a/H_a \qquad a_s=100A_s/H_s$$

$$F_a=FG_a \qquad F_s=FG_s$$

where A, H, and D have the same significance given them throughout this paper, but F_a and F_s are obtained as summations of the products of the fractions by volume of each constituent G of the gas mixtures and a factor F, called the "lifting constant" of the constituent. The constant F was chosen empirically from a consideration of lifting curves, not of flame velocities, and is based on the effect of unit mass of each constituent of the gas mixture, which is the reason for the appearance of specific gravity in the denominator of the expression defining K. For further details of the derivation of I_L, Bulletin 36 must be consulted.

In comparing the new index, J_L, with I_L it is first to be noted that one decreases while the other increases

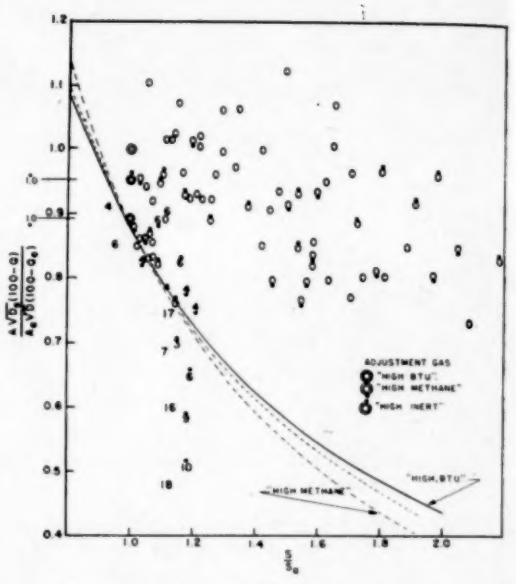

FIGURE 12. *Observations of lifting with appliances adjusted for natural gases recorded in Bulletin 36.*

Value of J_A modified to take account of oxygen in the gas.

with increasing tendency of the gas to cause lifting. This amounts to saying that $AS\sqrt{D_a}/A_aS_a\sqrt{D}$ corresponds more nearly to the reciprocal of I_L, which we may write

$$\frac{1}{I_L}=\frac{K_s}{K_a}\left\{\frac{f_a a_s}{f_s a_a}-\frac{1}{K_s}\log\frac{f_a}{f_s}\right\}.$$

Making the various substitutions indicated above, simplifying, and dropping the subscript (s) as in the remainder of this paper

$$\frac{1}{I_L}=\frac{KA\sqrt{D_a}}{K_aA_a\sqrt{D}}\left\{1-\frac{1}{K_a}\log\frac{H\sqrt{D_a}}{H_a\sqrt{D}}\right\}.$$

The term $1/K_a \log H\sqrt{D_a}/H_a\sqrt{D}$ is found to be rather small in most cases. If we neglect it for the moment and assume that values of K are proportional to values of S in index J_{L-1} one index becomes the reciprocal of the other. Next we should note that I_L contains no term relating specifically to oxygen, but as this is rarely an important constituent of a gas, the omission is relatively unimportant.

As K and S are derived in very different ways from observations of different kinds, no theoretical relation between them can be stated. A comparison was made by plotting with respect to each other their numerical values for the experimental gases described in Bulletin 36 and Report 1106–A. The assumed proportionality was not closely approximated; nevertheless there is a general agreement as to the nature of the index needed to represent lifting, with the principal difference appearing in the values and methods of determining constants that are essentially similar functions of flame velocity.

V. Selection of the Best Index of Interchangeability for Lifting

Figures 11 and 12 give a good general picture both of the agreement of J_L with observations and of the relations between the functions of composition of gas mixtures from which the index was derived, but they do not permit ready comparison of J_L with I_L or other indexes for predicting lifting based on different properties of the gases involved. Accordingly, the data of figure 11 are plotted in still a different manner in figures 13 and 14. In figure 13, the lifting index J_L for each substitute gas is plotted with respect to the number of appliances for which any lifting (+4 or +5 flames) was recorded. In figure 14, the abscissa is the number of burners with +5 flames only. The average index of limiting mixtures in each figure and the suggested limit of interchangeability correspond, respectively, to the solid and the dotted reciprocal curves of figure 11. Arrows at the edges of the figures indicate the direction of points off the figure, the inclusion of which would have unnecessarily reduced the scale used. Each of the two asterisks in the figures represents a substitute gas with which a single +4 flame was recorded. These points indicate the same gases (A1–32–90 and A1–32–55) that were represented by underlined X in figure 11. They appear to be quite anomalous; at least we should expect the gas represented by the lower point to produce many +5 flames. When the observations made with these two gases are plotted with respect to other functions of composition, I_L, AGA index C, Knoy Index C, J_H, J_A, the ratio of hydrogen to inert in the gas and to the observed adjustments of the Rochester Burner that produced lifting, they appear to be as much out of line as they are in figures 13 and 14. They are also highly improbable merely when compared with the other

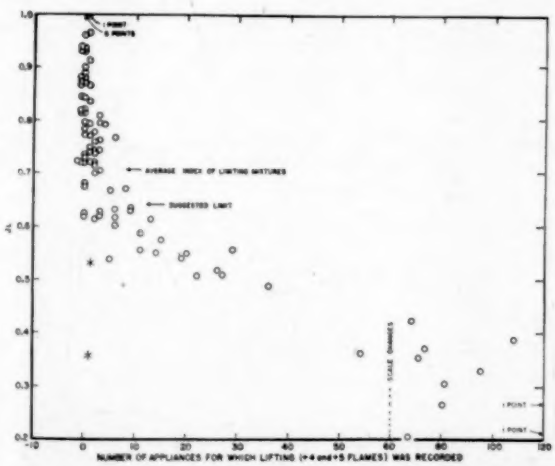

FIGURE 13. *Number of appliances showing any lifting (+4 and +5 flames) compared with values of J_L.*

Data from Report 1106A.

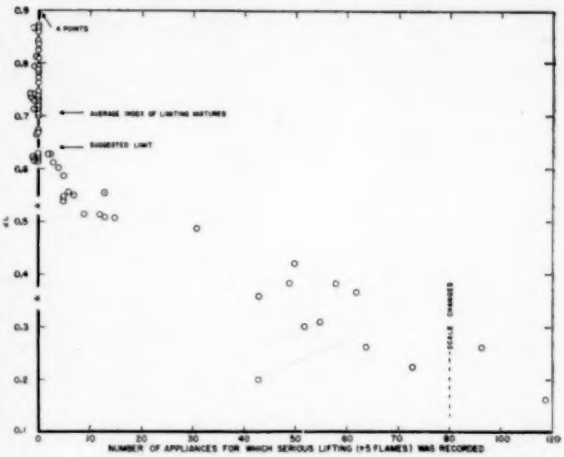
6 POINTS
AVERAGE INDEX OF LIFTING MIXTURES
SUGGESTED LIMIT
SCALE CHANGES
NUMBER OF APPLIANCES FOR WHICH SERIOUS LIFTING (+5 FLAMES) WAS RECORDED

FIGURE 14. *Number of cases of serious lifting (+5 flames) compared with J_L.*

Data from Report 1106A.

observations of mixtures with the same supplemental gas (A–32). This gas undiluted showed 71 cases of lifting, of which 55 were recorded as +5 flames, and the mixture of 40 percent of the gas with 60 percent of adjustment gas A–1 caused nine cases of +4 flames, but the anomalous mixtures containing 90 and 55 percent, respectively, of gas A–32 showed only one case of +4 flames each. For these reasons it seemed desirable to omit these two gases from all comparisons between the various indexes.

In selecting the limits of mixing of supplemental with adjustment gases, the AGA committee permitted some +4 flames and even a few +5 flames. Taking the first gas substituted, A1–11 as an example, the committee decided that a mixture containing 30 percent of the supplemental gas was to be considered interchangeable with the adjustment gas, although it was recorded as having produced four +5 and two +4 flames. The number of cases of serious lifting (+5 flames) therefore seems to be a more practical as well as an easier basis on which to compare various indexes than the number of cases of both +4 and +5 flames. Hence, only the more serious type of lifting will be included in most of the comparisons that follow.

In figure 15, lifting is plotted with respect to the AGA index for lifting, I_L. In figure 16, the same comparison is made with the AGA general index of interchangeability, C. Plots of the same kind were made for the Knoy index, for the ratio of hydrogen to inert, which is regarded as a general index of interchangeability by some operators, for several other functions of composition, and for comparisons of appliance burners with the Rochester test burner. The observations made after adjusting appliances with the other adjustment gases were treated in the same way. Then similar plots were made of the results of observations of the other types of appliance failure. In all, more than 100 plots were made to

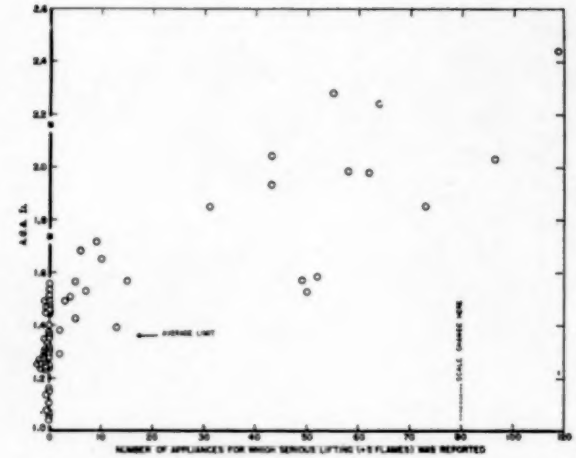

FIGURE 15. *Number of cases of serious lifting (+5 flames) compared with AGA Index I_L.*

Data from Report 1106A.

show the frequency of appliance failure of one kind or another in relation to some computed or experimental means of predicting failure.

Some of the plots resulted in nothing of interest, but to reproduce all those that did would require too much space and would be more confusing than helpful. Some times it is hard to determine from casual inspection which of two indexes better represents the observations. A method of summarizing in numerical form the information available from one of the figures is needed. The method devised will be explained with the aid of figure 17, assumed to represent a simple hypothetical case. It is assumed that five gases, *A* to *E* were tested with the results indicated in the figure, that is one appliance showed lifting with gas A, two with gas B, six with gas E, etc.

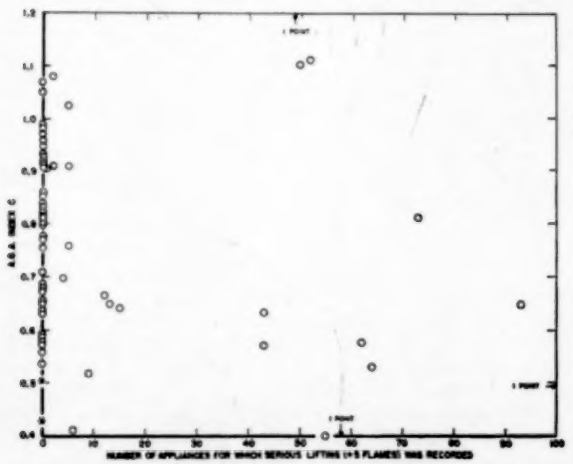

FIGURE 16. *Number of cases of serious lifting (+5 flames) compared with AGA Index C.*

Data from Report 1106A.

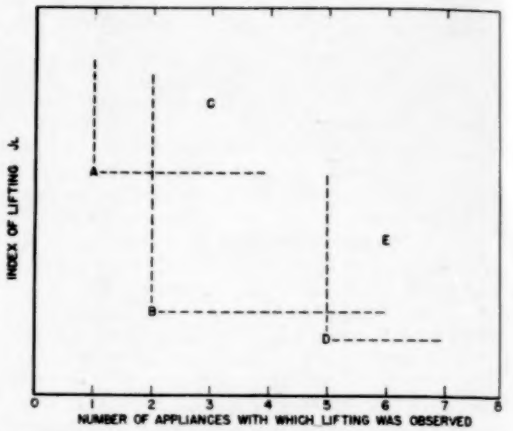

FIGURE 17. *Figure representing the hypothetical case used to explain the method of "summations" employed for comparing various indexes.*

We should expect the least appliance failures from *C*, because it has the highest index J_L, and the most failures from *D* with the lowest index. Table 2 is prepared to show the exceptions to the predictions that would be made from a knowledge of the indexes. In the column headed "summation A", one is entered for each gas with which lifting was recorded less frequently than with one or more gases having higher values of the index. In the case of each of these mixtures, the number of mixtures of higher index that produced lifting more frequently is noted and added together in the column headed "summation B." From the total number of cases of observed lifting with the mixtures indicated in summation B is subtracted the total number of cases occurring with the mixtures indicated in summation A. This gives "summation C", which is the total number of times lifting was observed from any appliance with any gas when it would not be expected to occur from the known extent of lifting with each of the other gases and the relative values of the indexes for the two gases.

The summations are easily made from the plotted data with the aid of a piece of transparent plastic

TABLE 2.—*Hypothetical case showing application of method of summation from figure*

Gas with which other gases are compared	Summation		
	A*	B	C
A	1	1	2
B	1	2	5
C	0	0	0
D	1	1	1
E	0	0	0
Total	3	4	8

* *Summation A represents the number of times we would be in error if we predicted, from their indexes, whether each gas mixture would cause lifting with more appliances than would occur with any other one gas mixture. Summation B represents the number of times we would be in error if we predicted from the index whether each gas mixture would cause more frequent lifting than each of the other gas mixtures. Summation C represents the number of cases in which we would be in error if we predicted whether each appliance would show lifting with each gas from a comparison of the index for that gas with the index for each other gas.*

with one right angle, the apex of which is successively placed on each of the plotted points as represented by dotted lines in figure 17. The numbers to be entered in each summation are then easily counted. In detail, mixture A has a lower value of J_L than mixture C, but caused lifting of two less appliances. Hence we enter 1 in summation A, one in summation B, and 2 in summation C. Mixture B has a lower value of the index than either C or E, hence 1 is added to summation A, and 2 to summation B. One more appliance lifted with C than with B and four more with E than with B, hence the total, 5, is entered in summation C. There were less failures with gas C than with any gas of lower index not already compared with it; hence there are no exceptions to the rule and nothing to enter in any of the summations. Mixture D has a lower value of the index than E, and one less appliance showed lifting with it than with E, hence 1 is added to summations A, B, and C.

The application of this method of descriptive summation to comparisons between indexes for other limiting conditions and the experimental observations should now be understandable. If the summation for one index results in smaller numbers than for another, the first is the better index because there are less exceptions to the predictions that can be made from its use.

The summations of observations made after adjustment with gas *A*1 for several indexes are shown in table 3. The data are confined to the gases for which I_L was given. The last series of numbers in the table, designated "possible", requires explanation. The AGA lifting index was given for 70 gases. If the one with the highest index had produced the most cases of lifting, the other 69 would have to be entered in summation A, and this in spite of the fact that the remainder of the observations might have been in perfect order. Hence summation A is not very significant. Summation B is prepared, in effect, by comparing the tests of each of the 70 gases with the tests of each of the remaining 69 gases, making a total of $70\times69/2=2{,}415$ comparisons. When there is a reversal of the anticipated relation, a unit is entered in summation B. Had all comparisons resulted in reversals, the fact would have represented a perfect inverse correlation between index and observation, that is a correlation that varied in the direction opposite to that anticipated. Had there been no correlation between the index and the number of appliance failures, we should expect about half this number in summation B. There were nine combinations of adjustment of each of 28 appliances, hence the possibility that in any one of the 2,415 possible reversals there would be $9\times28=252$ more failures with one gas than with the other. But this maximum difference could have existed in the maximum number of cases only had the gases been divided into a group each number of which produced 252 failures and an equal group that produced no failures. Comparisons between numbers of the same group would show no differences. The maximum number that could appear in summation C is $35\times35\times252=308{,}700$, but this again could occur only if there were complete reversal of the predicted relation of index to appliance failures, as well as arrangement in two extreme groups. The number of failures that would have appeared in summation C had there been no correlation between the index and appliance failure cannot be stated, because it depends greatly on the distribution of tendencies to lift among the appliances used, but it is of the order of magnitude of 10^5.

Table 3 shows that there is a strong correlation with the numerical value of the index even in the case of the worst one, which is AGA index C. We see at once that the number of times we would fail to predict lifting on individual appliances by the use of I_L, J_L, or J_{L-1}, indexes designed to show the tendency to lift only, is an order of magnitude less than the number of times we would fail when using any of the single expressions designed to show general interchangeability, except the ratio of hydrogen to inert which, for this set of data, is about as good as I_L. Index J_L is shown to be much better than I_L so far as this set of data is concerned, and the advantage of correcting J_{L-1} for the presence of oxygen in the gas is apparent.

TABLE 3. *Summations showing the application of various indexes to observations of lifting made after adjusting appliances with gas A1.*

(Only +5 flames and cases for which I_L is given are included. Tests A1-32-90 and A1-32-55 omitted).

Index	Summation		
	A	B	C
J_L	14	36	294
J_L-1	22	48	339
AGA I_L	37	120	1,402
AGA C	57	817	12,614
Knoy C	48	451	10,915
Hydrogen: inert	39	109	1,112
J_H	58	429	12,392
Possible	69	2,415	308,700

The superiority of J_L is even more evident if we omit from the summations the mixture A1–26–100, experimentation with which was on a different basis than with the other mixtures. This is explained in footnote in Report 1106–A as follows: "Data taken prior to the Committee's decision to adjust each burner for more than one kind of flame. First figure gives number of burners with unsatisfactory flames, second indicates the number of burners adjusted for the particular kind of flame". We find that of the seven, eight, or nine burners tested under five of the nine combinations of adjustment and pressure, all had +5 flames. We have no way of judging how many failures would have occurred had all 28 appliances been given all the adjustments. Omitting this gas gives the three lifting indexes with the summations listed in table 4.

Although data from the experiments with several adjustment gases have been plotted for various general indexes, the superiority of the lifting indexes I_L and J_L is so decisive that no further consideration

TABLE 4. *Summations of observations of lifting with appliances adjusted with gas* A1.

Tests A1-26-100, A1-32-90, and A1-32-55 omitted from the comparison

Index	Summation		
	A	B	C
J_L	13	27	125
J_{L-1}	21	39	170
I_L	36	113	1,101

need be given to AGA index C, Knoy index C, etc. Summations for the comparisons with natural gases are given in table 5. In this set of comparisons I_L certainly has the advantage. It might be concluded that J_L is generally unsuitable for use when burners have been adjusted with natural gases, but such a conclusion is probably not warranted by the experimental data, which show that J_L applied very well to all tests except those involving a single producer gas and its mixtures. Further work may be needed to establish the value of J_L when applied to very slow-burning gases, however. Again J_L appears to be superior to J_{L-1} by a margin wide enough to warrant dropping the latter from further discussion.

The interpretation of the experiments recorded in Research Report 1106, parts B, C, and D is affected by the fact, earlier mentioned, that varying numbers of appliances were actually tested with the different conditions of adjustment and gas supply. Usually the burners most susceptible to lifting were tested first. When enough of them had been tested without lifting to make it probable that most of those not tested would not show lifting, testing was discontinued. In these cases it is not likely that the number of failures would have increased greatly had all the appliances been tested; but there were other cases in which all appliances tested showed +5 flames, and it appears that testing was discontinued because the noninterchangeability of the substitute gas with the adjustment gas had been shown decisively and further experimentation seemed unnecessary for the original purpose of the investigation.

Even had the appliances been arranged as well as practicable in the order of susceptibility and had testing been continued with each gas until some of the burners had not shown lifting, there must have been some uncertainty as to the number that might have failed, for the order of susceptibility was by no means constant. When, under a given condition of adjustment and gas supply, no more than three appliances showed either +4 or +5 flames, they were designated by their identifying letters. In table 6 is a summary of the entries of this kind in Report 1106–A. When a given burner was the only one that showed +5 flames or the only one that showed +4 flames when none showed +5 flames, it was considered "most susceptible" to lifting and entered in column (A). If its greater tendency to lift was shared by one or two other burners, it is entered in column B, etc. Rated like an athletic event, a first in susceptibility to lifting is represented in column A, a tie for first with not more than two others in column B, second or a tie for second with not more than two others in C, third or a tie for third with not more than two others in D. Columns E and F merely show that the burner was not first or second, while the entries under G show definitely that the burner was often far less susceptible than numerous others. The burners are listed in order of the number of times they appeared to be most susceptible or among the two or three most susceptible, and 19 of 28 were in this position under at least one condition, but those most susceptible in many cases were as low as 16th in order of susceptibility in other cases.

If such variations appear in the relative susceptibility to lifting, we cannot expect greater regularity in their absolute susceptibilities, which determine the number of appliances on which lifting should occur with a given gas. Even if the index were the

TABLE 5. *Summations of observations of lifting with appliances adjusted with natural gases*

Adjustment gas	Index	Summation		
		A	B	C
"High Btu"	J_L	9	9	47
	J_{L-1}	8	12	64
	I_L	3	3	22
"High methane"	J_L	1	1	2
	J_{L-1}	3	6	24
	I_L	0	0	0
"High inert"	J_L	4	4	21
	J_{L-1}	4	8	30
	I_L	1	1	2

TABLE 6. *Relative tendency to lift shown by certain burners as recorded by burner designations in table 7 of Report 1106–A*

Column	A	B	C	D	E	F	G	Average number of more susceptible burners	Greatest number of more susceptible burners
Number of burners shown more susceptible	0	0	1	2	1	2	3 or more		
Number of burners shown equally susceptible	0	1 to 2	0 to 2	0 to 2	Not shown	Not shown	.....		
Burner	Number of cases								
e	12	17	0	1	9	24	18	6	15
o	6	20	1	0	12	8	5	4	6
n	10	14	3	2	7	21	18	8	15
af	0	14	5	2	9	18	7	4	12
y	3	6	0	0	20	27	13	3	6
x	3	4	1	0	.....	.....	.....	.....	.....
h	2	4	2	0	.....	.....	.....	.....	.....
z	3	2	0	0	.....	.....	.....	.....	.....
c	3	1	0	0	.....	.....	.....	.....	.....
t	0	4	0	0	.....	.....	.....	.....	.....
k	0	3	1	1	.....	.....	.....	.....	.....
g	0	3	0	0	.....	.....	.....	.....	.....
q	0	3	0	0	.....	.....	.....	.....	.....
d	1	1	2	0	.....	.....	.....	.....	.....
m	1	1	1	0	.....	.....	.....	.....	.....
w	1	0	0	0	.....	.....	.....	.....	.....
f	0	1	0	0	.....	.....	.....	.....	.....
p	0	1	0	0	.....	.....	.....	.....	.....
r	0	1	0	0	.....	.....	.....	.....	.....

TABLE 7. *Summations of all tests for lifting compared with I_L and J_L (comparisons with adjustment gas A1 limited to those for which I_L had been computed)*

Adjustment gas	Index I_L summations			Index J_L summations			Maximum possible summations		
	A	B	C	A	B	C	A	B	C
A1	37	120	1,402	14	36	294	69	2,415	308,700
B1	23	76	601	20	77	446	64	2,080	266,112
B2	14	44	188	17	35	92	56	1,596	204,624
B3	15	48	201	24	35	58	72	2,628	326,592
C1	32	105	611	30	42	258	93	4,418	344,824
D1	7	11	60	2	3	4	11	66	7,560
N1	3	3	22	9	9	47	47	1,128	145,152
N2	0	0	0	1	1	2	17	153	20,412
N3	1	1	2	4	4	21	21	231	30,492
Total	132	408	3,087	121	242	1,222	450	14,715	1,654,468

best possible guide in predicting appliance failure, and if all appliances had been tested with every gas, we should expect considerable irregularity among the results, because table 6 shows the variations to be unpredictable. When a varying number of appliances is tested, the scrambling of the results is much greater. Nevertheless, we have no alternative to using the data available. The apparent value of any index must be unfavorably affected by such irregularities as the variable number of appliances tested, but these variations are not too great to leave a high degree of correlation between the number of appliance failures and the properties of the gas supply, and the index that most perfectly represents these properties should still show the better correlation with the number of appliance failures.

It would be possible to omit from consideration certain results in Reports 1106-B, C, and D, for the same reasons given in the case of tests A1–32–90, A1–32–55, and A1–26–100, but their individual discussion would not be worth while. Accordingly, all the results recorded in these reports have been included in the "summations" made of them. The AGA index I_L was reported for only 57 of 65 gases for which tests were recorded with B1 as the adjustment gas, but all tests are included in the summations for J_L, although the larger number of gases leads necessarily to somewhat larger summations. In spite of this handicap, J_L shows the higher degree of correlation in this as in all other cases, except the tests reported in Bulletin 36. The summations for each group, including those previously discussed, are given in table 7. There is no room for uncertainty that J_L represents the results of this huge group of tests materially better than does I_L.

The Rochester Test Burner is a simple single-port burner with a graduated means of adjusting the primary air opening. When used to measure the lifting properties of a gas, a normal rate of gas flow is set with an adjustment gas, and with each substitute gas in turn the air shutter is opened until lifting occurs. A graduated scale attached to the air shutter provides a numerical reading that is taken to be the desired measure of the tendency of the substitute gas to produce lifting. The readings of the Rochester burner were not included in table 3 with the indexes, because neither they nor index I_L was applied to all the gases substituted for A1, and the ones omitted were not the same. Index J_L was plotted for the same gases used with the Rochester burner, however, and the usual summations taken. Including +4 and +5 flames, they were as follows: for J_L, A=25, B=72, C=481. For the Rochester-Burner Index, A=33, B=108, C=1,331. It appears that observations with the Rochester burner would have provided a more accurate means of predicting lifting than I_L but not as accurate a means as J_L. The same appeared to be true in plots of tests involving other adjustment gases, but summations were not made.

VI. Derivation of a New Index to Represent Flashback, and its Comparison With AGA Index I_F

The flashback curves shown in Report 847 are not complete enough, nor do they cover a sufficiently varied lot of gases to be of much use in preparing a formula for predicting flashback. It was therefore necessary to go much farther back, to 1922 and the Bureau's Technologic Paper 222 [11], which dealt with a considerable variety of rapidly burning gases and two range burners. The observations were made before methods of testing appliances were well developed and leave much to be desired in the way of completeness and accuracy, but they still represent the best data for this purpose available to the writer.

Essentially the same method was employed as in the preparation of the formula for lifting. Curves were replotted from the original figures to show the average rate of gas supply (in terms of the air required to burn it) at which the two appliances flashed back with each gas and at each of several percentages of primary air. Only a part of the 10 resulting flashback curves, for gases designated 103–106, are shown by heavy lines in figure 18; the

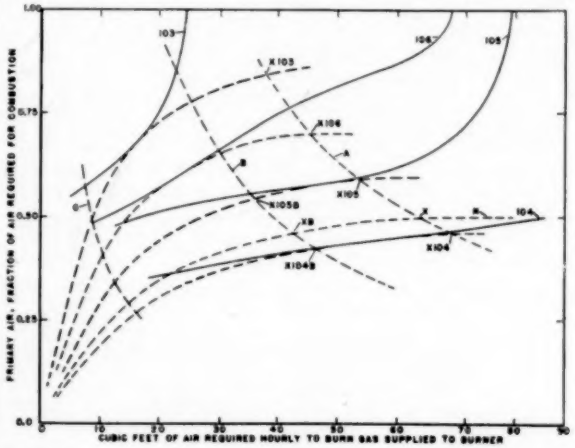

FIGURE 18. *Average flashback curves for four gases, and changes that occur in tendency to flash back when pressures and mechanical adjustments are changed.*

others are omitted to make the figure less confusing. In the case of lifting we were concerned only with what would happen when the gas-supply valve of an appliance is wide open. If lifting does not occur under that condition, it does not occur when the gas is turned down. The case of flashback is entirely different. Ranges and space heaters are usually manually controlled to whatever rate the user desires, and many appliances of other types have graduating thermostats that effect similar control automatically. Safety from flashback therefore requires that it shall not occur under any conditions produced by gradually reducing the pressure at the burner orifice, by closing a valve in the supply line or otherwise. What happens to the input of gas and the injection of primary air when this occurs is represented on the basic diagram by "normal injection curves," of which curves N_a and N of figure 2 are examples. Normal injection curves in figure 18 are broken curves converging at the origin. The point representing the operation of an appliance at its normal input rating may seem remote from flashback, but if the normal injection curve connecting it with the origin intersects the flashback curve, the appliance is subject to that hazard. The changes that take place in the flow of gas and primary air when one gas after another is supplied to an appliance with unchanged mechanical adjustments, including the burner valve, is again represented by a reciprocal curve (A).

The solution of our problem begins with the construction of a normal injection curve for a typical appliance, marked N in figure 18. Such curves differ somewhat from one appliance to another, but are enough alike to permit almost any one to represent appliances in general. Other normal injection curves to be used in the same problem must be related to the others as shown by the method of deriving one from another which follows. The intersection of curves A and N is marked X. From another point on curve A, say *X–105*, a normal injection curve is constructed in the following manner. Other reciprocal curves, of which B and C are shown, are constructed. Each represents a different pressure at the orifice. Curve N intersects curve B at a point marked X-B. The normal injection curve through point *X–105* will intersect curve B at a point *X–105–B*, whose abscissa has the same ratio to that of *X–105* as the abscissa of point X-B has to the abscissa of X. In this manner any number of points on the normal injection curve through *X–105* can be located, and any number of other normal injection curves can be drawn.

By trial and error, normal injection curves tangent to the experimental flash back curves were constructed in the manner described. Their intersections with curve A are marked *X–103*, *X–104*, . . . and have the same significance with respect to flashback as did the intersections of reciprocal curve Y with the lifting curves of figure 4. The abscissas of points *X–101*, . . ., *X–110* are plotted with respect to flame speed (S) in figure 19. The gas rate in terms of air required to burn it will be designated A_p. It was plotted in preference to its reciprocal, primary air, because a simpler relation was expected to appear. Actually, the points scatter badly, but they can be represented by a straight line as well as by any other simple function. The straight line obviously does not pass through the origin and the still simpler relation of direct proportionality does not exist. As each abscissa of a point of figure 19 is that of a point on the same reciprocal curve of figure 18,

$$A_p = kA/\sqrt{D}, \tag{2}$$

and the equation of the straight line of figure 19 can be written

$$S - kA/\sqrt{D} + C = 0 \tag{3}$$

in which k and C are constants. The significance of the equation is that, with single values of the constants, it represents in terms of three properties of the gas A, D, and S, and with as much accuracy as the accuracy of the observations and assumptions will permit, all gases that are equally susceptible to flashback.

The observations of flashback recorded in Report 1106–A are plotted in figure 20 with the coordinates used in figure 7. When flashbacks were reported without a qualifying note for any appliance, the point corresponding to the gas used is marked +, and when no flashback occurred, it is marked 0. When flashback was noted for a single appliance but marked "tendency" or "occasionally," the corresponding point was omitted from the figure as indeterminate. The diagonal straight line does not make a perfect separation of gases with which flashback was recorded from those with which it was not, but points very far on the wrong side of the line are not numerous.

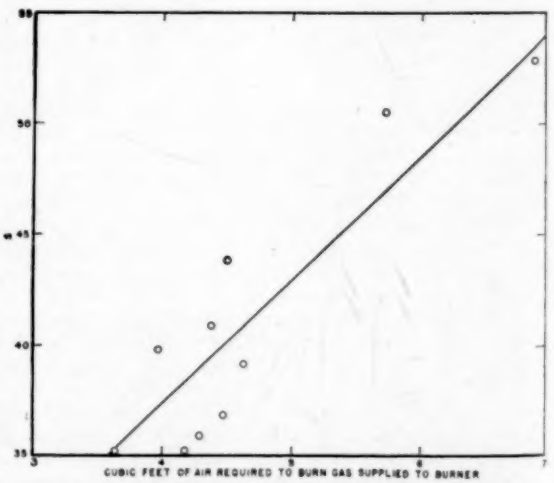

FIGURE 19. *Relation between flame speed (S) and rate of gas supply (in terms of air required to burn it) at initial adjustments of appliance with each gas such that flashback will just occur when pressure is gradually reduced.*

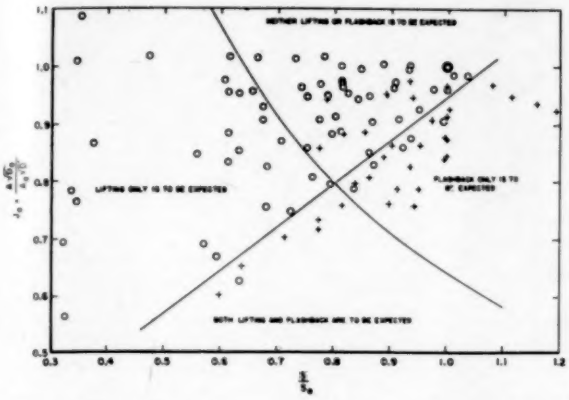

FIGURE 20. *Observations of flashback from Report 1106–A.*

Added curve for lifting shows generally the conditions for stable and unstable flames.

Actually, the line was drawn, in the first place, from the undetailed but considered data of the Anthes Report, with which it was in excellent agreement.

It is of interest to add, to the line indicating the limit of interchangeability with respect to flashback, the reciprocal curve indicating the limit of interchangeability with respect to lifting previously found. The curve in figure 20 corresponds to the "suggested limit" of figures 11, 13, and 14. Figure 20 is thus divided roughly into quadrants, only one of which represents gases with which flames may be expected to be stable (subject to neither lifting nor flashback).

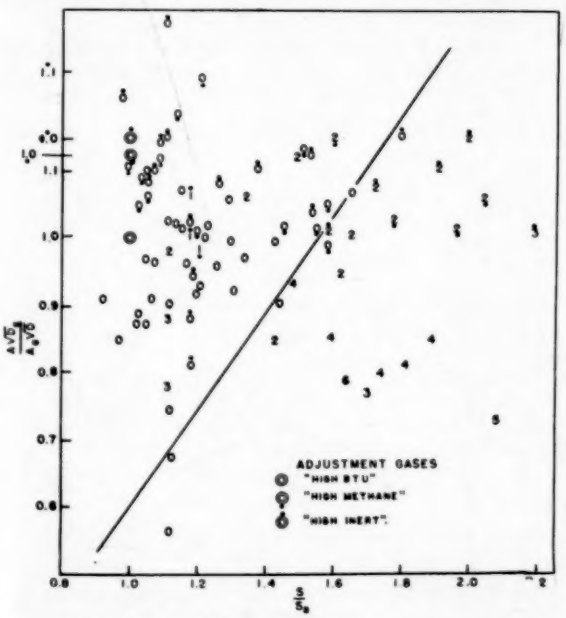

FIGURE 21. *Observations of flashback with appliances adjusted for natural gas.*

From Bulletin 36.

In figure 21, three plots showing the results of flashback tests with appliances adjusted for the three natural gases of Bulletin 36 are superposed. The figure is like figure 12 except that the numbers represent the number of appliances that flashed back with each gas instead of the number that showed lifting. The three figures that are combined in figure 21 were drawn separately, a line was drawn on each to represent what was considered to be the permissible limit of interchangeability with respect to flashback, and the three figures were superposed by sliding vertically (adjusting the ordinates) until the limiting curves coincided.

The slopes of the lines representing limits of interchangeability in figures 20 and 21 are identical, although they may not appear to be so because of a difference of scale. They may both be represented by the equation

$$S/S_a - 1.4A\sqrt{D_a}/A_a\sqrt{D} = C,$$

in which 1.4 is also the value of k in eq 3 derived from figure 19.[6] Assuming the relation to be quite general, gases that are identical ("exactly interchangeable") in their tendency to cause flashback will always be represented by points on a line parallel to those in figures 19 and 20. Then the "index," or measure of departure from exact interchangeability between two gases, can be taken as the difference between the final constants of the equations of the lines on which they lie, that is,

$$J_F = C - C_a = S/S_a - 1.4A\sqrt{D_a}/A_a\sqrt{D} + 0.4,$$

where J_F is the new index for susceptibility to flashback.

It is again of interest to examine the relation of the new formula to the corresponding AGA index defined by the equation $I_F = K_s F_s / K_a f_a \sqrt{h_s/1000}$. The various symbols have the same meaning as in the earlier equation defining I_L. By substituting the symbols used in this paper, simplifying, and rearranging terms to put those depending primarily on speed of combustion on one side of the equation and those having to do with "inputs" of gas and primary air on the other, this becomes $K/K_a = I_F(H\sqrt{D_a}/H_a\sqrt{D})\sqrt{1000/H}$, or making the now familiar approximate assumption that heating value and air requirement are proportional, $K/K_a = I_F(A\sqrt{D_a}/A_a\sqrt{D})\sqrt{1000/H}$.

The new expression for interchangeability put in the corresponding form becomes

$$S/S_a = 1.4(A\sqrt{D_a}/A_a\sqrt{D}) - \mathrm{C}.$$

Each of these equations is designed to represent a set of gases, all of which would be equally susceptible to flashback. Hence I_F is a constant for such a set. A fairly close relation between the two formulas is

[6] Of course this equality was obtained by adjusting the slopes of the lines a little at the time the figures were drawn, but it is difficult to say that the agreement of the line with the points it represents could be improved by a change of slope in any of the figures.

now apparent, but there are important differences. When we change to another set of gases all interchangeable among themselves, the values of I_F and C change. The formulas also differ because of the introduction of $\sqrt{H}$ as a factor in the denominator of the AGA expression. If several sets of mutually interchangeable gases are represented geometrically in terms of the AGA formula, the result is a series of curved lines passing through the origin with different slopes. The new formula results in a series of parallel straight lines.

The value of the new formula J_F was examined in the same manner as that of J_L by plotting it and other indexes with respect to the frequency of reported failures of appliances. It was found that, as in the case of the indexes for lifting, both I_F and J_F were decisively better for judging interchangeability with respect to the property in question than is any of the general indexes. The ratio of hydrogen to inert was considerably less closely related to recorded flashbacks than to recorded lifting. Accordingly, only I_F and J_F will be discussed. In figure 22, the number of appliances that flashed back with each gas is plotted with respect to J_F. As in figure 20, mixtures for which there were recorded flashbacks of a single burner marked "tendency" or "occasionally" have been omitted. Figure 23 shows similar data plotted with respect to I_F, but, as in the case of lifting, I_F was not recorded for all the substitute gases. Figure 24 shows J_F for only those mixtures for which I_F was reported.

The point that is most noticeable when comparing figures 23 and 24 is that when using I_F and either the adjustment gas (with which flashback did not occur) or the average of the gases selected by the investigators as limiting mixtures, there are many more flashbacks that would not be predicted than when J_F is used. Thus, 19 flashbacks were recorded for eight mixtures that had lower values of I_F than the adjustment gas, and only seven flashbacks in three mixtures that had lower values of J_F. The usual

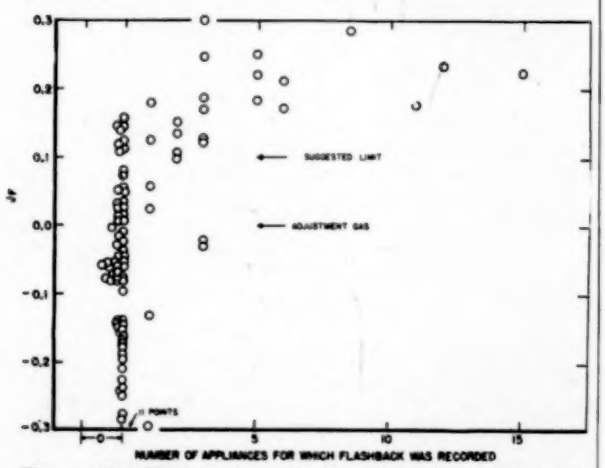

FIGURE 22. *Number of cases of observed flashback from Report 1106–A compared with the index for flashback J_F.*

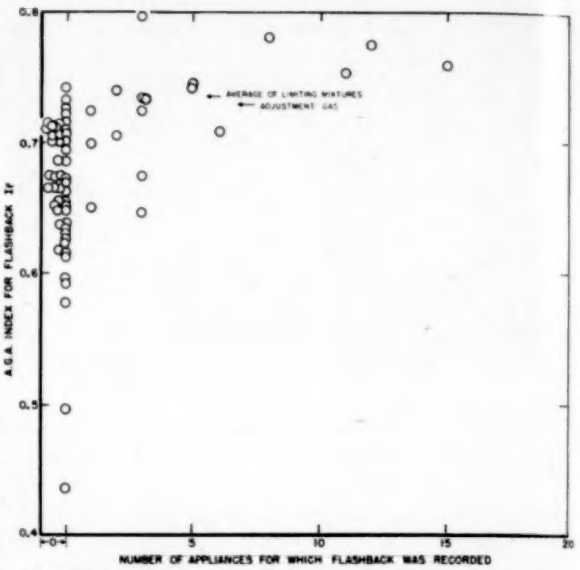
AVERAGE OF LIMITING MIXTURES
ADJUSTMENT GAS
A.G.A. INDEX FOR FLASHBACK I_F
NUMBER OF APPLIANCES FOR WHICH FLASHBACK WAS RECORDED

FIGURE 23. *Number of cases of observed flashback from Report 1106–A compared with the AGA Index for flashback, I_F.*

summations are given in table 8. As in table 4, the summations relating to comparisons with adjustment gas *A–1* are limited to those for which values of I_F are given in the report. In the other summations, all recorded results are included. Data from report 1106–B are not included because practically all the substitute gases were less subject to flashback than the adjustment gas, and the number of failures that occurred was too small to be significant.

The Rochester Test Burner could not be adjusted to flash back with four of the gases described in report 1106–A that did flashback in the appliance

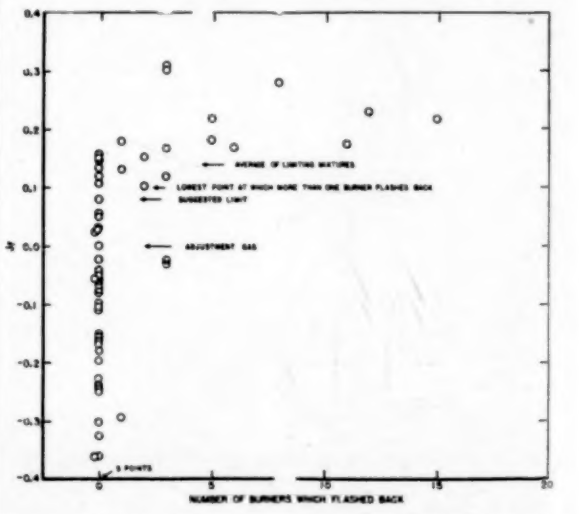
AVERAGE OF LIMITING MIXTURES
LOWEST POINT AT WHICH MORE THAN ONE BURNER FLASHED BACK
SUGGESTED LIMIT
ADJUSTMENT GAS
3 POINTS
NUMBER OF BURNERS WHICH FLASHED BACK

FIGURE 24. *Number of cases of observed flashback for the gases represented in figure 23 compared with J_F.*

TABLE 8. *Summations of tests for flashback compared with I_F and J_F*

Adjustment gas	Index I_F Summations			Index J_F Summations		
	A	B	C	A	B	C
A1	48	168	437	44	107	261
C1	53	115	337	22	73	186
N1	12	56	120	32	78	197
N2	1	2	2	5	10	15
N3	6	18	27	8	15	16
Total	120	359	923	111	283	675

burners; and there were 11 gases, including the adjustment gas, that did flash back with the Rochester Burner but not with any of the appliance burners. Summations of the readings for the gases that could be made to flash back in the Rochester burner and of J_F for the same gases gave the results in table 9. The two means of predicting flashback appear to be about equally good if the figures in the table only are considered, but it must be remembered that the Rochester burner was favored in the selection of these data because those gases that could not be made to flash back with it where the tests with the other burners would have led us to think that it could, have been eliminated from consideration. It is probably safe to conclude that flashback of appliances in service can be predicted with a little more certainty from a knowledge of the composition of two gases and the use of the index than from tests of the gases with the Rochester burner.

TABLE 9. *Summations comparing the readings of the Rochester Test Burner with J_F as means for estimating the probability of flashback*

Tests summarized are those with gases that could be made to flash back in the Rochester burner

Test gas	Index	Summations		
		A	B	C
A1	J_F	14	39	160
A1	Rochester burner	23	84	192
C1	J_F	8	30	94
C1	Rochester burner	6	27	84

VII. Interchangeability With Respect to Yellow Tips

Much the greater part of the heat of combustion of practically all gases distributed as public supplies comes from hydrocarbons. These compounds tend to be decomposed in the zone of primary reaction according to the chemical equation

$$C_nH_m+\frac{n}{2}\,0_2=n\mathrm{CO}+\frac{m}{2}\,\mathrm{H}_2. \qquad (4)$$

Although some of the carbon monoxide and hydrogen are oxidized at the same time to carbon dioxide and water, the amount is relatively small as long as an appreciable excess of hydrocarbon remains. If there is enough oxygen in the primary air to satisfy the equation, an insignificant quantity of hydrocarbon or none at all passes through the primary zone. Any hydrocarbon that does get through the zone is surrounded by an atmosphere devoid of oxygen and at a temperature high enough for the thermal decomposition of most hydrocarbons, but not high enough for methane, which is a particularly stable compound. The carbon formed by decomposition in the flame is in the solid form and imparts a yellow color to it. The carbon is most apparent near the tip of the flame. Once the solid carbon is formed, its reaction in the secondary zone of combustion is much slower than that of gases in the same region, and some of it usually escapes to form eventually a discoloring smudge of soot on nearby surfaces even when the amount is too small to produce a visibly smoky flame. This is the reason we wish to avoid "yellow tips."

The "yellow tip limit", expressing the quantity of primary air needed to avoid yellow tips, is usually near that which would be calculated from eq 4 including methane among the hydrocarbons, but since we get little or no carbon from methane itself, other hydrocarbons must be present also. Then we might expect any formula for interchangeability with respect to yellow tips to involve the amount of primary air injected, the air requirement of the gas, the total carbon in the hydrocarbons, the quantities of hydrocarbons other than methane, and their stability toward heat. Approximately a dozen different formulas involving combinations of these factors were tried, and three or four of them gave pretty good results for the data of Bulletin 36 and Report 1106–A. To make a long story short, it was found that a function of the familiar $A/\sqrt{D}$ and an easily found number N would give results as good as and more simply than anything else tried. N is the number of carbon atoms in the hydrocarbons of 100 molecules of gas minus the number of molecules of saturated hydrocarbons (methane, ethane, propane, butane, etc.) in the same.

The form of the function relating N and $A/\sqrt{D}$ had to be determined from the observations of Bulletin 36 and the Anthes Report because there were no adequate data from another source as for lifting and flashback. The data were plotted in figure 25 with J_A as ordinate and N as abscissa. N/N_a was not used because N_a may be close enough to zero to make the ratio embarrassingly large. In each case a straight line was drawn to divide as well as practicable the gases that produced yellow tips from those that did not. In figure 25 the AGA Committee's judgment of the interchangeability of the gases substituted for gas $A1$ as stated in the Anthes Report is given. The meaning of the symbols is the same as in figure 7, that is, + represents gases considered not interchangeable, O gases that were interchangeable, L limiting mixtures of supplemental gases for which yellow tips was one of the limiting conditions, and the concentric circles represent the adjustment gas. Figure 26 represents in more detail the experimental results from Report 1106-A on which the

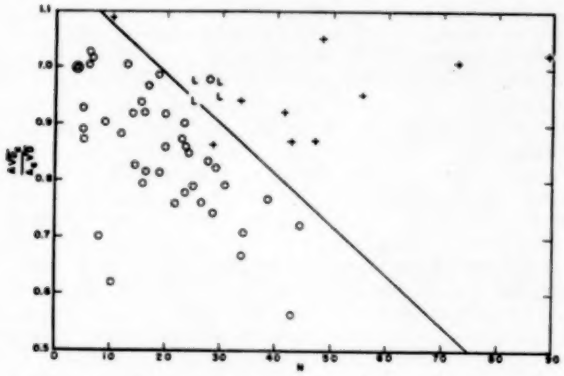

FIGURE 25. *Interchangeability of gases with respect to yellow tips as shown in the Anthes Report.*

Committee's decision as to interchangeability was based. In this figure + represents the occurrence, with some of the applicances tested, of −5 flames, *X* represents the appearance of −4 flames only, and O represents gases in whose flames no yellow was reported. Figure 27 again combines the data on the three sets of tests with different adjustment gases reported in Bulletin 36. In this case the data did not distinguish between degrees of yellow tips. Once more, the slopes of the lines in the three figures are the same, and again they separate satisfactory from unsatisfactory performance reasonably well.

The results can be expressed by the general equation

$$\frac{A\sqrt{D_a}}{A_a\sqrt{D}}+\frac{N}{110}=C,$$

in which C is a constant for any group of gases that are equally liable to produce yellow tips. As with

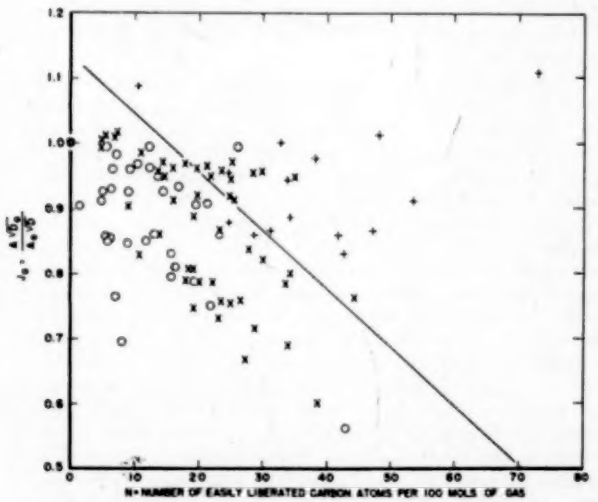

FIGURE 26. *Observations of yellow tips from Report 1106-A.*

+ Indicates −5 flames reported on some appliances, *X* only −4 flames reported. *O* no yellow reported in flames.

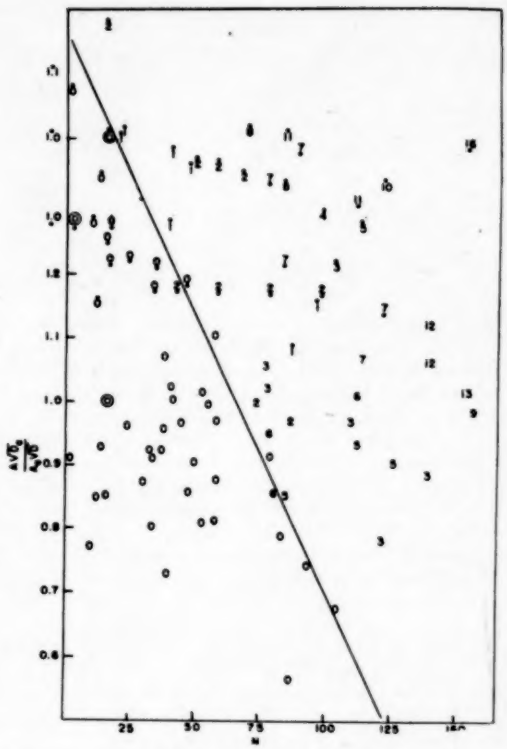

FIGURE 27. *Observations of yellow tips with appliances adjusted for natural gases as reported in Bulletin 36.*

the flashback formula, the value of C is different for another group of mutually interchangeable gases, and the difference between two values of C for two gases is a measure of their approach to interchangeability. Hence the index of interchangeability with respect to yellow tips is

$$J_Y=C-C_a=\frac{A\sqrt{D_a}}{A_a\sqrt{D}}-1+\frac{N-N_a}{110}.$$

The definition of the AGA index for Interchangeability with respect to yellow tips is

$$I_Y=\frac{f_s a_s Y_a}{f_a a_a Y_s},$$

in which

$$Y=\frac{100T}{A+7E-26.3\ O_2}.$$

The factor T is the experimentally observed number of cubic feet of primary air required to eliminate yellow tips per cubic foot of gas. It is tabulated for various constituents in Bulletin 36. Substituting the symbols of the present paper and simplifying

$$I_Y=\frac{A\sqrt{D_a}}{A_a\sqrt{D}}\frac{T_a}{T}\qquad\frac{A+7Z-26.3Q}{A_a+7Z_a-26.3Q_a},$$

in which Z is the volume of inert and Q the volume of oxygen in the gas.

To show more clearly the relation between the two formulas, they may be put in the forms

$$\frac{A\sqrt{D_a}}{A_a\sqrt{D}}=\frac{N_a-N}{110}+J_Y+1,$$

$$\frac{A\sqrt{D_a}}{A_a\sqrt{D}}=I_Y\,\frac{Y}{Y_A},$$

in which the factors representing the flow of gas and air into the burner are on one side of each equation, and those representing the chemical property of forming carbon in the flame are on the other. If $A\sqrt{D_a}/A_a\sqrt{D}$ is plotted with respect to N_a-N, the equation represents a series of parallel lines, one for each value of J_Y. For the second formula, $A\sqrt{D_a}/A_a\sqrt{D}$ is to be plotted against the ratio rather than the difference of quantities representing the chemical property of readiness to decompose when heated, and gives a series of lines, one for each value of I_Y converging at the origin. These differences between the treatment of the same phenomena by the two formulas is nearly the same as in the case of the formulas for flashback.

The indexes I_Y and J_Y were plotted with respect to the number of appliances for which yellow tips were recorded with each of the nine adjustment gases of Bulletin 36 and Reports 1106 A–D. Again, it would take too much space to display all these figures, and they will be represented only by the now familiar summations, which are given in table 10. In Bulletin 36 no distinction is made between −4 and −5 flames, and in Reports 1106–B, C, and D, −5 flames were not prevalent, hence the table represents all burners which showed yellow tips of any kind. For report 1106A, the entries are limited to gases for which I_Y was reported however. In the other cases, in which I_Y was reported for nearly

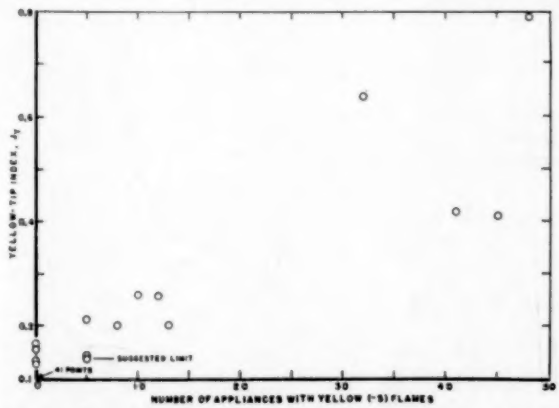

FIGURE 28. *Yellow (−5) flames recorded in Report 1106–A compared with yellow-tip index J_Y.*

Only cases for which I_Y was also given.

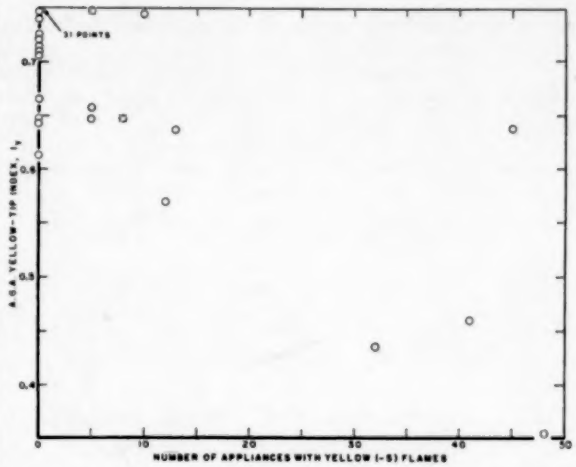

FIGURE 29. *Yellow (−5) flames recorded in Report 1106–A compared with AGA index I_Y.*

all mixtures, this distinction was not made, and the comparison is a little unfavorable to J_Y for this reason.

Actually, the appearance of a little yellow in a flame cannot be considered a serious failure of an appliance in the sense that lifting, flashback, and the liberation of carbon monoxide are; and this was evidently the opinion of the AGA Committee in charge of the investigation, for the gases selected as interchangeable included many that produced some −4 flames. It is of interest, therefore, to consider only those appliances that produced −5 flames. Figures 28 and 29 show plots of the two indexes with respect to the number of recorded cases of −5 flames among the gases of Report 1106A for which I_Y was recorded. Their summations are given in table 11, together with the summations for the observations made with the Rochester Test Burner and the Caloroptic.

TABLE 10. *Summation of observations of yellow tips (−4 and −5 flames) compared with indexes I_Y and J_Y*

Adjustment gas	I_Y Summations			J_Y Summations		
	A	B	C	A	B	C
A1	42	210	1,200	38	203	1,082
B1	38	134	402	22	76	253
B2	32	153	535	33	110	485
B3	40	288	1,351	37	185	1,102
C1	60	461	1,763	55	379	1,253
D1	7	11	60	3	4	6
N1	11	21	50	17	31	84
N2	0	0	0	1	1	1
N3	6	13	22	8	16	52
Totals	236	1,291	5,383	214	1,005	4,318

The table shows a very definite advantage of the new index, both over the old one and the test burners in predicting serious cases of failure for the group of gases considered. The new index again does not agree as well as the old with the observations recorded

in Bulletin 36, but on the whole it appears to be the better for general use.

TABLE 11. *Summation of observations of yellow (−5) flames compared with indexes I_Y, J_Y, and the settings of the caloroptic and Rochester Burners*

For adjustment gas A1 and all substitute gases for which all the data are recorded

Index	Summation		
	A	B	C
I_Y	18	39	356
J_Y	6	11	59
Rochester burner	32	39	221
Caloroptic	17	29	161

VIII. Interchangeability With Respect to Completeness of Combustion

The most important potential hazard in connection with the use of gas is that of the liberation of carbon monoxide through incomplete combustion. Where there is a uniform supply of gas, this hazard has been almost eliminated by the testing of appliances under American Standard approval requirements, the designing of appliances to meet the requirements, the assignment of safe "input ratings," and the training of service men to adjust burners to their ratings and to "normal" supplies of primary air. When the gas supply is changed, the rating in general is no longer normal, and the effect of the change on possible release of carbon monoxide must be given the most careful consideration.

It was mentioned previously that the important chemical reactions in the Bunsen flame are concentrated in two thin zones, the inner cone in which the principal reaction is usually the formation of hydrogen and carbon monoxide and the outer cone, or mantle, in which the carbon monoxide and hydrogen react with secondary air, usually completely. The size and shape of the zone of primary reaction are determined by the flame speed, or ignition velocity, with which the flame front moves into the streaming mixture of gas and primary air. The location of the secondary zone is determined by the interdiffusion of the surrounding air and the gases within or produced by the flame. If we were to plot the concentration of oxygen with respect to distance as we approach the flame surface from the outside, we would find a steadily falling curve dropping suddenly to zero at the flame surface. The concentration of carbon monoxide, hydrogen, and any hydrocarbons not already decomposed declines in the same manner as the outer cone is approached from the inside. The very thin zone of reaction itself is always located just where the concentrations of oxygen and combustible gas are exactly chemically equivalent. That this is true is easily seen if we think of how promptly any combustible gas that got into the hot, relatively concentrated oxygen just outside the zone would burn, or the speed with which oxygen would react in the concentrated fuel just inside it.

When a flame burns in the open, provided it is not too much disturbed by air currents, the zone of secondary reaction is a continuous surface, and there is no chance for carbon monoxide to escape from the region of the flame without passing through it, which it cannot do. If we thrust a cold object into the flame, the zone of secondary reaction spreads out to the extent necessary for the fuel gases to find their chemical equivalent of oxygen, and generally the surface of the solid seems to cut the flame cone sharply. Just at the cold surface, however, there is a zone in which the temperature is too low for combustion so that the continuity of the flame is broken, and through the gap a little carbon monoxide can escape. As the temperature of the solid increases, the width of the gap narrows and finally disappears entirely. The amount of carbon monoxide liberated in a case of flame impingement obviously depends on the temperature of the solid object and the length of the line of intersection between it and the flame surface. An increase in the size of the flame may lead to a greatly increased area of escape for the unburned gas, but generally the amount of carbon monoxide that gets away is not dangerous unless the flame is inclosed by solid walls, which prevent the access of as much secondary air as is needed. In this case the flame fills the combustion space and the gases that cannot be burned for lack of secondary air are too cold to burn by the time they escape from the confining walls and have access to adequate secondary air. Hence, we have two cases to consider (1) that of flame impingement in open space with adequate access of secondary air to the boundaries of the flame, which usually results in the release of measurable but not dangerous amounts of carbon monoxide, and (2) that of inclosure, which excludes the secondary air needed. In the first case, an increase in the size of the flame, whether produced by burning more gas or otherwise, has only a minor and gradual effect on the liberation of carbon monoxide; in the second case, increasing the size of the flame has no effect until the capacity of the combustion chamber and flue passages to take secondary air is almost reached, but beyond that point carbon monoxide is suddenly liberated in dangerous quantity. There are appliances in which the two effects of flame impingement and exclusion of secondary air are somewhat merged and hard to distinguish. The burning of gas in and around the glowers of radiant heaters is an example.

The case of insufficient secondary air is most important and easiest to deal with when considering interchangeability of gases. In most appliances the hydrocarbons are pretty completely decomposed in the primary cones so that only carbon monoxide and hydrogen remain to be burned. Moreover, these two gases have nearly the same heating value and exactly the same air requirement, though both they and their products of combustion, carbon dioxide and water vapor, have different rates of diffusion that affect the size of the flame appreciably. It follows that if the volume of air required, in cubic feet per hour, to burn two gases supplied to

the same appliance is the same, and if the same percentage of it is entrained as primary air, the same quantity of secondary air is also involved in the final combustion. Both these conditions are met if $A/\sqrt{D}$ is the same for the two gases. Moreover, because heating value is nearly proportional to air requirement, nearly the same total heat is produced, and the volume of secondary air, which depends on thermal convection, is nearly the same in the two cases. The result is that we can predict from basic relations that $A\sqrt{D_a}/A_a\sqrt{D}$ will be a fairly good index of interchangeability for the important case of incomplete combustion because of a lack of secondary air.

This is well confirmed by observation. It was found in the early work at the National Bureau of Standards that the curve showing the limit of complete combustion on a diagram like figure 1 was displaced much less by moderate changes in the composition of gases than were the lifting and flashback curves. Additional evidence comes from the fact that the manufacturers of many appliances wish to "rate" them as high as possible and that the upper limit is usually determined by completeness of combustion. When the rating in Btu per hour has been pushed to the limit, it has usually been necessary to assign a rating for natural gas a little lower than for manufactured gas, but the ratio about corresponds to the difference in the air requirement of the two gases. The same conclusion can be reached from several statements in the Report of the Mixed Gas Research.

The degree to which impingement occurs in an appliance depends on the size of the flame, and this is affected by the completeness of decomposition of the hydrocarbons in the primary zone and the proportions of hydrogen and carbon monoxide that result. Carbon monoxide diffuses more slowly than hydrogen, carbon dioxide more slowly than water vapor. The result is that when carbon monoxide rather than hydrogen is burned the concentrations of the reactants fall more slowly, and the position of the zone in which they are equivalent is moved outward. Of course more carbon monoxide also escapes through a gap in the zone of reaction if the concentration inside is higher. The general result may be expected to be a function of the relative amounts of carbon monoxide and hydrogen in the mixture that leaves the primary zone. It was first assumed that this could be represented by the ratio of the total number of hydrogen atoms to carbon atoms in all constituents of the gas, and this ratio was plotted with respect to $A\sqrt{D}$, but gases with large initial contents of carbon monoxide appeared from the diagram to be more susceptible to incomplete combustion than from the results of observation. If we were dealing with a gas containing no hydrocarbon, primary air would react in the primary zone to oxidize carbon monoxide; when much hydrocarbon is present it serves to produce carbon monoxide in that zone. It seems reasonable, therefore, to differentiate between the carbon in hydrocarbons and that initially present as carbon monoxide, and the ratio of the total hydrogen in the gas to the carbon in hydrocarbons only, designated R, was substituted for the previous ratio.

When $A\sqrt{D_a}/A_a\sqrt{D}$ is plotted with respect to R/R_a for appliances adjusted with gas $A1$, the result is figure 30. Gases with which incomplete combustion was reported are marked (+), those which burned completely in all appliances are marked (O). If $A\sqrt{D_a}/A_a\sqrt{D}$ which we previously called J_a were the sole determining factor in incomplete combustion, the best line we could draw to separate the two symbols of figure 30 should be a horizontal line. Apparently it is not. Similar figures were drawn for each of the sets of observations with other gases, and the slope of the limiting straight line that would give the best general separation was chosen by considering all the figures.

If the relation represented by the straight line chosen is right, equal susceptibility of gases to produce carbon monoxide occurs when

$$\frac{A\sqrt{D_a}}{A_a\sqrt{D}}-0.366\,\frac{R}{R_a}=C,$$

where R and R_a are the ratios of the number of hydrogen atoms in all forms of combination to carbon in hydrocarbons only, and C is a constant that is the same for all exactly interchangeable gases.

Again we can take as the index of interchangeability the difference between the values of C for two gases when the properties of the two gases represented by A, D, and R are put into the equation, that is,

$$J_I=\frac{A\sqrt{D_a}}{A_a\sqrt{D}}-0.366\,\frac{R}{R_a}-0.634.$$

When the substitute gas is exactly interchangeable with the adjustment gas, $J_I=0$.

No coefficient of interchangeability for incomplete combustion was considered necessary by the authors

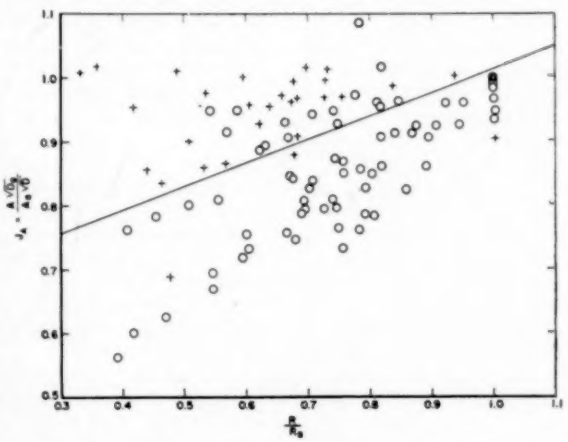

FIGURE 30. *Observations of incomplete combustion from Report 1106–A.*

Relation to J_A and R/R_a.

of Bulletin 36 because it was found that gases interchangeable with respect to the other limiting conditions were interchangeable with respect to completeness of combustion also. This was by no means always true of the observations recorded in Reports 1106–A–D. This is not hard to explain by reference to figures 2 and 3.

The adjustment gases of Bulletin 36 were all slow-burning natural gases, and at least some of the appliances were adjusted rather close to the condition of lifting. In most cases the substitute gases were of faster-burning types (with shorter flames and less chance for impingement) which, tend to produce less carbon monoxide unless the input to the burner is greatly increased. With most of the substitutions, the displacement of the limit of complete combustion was therefore in the direction of safety, and the imminence of lifting prevented too great an increase of input. The only substitute gases for which the shift of the limit of complete combustion could have been away from safety were those containing a considerable amount of inert. Because inerts inject air without "requiring" any for chemical reaction and increase the velocity of flow through the ports without increasing the heat liberated, they affect the tendency of the flame to lift more than the tendency to burn the gas incompletely. The substitute gases also generally contained higher percentages of easily decomposed hydrocarbons than the adjustment gases, so that any displacement of the "adjustment" toward less primary air, which might have precluded danger from lifting, caused the higher yellow-tip limit to be encountered.

The case was quite different with the gases covered by Report 1106. The adjustment gases were all of rapid-burning types; they contained readily decomposed hydrocarbons; and the adjustments were nearly all rather far from lifting conditions. Introducing natural gas or even propane or butane into these burners, tended to reduce the input at which incomplete combustion is encountered without adversely affecting the yellow-tip limit and often without crossing the initially wide margin of safety from lifting. Therefore the fact that an index relating to completeness of combustion was not needed when considering the tests recorded in Bulletin 36 does not mean that such an index is not needed in general.

Table 12 shows this rather clearly. In it are listed the number of substitute gases for which only one type of failure was recorded in Report 1106, the number of times the AGA Committee attributed to only one limiting condition the amount of a supplementary gas that could be satisfactorily added to the base gas, and the total number of times a given type of failure was said to be one "reason for limiting further addition of the supplemental gas".

In figure 31, the numbers of appliances reported in Report 1106–A to have burned the gases incompletely are plotted with respect to J_1. The most notable thing about the figure is that a relatively large number of appliances begin to show failure at approximately the same value of the index, and this

TABLE 12. *Importance of various types of failure in determining interchangeability*

	Type of failure			
	Lifting	Yellow tips	Flash back	Incomplete combustion
Number of substitute gases with which only one type of failure was reported	35	59	24	12
Number of supplementary gases the limit of interchangeability of which was attributed to only one type of failure	32	4	7	9
Number of times a type of failure was stated as one reason for limiting "the further addition of a supplemental gas"	69	46	13	40

index is nearly that of the adjustment gas. The same statement applies also to the data of reports 1106–B–D. The reason is not hard to find. An inspection of figure 2 shows that in a typical appliance the normal injection curve, N, along which the point representing the adjustment of an appliance moves when pressure is increased, is nearly parallel to the yellow-tip limit and approaches the lifting curve only at a sharp angle but is nearly perpendicular to the limit of complete combustion, C. Moreover the typical appliance is safest and most efficient when it is adjusted to take just a little more primary air than is necessary to avoid yellow tips. The only reason for supplying still more primary air is to permit more gas to be burned completely. Hence the danger of incomplete combustion is the usual reason for limiting the input of an appliance. The general method of increasing the amount of gas that can be burned is to increase the size of the appliance, giving it more ports, a larger combustion chamber, larger flue passages, etc.; but this costs money. At the time it is approved under ASA standards every appliance is assigned an "input rating" in Btu per hour, and when adjusted to this rating during testing it must take a 50-percent increase of pressure (25% in the case of range burners and some others) without incomplete

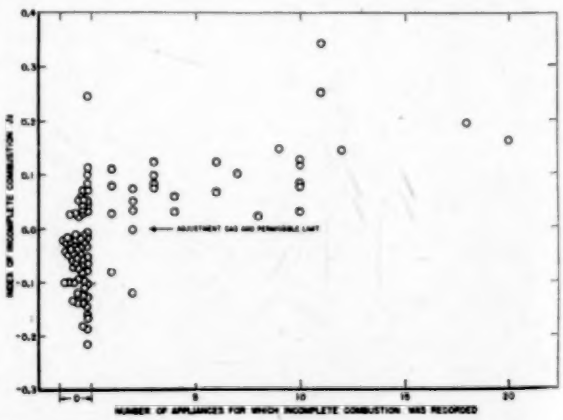

FIGURE 31. *Number of appliances for which incomplete combustion was recorded in Report 1106–A compared with J_1.*

combustion. As appliances of increasing input rating command increasing prices, manufacturers tend to rate their appliances as high as they can and still meet the combustion requirement. When the tests of Report 1106 were made, each appliance was given its normal adjustment, which includes the "rated input." Because this rating probably was usually determined as just described, we should expect the burner to approach closely the limit of complete combustion if the pressure of the adjustment gas were increased 50 percent (range burners, 25%). If the substitute gas then had only a slightly higher index of complete combustion than the adjustment gas, we should expect incomplete combustion with most of the appliances when the substitute gas is supplied at a pressure 50 percent above normal. This is precisely what happened. The much greater dependence on pressure of incomplete combustion than of other types of failure and the fact that substituting other gases rarely resulted in incomplete combustion except at the higher pressures are clearly shown in table 13.

TABLE 13. *Number of failures recorded in Report 1106–A at different pressures*

Type of failure	Pressure 0.5 N	N	1.25 N or 1.5 N *
Lifting	239	519	732
Flashback	84	51	21
Yellow tips	213	288	307
Incomplete combustion	0	9	173

* 1.25 times normal pressure with range burners, 1.50 N with others.

Another feature of figure 31 is the wider spread of the index corresponding to the same number of appliance failures than is the case with other indexes, and this in spite of a more definite limit at which failures begin. This is probably the result of the fact that, as already explained, failure to burn gas completely results from two independent conditions, lack of enough secondary air, and cooling of flames by impingement. Since we know that $J_A = A\sqrt{D_a}/A_a\sqrt{D}$ should be a good index for the first (and much the most dangerous) condition, it is probable that we should give as much weight to it as to J_I when predicting interchangeability. If this is done, a better index for cases of severe flame impingement could probably be worked out. The coefficient of R/R_a in the expression for J_I should probably be increased if the two indexes are used.

IX. Application of Indexes of Interchangeability

If we had to decide whether a plank would be long enough to span a brook, we would have two things to consider, the length of the plank, which we could measure accurately, and the width of the brook at which we might have to guess. A gas company or a public utility commission that must decide what modification of a gas supply to make or to permit has a very similar problem. The several indexes of interchangeability supply a means of measuring the length of the plank (the effect of a change of composition of the gas supply on the operation of any one appliance with a definite adjustment). The width of the brook corresponds to the existing adjustments of all or a great proportion of the appliances in service. The figure of speech may be carried even further. If the margins of the brook are muddy, we may know that the plank will not reach to solid ground and that we will have an unsatisfactory bridge, but it may be better than no bridge at all. Correspondingly, we may be sure that a given change of the gas supply will cause trouble with some appliances; whether they will be too numerous and the trouble of too serious a nature to justify the change can only be estimated. So far in this paper only the easy part of the problem has been discussed; unfortunately, the difficult part will have to be left almost entirely to the observation, ingenuity, and judgment of those immediately concerned. Some discussion of this may, however, be helpful.

The most obvious thing is that not all brooks are of the same width and that not all groups of gas appliances will tolerate, without readjustment, the same change in, let us say, the index for lifting. If appliances in service have been adjusted to burn natural gas, it is probable that nearly all of them have been set very close to lifting in order to burn the gas completely at a rate to supply a satisfactory amount of heat. Probably many of them are also on the verge of incomplete combustion, but they have a wide margin of safety from flashback and a reasonable one from yellow tips. Bulletin 36 probably gives us a fair guide in deciding how wide these margins are.

Similarly, a community that has been burning a by-product oil gas is likely to have appliances most of which are adjusted as close as permissible to flashback in order to have primary air enough to prevent smoking; but because of the large percentage of hydrogen present, they are remote from lifting and have at least the usual margin of safety from incomplete combustion. If it has been the gas company's policy to adjust appliances in a given district only when the pressure is near its maximum and has trained its employees to adhere closely to the input rating of the appliance, a gas with a value of J_I of 0.10 or 0.15 when the adjustment gas is the customary supply, may be introduced with reasonable safety. But a company with many unvented space heaters on its system, which has adjusted appliances without much regard to the momentary stage of a variable pressure, and has tended to leave appliances with more than their normal input rating because its customers like it that way, may risk the lives of some of those customers if it increases J_I by even a small amount. Of course it is impossible to set a positive limit to any change of properties of the gas on one side of which is safety and on the other danger. We have no sharp-edged precipice, but we do have a much narrower margin of uncertainty than in many other things that have to be

decided for the sake of safety, the permissible speed of automobile traffic, for example, or the safe spacing between a heated chimney and wooden building materials.

The method of using the indexes in determining the composition of a gas supply, after the margins of safety of existing adjustments have been estimated, will be illustrated by the following problem.

Problem: A company distributing a coke oven gas of the composition of gas A1 wishes to supplement its supply as much as permissible during peak loads by mixing in propane and air. How much propane can be and how much air should be used?

The first step is, if possible, to assign permissible limits to the various indexes; the second is to make a quick estimate, by means of a few preliminary calculations, to determine which conditions may be limiting factors and to obtain some idea of the permissible changes; and the final step is to compute the indexes that may determine the limit with as much accuracy as the available data seem to justify.

For the difficult first task of assigning permissible limits to the indexes, we have a much better basis in the experiments of Report 1106A than will usually be available to a gas company or a regulatory body. Permissible limits for appliances adjusted with gas A1 have already been assigned in the various figures. They are:

The lifting index, J_L, should not be less than 0.64.

The flashback index, J_F, should not be greater than 0.08.

The yellow tip index, J_Y, should not be greater than 0.14.

The index for incomplete combustion, J_I, should not be greater than zero.

For the second step it will probably be sufficient to assume that all the indexes are linear functions of composition. After computing the indexes for changes from the adjustment gas to propane and to propane with 50 percent of air, one can quickly determine by linear interpolation (if one did not already know it) that the addition of propane will produce values of J_F less than zero unless a very large amount of air is added, and that lifting will result from the addition of much less air, so that flashback is entirely eliminated from consideration. It will be found that incomplete combustion will not permit much propane to be used unless at least an equal volume of air accompanies it, and that if four times as much air as propane is used, very little of the mixture can be used without producing lifting. Yellow tips are found to be indicated under about the conditions that produce incomplete combustion. It is rather quickly found that we cannot hope to use more than about one-fourth as large a volume of propane as of the coke oven gas, and that something between one volume and four volumes of air will have to accompany each volume of propane.

The third step is to compute accurately and plot the indexes for several mixtures of air with propane in the range of interest outlined by the preliminary survey and for several mixtures of these mixtures with the coke oven gas. The plots obtained are

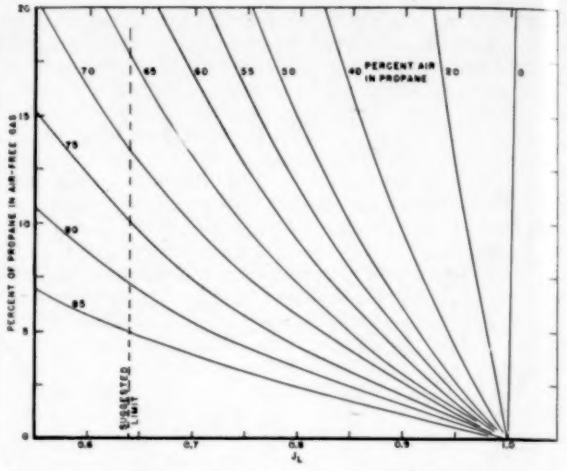

FIGURE 32. *Values of index J_L for mixtures of propane and air with coke oven gas.*

shown in figures 32 to 34, and should be understandable without further explanation. The intersections of the lines representing suggested limits with the curves representing definite percentages of air in propane are plotted in figure 35. From this figure, the permissible quantity of propane, if our preselected limits are not to be violated in any respect, is shown to be 16 percent by volume of the air-free gases, an increase in the amount of fuel that can be sent out of about 87 percent, as shown by the right hand scale of ordinates. The optimum percentage of air to be mixed with the propane is 67 percent. If during an emergency we are willing to tolerate some yellow flames but no carbon monoxide, we can use 18 percent of propane in the air-free fuel, but to avoid lifting we must reduce the amount of air mixed with the propane to 64.5 percent.

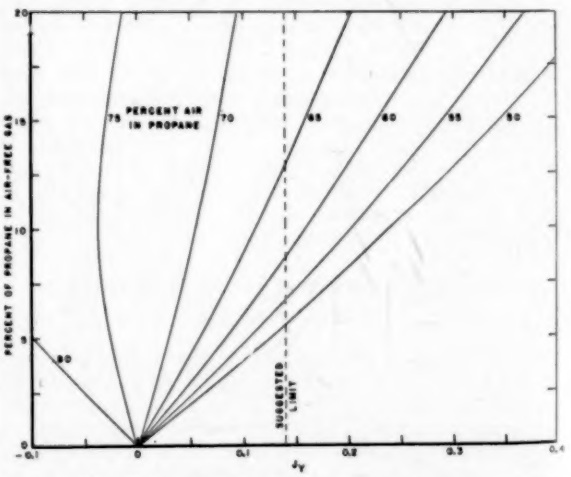

FIGURE 33. *Values of index J_Y for mixtures of propane and air with coke-oven gas.*

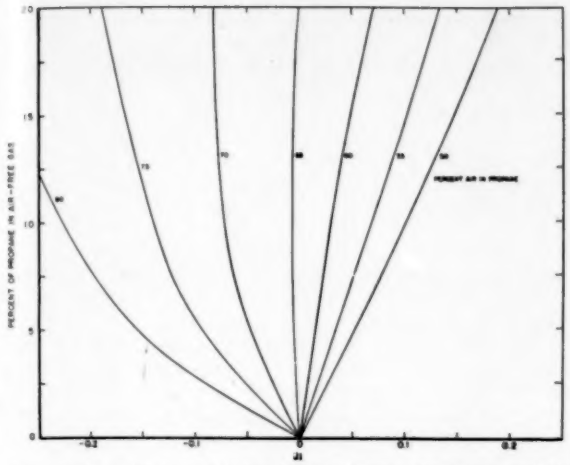

FIGURE 34. *Values of index J_I for mixtures of propane and air with coke-oven gas.*

It is interesting to check this diagram with the direct results of the observations of propane-air mixtures recorded in Report 1106–A. It may seem that this is reasoning in a circle since the "suggested permissible limits" were based on the report. To some extent the objection is valid, but the general expression for J_L was derived without the use of data from Report 1106–A, the expressions for J_Y and J_I were based on the whole group of about 400 experimental gases covered in the five reports of experimental work, and the selection of permissible limits for the indexes was made by considering all the 97 "substitute" gases of the Report 1106–A without special consideration being given to the mixtures of propane and air.

Two mixtures of propane and air were used as supplemental gases. Gas A1-11–100 contained 78.2 percent of air and had the same heating value as the adjustment gas. Gas A1-13–100 contained 62.8 percent of air. Each was mixed in several proportions with the adjustment gas to make substitute gases, the compositions of which are represented in the figure by circles and by numbers from which the initial A1 has been omitted. In both cases the AGA Committee decided that 30 percent of the substitute gases was the limit of practicable interchangeability. These mixtures are represented by the X marks labeled 11–30 and 13–30, respectively. In the first case the limiting mixture was tried experimentally; in the second it was estimated from observations of 25- and 50-percent mixtures of the supplemental gas with the adjustment gas.

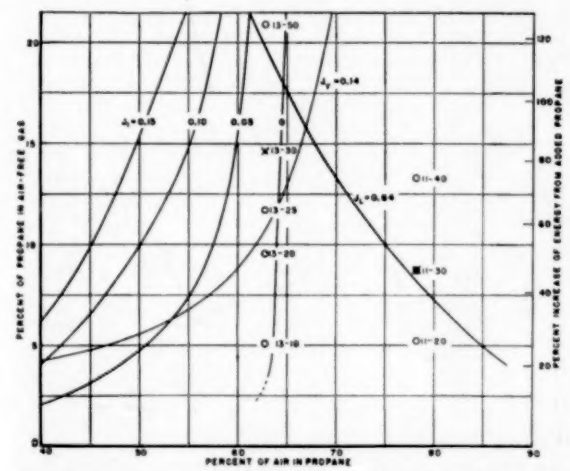

FIGURE 35. *General diagram showing the amounts of propane that can be used to supplement coke-oven gas when mixed with any quantity of air.*

We will now compare, point by point, the predictions that might have been made from the chart with the actual observations. From the chart we could predict that neither incomplete combustion nor yellow tips would occur with supplemental gas 11, either when mixed with the adjustment gas in the proportions shown or when used alone. The record shows no incomplete combustion and no yellow tip for the unmixed supplemental gas and only one appliance with a −4 flame (slight yellow tip) at the softest adjustment with 40 and 60 percent of the supplemental gas in the mixture. We should predict severe lifting for the mixture containing 40 percent of supplemental gas and none with the mixture containing 20 percent. There were 22 recorded cases of failure, of which 15 involved +5 flames, with the 40-percent mixture and none with the 20-percent mixture. We should predict some show of lifting with the 30 percent mixture, because the point 11–30 is a little over the line, and we find six cases of which four involved +5 flames. These were considered by the Committee not severe enough to make a reduction of the limit necessary, however.

With supplemental gas 13, we should predict that the 50-percent mixture, marked 13–50, would produce yellow tips, with a little lifting and some incomplete combustion. We find 37 recorded cases of yellow tips of which 12 were −5 flames, 20 cases of lifting of which only five involved +5 flames, and 12 cases of incomplete combustion. It was previously pointed out that the +5 flames more sharply define lifting conditions than the +4 flames. The five cases of +5 flames in a total of 20 with the 13–50 mixture checks rather well with the four +5 flames in a total of six with the 11–30 mixture, combined with the fact that the point 13–50 is a little farther inside the lifting limit than the point 11–30.

We should predict no trouble from lifting with the experimental mixture containing less than 50 percent of supplemental gas 13, and we find only one appliance showing +4 flame under the most severe condition of adjustment and pressure with both the 20- and 25-percent mixtures. This is clearly negligible if the committee was justified in accepting as interchangeable with the adjustment gas the four +5 and two +4 flames of gas 11–30. We should expect severe yellow tip conditions (−5 flames) to disappear with about 24 percent of supplemental gas 13, and we find

seven −4 flames at 25 percent and six of the same at 20 percent. We should expect to find some incomplete combustion with the higher percentages of gas 13, but not much since we are just under the percentage of air in propane that would be exactly interchangeable with the adjustment gas; and we should expect only a little change in the tendency toward incomplete combustion with diminishing percentages of the supplemental gas because we have assumed some of the appliances to be rated so close to the margin permitted by approval requirements that no increase in J_I is permissible. We find 11, 12, 3, 2, and 2 recorded cases of incomplete combustion respectively with mixtures containing 100, 50, 25, 20, and 10 percent of gas 13, which is in good accord with the prediction.

The most outstanding point of practical importance shown by figure 35 is that whatever limits we assume as permissible for the several indexes, the addition of air must be carefully controlled if we wish to make maximum use of propane as a supplement to the fuel supply.

It is now possible to outline quite definitely the practice desirable when coke-oven gas must be supplemented with propane. Because it is desirable to maintain constant the selling price of the gaseous fuel, a 535-Btu mixture containing about 22 percent of propane and 78 percent of air should be used until the first hazard from lifting is encountered. This occurs when the demand for fuel exceeds the supply of coke oven gas by about 40 percent. When this occurs, about 8 percent by volume of the air-free gas will be propane. If the demand continues to increase, the addition of propane can be continued, but the percentage of air in the propane must be gradually reduced until the air constitutes about 65 percent of the mixture with propane and the propane constitutes about 18 percent of the air-free gas by volume and has added about 105 percent to the available fuel supply. The heating value of the propane-air mixture will then be about 890 Btu per cubic foot and that of the gas as a whole about 676 Btu. Appliances with fixed orifice and valve settings will be delivering about 95 percent as much heat at the same pressure as with the unmixed coke-oven gas.

Some time before this mixture is reached complaints of yellow or even smoky flames may be expected, but a little smoke is preferable to lifting flames or to an inadequate fuel supply. A further increase in the use of propane will result in either lifting flames or the release of carbon monoxide unless pressure is lowered. Lowering the pressure will not, of course, prevent trouble with the appliances controlled by regulators already set at pressures materially lower than those in the mains, nor will it relieve the tendency to deposit carbon very much.

X. Summary and Conclusions

The conditions that determine whether one fuel gas can be satisfactorily substituted for another have been described in relation to a general diagram by the use of which the complicated subject can be explained much more clearly than otherwise. All the commonly used formulas for predicting the effects of supplying one gas mixture to appliances already adjusted to burn another have been discussed and compared, and a new group of indexes (which includes some old ones) has been proposed for use. The term index is used in this case for any mathematical expression that shows approximately the relative tendencies of the two gases to give unsatisfactory results of some kind when supplied to the same appliances without readjusting them. The symbols used in the new indexes all represent properties of gas mixtures that are easily computed from their composition.

The new indexes were derived in part from theory and in part empirically from recorded observations, chiefly those made in the Laboratory of the American Gas Assn. For a substantially complete survey of the interchangeability of two gases, the following indexes are recommended

$$J_H=\frac{H\sqrt{D_a}}{H_a\sqrt{D}}, \qquad (1)$$

where H stands for heating value and D for density or specific gravity. The subscript a indicates the gas with which the appliance was adjusted. J_H is a well-known expression that shows quantitatively the effect of a change of composition on the rate at which heat is produced in an appliance. If I_a is the heat input into an appliance when adjusted, $I=J_H I_a$ is the heat input after the change of gases.

$$J_A=\frac{A\sqrt{D_a}}{A_a\sqrt{D}}; \qquad (2)$$

A stands for the number of cubic feet of air required to burn 1 cu ft of gas. J_A, also well known, shows the change in the primary air that accompanies a change of gas. If P_a is the primary air injected into an appliance, expressed as a fraction of the volume required to burn the gas at the time of adjustment, $P=P_a/J_A$ is the primary air, expressed in the same terms, which enters the burner after the change of gases. J_A not only provides an accurate measure of the relative conditions of supply of primary air to burn two gases but an almost accurate measure of secondary air as well, and in consequence it is a measure of the hazard of incomplete combustion in the important group of water heaters, space heaters, ovens, etc., in which flame impingement is not involved and secondary air is adjusted close to the safe minimum in order to increase thermal efficiency.

$$J_L=J_A\frac{S}{S_a}\frac{100-Q}{100-Q_a} \qquad (3)$$

S/S_a is the ratio of flame speeds in corresponding mixtures of the two gases with air, and Q is the percentage of oxygen in the gas. J_L is the new index for lifting and shows the relative tendency of flames of the two gases to lift from the burner ports. When the

two gases are exactly interchangeable with respect to lifting, $J_L=1$.

$$J_F=\frac{S}{S_a}-1.4J_A+0.4 \tag{4}$$

J_F shows the relative tendency for flames of the two gases to flash back into the burners. When $J_F=0$, there is no difference between the gases in this respect.

$$J_Y=J_A+\frac{N-N_a}{110}-1. \tag{5}$$

N represents the number, in 100 molecules of gas, of the carbon atoms easily liberated during combustion. It is taken to be the total number of carbon atoms in the hydrocarbons except one in each molecule of the methane (saturated) series. J_Y is a measure of the relative tendency of the two gases to produce yellow flames and release soot. When $J_Y=0$ there is no difference between the gases in this respect.

$$J_I=J_A-0.366\,\frac{R}{R_a}-0.634. \tag{6}$$

R is the ratio of the number of hydrogen atoms in the gas to the number of carbon atoms in the hydrocarbons only. J_I is a general expression for the relative tendencies of the two gases to liberate carbon monoxide and is a correction of J_A, which would otherwise apply, to take into account the effect of flame impingement in appliances of some types. When the two gases are equally likely to liberate carbon monoxide during combustion, $J_I=0$.

Extensive comparisons of the last four indexes with the results of experimental studies made by the American Gas Assoc. and recorded in its Bulletin 36 and Research Report 1106 show them to give a somewhat closer representation of the observations than any other method that has been proposed. Detailed comparisons were made with the three indexes of performance developed by the Association and designated I_L, I_F, and I_Y, which have the same purpose as the indexes designated by J with the corresponding subscripts. It is clearly shown that no single index, such as that commonly referred to as AGA "Index C" and which was developed during the "mixed Gas Research" of 1927–32 can be considered useful in comparison with the use of either group J_L, J_F, J_Y, and J_I or I_L, I_F, and I_Y.

It is also rather clearly shown that, for the general purpose of predicting the effect of a change of gas supply on the large number of gas appliances in service, any uncertainty as to the accuracy with which either of these sets of indexes represents the relative properties of the gases is small compared with the uncertainties connected with the initial adjustments of the appliances themselves.

Without doubt the interpretation of the observations made by the AGA is complicated (1) by the difficulty of reproducing appliance adjustments and making gas mixtures exactly to specifications; (2) by variations in the number of appliances tested; and (3) by errors of computation and plotting by the writer of this paper. All these things combine to make the indexes appear less reliable than they really are. The first two sources of difficulty have been discussed at some length, particularly in connection with tables 3, 4, and 6. These two sources of error offer the best explanation of the fact that the agreement between the behavior of appliance burners and that of test burners was never much better and was sometimes worse than the agreement of either appliance or test burners with the somewhat theoretical "indexes". Several errors that had been made in the long computations were found, but without doubt others remain. To have eliminated them by checking all the computations would have necessitated a long delay in publication and could not have changed the picture greatly.

The writer acknowledges the assistance of John H. Eiseman, who not only helped greatly in the preparation of the present paper but whose work with fuel gases for many years supplied much of the necessary background. The paper is of course, based mainly on experiments at the Laboratory of the American Gas Assoc. whose Director, E. L. Hall, generously facilitated the work of preparation by supplying copies of the several sections of Report 1106 in advance of publication. Paul Bannar, formerly of this Bureau, did much of the burdensome computing.

XI. References

[1] Mixed Gas Research, American Gas Association Reports 597, 645, and 689 (1930, 1932, 1933).
[2] Standards for gas service, NBS Circular 405 (1934).
[3] Requirements Committee Investigation of Laboratories Test Gases and Pressures. Report Number 847, AGA Testing Laboratories (1938).
[4] Combustion experiments with liquefied petroleum gases, Frank Knoy, Gas (Los Angeles) **17**, 14 to 19 (June 1941).
[5] Interchangeability of other gases with natural gases. Research Bulletin 36, American Gas Association Testing Laboratories (1946).
[6] Progress report on mixed gas research Project T L—1, J. F. Anthes. Presented at the 1948 Joint Production and Chemical Committee Conference (May 24 to 26, 1948).
[7] Interchangeability of other fuel gases with coke-oven gas. Resarch Report No. 1106–A Gas Production Research Committee, Testing Laboratories (1948).
[8] Interchangeability of other fuel gases with carburetted water gases. Research Report 1106–B. AGA Testing Laboratories (1948).
[9] Interchangeability of other fuel gases with a mixed coke-oven carburetted water gas. Research Report 1106–C. AGA Laboratories (1949).
[10] Interchangeability of carburetted water gases with a mixed natural gas—blue gas—cracked natural gas—producer gas. Research Report 1106–D. AGA Laboratories (1949).
[11] Relative usefulness of gases of different heating value and adjustments of burners for changes in heating value and specific gravity, W. M. Berry, I. V. Brumbaugh, J. H. Eiseman, G. F. Moulton, and G. B. Shawn, NBS Tech. Pap. T222 (1922).

Washington, August 31, 1950

Journal of Research of the National Bureau of Standards Vol. 46, No. 3, March 1951 Research Paper 2184

Absorption Spectra of Water Vapor and Carbon Dioxide in the Region of 2.7 Microns

W. S. Benedict and Earle K. Plyler

The absorption due to atmospheric H_2O and CO_2 in the region of 2.7μ has been remeasured under higher resolution than previously reported. By using a 15,000-line grating and a lead sulfide photoconductive cell, some 450 lines have been measured between 2.43 microns (4,090 cm^{-1}) and 2.87μ (3,500 cm^{-1}). A rotational analysis may be given for nearly all the lines. In addition to the known ν_3 fundamental of H_2O which causes the strongest absorption in the region, a number of lines due to the ν_1 fundamental of H_2O, and the $\begin{cases}02^\circ 1\\10^\circ 1\end{cases}$ combination bands of CO_2 may be recognized. The ν_1 analysis does not agree with one suggested previously. The following are the principal molecular constants derived from the new analyses:

Molecule	v_1 v_2 v_3	ν_0	A	B	C
		cm^{-1}	cm^{-1}	cm^{-1}	cm^{-1}
H_2O	0 0 1	3755.79	26.64	14.40	9.16
H_2O	1 0 0	3657.05	27.13	14.29	9.11
CO_2	0 2 1	3612.91	-------	0.3875_3	------
CO_2	1 0 1	3714.59	-------	$.3872_3$	------

I. Introduction

Since the beginning of infrared spectroscopy, the existence of a region of strong atmospheric absorption near 2.7μ has been recognized. With each advance in experimental techniques, permitting higher resolving power, more and more fine structure has been observed in the absorption band. The lines have the highly irregular spacing characteristic of an asymmetric rotator, and it has long been recognized that the strongest absorption is due to the H_2O molecule, in a fundamental vibration-rotation band. The first rotational analysis of this molecule was achieved by Mecke [1],[1] who was able to assign the strongest lines, as resolved by Plyler and Sleator [2], to transitions of low J in the asymmetrical valence vibration, ν_3. Nielsen, [3], with improved resolution, made a more extensive analysis of the ν_3 band, and also attributed some of the weaker lines at longer wavelength to the symmetrical valence vibration, ν_1, which appears strongly in the Raman effect.

In the course of a study [4] of the structure of a large number of the overtone and combination bands of H_2O, it appeared that the reported identification of ν_1 in the infrared was questionable. We have accordingly reinvestigated the atmospheric absorption in the 2.7-μ region, making use of a recently developed grating spectrograph of high resolution [5]. In the course of the present investigation, we have arrived at a new identification of ν_1, have extended the analysis of ν_3 to higher values of J, and in addition have identified a number of lines of two combination bands of CO_2 [6], which had not previously been studied under high resolution. The present analysis of the spectrum accounts for nearly all of the more than 450 lines that have been observed between 2.43μ (4,090 cm^{-1}) and 2.87μ (3,500 cm^{-1}). The resulting energy levels are in good agreement with theoretical considerations and with the observations on the overtone and combination bands.

II. Experimental Procedure

The spectrometer, which uses a 15,000-line, 7¼-in. ruled surface as the dispersing element and a lead-sulfide photoconductive cell as the receiver, has been described [5]. In order to reach the longest wavelengths desired in this study, it was necessary to use the grating at its extreme angle, thus reducing the intensity of radiation. The sensitivity of the PbS detector also falls off at the longest wavelengths, so that relatively wide slits were required beyond 2.8μ. However at wavelengths shorter than 2.75μ(ν>3,640 cm^{-1}) the instrument could be operated at its maximum resolving power. Under these conditions records with good signal-to-noise ratios were obtained with spectral slit widths of 0.12 cm^{-1}. This is comparable to, or less than the width of the H_2O lines, when the water-vapor content of the optical path in the room and the spectrometer was that prevailing on a dry February day. It is often possible to distinguish the presence of two components in lines separated by 0.15 cm^{-1}, and lines 0.30 cm^{-1} apart are clearly resolved. Further lowering of the water-vapor content might result in some further improvement in resolution, but as the present resolution was adequate, and as it was desired to record as many of the weaker lines as possible, this was not attempted.

[1] Figures in brackets indicate the literature references at the end of this paper.

The source was a tungsten lamp with quartz window, operated at 38-amp current. Radiation of second and higher orders was removed by a tellurium filter. This completely eliminated wavelengths below 1.35μ, so that the spectrum below 2.70μ was free from higher-order radiation. Above that wavelength the filter reduced but did not completely eliminate the second-order radiation. The resultant overlapping of first- and second-order absorption lines (second-order absorption, due to the 1.4μ combination band of H_2O, is relatively strong) complicates the appearance of the observed spectrum. It does not, however, lead to any difficulty in assigning the first-order lines, which appear broader because of their greater natural width in cm^{-1}; and the presence of the second-order lines is of some value in providing frequent standards for wavelength determinations, as they have been measured with high accuracy [7].

A number of runs through the entire spectral region in question, or through various portions of it, were made at different humidities and with different slit widths. Runs were made with the grating drive operating both toward longer and toward shorter wavelengths, and with both positive and negative values of the grating angle. By intercomparison of these various tracings, it was possible to distinguish weak true absorption lines close to the noise level. In addition, several spectra were obtained with an absorption cell 5 cm long containing CO_2 gas at a pressure of 40 cm in the optical path, in order to confirm that the lines attributed to CO_2 in the atmospheric path were indeed due to that molecule.

The wavelengths of the absorption lines were obtained as follows. The primary standards of wavelength were higher-order lines from a mercury-vapor lamp, which was placed at the center of focus of the spectrometer, so that the mercury lines in emission were superimposed upon the absorption spectrum. This yielded 8 or 10 lines in the region between 2.4 and 2.9μ whose positions were known with accuracy. The second-order water-vapor lines provided numerous other standards between 2.7 and 2.85μ. A dispersion curve, representing wavelength as a quadratic function of the reading of the Veeder counter, which in turn related position on the recording chart to the grating angle, was passed through the standard lines. This gave the frequency of a number of the first-order absorption lines, namely those close to the standards, with good accuracy. To establish additional standard wavelengths in spectral regions further from the primary standards, use was made of the characteristic frequency differences between the lowest rotational levels of the H_2O molecule. These are known, from their occurrence in a large number of vibrational bands [4] with an accuracy of ± 0.02 cm^{-1}, and hence provide a set of reliable internal frequency standards, when the lines in question are not overlapped by other lines. The dispersion curve that was finally adopted was fitted to a number of these secondary standards. The measurement of the positions of the absorption lines, and their reduction to wavelengths, was carried out independently by different observers on several tracings. The final values reported are the averages of these reductions, and are believed accurate to within ± 0.20 cm^{-1}. The precision of measurement of the frequency difference between neighboring lines, or of lines close to the primary standards, should be considerably better, about ± 0.05 cm^{-1}. The reported frequencies are also subject to a minor uncertainty associated with the conversion factor from wavelengths in air to wave numbers in vacuum. The adopted value was $\nu_{vac}=(\lambda_{air}\times 1.0002706)^{-1}$.

III. Results

A reproduction of a tracing made from a recording of the entire region from 4,090 to 3,498 cm^{-1} is shown in figures 1 to 4. The tracing is broken into segments approximately 50 cm^{-1} in length, with an overlap of one or two lines at either end. The wave numbers (in vacuum) of a number of the more prominent lines are indicated in the figure. As explained previously, the spectrum below 3,700 cm^{-1} is not pure, and hence contains some second-order lines.

The wave numbers and approximate intensities of all the observed lines, together with the identification proposed for most of them, are given in table 1. The first column of the table presents the intensity, on an estimated scale 0 to 100, which corresponds roughly to the percentage absorption at the maximum. The intensity scale is of least significance for very intense lines ($I>95$), of which a few show complete absorption over a width approaching 1 cm^{-1}, for lines that are members of incompletely resolved groups, and for the lines of longest wavelength, where the second-order energy and absorption is a complicating factor. However it is of some quantitative usefulness for well-resolved lines between 10 to 90 in the shorter wavelength region, and serves as a qualitative indication of relative intensity throughout the table. The second column of table 1 gives the vacuum wave number of the line center, or what is judged to be the position of maximum absorption of an incompletely resolved component.

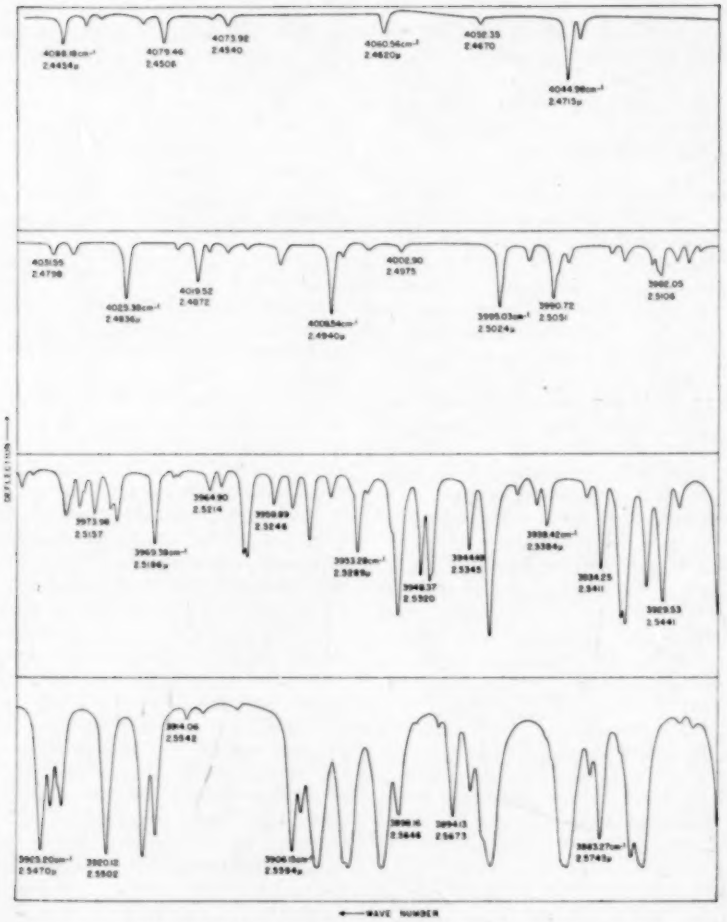

FIGURE 1. *Observed absorption due to* H_2O *and* CO_2, *4,000 to 3,875* cm^{-1}.

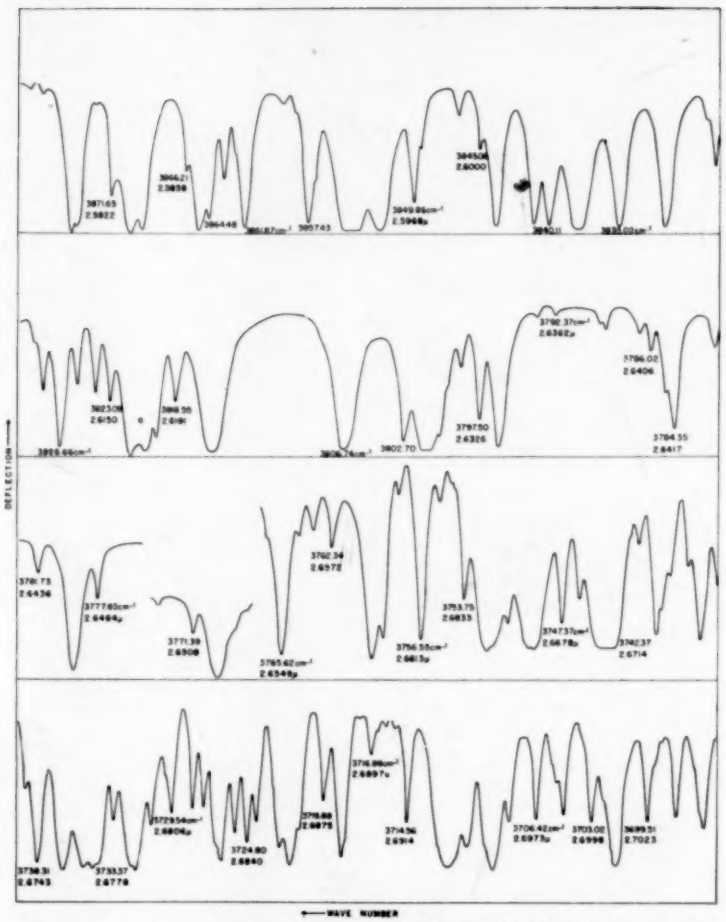

FIGURE 2. *Observed absorption due to* H_2O *and* CO_2, *3,877 to 3,692* cm^{-1}.

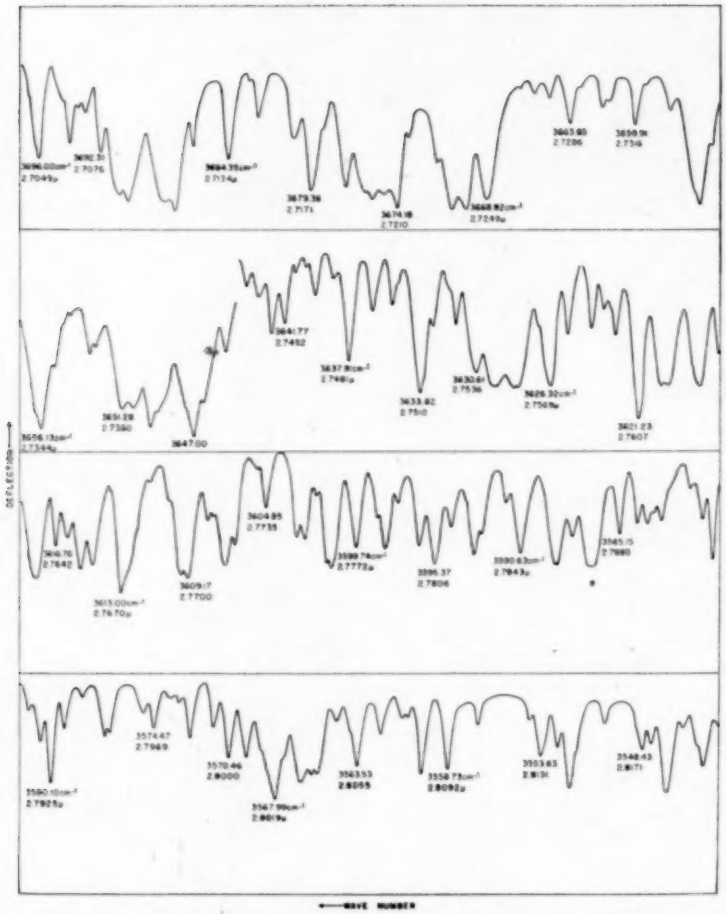

FIGURE 3. *Observed absorption due to* H_2O *and* CO_2, *3,697 to 3,544* cm^{-1}.

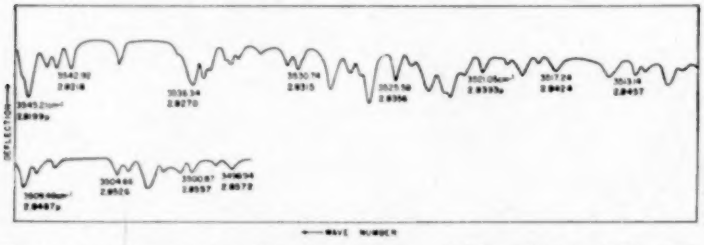

FIGURE 4. *Observed absorption due to* H_2O *and* CO_2, *3,546 to 3,498* cm^{-1}.

TABLE 1. *Absorption lines in the region of 2.7 μ due to* H_2O *and* CO_2

Observed		Identification	Calculated	
Intensity	ν_{vac}	$J'_\tau - J''_\tau$	Intensity	ν
	cm^{-1}			
10	3498.94			
5	3499.70	$8_2 - 9_1$	0.066	99.60
		$9_{-5} - 10_{-6}$	.041	99.95
12	3500.87	7001.9/2	(25)	00.90
10	3501.45	$8_0 - 9_{-1}$	0.143	01.41
6	3502.40	$10_{-9} - 11_{-9}$	.080	02.46
		$10_{-7} - 11_{-8}$	.026	02.58
		$9_{-4} - 10_{-5}$	.111	02.67
40	3503.09	7006.1/2	(20)	03.02
		$2_1 - 3_2$	15.06*	03.18
12	3504.08	$11_{-10} - 12_{-11}$	0.107	04.15
15	3504.66	$2_2 - 3_2$	5.16*	04.59
8	3507.87	7015.9/2	(20)	07.93
15	3508.80	$6_{-6} - 7_{-6}$	2.55*	08.72
35	3509.48	$6_{-5} - 7_{-7}$	7.67*	09.41
		$8_{-2} - 9_{-3}$	0.232	09.36
5	3510.89	$8_{-1} - 9_{-2}$	.053	10.45
		$6_{-1} - 7_{-3}$	.647*	10.75
25	3511.45	7022.7/2	(30)	11.35
		$4_{-2} - 5_{-2}$	2.60*	11.51
10	3512.61	7025.3/2	(20)	12.67
12	3513.14	$3_{-2} - 4_1$	0.081	12.94
		7026.4/2	(20)	13.23
15	3414.47	$5_3 - 5_3$	0.61*	14.36
10	3517.24	7034.4/2	(15)	14.14
		$7_{4,5} - 8_{3,4}$	0.052	17.44
6	3518.13	7036.4/2	(10)	18.20
15	3518.92	$4_{-2} - 5_1$	0.213	18.90
5	3519.57	7038.4/2		
12	3521.05	7042.1/2	(30)	21.05
15	3521.92	$5_{-2} - 6_{-4}$	1.45*	21.97
		7044.0/2	(30)	22.00
35	3522.69	$2_{-1} - 3_1$	8.83*	22.72
30	3522.99	$8_{-4} - 9_{-5}$	0.381	23.07
25	3523.80	7047.4/2	(40)	23.7
		$9_{-7} - 10_{-8}$	0.088	24.00
8	3524.28	$9_{-6} - 10_{-7}$	.25	24.26
10	3524.69	$8_{-3} - 9_{-4}$	.110	24.71
20	3525.58	$10_{-10} - 11_{-11}$	.337	25.66
		$7_3 - 8_2$	.056	26.92
40	3526.98	$3_{-1} - 4_{-1}$	11.73*	27.03
		7054.1/2	(40)	27.11
18	3527.43	$7_2 - 8_1$	0.170	27.58
18	3528.07	$4_{-4} - 5_{-1}$	0.261	28.04
35	3528.97	$5_{-5} - 6_{-5}$	15.89*	28.99
15	3530.74	$5_{-4} - 6_{-6}$	4.48*	30.64
13	3531.51	$7_1 - 8_0$	0.134	31.33
5	3532.71	7065.5/2	(15)	32.76
8	3533.85	7067.7/2	(20)	33.82
12	3534.25	7068.5/2	(20)	34.27
5	3534.55	7069.0/2	(15)	34.55
18	3535.27	7070.7/2	(45)	35.38
25	3535.72	7071.4/2	(60)	35.73
32	3536.34	$7_0 - 8_{-1}$	0.436	36.12
		$7_{-1} - 8_{-2}$	.240	36.50
10	3537.18			
8	3540.23	$5_0 - 5_2$	.75*	40.23
20	3540.38	7080.5/2	(50)	40.28
20	3542.92	$3_{-1} - 4_2$	0.098	42.89
		$6_{-3} - 6_{-3}$	2.72*	42.92
20	3543.73	$6_6 - 7_5$	0.107	43.41
		$5_1 - 5_3$	2.31*	43.66
		$4_1 - 4_3$	2.34*	43.80
18	3544.25	$2_0 - 3_0$	5.49*	44.27

TABLE 1. *Absorption lines in the region of 2.7 μ due to* H_2O *and* CO_2—Continued

Observed		Identification	Calculated	
Intensity	ν_{vac}	$J'_\tau - J''_\tau$	Intensity	ν
	cm^{-1}			
45	3545.21	$7_{-3} - 8_{-4}$	0.36	44.88
		$8_{-6} - 9_{-7}$	.75	45.19
25	3545.56	$8_{-5} - 9_{-6}$	0.24	45.35
12	3546.28	7092.5/2	(35)	46.23
65w	3547.15	$9_{-8} - 10_{-9}$	0.97	46.86
		$7_{-2} - 8_{-3}$	.91	47.03
		7094.7/2	(60)	47.35
23	3547.95	7095.9/2	(55)	47.92
		$2_{-1} - 3_2$	0.023	48.11
25	3548.43	$4_{-4} - 5_{-4}$	6.84*	48.43
10	3548.74	7097.4/2	(30)	48.75
15	3550.42	$6_{-3} - 6_{-1}$	2.70*	50.33
		$6_0 - 6_2$	0.52*	50.35
20	3551.96	$4_{-1} - 5_{-3}$	5.73*	51.76
		$6_1 - 7_{-1}$	0.17**	52.12
65	3552.29	$4_{-3} - 5_{-5}$	20.39*	52.24
		7104.7/2	(55)	52.30
		$6_{-6} - 6_{-4}$	0.99*	52.28
28	3552.90	7105.9/2	(60)	52.94
35	3553.83	$6_4 - 7_3$	0.57	53.83
12	3554.36	7108.6/2	(30)	54.33
15	3557.12	$1_0 - 2_2$	5.98*	57.11
50	3558.73	7117.6/2	(90)	58.72
55	3560.12	$6_2 - 7_1$	0.94	60.12
		7120.3/2	(35)	60.20
10	3560.86	$5_{-2} - 5_0$	1.72*	60.84
		7120.3/2	(25)	60.88
		$7_{-1} - 7_1$	0.84*	60.91
12	3561.12	$5_{-4} - 5_{-2}$	1.82*	61.23
25	3562.33	$6_1 - 7_0$	0.32	62.30
50	3563.53	$1_1 - 2_1$	21.8*	63.53
25	3563.89	$7_{-5} - 7_{-3}$	1.87*	64.01
10	3564.67	(a)		
60	3565.69	$6_0 - 7_{-1}$	1.85	65.64
60	3566.02	$7_{-5} - 8_{-6}$	0.57	65.98
		$7_1 - 8_{-3}$	.05**	66.23
65	3566.51	$3_{-2} - 4_{-3}$	25.8*	66.52
		$7_{-4} - 8_{-5}$	1.85	66.82
40	3567.47	7134.9/2	(55)	67.42
80	3567.99	$8_{-8} - 9_{-9}$	2.46	68.00
		7136.0/2	(40)	68.04
40	3568.35	$6_{-2} - 7_{-3}$	2.84	68.33
30	3568.69	$4_{-1} - 4_1$	7.07	68.72
45	3569.48	7139.0/2	(80)	69.52
47	3570.46	$6_{-1} - 7_{-2}$	0.70	70.53
25	3571.27	7142.6/2	(65)	71.30
32	3572.55	7145.1/2	(80)	72.57
10	3573.16	$7_3 - 8_{-1}$	0.31**	73.09
8	3573.59	$3_0 - 3_2$	2.23*	73.57
25	3574.47	$3_{-2} - 4_{-4}$	9.95*	74.47
15	3575.10	$3_{-3} - 4_0$	0.193	75.07
30	3576.88	$5_{-3} - 5_{-3}$	6.59*	76.78
35	3577.17	$4_{-2} - 4_{-1}$	9.31*	77.22
15	3577.40	CO_2 P_{40}		77.38
8	3578.38	7156.7/2	(35)	78.38
25	3579.39	$3_1 - 3_2$	7.04*	79.17
		$CO_2 - P_{38}$		79.36
70	3580.10	$5_4 - 6_3$	0.61	79.87
		7160.2/2	(65)	80.08
40	3580.66	7161.3/2	(75)	80.66
20	3581.33	CO_2 P_{36}		81.33
15	3582.44	$9_{-8} - 9_{-7}$	0.040	82.41
40	3582.95	7165.7/2	(65)	82.84
20	3583.33	CO_2 P_{34}		83.26
		$3_0 - 4_{-2}$	1.89*	83.38

[a] This line very probably is $5_0 - 4_3$ in the overtone band $2\nu_2$, the strongest expected line of that band in this region.

TABLE 1. *Absorption lines in the region of 2.7 μ due to* H_2O *and* CO_2—Continued

Observed		Identification	Calculated	
Intensity	ν_{vac}	$J'_\tau - J''_\tau$	Intensity	ν
	cm^{-1}			
55	3583.66	$2_{-2} - 3_{-2}$	10.3*	83.60
52	3584.17	7168.3/2	(80)	84.17
65	3585.15	7170.1/2	(45)	85.08
		CO_2 P_{32}		85.18
		$6_2 - 7_{-2}$	0.054**	85.49
100	3586.58	$6_{-4} - 7_{-5}$	4.36	86.52
		$5_1 - 6_0$	1.28	86.56
		$5_{-1} - 5_1$	6.67*	86.87
100	3586.93	$6_{-3} - 7_{-4}$	1.38	86.89
		CO_2 P_{30}		87.08
65	3587.79	$5_0 - 6_2$	0.56	87.87
		$5_2 - 6_1$	1.69	88.63
100	3588.70	$7_{-6} - 8_{-7}$	6.39	88.79
		CO_2 P_{28}		88.97
90	3590.63	7181.1/2	(80)	90.54
		CO_2 P_{26}		90.84
30	3591.47	7182.9/2	(5)	91.46
65	3592.74	CO_2 P_{24}		92.66
90	3593.21	$5_{-1} - 6_{-2}$	2.09	93.13
10	3593.62			
45	3594.47	CO_2 P_{22}		94.48
100	3595.37	$6_2 - 7_1$	0.51**	95.2
		$5_0 - 6_{-1}$	4.10	95.38
75	3596.23	$5_2 - 6_0$	0.09**	96.21
		CO_2 P_{20}		96.27
30	3597.44	7194.7/2	(60)	97.35
77	3598.17	CO_2 P_{18}		98.02
50	3598.56	$2_{-1} - 3_{-3}$	25.0*	98.11
		$6_0 - 7_{-4}$	0.059**	98.55
75	3599.74	7199.4/2	(35)	99.62
		CO_2 P_{16}		99.75
		$2_{-1} - 2_1$	12.1*	99.97
100	3601.14	$1_{-1} - 2_{-1}$	29.4*	00.88
		$5_1 - 6_{-3}$	0.41**	01.08
95	3601.41	CO_2 P_{14}		01.46
		7203.0/2	(55)	01.47
40	3601.95	7204.0/2	(45)	01.97
70	3602.61	$8_{-8} - 8_{-5}$	0.109	02.57
		7205.3/2	(85)	02.63
65	3603.07	$5_{-3} - 5_{-1}$	11.5*	03.01
		CO_2 P_{12}		03.15
50	3604.85	CO_2 P_{10}		04.84
		$8_{-7} - 8_{-6}$	0.036	05.24
80	3606.51	7212.9/2	(60)	06.42
		CO_2 P_8		06.51
100	3607.07	$5_{-3} - 6_{-4}$	2.95	07.11
30	3607.51	$5_3 - 6_{-1}$	0.25**	07.49
50	3607.83	7215.4/2	(50)	07.74
52	3608.13	7216.2/2		08.07
		CO_2 P_6	(25)	08.15
100	3609.17	$6_{-6} - 7_{-7}$	8.63	09.21
		$6_{-5} - 7_{-6}$	2.87	09.53
98	3609.62	CO_2 P_4		09.76
		7219.6/2	(75)	09.80
35	3610.30	7220.7/2	(50)	10.38
10	3611.39	CO_2 P_2		11.35
50	3612.10	$4_{-2} - 4_0$	6.68*	11.90
90	3612.50	$5_{-2} - 6_{-3}$	8.02	12.53
100	3613.00	$2_{-2} - 3_1$	0.74	12.78
		7226.0/2	(80)	13.00
5	3613.61	CO_2 R_0		13.69
		$2_0 - 2_2$	6.04*	14.40
90	3614.62	$4_4 - 5_3$	2.03	14.54
		$4_2 - 5_2$	0.67	14.75
		CO_2 R_2		15.22
95	3615.31	$3_{-1} - 3_1$	24.3*	15.25
		7230.8/2	(80)	15.44

TABLE 1. *Absorption lines in the region of 2.7 μ due to* H_2O *and* CO_2—Continued

Observed		Identification	Calculated	
Intensity	ν_{vac}	$J'_\tau - J''_\tau$	Intensity	ν
	cm^{-1}			
60	3616.08	7231.9/2	(90)	16.14
65	3616.76	7233.2/2	(80)	16.70
		CO_2 R_4		16.73
100	3617.82	$4_2 - 5_1$	6.22	17.83
		$3_{-3} - 3_{-1}$	25.7*	17.99
98	3618.18	$8_{-6} - 8_{-3}$	0.080	18.18
		CO_2 R_6		18.22
		$4_0 - 5_{-1}$	11.5	19.66
100w	3619.81	CO_2 R_8		19.69
		$0 - 1_0$	3.33*	19.92
		CO_2 R_{10}		21.14
100	3621.23	$4_1 - 5_0$	2.13	21.19
		7242.6/2	(80)	21.32
45	3622.59	CO_2 R_{12}		22.57
15	3622.82	7245.5/2	(55)	22.76
		$1_0 - 2_{-2}$	5.18*	23.20
25	3623.25	$7_{-7} - 7_{-4}$	0.09	23.29
40	3623.95	CO_2 R_{14}		23.96
45	3625.33	CO_2 R_{16}		25.33
99	3626.32	$4_2 - 5_1$	0.23**	26.37
		7252.7/2	(55)	26.35
75	3626.61	CO_2 R_{18}		26.67
20	3626.94	7253.9/2	(50)	26.97
100	3628.14	CO_2 R_{20}		28.00
100	3628.42	$4_{-2} - 5_{-3}$	16.25	28.24
		CO_2 R_{22}		29.30
99	3629.35	$5_{-5} - 6_{-6}$	5.21	29.35
100	3629.65	$5_{-4} - 6_{-5}$	15.6	29.62
		CO_2 R_{24}		30.59
85	3630.61	$4_4 - 5_0$	0.075**	30.69
		$2_{-2} - 2_0$	12.4*	30.70
		7262.3/2	(75)	31.12
35	3631.80	CO_2 R_{26}		31.86
10	3632.17	$7_{-5} - 7_{-2}$	0.057	32.30
35	3633.09	CO_2 R_{28}		33.10
20	3633.64			
98	3633.82	$4_{-1} - 5_{-2}$	4.39	33.82
		7267.9/2	(50)	33.94
50	3634.40	CO_2 R_{30}		34.33
10	3635.14	$3_2 - 4_{-1}$	0.78**	34.79
30	3635.48	CO_2 R_{32}		35.52
35	3636.57	CO_2 R_{34}		36.69
70	3637.99	CO_2 R_{36}		37.83
		$1_{-1} - 1_1$	36.3*	37.99
10	3638.88	CO_2 R_{38}		38.95
		$3_1 - 4_{-3}$	1.09**	39.74
18	3639.98	$4_0 - 5_{-4}$	0.19**	39.88
		CO_2 R_{40}		40.06
5	3640.47	7281.1/2	(40)	40.53
6	3641.11	CO_2 R_{42}		41.13
50	3641.77	$3_{-1} - 3_2$	0.037	41.50
		$6_{-4} - 6_{-1}$	.28	41.75
55	3642.53	$6_{-6} - 6_{-3}$	.59	42.57
		$8_{-5} - 8_{-4}$	.038	42.76
20w	3643.30	$1_{-1} - 2_2$	.14	43.21
		7287.0/2	(60)	43.52
15	3643.93	7288.1/2	(65)	44.02
30	3645.12	$4_{-2} - 4_1$	0.24	45.20
90	3646.41	$5_{-3} - 5_3$	.106	45.98
		$3_1 - 4_2$	2.23	46.41
100	3647.00	7294.1/2	(95)	47.03
		$3_1 - 4_3$	5.53	47.10
95	3647.48	$3_2 - 4_1$	6.71	47.53
100	3649.19	$4_{-4} - 5_{-5}$	24.9	49.18
100	3649.67	7299.3/2	(85)	49.67
98	3650.63	$4_{-3} - 5_{-4}$	8.13	50.68
99	3651.28	$3_{-1} - 4_{-2}$	8.38	51.27

TABLE 1. *Absorption lines in the region of 2.7 μ due to* H_2O *and* CO_2—Continued

Observed		Identification	Calculated	
Intensity	ν_{vac}	$J'_\tau - J''_\tau$	Intensity	ν
	cm^{-1}			
20	3653.05	$6_{-5} - 6_{-4}$	0.23	53.09
22	3653.32	7306.6/2	(95)	53.33
5	3654.47			
10	3654.91			
30	3655.35	7310.7/2	(85)	55.32
100	3656.13	7312.2/2	(70)	56.07
85	3656.46	$3_0 - 4_{-1}$	17.7	56.22
15	3657.88	7315.7/2	(70)	57.83
5	3659.25	7318.6/2	(25)	59.37
30	3659.91	$5_{-5} - 5_{-2}$	0.35	59.94
15	3661.51	7322.8/2	(60)	61.43
18	3661.87	7323.8/2	(60)	61.93
10	3662.05			
10	3661.22			
30	3663.85	7327.7/2	(90)	63.91
15	3665.08	7330.2/2	(60)	65.11
10	3666.00	$9_{-4} - 9_{-3}$	0.036	65.92
3	3666.90	7333.8/2	(15)	66.92
99	3668.82	$3_{-3} - 4_{-4}$	11.6	68.76
100	3670.03	7339.9/2	(90)	70.00
95	3670.41	$7_{-4} - 7_{-3}$	0.37	70.05
100	3670.92	$3_{-2} - 4_{-3}$	33.2	70.60
40	3671.83	7343.7/2	(85)	71.89
30	3673.56	7347.0/2	(65)	73.52
100	3674.18	$4_{-4} - 4_{-1}$	1.51	74.16
		7348.3/2	(80)	74.20
98	3674.95	$1_1 - 1_{-1}$	39.3*	74.65
		$2_2 - 3_1$	12.5	74.98
100	3675.72	7351.5/2	(35)	75.72
95	3676.07	$2_0 - 3_{-1}$	43.7	75.77
90	3677.30	$5_{-4} - 5_{-3}$	1.53	77.41
30	3678.67	CO_2 P_{40}		78.54
92	3679.36	$2_1 - 3_0$	5.49	79.36
		$2_0 - 2_{-2}$	14.2*	80.49
50	3680.45	7361.5/2	(80)	80.70
		CO_2 P_{38}		80.58
30	3682.57	7365.1/2	(50)	82.54
		CO_2 P_{36}		82.61
5	3683.05			
65	3684.35	7368.5/2	(80)	84.17
		7368.9/2	(50)	84.41
30	3684.53	$3_{-3} - 3_0$	0.48	84.52
		CO_2 P_{34}		84.58
55	3686.54	CO_2 P_{32}		86.54
100	3687.69	7375.7/2	(90)	87.76
100w	3688.28	$2_{-2} - 3_{-3}$	37.1	88.17
		CO_2 P_{30}		88.48
98	3690.66	CO_2 P_{28}		90.40
		7381.6/2	(75)	90.80
96	3691.08	$2_{-1} - 3_{-2}$	12.3	91.09
		$3_1 - 3_{-1}$	30.0*	91.21
60	3692.31	CO_2 P_{26}		92.29
25	3693.20	1_0 0	10.0*	93.26
18	3693.66	$6_{-3} - 6_{-2}$	0.37	93.72
50	3694.14	CO_2 P_{24}		94.16
15	3694.60	7390.2/2	(60)	95.06
60	3696.00	CO_2 P_{22}		96.01
40	3696.22	$5_{-1} - 5_{-3}$	8.76*	96.21
20	3696.72	7393.9/2	(50)	96.95
52	3697.73	CO_2 P_{20}		97.83
3	3698.56			
15	3699.08	7397.7/2	(40)	98.84
50	3699.51	CO_2 P_{18}		99.59
		$7_0 - 7_7$	0.30	01.28
98	3701.45	CO_2 P_{16}		01.35
		$1_1 - 2_0$	23.0	01.58
80	3701.80	$4_{-3} - 4_{-2}$	1.10	01.79

TABLE 1. *Absorption lines in the region of 2.7 μ due to* H_2O *and* CO_2—Continued

Observed		Identification	Calculated	
Intensity	ν_{vac}	$J'_\tau - J''_\tau$	Intensity	ν
	cm^{-1}			
40	3702.15	7405.1/2	(45)	02.56
50	3703.02	CO_2 P_{14}		03.08
45	3704.74	CO_2 P_{12}		04.78
30	3705.24	$5_1 - 6_{-4}$	0.025	05.23
		$6_0 - 6_{-2}$	1.89**	05.38
15	3705.44	$4_{-2} - 4_{-4}$	6.14*	05.59
48	3706.42	CO_2 P_{10}		06.49
50	3708.08	$5_1 - 5_{-1}$	9.34*	07.50
		CO_2 P_8		08.07
99	3709.16	$2_1 - 2_{-1}$	16.3*	09.10
		$1_{-1} - 2_{-2}$	13.5	09.30
80	3709.71	CO_2 P_6		09.82
80	3710.80	$7_{-2} - 7_{-1}$	0.60	10.82
95	3711.44	$2_{-1} - 1_{-1}$	39.6*	11.09
		CO_2 P_4		11.44
100	3712.01	$3_{-3} - 2_{-1}$	34.1*	11.87
		$1_0 - 2_{-1}$	29.3	12.04
90	3712.60	$7_4 - 7_3$	0.55	12.64
		CO_2 P_2		13.03
70	3714.56	$6_6 - 6_5$	1.59	14.65
5	3715.41	CO_2 R_0		15.37
5	3715.94	$4_2 - 4_3$	4.29*	16.02
		$9_0 - 9_1$	0.052	16.03
5	3716.50	$3_0 - 3_{-2}$	6.03*	16.55
20	3716.88	CO_2 R_2		16.90
3	3717.68			
60	3718.49	CO_2 R_4		18.41
95	3718.80	$5_{-2} - 5_{-1}$	3.17	18.95
50	3719.88	CO_2 R_6		19.83
80	3821.42	CO_2 R_8		21.35
100	3722.03	$8_2 - 8_1$	0.19	21.87
		$3_{-2} - 3_{-1}$	7.01	22.07
90	3722.64	CO_2 R_{10}		22.79
		$7_2 - 7_3$	0.64	22.88
50	3723.06	$3_3 - 3_1$	10.45*	23.01
		$7_3 - 7_2$	0.21	23.22
70	3724.11	$5_{-3} - 5_{-3}$	10.74*	24.15
		CO_2 R_{12}		24.20
85	3724.80	$6_4 - 6_3$	2.55	25.03
80	3725.49	CO_2 R_{14}		25.58
		$6_{-1} - 6_0$	0.68	25.64
50	3726.00	$4_{-1} - 4_{-3}$	14.0*	26.38
98	3726.37	$5_4 - 5_5$	6.62	26.45
80	3726.80	CO_2 R_{16}		26.93
60	3727.48	$7_0 - 7_1$	0.79	27.67
60	3728.20	CO_2 R_{18}		28.25
65	3729.54	CO_2 R_{20}		29.56
35	3729.93	$7_1 - 7_{-1}$	.84**	29.99
		$4_1 - 4_{-1}$	11.0*	30.33
70	3730.87	CO_2 R_{22}		30.83
100	3732.00	$0 - 1_{-1}$	26.4	32.00
		CO_2 R_{24}		32.09
80	3732.58	$6_1 - 6_2$	0.81	32.36
		$4_{-4} - 3_{-2}$	13.2*	32.75
70	3733.37	CO_2 R_{26}		33.33
		CO_2 R_{28}		34.53
100	3734.55	$6_2 - 6_1$	2.43	34.59
		$5_2 - 5_3$	6.46	35.05
		$5_3 - 5_2$	2.15	35.45
		$7_1 - 7_0$	0.27	35.45
100	3735.32	$5_0 - 5_1$	5.94	35.56
		CO_2 R_{30}		35.72
100	3736.67	$4_4 - 4_3$	20.5	36.71
		CO_2 R_{32}		36.88
		CO_2 R_{34}		38.01
95	3738.31	$2_{-1} - 2_0$	5.16	38.19
		$5_{-2} - 5_{-4}$	2.95*	38.25

TABLE 1. *Absorption lines in the region of 2.7 μ due to* H_2O *and* CO_2—Continued

Observed		Identification	Calculated	
Intensity	ν_{vac}	$J'_\tau - J''_\tau$	Intensity	ν
	cm^{-1}			
45	3739.17	CO_2 R_{36}		39.11
		$8_0 - 8_{-1}$	0.24	39.19
50	3740.34	CO_2 R_{38}		40.19
		$6_2 - 6_0$	.83**	40.60
70	3740.84	$4_0 - 5_{-5}$	0.14	40.80
		$4_{-3} - 3_{-3}$	43.1*	40.83
80	3741.26	$4_1 - 4_2$	5.01	41.33
		CO_2 R_{40}		41.25
25	3742.37	CO_2 R_{42}		42.28
15	3742.87	$6_{-4} - 6_{-6}$	1.65*	42.99
		$5_1 - 5_0$	2.03	44.10
100	3743.9	$4_2 - 4_1$	15.0	44.13
		$3_0 - 3_1$	21.5	44.44
100	3745.1	$3_2 - 3_3$	33.6	44.62
		$3_2 - 3_2$	11.2	45.02
60	3746.23	$2_1 - 1_1$	35.8*	46.21
85	3747.37	$5_2 - 5_1$	4.00**	47.67
100	3749.18	$5_{-3} - 4_{-1}$	9.21*	49.13
		$1_0 - 1_1$	35.8	49.15
100	3749.49	$2_1 - 2_2$	15.8	49.49
70	3750.84	$4_1 - 4_2$	1.38**	50.83
90	3751.31	$5_{-3} - 4_{-3}$	45.0*	51.40
		$6_{-2} - 6_{-5}$	4.80*	52.06
100	3752.14	$2_2 - 2_1$	47.4	52.23
		$4_3 - 4_1$	4.15**	52.67
		$2_2 - 1_0$	10.2*	52.71
65	3753.75	$5_2 - 5_0$	1.35**	53.75
3	3754.47	$3_{-3} - 2_2$	.066	54.65
		$3_3 - 4_{-2}$	.011	54.79
12	3755.33	$5_{-4} - 4_{-4}$	12.0*	55.31
95	3756.55	$3_1 - 3_0$	7.20	56.55
10	3758.02			
90	3758.98	$6_0 - 6_{-1}$	2.19	59.03
99	3759.76	$1_1 - 1_0$	12.3	59.62
		$7_{-5} - 7_{-7}$	2.32*	60.14
30	3762.34	$4_{-4} - 3_1$	.26	62.38
20	3763.61	$3_0 - 2_2$	9.98*	63.65
20	3764.54	$7_{-7} - 6_{-2}$	.018	64.46
		$7_3 - 7_1$	.61**	64.64
98	3765.62	$4_0 - 4_{-1}$	9.28	65.78
10	3766.58			
3	3767.95	$7_2 - 7_0$	.20**	68.09
20	3768.47	$6_{-6} - 5_{-4}$	8.64*	63.56
100	3769.72	$2_0 - 2_{-1}$	16.3	69.65
		$6_3 - 6_1$	1.06**	69.7
60	3770.17	$7_{-1} - 7_{-2}$	.23	70.05
		$6_{-5} - 5_{-5}$	25.9*	70.58
30	3771.39	$5_3 - 5_2$	1.24*	71.39
5	3773.72	$6_{-4} - 5_{-2}$	2.85*	73.58
35	3777.65	$4_{-1} - 3_{-1}$	23.9*	77.85
99	3779.41	$1_{-1} - 0$	10.0	79.36
		$5_{-1} - 5_{-2}$	1.25	79.68
22	3781.73	$6_{-4} - 5_1$	.089	81.93
90	3784.35	$3_{-1} - 3_{-2}$	2.76	84.49
55	3784.97	$7_{-7} - 6_{-5}$	19.1*	85.01
		$3_1 - 2_{-1}$	18.0*	85.09
20	3786.02	$8_{-2} - 8_{-3}$	.20	86.23
15	3786.72			
12	3789.08			
10	3789.43	$5_{-2} - 4_{-2}$	5.50*	89.36
3	3792.37	$5_2 - 6_{-3}$	.007	92.47
5	3793.63	$7_{-5} - 6_{-3}$	5.80*	93.50
99	3796.13	$2_{-1} - 1_0$	12.3	96.23
80	3797.50	$6_{-2} - 6_{-3}$	1.45	97.82
30	3798.78	$3_2 - 2_2$	11.2*	98.83
30	3799.66	$6_{-3} - 5_{-3}$	10.9*	99.85
90	3800.26	$3_2 - 2_1$	33.4**	00.26

TABLE 1. *Absorption lines in the region of 2.7 μ due to* H_2O *and* CO_2—Continued

Observed		Identification	Calculated	
Intensity	ν_{vac}	$J'_\tau - J''_\tau$	Intensity	ν
	cm^{-1}			
100	3801.15	$2_{-2} - 1_{-1}$	52.0	01.15
95	3802.70	$4_{-2} - 4_{-3}$	4.33	02.86
100	3806.74	$2_0 - 1_1$	34.9	06.76
100	3815.96	$2_1 - 2_{-2}$	0.34	15.58
		$3_{-2} - 2_{-1}$	51.9	15.95
60	3818.55	$7_{-3} - 7_{-4}$	0.18	18.47
		$4_1 - 3_1$	22.1*	18.55
92	3819.88	$3_0 - 3_{-3}$	2.10	19.83
100	3820.65	$3_{-3} - 2_{-2}$	19.9	20.74
100	3821.70	$3_0 - 2_1$	24.2	21.69
55	3823.09	$5_{-3} - 5_{-4}$	0.75	23.39
50	3824.23	$4_0 - 3_{-2}$	2.81**	24.20
45	3825.50	$4_2 - 3_0$	7.13**	25.47
95	3826.66	$3_1 - 2_2$	8.04	26.68
50	3827.94	$4_{-1} - 4_{-4}$	0.77	27.90
10	3828.61	$5_1 - 5_{-5}$	.33**	28.64
99	3831.68	$3_{-1} - 2_0$	15.9	31.58
100	3835.02	$4_{-3} - 3_{-2}$	17.3	35.00
100	3837.99	$4_{-4} - 3_{-3}$	55.0	37.77
		$8_{-4} - 8_{-5}$	0.19	39.47
98	3840.11	$4_1 - 3_2$	3.79	39.94
		$5_{-2} - 5_{-5}$	1.75	40.09
98	3841.22	$4_2 - 3_3$	11.3	41.22
		$6_{-4} - 6_{-5}$	1.15	43.48
99	3843.89	$4_{-1} - 3_0$	9.85	43.66
		$6_{-1} - 6_{-4}$	0.16	44.31
35	3845.06	$5_0 - 5_{-3}$	.62	44.90
15	3846.60	$6_{-1} - 5_{-1}$	6.64*	46.68
30	3849.35	$7_{-2} - 7_{-3}$	0.31	48.98
		$4_3 - 3_2$	7.3**	49.44
		$6_{-3} - 6_{-4}$	0.35	49.68
80	3849.86	$4_1 - 4_{-2}$	.14	49.71
		$4_3 - 3_3$	21.9**	49.76
20	3850.54			
100	3852.29	$5_{-4} - 4_{-3}$	42.4	52.03
		$4_0 - 3_1$	29.0	54.00
100	3854.3	$5_{-3} - 4_{-4}$	14.4	54.02
		$4_{-2} - 3_{-1}$	43.6	54.03
60	3856.95	$3_2 - 3_{-1}$	0.19	56.61
95	3857.43	$5_2 - 4_3$	3.91	57.22
		$5_3 - 4_4$	1.31	57.40
10	3858.32	$8_{-3} - 8_{-4}$	0.051	58.11
5	3859.24	$6_2 - 6_{-4}$	.004**	59.27
98	3861.87	$5_0 - 4_1$	12.26	61.86
50	3862.52	$7_{-5} - 7_{-6}$	0.21	62.52
60	3863.48	$2_2 - 1_{-1}$	.77	63.35
90	3864.48	$5_1 - 4_2$	4.06	64.24
100	3865.22	$5_{-2} - 4_{-1}$	24.8	65.07
50	3866.21	$7_{-4} - 7_{-7}$	0.53	66.18
100	3869.37	$6_{-5} - 5_{-4}$	9.92	69.37
100	3870.21	$9_{-4} - 9_{-7}$	0.062	69.80
		$6_{-6} - 5_{-3}$	30.0	70.13
65	3871.65	$5_{-1} - 4_{-3}$	3.40*	70.83
5	3872.64	$6_4 - 5_3$	1.35	71.62
98	3874.03	$5_2 - 4_3$	4.14**	73.89
		$5_3 - 4_1$	12.4**	73.97
100	3874.53	$5_{-3} - 4_{-2}$	10.55	74.50
5	3876.66	$7_0 - 7_{-3}$	0.065	76.49
3	3877.52	$10_{-6} - 10_{-7}$	0.022	77.58
100	3880.07	$6_1 - 5_2$	1.25	79.94
		$5_{-1} - 4_2$	7.97	80.07
100	3880.33	$6_{-3} - 5_{-2}$	5.60	80.27
95	3881.05	$6_2 - 5_3$	3.74	81.01
20	3881.82	$8_{-5} - 8_{-8}$	0.077	81.72
80	3883.27	$6_{-1} - 5_0$	2.98	83.18
30	3884.08	$7_4 - 6_3$	0.32	83.88

TABLE 1. *Absorption lines in the region of 2.7 μ due to* H_2O *and* CO_2—Continued

Observed		Identification	Calculated	
Intensity	ν_{vac}	$J'_\tau - J''_\tau$	Intensity	ν
	cm^{-1}			
100	3885.77	$7_{-6} - 6_{-5}$	18.4	85.68
		$6_1 - 5_1$	6.10**	85.69
100	3886.08	$7_{-7} - 6_{-6}$	6.10	86.08
15	3886.92			
10	3887.30	$6_1 - 6_{-2}$	0.026	37.39
		$3_2 - 3_{-2}$	.033	88.00
100	3891.30	$6_{-4} - 5_{-3}$	19.7	91.27
85	3891.92	$6_0 - 5_{-2}$	1.49**	91.33
50	3892.80	$3_1 - 2_{-2}$	0.54	92.77
		$5_5 - 4_3$	3.15*	93.57
70	3894.13	$7_2 - 6_3$	.84	94.08
		$4_1 - 3_{-3}$	0.60**	94.19
8	3895.18	$8_6 - 7_7$	.042	94.97
5	3896.88	$9_{-7} - 9_{-8}$	.031	97.01
10	3897.62	$9_{-6} - 9_{-9}$	0.093	97.85
65	3898.16	$6_2 - 5_0$	.13**	98.14
		$5_2 - 5_{-1}$	.075	98.89
100	3899.38	$6_0 - 5_1$	8.75	99.21
		$7_{-4} - 6_{-3}$	9.62	99.54
		$7_0 - 6_0$	2.40*	01.41
100	3901.91	$8_{-7} - 7_{-6}$	3.30	01.78
		$8_{-5} - 7_{-7}$	9.90	01.93
98	3902.15	$7_0 - 6_1$	2.41	02.14
100	3904.22	$7_{-2} - 6_{-1}$	5.18	04.21
		$6_{-2} - 5_{-1}$	14.55	04.24
60	3905.51	$7_1 - 6_2$	0.80	05.51
90	3906.15	$8_4 - 7_5$	.20	06.01
		$7_{-5} - 6_{-4}$	3.47	06.08
3	3910.32	$4_3 - 4_{-3}$	0.10**	10.33
		$9_0 - 9_{-3}$	.004	10.47
5	3912.86	$10_{-6} - 10_{-9}$	.030	12.80
8	3914.06	$8_{-1} - 7_{-1}$	.99*	14.09
		$6_3 - 5_3$	4.78*	16.1
80	3916.35	$8_{-5} - 7_{-4}$	1.61	16.35
		$8_1 - 7_2$	0.16	16.42
92	3917.32	$8_2 - 7_3$	.48	17.17
		$9_{-6} - 8_{-7}$	6.36	17.42
90	3920.12	$8_{-6} - 7_{-5}$	4.99	20.13
60	3923.46	$7_1 - 6_{-1}$	2.70**	23.38
40	3923.70	$8_{-1} - 7_0$	0.41	23.70
60	3924.38	$8_{-3} - 7_{-2}$	.84	24.43
		$7_{-1} - 6_0$	1.63	25.16
88	3925.20	$7_{-3} - 6_{-2}$	2.49	25.20
15	3928.19	$9_2 - 8_3$	0.101	28.11
		$4_0 - 3_{-3}$	1.53	29.39
75	3929.53	$5_2 - 5_{-2}$	0.021	29.45
65	3930.83	$8_0 - 7_1$	1.20	30.74
88	3932.42	$9_{-4} - 8_{-5}$	2.12	32.42
85	3932.76	$10_{-10} - 9_{-9}$	2.74	32.67
55	3934.25	$9_{-7} - 8_{-6}$	0.71	34.25
10	3935.29	$3_3 - 2_0$	.094	35.10
25	3938.42	$9_3 - 8_1$	.217	38.30
		$6_2 - 6_{-3}$	.054	38.43
15	3939.24	$7_3 - 6_1$	2.15**	39.11
		$7_{-1} - 6_{-3}$	1.82*	39.22
6	3940.80	$9_1 - 8_2$	0.072	40.65
90	3942.86	$8_{-4} - 7_{-3}$	3.26	42.70
		$9_{-4} - 8_{-3}$	1.05	42.79
45	3944.49	$9_{-3} - 8_{-1}$	.51	44.40
55	3947.39	$10_{-7} - 9_{-6}$	.28	47.39
60	3947.59	$11_{-10} - 10_{-9}$	1.06	47.53
55	3948.37	$10_{-8} - 9_{-7}$	.84	48.35
80	3950.12	$8_{-2} - 7_{-1}$	2.23	50.02
25	3950.51	$3_2 - 2_{-1}$	.202	50.54
10	3952.57			
40	3953.28	$4_2 - 3_{-1}$	.57	53.26

TABLE 1. *Absorption lines in the region of 2.7 μ due to* H_2O *and* CO_2—Continued

Observed		Identification	Calculated	
Intensity	ν_{vac}	$J'_\tau - J''_\tau$	Intensity	ν
	cm^{-1}			
10	3953.70	$8_0 - 7_{-2}$	.29**	53.60
		$7_1 - 7_{-4}$	.010	53.71
15	3955.30			
35	3957.05	$9_{-5} - 8_{-4}$	.32	56.74
20	3958.43	$9_{-1} - 8_0$	.164	58.07
18	3959.89	$10_{-5} - 9_{-4}$	.142	59.73
		$6_0 - 6_{-3}$	.046	60.76
50	3961.92	$4_3 - 3_{-1}$	.053**	61.78
		$12_{-12} - 11_{-11}$	.37	61.92
48	3962.21	$11_{-8} - 10_{-7}$	.29	62.21
10	3963.99	$10_{-3} - 9_{-2}$	.055	63.89
12	3964.90	$6_0 - 6_{-1}$	.015	64.73
		$10_0 - 9_1$	.079	64.83
3	3967.39			
3	3967.69	$6_{-1} - 5_{-5}$	.62*	67.80
42	3969.38	$10_{-6} - 9_{-5}$	.42	69.34
28	3972.16	$9_{-3} - 8_{-2}$	.28	72.10
20	3972.70	$5_1 - 4_{-2}$	.27	72.62
25	3973.98	$5_{-1} - 4_{-4}$	.29	73.76
6	3974.88	$10_{-1} - 9_{-1}$	.076**	74.88
20	3975.10	$11_{-6} - 10_{-5}$	.123	75.06
3	3975.77			
26	3976.26	$13_{-12} - 12_{-11}$	.116	76.26
10	3976.49	$12_{-10} - 11_{-9}$	.123	76.49
2	3978.78			
8	3979.68			
6	3980.75			
15	3982.05			
10	3982.27	$5_2 - 4_{-2}$	.13**	82.27
10	3982.64	$4_1 - 3_{-2}$	.099	82.92
8	3984.87			
5	3985.83			
10	3989.56			
15	3990.22			
28	3990.72	$10_{-4} - 9_{-3}$	.273	90.65
8	3992.48	$4_4 - 3_{-2}$	0.008**	92.42
10	3994.78	$10_{-2} - 9_{-1}$	.167	94.89
30	3995.03	$6_1 - 5_{-3}$	.21**	95.03
3	4002.90			
3	4005.53			
6	4007.57			
35	4008.54	$6_3 - 5_{-3}$	.586	08.55
10	4012.71	$4_4 - 3_1$	.117	12.72
3	4015.37			
6	4017.00			
5	4018.59	$4_3 - 3_0$	.039	18.59
15	4019.52	$5_0 - 4_{-3}$	.268	19.52
3	4021.18	$7_0 - 6_{-4}$	.078**	21.08
25	4025.38	$6_{-2} - 5_{-5}$	.376	25.38
5	4029.88	$5_3 - 4_0$	.063	29.84
5	4031.55	$5_3 - 4_{-3}$	.037**	31.63
10	4043.86	$7_{-1} - 6_{-4}$	.108	43.83
25	4044.98	$6_2 - 5_{-1}$	.166	44.85
		$5_2 - 4_{-1}$	.160	45.01
4	4052.35	$8_{-1} - 7_{-3}$	.147*	52.25
5	4060.19			
12	4060.56	$7_1 - 6_{-2}$	.031	60.54
		$6_{-1} - 5_{-4}$	.051	60.59
6	4073.92	$6_1 - 5_{-2}$	.047	73.94
2	4075.27	$6_2 - 5_{-4}$	.012**	75.55
14	4079.46	$8_0 - 7_{-3}$	.083	79.54
4	4081.26	$7_{-3} - 6_{-6}$	.040	81.26
2	4084.83	$5_3 - 4_2$	.014	84.79
5	4086.17	$5_4 - 4_1$	.043	86.06
15	4088.18	$8_{-2} - 7_{-5}$	.121	88.18

The third and fourth columns of table 1 give the identifications of the line, or, if several transitions overlap to give an unresolved blend, the strongest such components are listed. The entries in these columns take three forms. (a) First-order H_2O lines. These may belong to either the ν_3 or the ν_1 fundamental. In either case we list first the rotational quantum numbers J_τ' belonging to the upper vibrational level, and next the corresponding rotational quantum numbers J_τ'' of the lower (vibrationless) level. ν_3 lines may be distinguished from ν_1 lines by the different selection rules that apply. These may most simply be stated as follows: in ν_3 (a so-called type A band, where the change of dipole moment is along the least axis of inertia) the parity of τ must change (odd $\longleftrightarrow$ even); whereas in ν_1 (a type B band, where the change of dipole moment is along the intermediate axis of inertia) the parity of τ is fixed (odd $\longleftrightarrow$ odd, or even $\longleftrightarrow$ even). (b) Second-order H_2O lines. The entry here is the wave number reported by Nelson [7] for the line in question, followed by the symbol /2. (c) CO_2 lines. The entry for these reads CO_2 R_J (or P_J), where the J signifies the rotational quantum number J'' of the ground state, and R or P is the conventional symbol for the R branch ($J'=J''+1$) or the P branch ($J'=J''-1$), respectively. As the two CO_2 bands, whose centers fall near 3,613 cm^{-1} and 3,715 cm^{-1}, do not overlap each other, no differentiation between them is given in the table.

The fifth and sixth columns of table 1 give calculated values of the intensity and frequency. The intensity values in the fifth column, when referring to first-order H_2O lines are relative values within each band, ν_3 or ν_1. The latter lines are distinguished by the symbol *, and a few lines of ν_1, for which abnormally high intensities are expected because of the perturbation phenomenon to be discussed in greater detail later, are further distinguished by a double asterisk (**). The calculated intensity has the following significance. It is proportional to the product of the "line strength", or probability of rotational transition $J_\tau'-J_\tau''$, into the Boltzmann factor $ge^{-E''/kT}$, where g is the statistical weight (3 for odd τ, 1 for even τ), E'' is the rotational term value of the ground level J_τ'' (these are listed in table 2), k is the Boltzmann constant, and T is the Kelvin temperature. In making the calculation, the line strengths were taken from the very useful tabulation of Cross, Hainer, and King [8], for the case of an a symmetric rotor with the asymmetry parameter $\kappa=-0.5$ in both upper and lower states. Hence the results should not precisely apply to the H_2O bands in question, where $\kappa''=-0.437$ and $\kappa'=-0.400$ for ν_3 and -0.425 for ν_1, but should be a good approximation to the true line strengths. Furthermore, in the calculation the temperature was taken as 267° K, for which the intensities had already been calculated [4] rather than the actual temperature of about 291° K; this would introduce an appreciable error only in a few of the transitions of highest E''. The absolute absorption intensity of a line, in addition to the relative factors tabulated, would depend upon the number of molecules in the absorbing path in the ground vibrational state, which is a constant of the experiment; upon the line width and slit width, which is approximately a constant of the experiment; upon the frequency, which varies by little more than 10 percent from one limit of the band to the other; and upon a factor representing the effective change of dipole moment in the vibrational transition. This last factor should be a constant for all lines of ν_3 and another constant for all lines of ν_1, to the approximation that the vibrational-rotational wave functions may be separated into vibrational and rotational portions. From a comparison of the observed intensities with those calculated it will be noted that the vibrational transition probability for ν_3 must be considerably stronger than that for ν_1. The proportionality factor seems to vary, however, being greater for lines in the R branches, where it is of the order of 50:1, than for lines in the P branches, where it is of the order of 15:1. This point will be discussed at greater length.

For second-order H_2O lines, the entry in column five of table 1 is the reported intensity, from reference [7], enclosed in parentheses. No entry is given for the intensity of the CO_2 lines; it is sufficient to note that a regular increase in intensity with J is expected, up to $J=20$, followed by a regular decrease. The weakest lines, R_0, R_{40}, P_{40}, etc., should have an intensity of the order of one-twentieth that of the strongest lines.

The calculated frequencies of the first-order H_2O lines in column six of table 1, are derived from the term values for the corresponding rotational states, which are listed in table 2. A calculated frequency is the difference between the two energy levels, J_τ' and J_τ'', involved in the transition. The term values for the ground state are those derived from the analysis of a large number of rotation-vibration bands [4]; they differ only very slightly from previously published values [9]. The term values for the upper levels ν_3 (001) and ν_1 (100) are derived from the present data. As each upper level gives rise to from two to six lines that are observably strong, and of which usually three or four are free from overlapping, the upper term values are obtained by adding the known lower term value to the observed ν for each line, and averaging the results. The concordance of the observed and calculated ν's, in which the disagreement rarely exceeds 0.2 cm^{-1}, thus indicates the consistency of the measurements. The correctness of the analysis is more definitely indicated by the agreement in relative intensities, and by the degree to which the observed term values of table 2 agree with theoretical calculations, which will be discussed later.

The calculated frequencies of the second-order H_2O lines are obtained in the same manner, the identification of the quantum transitions and the term values being given elsewhere [7, 4]; the calculated frequencies were then divided by 2. The calculated frequencies for the CO_2 lines were obtained by fitting the data to the well-known formula for a linear molecule [10]. The value of B'', 0.3904 cm^{-1}, was taken from the analysis of other well-resolved

TABLE 2. *Energy levels (cm^{-1}) of H_2O leading to lines in table 1*

J_τ	$v_1v_2v_3$		
	000	100	001
0_0	0. 00	(3657. 05)	3755. 79
1_{-1}	23. 79	3680. 36	3779. 36
1_0	37. 13	3693. 26	3791. 52
1_1	42. 37	3698. 44	3796. 75
2_{-2}	70. 06	3725. 87	3824. 94
2_{-1}	79. 48	3734. 88	3833. 36
2_0	95. 17	3750. 55	3849. 13
2_1	134. 91	3788. 58	3885. 58
2_2	136. 15	3789. 84	3887. 14
3_{-3}	136. 77	3791. 35	3890. 80
3_{-2}	142. 27	3796. 51	[1] 3895. 43[a]
3_{-1}	173. 36	3827. 41	3926. 75
3_0	206. 28	3858. 82	3956. 60[e]
3_1	212. 16	3864. 57[a]	3962. 83[b]
3_2	285. 25	3934. 98[b]	4030. 02
3_3	285. 40	3935. 17[c]	4030. 27
4_{-4}	222. 04	3875. 02	3974. 54
4_{-3}	224. 83	3877. 60	3977. 27[d]
4_{-2}	275. 48	3927. 63	4027. 69
4_{-1}	300. 38	3951. 21	4049. 94[f]
4_0	315. 73	3966. 47[d]	4066. 16[e]
4_1	382. 49	4030. 71[e]	4125. 19[b]
4_2	383. 86	4031. 75[f]	4126. 62[e]
4_3	488. 16	4135. 16[g]	4224. 87
4_4	488. 17	4134. 69[b]	4224. 88
5_{-5}	325. 36	3976. 23	4076. 06
5_{-4}	326. 59	3977. 35	4076. 86[f]
5_{-3}	399. 45	4049. 51	4149. 98
5_{-2}	416. 12	4064. 84	4165. 45[f]
5_{-1}	446. 50	4095. 66[f]	4195. 80
5_0	504. 00	4150. 35	4244. 35[f]
5_1	508. 79	4154. 00[f]	4248. 10[h]
5_2	610. 12	4257. 75[h]	4345. 39
5_3	610. 34	4256. 46[f]	4345. 57
$5_{4,\ 5}$	742. 10	4381. 73	4468. 55
6_{-6}	446. 71	4095. 15	4195. 49
6_{-5}	447. 24	4095. 84	4195. 96
6_{-4}	542. 87	4189. 70	4290. 72
6_{-3}	552. 92	4199. 30	4296. 39[m]
6_{-2}	602. 67	4249. 53	4350. 74
6_{-1}	648. 97	4293. 16	4387. 18[o]
6_0	661. 54	4308. 05[m]	4408. 00[n]
6_1	756. 76	4394. 48[n]	4490. 06
6_2	757. 70	4402. 14[o]	4491. 35
$6_{3,\ 4}$	888. 69	(4526. 4)	4613. 72
$6_{5,\ 6}$	1045. 15	----------	4759. 80
7_{-7}	586. 28	4232. 25	4332. 79
7_{-6}	586. 43	----------	4332. 92
7_{-5}	704. 20	4346. 42	4448. 95
7_{-4}	709. 50	----------	4452. 46
7_{-3}	782. 41	4430. 69	4527. 97
7_{-2}	816. 65	----------	4553. 18[q]
7_{-1}	842. 36	4492. 14	4586. 70[p]
7_0	927. 76	4563. 95[p]	4658. 90
7_1	931. 23	4572. 35[q]	4663. 21
7_2	1059. 68	4695. 85	4782. 77
7_3	1059. 89	4695. 87	4782. 90
$7_{4,\ 5}$	1216. 39	----------	4929. 03
$7_{6,\ 7}$	1394. 96	----------	5096. 24

TABLE 2. *Energy levels (cm^{-1}) of H_2O leading to lines in table 1*—Continued

J_τ	$v_1v_2v_3$		
	000	100	001
$8_{-8,\ -7}$	744. 13	----------	4488. 21
8_{-6}	882. 97	----------	4624. 33
8_{-5}	885. 64	----------	4625. 85
8_{-4}	983. 09	----------	4725. 11
8_{-3}	1006. 15	----------	4741. 08[s]
8_{-2}	1050. 20	----------	4792. 38[r]
8_{-1}	1122. 78	4756. 45[r]	4851. 46
8_0	1131. 88	4770. 25[s]	4861. 97
8_1	1255. 19	----------	4976. 10
8_2	1255. 98	----------	4977. 06
$8_{3,\ 4}$	1411. 59	----------	5122. 40
$8_{5,\ 6}$	1591. 11	----------	(5289. 9)
$8_{7,\ 8}$	1789. 36	----------	----------
$9_{-9,\ -8}$	920. 21	----------	4661. 55
9_{-7}	1079. 14	----------	4817. 22
9_{-6}	1080. 51	----------	4818. 06
9_{-5}	1202. 04	----------	4939. 83
9_{-4}	1216. 37	----------	4948. 94
9_{-3}	1283. 02	----------	5022. 30
9_{-2}	1341. 01	----------	5067. 18
9_{-1}	1360. 56	----------	5089. 95[t]
9_0	1475. 14	5108. 35[t]	5193. 49
9_1	1477. 46	----------	5196. 63
$9_{2,\ 3}$	1631. 56	----------	5339. 70
$10_{-10,\ -9}$	1114. 69	----------	4852. 88
10_{-8}	1293. 22	----------	5027. 49
10_{-7}	1293. 80	----------	5027. 90
10_{-6}	1439. 88	----------	5171. 38
10_{-5}	1446. 37	----------	5176. 10
10_{-4}	1538. 11	----------	5273. 67
10_{-3}	1581. 53	----------	5304. 90
10_{-2}	1614. 07	----------	5355. 45[u]
10_{-1}	1719. 36	5335. 44[u]	----------
10_0	1725. 84	----------	5442. 27
$11_{-11,\ -10}$	1327. 22	----------	5062. 22
11_{-9}	1525. 03	----------	----------
11_{-8}	1525. 32	----------	5256. 01
11_{-7}	1690. 75	----------	----------
11_{-6}	1694. 33	----------	5421. 43
11_{-5}	1810. 78	----------	----------
$12_{-12,\ -11}$	1558. 07	----------	5289. 14
$12_{-10,\ -9}$	1774. 88	----------	5501. 52
$13_{-13,\ -12}$	1806. 94	----------	5534. 33

[1] The letters a, b, etc., identify pairs of levels in (100) and (001) that are particularly strongly connected by perturbation interactions. See text.

bands of this molecule [11]; the resulting values of B''-B' and ν_0 are listed in table 3. The observed values of these parameters are in good agreement with the values calculated from an empirical equations whose constants fit the other CO_2 bands.[2]

[2] In a paper published after the completion of this work, Jones and Bell (Phys. Rev. **79**, 1004 (1950)) have reported measurements of the CO_2 bands in a vacuum grating spectrometer. The constants they derive are in excellent agreement with ours for B'-B'', but differ by about 1 cm^{-1} for the ν_0's. Their values of B'' also do not agree well with the published values we have adopted [11]. These discrepancies must be due to different methods used in establishing the wavelength scales; it is difficult to believe that our values, based on accurately known lines in higher orders, could be in error by as much as 1 cm^{-1}.

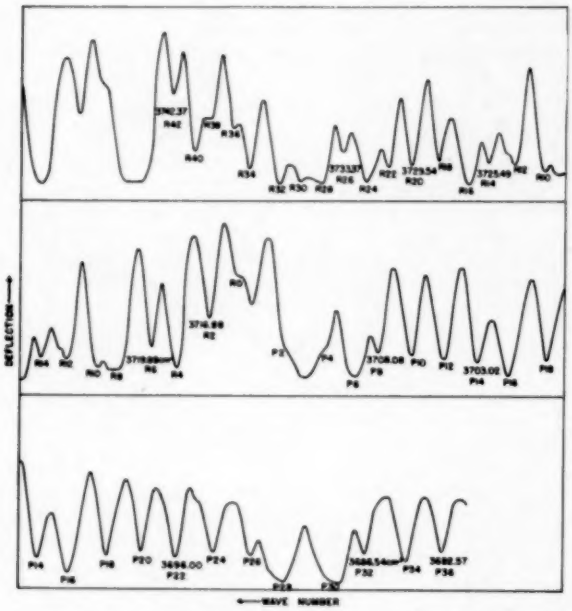

FIGURE 5. *Observed absorption enhanced by absorption cell containing* CO_2, *3,750 to 3,680* cm^{-1}.

TABLE 3. *Constants of* CO_2 *bands in 2.7-μ region*

v_1	v_2	v_3	ν_0		B''	B'
			Observed	Calculated	Observed	Calculated
			cm^{-1}	cm^{-1}	cm^{-1}	cm^{-1}
0	2	1	3612. 91	3613. 64	0. 0027_9	0. 00274
1	0	1	3714. 59	3714. 76	. 0030_9	. 00312

The absorption due to CO_2, when an absorption cell filled with this gas was added to the optical path, is shown in figure 5, covering the region of the higher-frequency band of the resonance doublet, from 3,680 to 3,748 cm^{-1}. Comparison with the corresponding region in figures 2 and 3 shows a marked enhancement of the lines that have been attributed to CO_2. Figure 5 also shows the rotational numbering for the band and makes it clear that the center of the band has been correctly located.

IV. Discussion

The rotational analysis of the ν_3 band is rather complete, in that nearly all the theoretically expected lines of intensity 0.2 or greater (on the adopted relative scale on which the strongest line, 4_{-4}-3_{-3}, has intensity 55.0) have been located. A few lines as weak as 0.03 appear, giving about 5-percent maximum absorption, in regions where there is no overlapping from stronger lines. The identified levels of ν_3 include all levels with $J'=8$, and a number of the lower-energy levels of higher J, as listed in table 2. The ν_1 analysis is less complete, because of the much lower intensity of the lines of this band, particularly in the R branch, where our measurements are most satisfactory. Many of the strongest lines of the P branch of ν_1, and some of the higher-J lines of the P branches of ν_3, fall in the region beyond 3,500 cm^{-1}, to which our measurements do not extend. These lines may be recognized in other published and unpublished measurements of this region [12], overlapping the R branches of the weaker overtone band $2\nu_2$. The known values of ν_1 used here are partially based on the longer wavelength data. Table 1 shows that nearly 98 percent of the lines, and all of the stronger ones, are satisfactorily accounted for.

As an illustration of the agreement between observation and the analysis, figure 6 represents a portion of the observed spectrum, together with the calculated spectrum. The latter is represented by lines at the calculated frequency, whose length is the theoretical relative intensity, on a scale that exaggerates the importance of the weaker lines. The region depicted, between 3,845 to 3,895 cm^{-1}, is dominated by the stronger lines of the R_0 branch from $J'=4$ to $J'=7$, with calculated intensities >3. These give observed absorptions of 80 percent or greater; lines with intensity >10 show practically complete absorption; and the overlapping of three such lines, with calculated ν's 3854.0 ± 0.1 cm^{-1}, gives rise to a region of complete absorption over 1 cm^{-1} broad. The weaker lines in the region include the lowest members of the ν_3 $R_{2\bar{1}}$ branch (e. g., 2_2-1_{-1}; Int calc=0.77, Int obs=60%), a few lines of the $\nu_3{}^{0}_{2,\bar{1}}$ branch (e. g., 7_0-7_{-3}; Int calc=0.065, Int obs=5%); and some of the stronger members of the R branches of ν_1. Many of the latter give quite weak absorption; for example 6_{-1}-5_{-1}, with Int calc=6.6, shows only 15-percent absorption. It is from comparisons of this kind that the statement was made above that the intensity of ν_1 relative to ν_3, in the R branch, was of the order of 1:50.

There are, however, some isolated members of the ν_1 R branches that show much more intense absorption. For example, the strong absorption (85%) at 3891.92 cm^{-1} is assigned to 6_0-5_{-2} whose calculated intensity is only 1.99, much less than the 6_{-1}-5_{-1} line. Similarly the pair 5_3-4_1, 5_2-4_2 at 3874.0 cm^{-1} show an observed absorption more nearly characteristic of ν_3 than of ν_1. These observations find a natural interpretation in the perturbation of a rotation-vibration level of ν_1 by a close-lying one of ν_3. It will be noted in table 2 that letters have been suffixed to certain levels in pairs, one in each vibration state. The pairs have the characteristic that they are of the same J, the same total (vibrational$\times$rotational) symmetry properties, and are of approximately the same energy (<30 cm^{-1} apart). Such pairs are subject to a mutual perturbation, induced by the Coriolis forces interacting between the vibrations and the rotation [13]. The perturbation results in a displacement of the frequencies, and a mixing of the wave-functions of the two levels. The frequency shifts will be discussed quantitatively later;

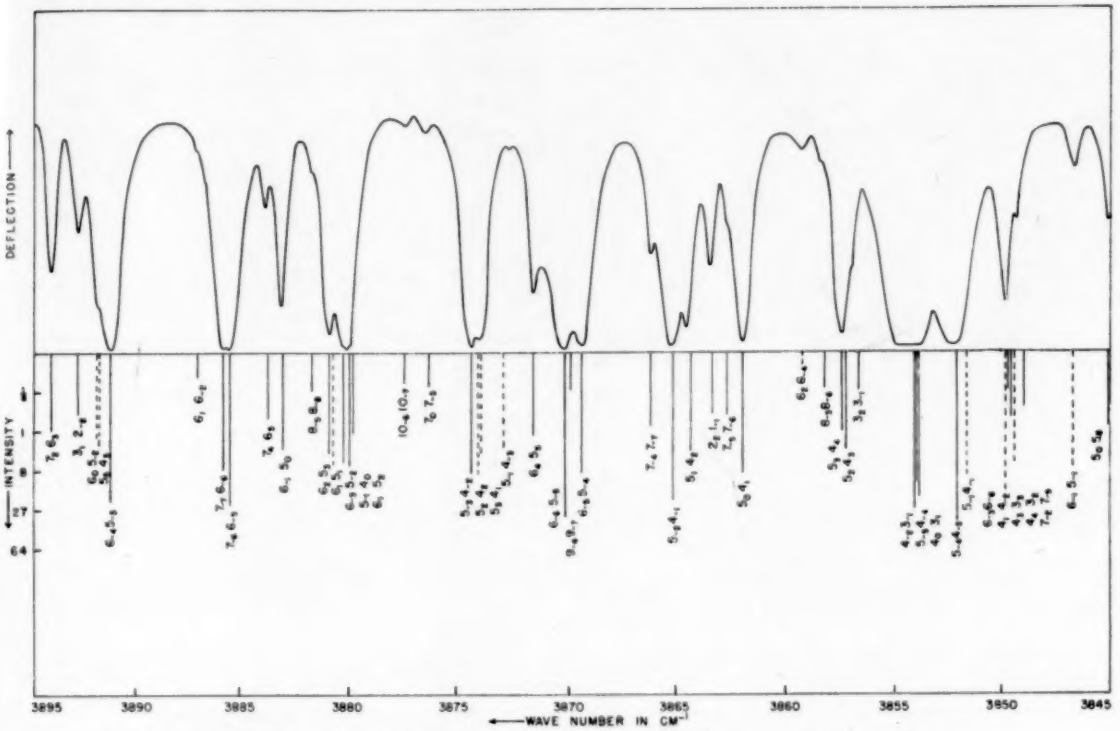

FIGURE 6. *Comparison of observed and theoretically calculated spectra, 3,895 to 3,845 cm⁻¹.*

they are small, but are apparent in table 2 in such instances as levels k and l of (100), which are inverted from their normal order, or n and o of (100) which are separated by 7.66 cm^{-1} instead of 1 cm^{-1}, which would be normal for the close doublet 6_1-6_2. These are precisely the levels that give rise to the ν_1 lines of abnormally high intensity, as indicated by ** in table 1. The perturbation has, for example, caused the ν_1 line 6_0-5_{-2} to partially merge its identity with the ν_3 line 6_{-3}-5_{-2}, with a resultant merger of the intensity of the two lines. Even more striking is the appearance of such a weak transition as ν_1 6_2-6_{-4} (Int calc=0.004); this is due to its perturbation by ν_3 6_{-1}-6_{-4} (Int calc=0.16).

Figure 7 is a similar illustration of the agreement between observation and calculation in the region 3,775 to 3, 25 cm^{-1}. The strong lines in this region are the first members of the $R_{0,1}$ branch of ν_3. Some of the very weak lines of the ν_3 R and P branches appear. The relatively low intensity of the ν_1 R-branch lines is again to be noted.

Figure 8 similarly depicts the situation from 3,505 to 3,590 cm^{-1}. Here the second-order radiation is a complicating factor in evaluating relative intensities, but it is clear that in this region, which includes higher-J members of the P branch of ν_3 and the stronger members of the P branch of ν_1, the relative intensity of ν_1:ν_3 is considerably higher than in the R branches. It seems certain that this anomaly occurs in ν_1 rather than ν_3; similar anomalous intensities have also been found in other of the type B bands of H_2O [4]. For example, the type B band (130) has a P branch that is about one-half the observed intensity of the P branch of the adjoining type A band (031), whereas the relative intensities in the corresponding R branches are about 1:10. A very similar anomaly has also been observed in H_2S [14], where the R branch of the ν_3 fundamental is very much stronger than the P branch. A quantitative explanation of this behavior cannot be offered but it undoubtedly is associated with the breakdown of the assumption of separability of the molecular wave-function into vibrational and rotational portions. The interaction terms in the molecular potential function, which result in different effective moments of inertia for different vibrational states, will also affect the transition probabilities, and it may be expected that anomalous intensities will result. This effect should, however, be roughly constant for all transitions of a similar type, so that the relative intensities within a particular branch should agree with those calculated on the assumption of separability, in agreement with observation.

Another way in which the correctness and completeness of the rotational analysis may be demonstrated is by arranging the lines of a given branch in series. This is done in table 4 for the $R_{0,1}$ branch of ν_3. The observed ν, observed intensity, and calculated intensity are listed for all lines, arranged vertically in order of increasing J, horizontally in

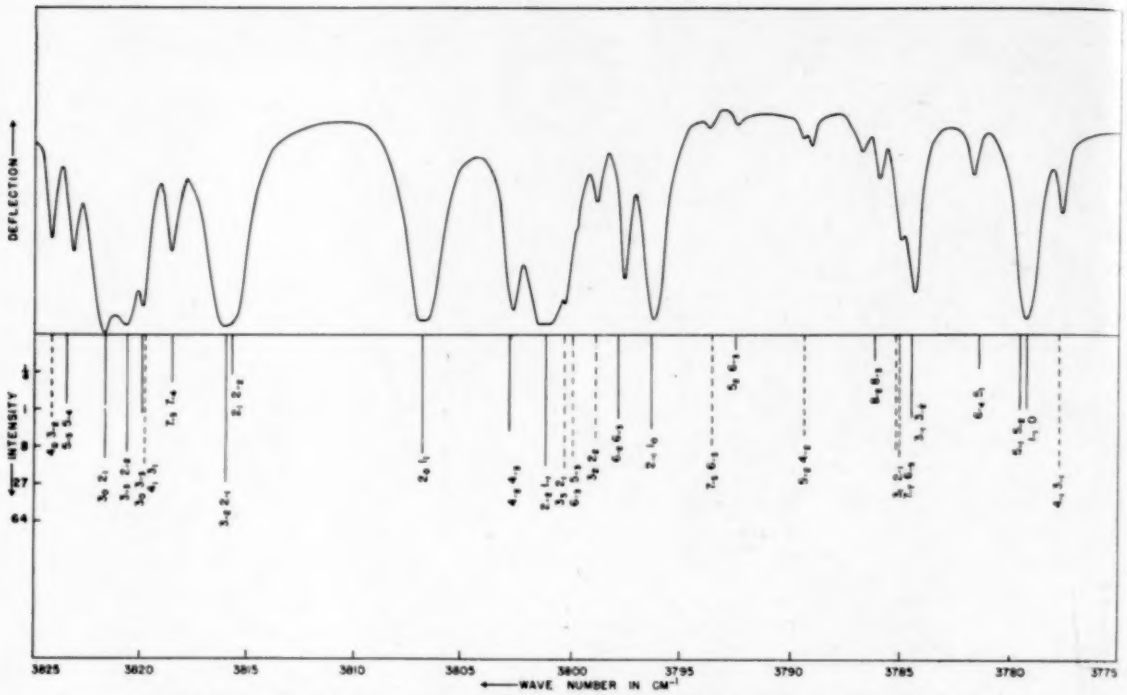

FIGURE 7. *Comparison of observed and theoretically calculated spectra, 3,825 to 3,775 cm⁻¹.*

order of increasing τ. Regularities in both position and intensity are apparent, except that for a few of the τ series there is an irregularity, which is seen to be associated with the perturbation of the ν_3 levels by close-lying ν_1 states. Similar series arrangements may be made of the lines of the other branches and of ν_1, but will not be reproduced here.

In table 4, spaces have been left for lines that have not yet been identified. By following the indicated regularities, provisional assignments may readily be made for the stronger of these expected lines, and some of these have been listed in table 4. In order to confirm the assignments, it would be necessary to locate the lines of corresponding $J\tau'$ in other branches. As these are either too weak to observe, or fall outside the present limits of observation, such lines and levels have not been included in tables 1 and 2. By making observations of the absorption of heated water vapor, over the spectral range 3,350 to 4,300 cm^{-1}, it should be possible to confirm these and extend the analysis to higher energies; it is hoped to do this in the near future. Observations [4, 12] of the absorption of the whole atmosphere (between 3,300 to 3,500 cm^{-1} and 3,000 to 4,320 cm^{-1}) have located a number of lines, of calculated intensity down to 0.001, that belong to the $R_{2,\bar{1}}$ and $P_{2,1}$ branches of the levels listed here. A few of the stronger lines of the $R_{4,\bar{3}}$ branch also appear in the solar absorption. It is of further interest to note that in the solar absorption curve obtained by Migeotte on the Jungfraujoch, the relative intensity of the lines between 3,900 to 4,020 cm^{-1} differs from our laboratory observations, in that on his tracings the lines of the $R_{2,\bar{1}}$ series are stronger relative to the $R_{0,1}$ series than on ours. This is to be expected, in view of the much lower temperature (surface temperature $\sim$257° K) prevailing on the Jungfraujoch. As the $R_{0,1}$ lines in a given region of the spectrum originate on much higher energy levels than the $R_{2,\bar{1}}$ lines in the same region, there is a pronounced temperature coefficient of their relative intensity, as observed. Indeed, it would seem possible to use this effect as a thermometric device, accurate to a few degrees.

The essential correctness of the rotational analysis may also be shown by a comparison of the energy levels of table 2 with those calculated from the theory of the asymmetric rotor. This calculation is relatively simple [15], if one ignores both the influences of centrifugal distortion and of the ν_1-ν_3 perturbation. There should then be three constants, the effective reciprocal moments of inertia, $A_v > B_v > C_v$, in terms of which the energies may be calculated. A procedure by which these constants may be evaluated from the energy levels, together with some of the constants that characterize the centrifugal stretching, has been developed [16] and will be described in detail elsewhere. The method (which is an extension of that suggested by Mecke [1]) consists in taking certain sums and differences of the observed energy levels, grouped according to the levels of like symmetry type for each J, and dividing by appropriate

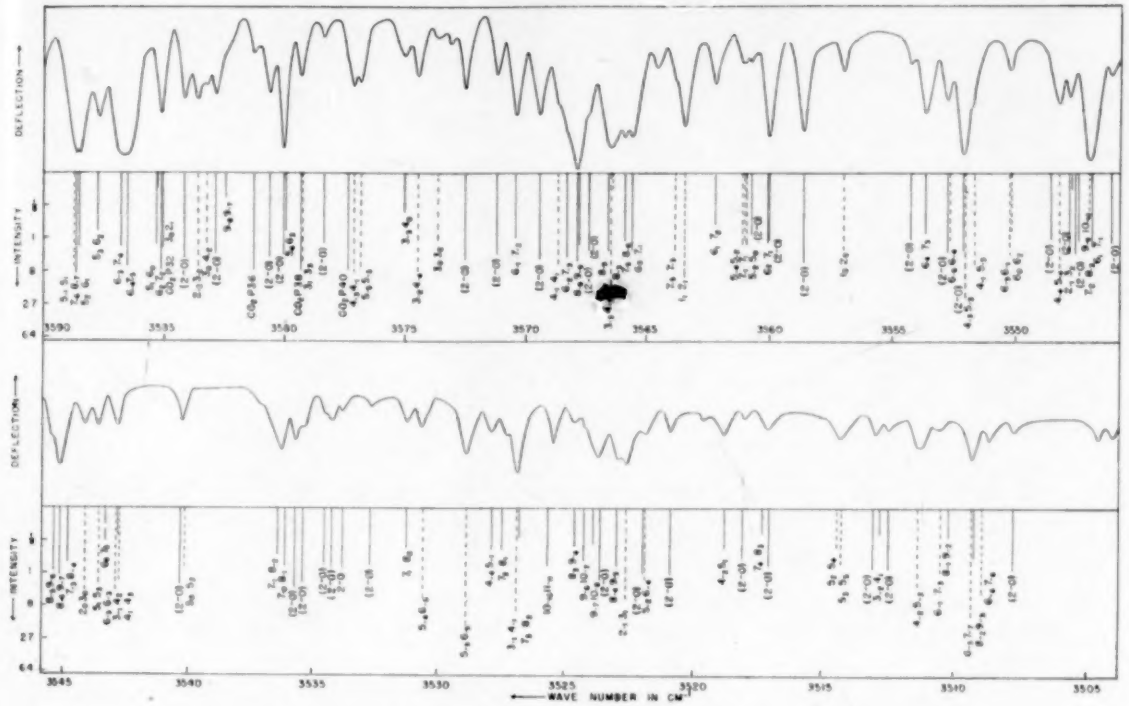

FIGURE 8. *Comparison of observed and theoretically calculated spectra, 3,590 to 3,505 cm⁻¹.*

functions of J. Each such operation yields a parameter that we designate $A'_v(J)$, $A''_v(J)$, $A'''_v(J)$, etc., and which, if there were no centrifugal stretching nor perturbation, should be the desired constant A_v, etc. If there is no perturbation, each such set, when plotted against J^2, should fall on smooth curves, whose zero intercept is close to A_v, and whose initial slope yields one of the centrifugal stretching constants. The three sets, denoted by $'$, $''$, and $'''$ do not coincide precisely, but may be brought into coincidence by making a correction involving one of the minor centrifugal stretching constants, and plotting against J^{2*}, which takes the value J^2-J, J^2-1, or J^2, depending upon the particular set.

In figure 9 the values of the parameters, obtained in the above manner from the data of table 2, are plotted against J^{2*}. The data for the ground state (000), which are obtained from many observed bands, are by far the most precise; it is seen that they fall excellently on smooth, nearly linear curves. (As the quantities plotted are of the order of $\Delta E/J^2$, it follows that an error of 0.5 cm^{-1} in any single energy at $J=7$ would lead to a deviation of 0.01, a scatter which the (000) curves do not exceed). The effective moments of the ground state are believed accurate to ± 0.005 cm^{-1}. The points for the vibrationally excited levels, denoted by the filled symbols, show much greater scatter from smooth curves in figure 9. This is to be expected, because of the less accurate data, and particularly because of the vibrational-rotational perturbation. The latter may be computed by an approximate calculation, to be described presently; from the "unperturbed" levels obtained by subtracting the corrections from the observed levels, new values of the parameters may be calculated. These are represented by the open symbols in figure 6. They show considerably less deviation from the smooth curves that have been drawn to fit them. In drawing the curves, the slopes for B and C were drawn approximately parallel to those for (000), as similar treatments of other vibrational levels has shown that these do not vary widely with the vibrational state. The slope of the A curves are somewhat lower for the excited states than for (000), again in conformity with the general finding. From the curves as drawn, values of the effective moments were obtained and are listed in table 5. These are believed accurate to about ± 0.02 cm^{-1}. The value of $C_{100}+C_{001}$ does not involve the perturbation corrections, and should be somewhat more accurate.

From the values of the effective rotational constants, the value of each energy level may now be calculated and compared with the observed energy. This is done for the levels up to $J=9$ (ν_1 up to $J=6$) in table 6. The first entry is the difference between the calculated and the observed energy; this is the

TABLE 4. *Series regularities in the $R_{0,1}$ branch of ν_2*

J'	$J+\tau$	0	1	2	3	4	5	6	7	8	9	10	11	12	13–14	15–16	17–18
1	ν	3779.41															
	I_{obs}	99															
	I_{calc}	10.0															
2	ν	3801.15	3796.13	3806.74													
	I_{obs}	100	99	100													
	I_{calc}	32.0	12.3	35.0													
3	ν	3820.65	3815.96	3831.68	3821.70	3826.66											
	I_{obs}	100	100	99	100	95											
	I_{calc}	19.9	52.0	15.9	24.2	8.04											
4	ν	3837.99	3835.02	(3854.3)	3843.89	(3854.3)	3840.11	3841.22									
	I_{obs}	100	100	(100)	99	(100)	98	98									
	I_{calc}	55.0	17.3	43.7	9.83	28.9	3.79	10.13									
5	ν	(3854.3)	3852.29	3874.53	3865.22	3880.07	3861.87	3864.48	3857.43								
	I_{obs}	(100)	100	100	100	100	98	90	95								
	I_{calc}	14.4	42.4	10.06	24.8	7.76	12.2	4.06	5.21								
6	ν	3870.21	3869.37	3891.30	3880.33	3904.22	3883.27	3899.38	3880.07	3881.05	3871.65						
	I_{obs}	100	100	100	100	100	80	(100)	(100)	95	65						
	I_{calc}	30.0	9.91	19.4	5.60	14.6	2.98	8.75	1.25	3.74	1.35						
7	ν	3886.08	3885.77	3906.15	3899.38	3925.20	3904.22	3925.20	3902.15	3905.51	3894.13		3884.08				
	I_{obs}	100	100	90	(100)	88	(100)	(88)	98	60	(70)		30				
	I_{calc}	6.10	18.2	3.47	9.62	2.49	5.18	1.63	2.41	0.80	1.12		0.32				
8	ν	3901.91		3920.12	3916.35	3942.86	3924.38	3950.12	3923.70	3930.83	3916.35	3917.32	3906.15		3895.18		
	I_{obs}	100		90	80	90	60	80	40	65	(80)	(92)	(90)		8		
	I_{calc}	13.20		4.99	1.61	3.25	0.84	2.23	0.41	1.20	0.16	0.48	0.20		0.041		
9	ν	3917.32		3934.25	3932.42	3957.05	3942.86	3972.16	3944.49	3958.43	3938.42	3940.80	3928.19		(3916.35)?		
	I_{obs}	92		55	88	35	(90)	28	45	20	25	6	15		(80)		
	I_{calc}	5.36		0.71	2.12	0.41	1.05	0.28	0.51	0.165	0.217	0.072	0.101		0.028	0.005	
10	ν	3932.76		3948.37	3947.39	3969.38	3959.89	3990.72	3963.99	3994.78	3959.89?	3964.90	3950.51?				
	I_{obs}	85		55	55	42	18	28	10	10	(18)	12	(25)				
	I_{calc}	2.74		0.84	0.28	0.42	0.128	0.27	0.055	0.166	0.027	0.079	0.040		.012	.003	0.005
11	ν	3947.59		3962.11	3961.92	3979.68?	3975.10	4005.52?	3982.05?	4019.52?	3980.75?		3975.77?				
	I_{obs}	60		(48)	50	8	20	3	15	(15)	6		3				
	I_{calc}	1.66		0.998	0.291	0.040	0.123	0.026	0.057	0.016	0.025	.008	0.010	.003	.004	.001	.0003
12	ν	3962.11		3976.49				4018.59?		4031.55?							
	I_{obs}	48		10				(5)		5							
	I_{calc}	0.368		0.125		.036	.012	0.019	.005	0.012	.002	.006	.001	.003	.0012	.0004	
13	ν	3976.26		3989.56?													
	I_{obs}	26		10													
	I_{calc}	0.116		0.034		.003	.008	.002	.005	.001	.002	.0004					
14	ν	3990.227		4005.53?													
	I_{obs}	15		3													
	I_{calc}	0.032		0.009		.002		.001									
15	ν	4007.57?															
	I_{obs}	6															
	I_{calc}	0.008		.002													

combined result of the effects of centrifugal distortion and perturbation, together with any errors resulting from experimental inaccuracy in locating the levels, or in deriving the rotational constants. It is seen that the differences are roughly alike for the three vibrational states, and increase in a regular manner with J and with $J+\tau$, except for the more strongly perturbed levels, which have been given letter suffixes.

The second number entered in table 6 for each rotational level of ν_1 and ν_3 is an estimate of the energy shift due to the perturbation. These are, of course, of equal magnitude and opposite sign in ν_1 and ν_3 for each symmetry group of each J. They were obtained by the following approximate procedure. An exact calculation [13] would involve setting up and solving secular determinants of order J or $J+1$, in which the elements are the usual rotational energy constants of the Wang determinant, plus perturbation elements of the form $W_p=G_{zz}(J+K+1)(J-K)$. G_{zz} is a constant that depends on the potential constants of the molecular motion and on the vibrational wave functions of ν_1 and ν_3. It might be calculated from the potential function,

TABLE 5. *Rotational constants for H_2O bands*

v_1 v_2 v_3	A_v	B_v	C_v	κ	$10^{40}I_{A_v}$	$10^{40}I_{B_v}$	$10^{40}I_{C_v}$	Δ
	cm^{-1}	cm^{-1}	cm^{-1}		$g\ cm^2$	$g\ cm^2$	$g\ cm^2$	
0 0 0	27.877	14.512	9.285	−0.4377	1.004	1.928	3.014	0.082
1 0 0	27.13	14.29	9.105	− .4247	1.031	1.958	3.073	.084
0 0 1	26.636	14.40	9.156	− .4000	1.051	1.943	3.056	.062

but is better treated as an empirical constant, inasmuch as it is found [4] to vary with the particular pair of interacting levels; that is, it has a different value in the interacting combination bands (011-110); (021-120); (111-210), etc., than is found here. It is now assumed that each rotational level is perturbed by each interacting level $K\pm1$ separately, so that the perturbed energy may be given by $E=E_0+\sum_i \delta_i$ where E_0 is the "unperturbed" energy (such as would result from a solution of each Wang secular equation, with appropriate centrifugal stretching terms), and

$$\delta_i=\frac{\{(E_0-E_i)^2+W_{pi}^2\}^{1/2}-(E_0-E_i)}{2}$$

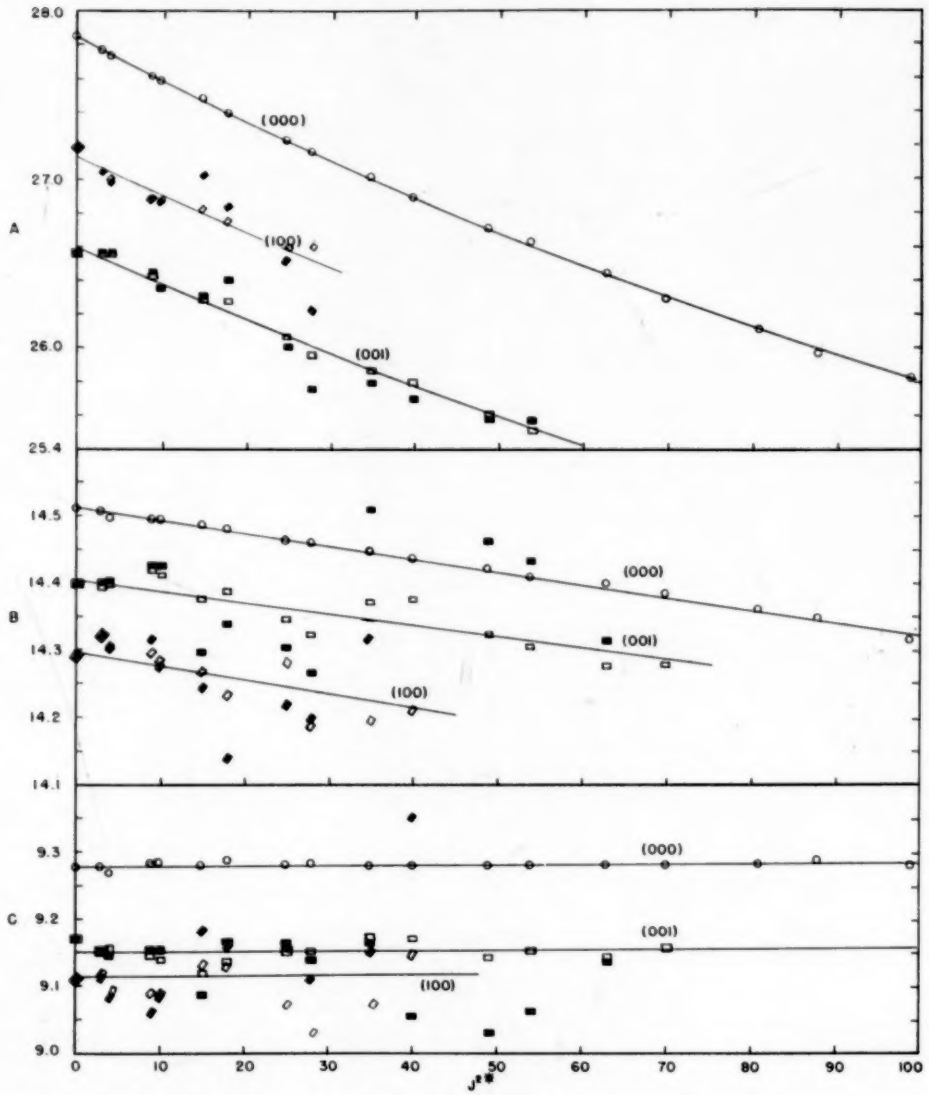

FIGURE 9. *Curves from which may be derived the inertial and centrifugal-stretching constants, associated with rotation about the least axis of inertia (A), the intermediate axis (B), and the greatest axis (C).*

○, Ground vibrational state (000); ◆, ν_1 (100), uncorrected for perturbation; ◇, ν_1 (100), corrected for perturbation; ■, ν_3 (001), uncorrected for perturbation; □, ν_3(001), corrected for perturbation.

TABLE 6. *Centrifugal and perturbation energies* (cm^{-1})

J	$J+\tau$ v_1 v_2 v_3	0	1	2	3	4	5	6	7	8	9	10	11-12	13-14
1	0 0 0	0.00	0.03	0.02										
	1 0 0	.09	.03	.03										
	0 0 1	−.01	.06	.08										
2	0 0 0	.35	.04	.04	0.41	0.40								
	1 0 0	.08−0.01	.05−0.02	−.10	.38−0.02	.42−0.03								
	0 0 1	.16+0.02	.09+0.04	.04+0.02	.24	.09								
3	0 0 0	.16	.11	.18	.40	.42	2.06	2.06						
	1 0 0	.11−0.02	.07−0.03	.07−0.01	.33−0.06	.54−0.11	2.05−0.14	2.07−0.19						
	0 0 1	.05+0.03	.06+0.11	−.05+0.04	−.06+0.20	−.01+0.14	1.56+0.02	1.54+0.02						
4	0 0 0	.34	.26	.54	.56	.71	2.01	2.01	6.44	6.44				
	1 0 0	.22−0.05	.12−0.05	.56−0.04	.51−0.10	.99−0.54	1.96−0.31	2.31−0.52	3.77+1.20	4.25+1.04				
	0 0 1	.34+0.05	−.20+0.55	.27+0.07	−.24+0.52	−.04+0.27	2.77−0.98	2.87−1.16	5.25+0.04	5.25+0.04				
5	0 0 0	.58	.51	1.17	.87	1.39	2.22	2.31	6.31	6.31	15.42			
	1 0 0	.50−0.07	.46−0.08	0.96−0.07	1.13−0.09	1.20+0.30	1.99−0.32	3.46−1.57	0.98+2.80	2.51+1.86	13.29+0.51			
	0 0 1	.67+0.08	.78−0.32	.67+0.09	−0.97+1.54	0.79+0.36	4.18−1.85	6.06−2.88	5.47−0.41	5.57−0.41	13.24+0.08			
6	0 0 0	.95	.89	2.00	1.58	2.75	2.92	3.32	6.47	6.48	14.92		31.16	
	1 0 0	.84−0.10	.74−0.11	2.24−0.12	1.40−0.12	2.34+0.06	2.42−0.54	0.93+1.80	8.71−3.39	2.09+2.51	12.23+0.98		? +0.48	
	0 0 1	1.03+0.10	.92−0.11	1.64+0.12	3.57+1.90	1.85+0.42	5.59−2.54	−.67+3.31	6.45−0.91	6.48−0.96	12.91−0.30		26.95+0.13	
7	0 0 0	1.46	1.45	3.05	2.55	4.93	4.20	5.37	7.36	7.30	14.98	14.95	30.20	5.86
	0 0 1	1.63+0.14	1.63−0.02	2.71+0.16	2.90−0.64	3.89+0.53	6.68−2.75	2.60+2.50	8.12−1.50	8.27−1.82	13.64−0.73	13.76−0.73	26.53−0.28	8.73+0.20 4
8	0 0 0	2.08		4.04	3.67	7.04	6.07	8.53	9.08	9.65	16.02	15.99	29.77	54.16
	0 0 1	2.33		3.95	4.07	6.41	7.80−2.15	6.60+1.85	10.77	11.94−3.65	15.59	15.67	27.27	48.38
9	0 0 0	2.99		5.53	5.18	9.98	8.44	13.04	11.97	13.63	17.71	18.28	30.92	53.89
	0 0 1	3.33		5.34	5.19	9.32	9.72	11.50	14.00	16.04	18.59	18.75	29.01	

E_i being the unperturbed energy of the neighboring level, with the perturbation parameter W_{pi}. This is the usual first-order perturbation formulation; and tests with a few secular equations of low order have shown it to be a good approximation to the more complicated exact procedure, when as is the case for these states, there is only one level E_i close to E_0.

With the approximate procedure, and an estimate for the unperturbed energies obtainable by inspection from table 6, it is thus possible to calculate from the observed levels a value of W_p and hence G_{zz} for each strong perturbation. The values thus obtained for G_{zz} do not agree well, showing a quite regular tendency to increase with higher K. This might mean that the Coriolis interaction is augmented by the centrifugal distortion associated with rotation about the least axis of inertia, which is not surprising. By assuming for G_{zz} the value $1.00+0.65\ K\ (K+1)$, we obtain the perturbation corrections listed in table 6. It is seen that these produce a gratifying smoothing of the entries, so that the sums, which now should be due to centrifugal stretching alone, vary quite regularly with J and $J+\tau$. Without further calculation, one should not ascribe great significance to this empirical perturbation correction, but it appears to yield results, for low J at least, that are quite reasonable, and further confirms the energy levels and molecular constants reported here.

The very small residuals in table 6 for the lowest J values may also be taken as confirmation of the values of the band origins listed in table 2. Except for some systematic error that would affect all our frequencies, they are probably accurate within ± 0.05 cm^{-1}. The 0_0 level of ν_1 is not directly observed, as the only line to which it would lead ($0-1_0$, at 3619.92 cm^{-1}) is overlapped by strong lines of ν_3 and of CO_2, but the consistency of the other ν_1 lines and levels here reported establishes it with good accuracy.

The lower levels of ν_3 here identified agree with those reported earlier [3]. However, beginning at $J=4$ there are numerous differences. Our ν_1 levels do not agree in any particular with the earlier analysis. It may be noted that the present results for ν_1 are in agreement with the frequency shifts observed in the Raman effect [17], when the vibrational-rotational selection rules applicable to the latter are considered. The Raman observations yield a broad unresolved "line" with two maxima at 3646.1 ± 1.5 and 3653.9 ± 1.5 cm^{-1}. The selection rules [18] show that this is really an unresolved Q branch in which are superposed all lines with $\Delta J=0$, $\Delta\tau=0$. For each J, the strongest lines are those with the highest and lowest τ. Because of the lower rotational constants in the upper vibrational state, the shifted lines will be below the band origin of 3657.05 cm^{-1}. The center of gravity of the unresolved band may be approximately calculated from the energy levels of table 2, with the unobserved higher levels estimated from the rotational constants. Such a calculation, assuming a scattering temperature of 150° C and an effective slit width of 3 cm^{-1} leads to the observed doublet structure, in which the higher frequency shifts are due principally to the lines of lowest τ, with maxima at 3654.3 cm^{-1} and 3647.5 cm^{-1}.

V. Conclusion

With the present identification of ν_1, and the derivation of quite accurate rotational constants for ν_1 and ν_3, the last significant gap in our knowledge of

the vibration-rotation spectrum of H_2O is filled. Additional studies at elevated temperature would undoubtedly be of value in establishing higher rotational term values, and improved resolution, by splitting some of the still blended lines, might lead to a slight revision in the energy levels. Moreover, studies in the region 3,300 to 3,600 will undoubtedly permit extension of the ν_1 analysis. With an asymmetric rotor of the complexity of H_2O, one can never consider the spectral analysis complete. Nevertheless, it is believed that the atmospheric absorption in the 2.7-μ region is now rather satisfactorily accounted for.

Our thanks are due to N. Acquista and Mary A. Lamb, who assisted in obtaining and measuring the spectra. We are also indebted to O. C. Mohler of the Mc-Math Hulbert Observatory, University of Michigan, to W. A. Benesch of the Johns Hopkins University, and to M. Migeotte of Liége, Belgium, for communicating their results on the atmospheric absorption, which were of assistance in interpreting the data.

VI. References

[1] R. Mecke, Z. physik **81**, 373 (1933).
[2] E. K. Plyler and W. W. Sleator, Phys. Rev. **37**, 1493 (1931).
[3] H. H. Nielsen, Phys. Rev. **62**, 422 (1942).
[4] W. S. Benedict, in preparation; cf. Phys. Rev. **74**, 702, 703, 1246 (1948).
[5] E. K. Plyler and M. A. Lamb, National Bureau of Standards, publication pending.
[6] E. F. Barker, Astrophys. J. **55**, 391 (1922).
[7] R. C. Nelson, The absorption of water vapor in the regions 1.33 to 1.48 and 1.77 to 1.98 microns, Summary Report No. 4 on Contract Nobs 28373 (Northwestern Univ., May 23, 1949).
[8] P. C. Cross, R. M. Hainer, and G. W. King, J. Chem. Phys. **12**, 210 (1949).
[9] D. M. Dennison, Rev. Mod. Phys. **12**, 189 (1940).
[10] G. Herzberg, Infra red and raman spectra of polyatomic molecules, p. 390 (D. Van Nostrand, New York, N. Y., 1945).
[11] L. Goldberg, O. C. Mohler, R. R. McMath, and A. K. Pierce, Phys. Rev. **76**, 1948 (1949); also G. Herzberg, private communication.
[12] Plyler and Sleator, Phys. Rev. **37**, 1493 (1931); H. H. Nielsen, Phys. Rev. **59**, 565 (1941); W. A. Benesch, private communication; M. Migeotte, private communication.
[13] E. B. Wilson, J. Chem. Phys. **4**, 313 (1936); also [10], p. 466.
[14] R. M. Hainer and G. W. King, J. Chem. Phys. **15**, 89 (1947).
[15] G. W. King, R. M. Hainer, and P. C. Cross, J. Chem. Phys. **11**, 27 (1943).
[16] W. S. Benedict, Phys. Rev. **75**, 1317 (1949).
[17] D. H. Rank, K. D. Larsen and E. B. Bordner, J. Chem. Phys. **2**, 464 (1934).
[18] G. Placzek and E. Teller, Z. Physik, **81**, 209 (1933).

WASHINGTON, July 19, 1950.